

Úvod do fyziky pevných látek

Václav Holý

Katedra fyziky kondenzovaných látek

Verze 2

Gert R. Strobl, Steven P. Brown: Condensed Matter Physics: Crystals, Liquids, Liquid Crystals, and Polymers, Springer Verlag; (September 2003) ISBN: 3540003533

R. A. L. Jones, Soft Condensed Matter, OUP 2002, ISBN 0-19-8505892

Neil W. Ashcroft, N. David Mermin, David Mermin: Solid State Physics, International Thomson Publishing; 1st edition (1976) ISBN: 0030839939

Ch. Kittel: Introduction to solid state physics, various editions (also in Czech)

Ch. Kittel: Quantum theory of solids, various editions (also in Slovak)

J. R. Hook, H. E. Hall, Solid state physics, J. Wiley 2000

H. Ibach, H. Lueth, Solid state physics, Springer 2003

R. E. Hummel, Electronic properties of materials, Springer 1992

P. M. Chaikin, T. C. Lubensky, Principles of Condensed Matter Physics, Cambridge University Press 2000.

I STRUCTURE OF CONDENSED MATTER IN 3D

Several numbers at the beginning:

characteristic distance on an atomic scale is the angstrom 10^{-8} cm. The electrostatic energy at this scale is of the order $e^2/(1 \text{ \AA}) \sim 2.3 \times 10^{-11} \text{ erg} \cong 14 \text{ eV} \cong 1.6 \times 10^5 \text{ K}$.

The kinetic energy associated with localizing an electron in a box of side 1 \AA is

$$\frac{\hbar^2}{2m} \left(\frac{1}{\text{\AA}} \right)^2 \simeq 6.1 \times 10^{-12} \text{ erg} \simeq 3.8 \text{ eV} \simeq 4.4 \times 10^4 \text{ K}$$

These two energies are comparable and much larger than room temperature $300 \text{ K} \sim 0.025 \text{ eV}$. Thus a large number of ions could form a very stable salt like NaCl with binding energy several eV per atom.

In a metal – the binding energy can be approximated by allowing some electrons to extend over the whole solid – this lowers the kinetic energy by several eV per atom.

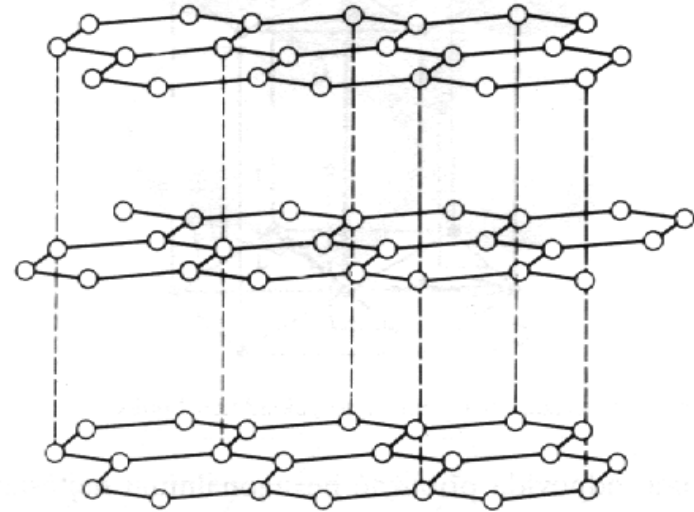
Two main effects – Coulomb attraction (or repulsion) and delocalization of quantum states of free electrons

I.1. Inter-atomic and inter-molecular bonds

Types of bonds and their energies:

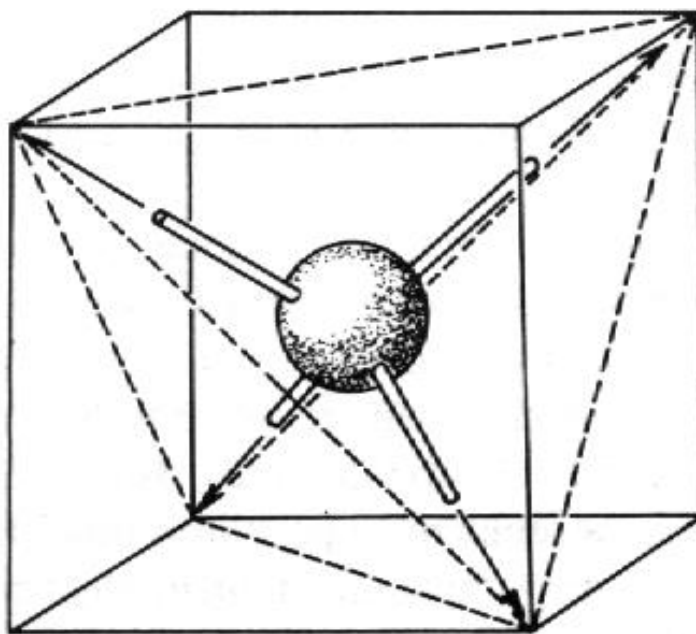
1. covalent $4 - 6 \cdot 10^5$ J/mol,
2. metallic $2 - 4 \cdot 10^5$ J/mol,
3. ionic $2 - 4 \cdot 10^5$ J/mol,
4. hydrogen $0,2 - 0,3 \cdot 10^5$ J/mol,
5. van der Waals $0,04 - 0,08 \cdot 10^5$ J/mol

Usually, several types of bonds are present in a solid. In graphite, for instance the strong covalent bonds give rise to carbon hexagons, the inter-plane bonds are weak



Directional and non-directional bonds:

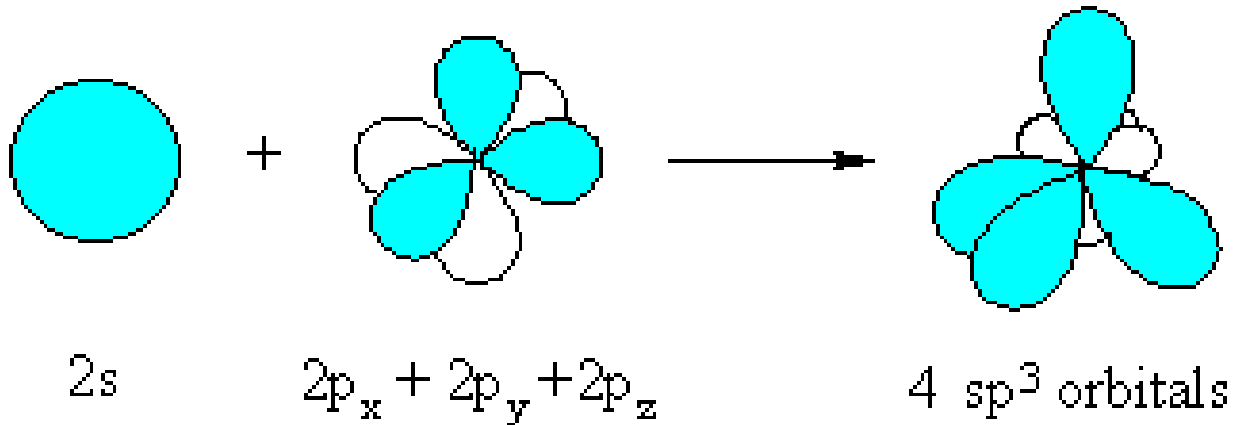
directional covalent bonds in the molecule CH_4 ; the bonds between the molecules are non-directional and weak (van der Waals bonds)



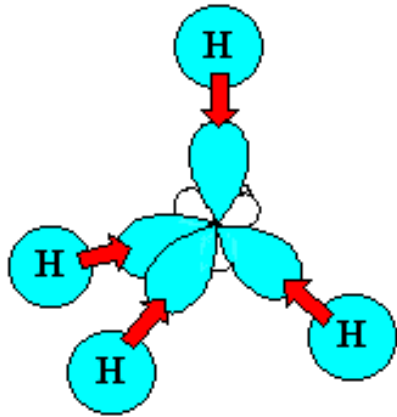
Covalent bond

Overlap of atomic orbitals occupied by single electrons with opposite spins – semiconductors (Si, Ge) and dielectrics (C-diamond) with the gaps 0.67 eV (Ge), 1.1 eV (Si) and 5.5 eV (C).

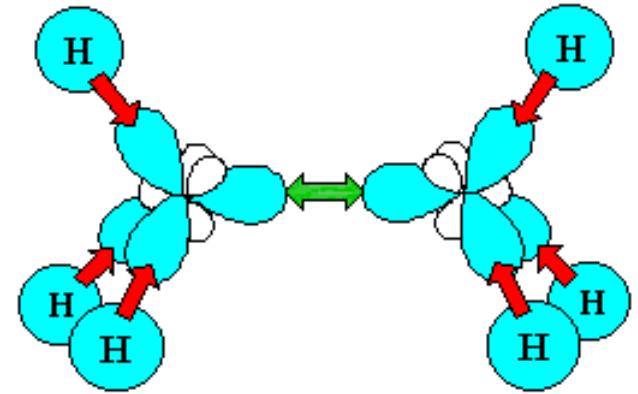
sp^3 hybridization in a C atom (electron configuration $1s^2 2s^2 2p^2$)



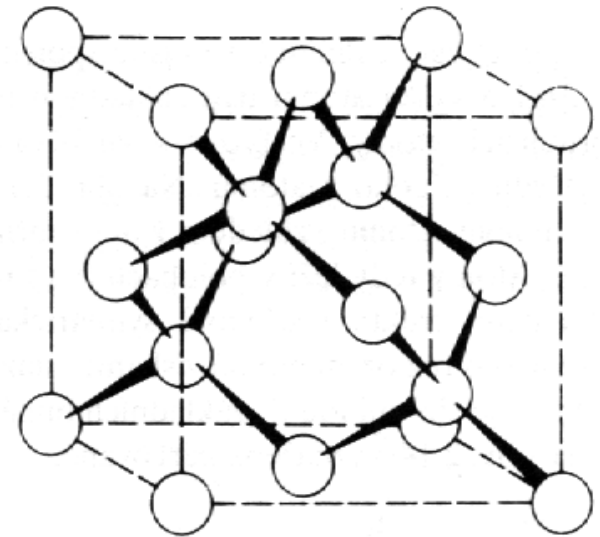
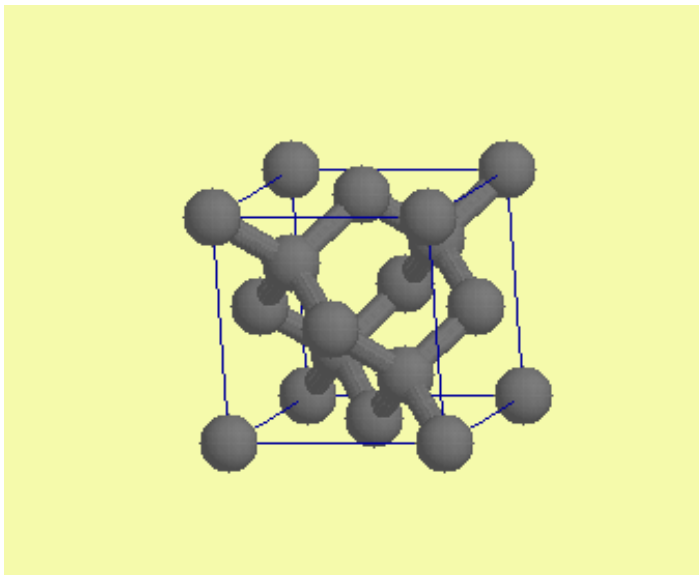
In methane:



In ethane:

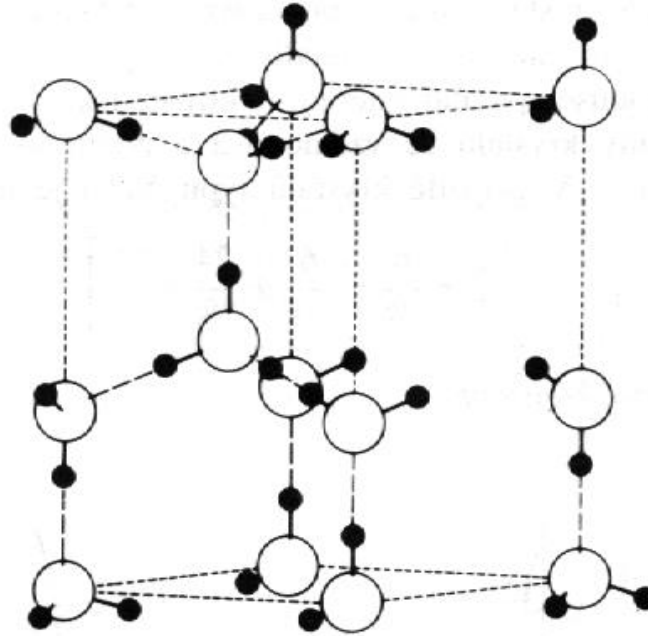


In Si



Hydrogen bond

Crystal structure of ice:

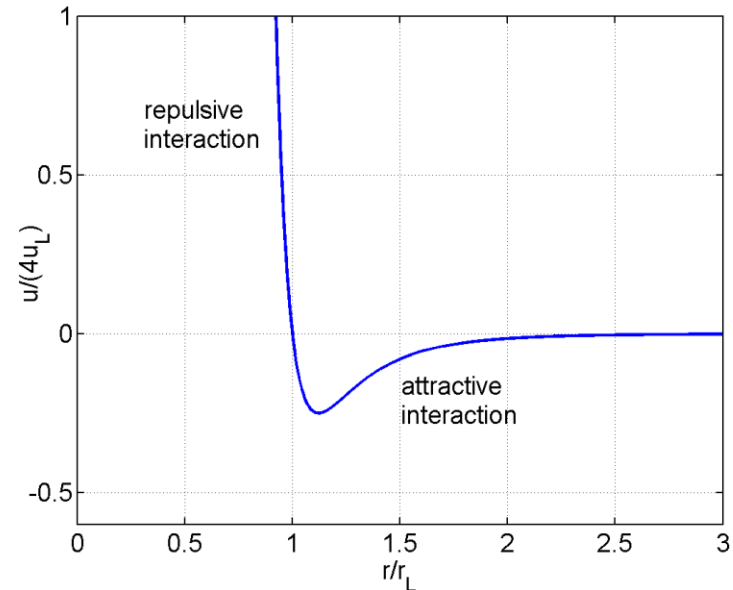


induced dipole moment of the hydrogen atom mediates the attractive interaction between the oxygen atoms

van der Waals bond

between molecules or neutral atoms

$$u(r) = 4u_L \left[\left(\frac{r_L}{r} \right)^{12} - \left(\frac{r_L}{r} \right)^6 \right]$$

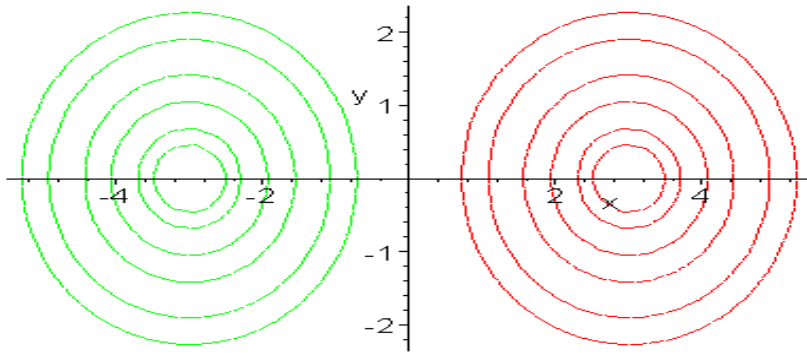


Equilibrium position: $\left. \frac{du(r)}{dr} \right|_{r_{min}} = 0 \Rightarrow r_{min} = r_L 2^{1/6}$

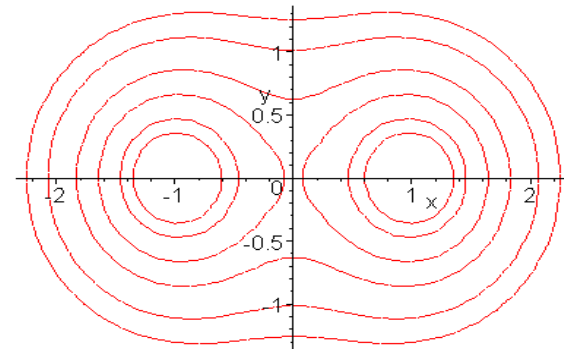
Attractive interaction: electrical interaction between permanent and/or temporary dipole moments.
Electric field of a dipole moment $\propto r^{-3} \Rightarrow$ the energy of the interaction $\propto r^{-6}$

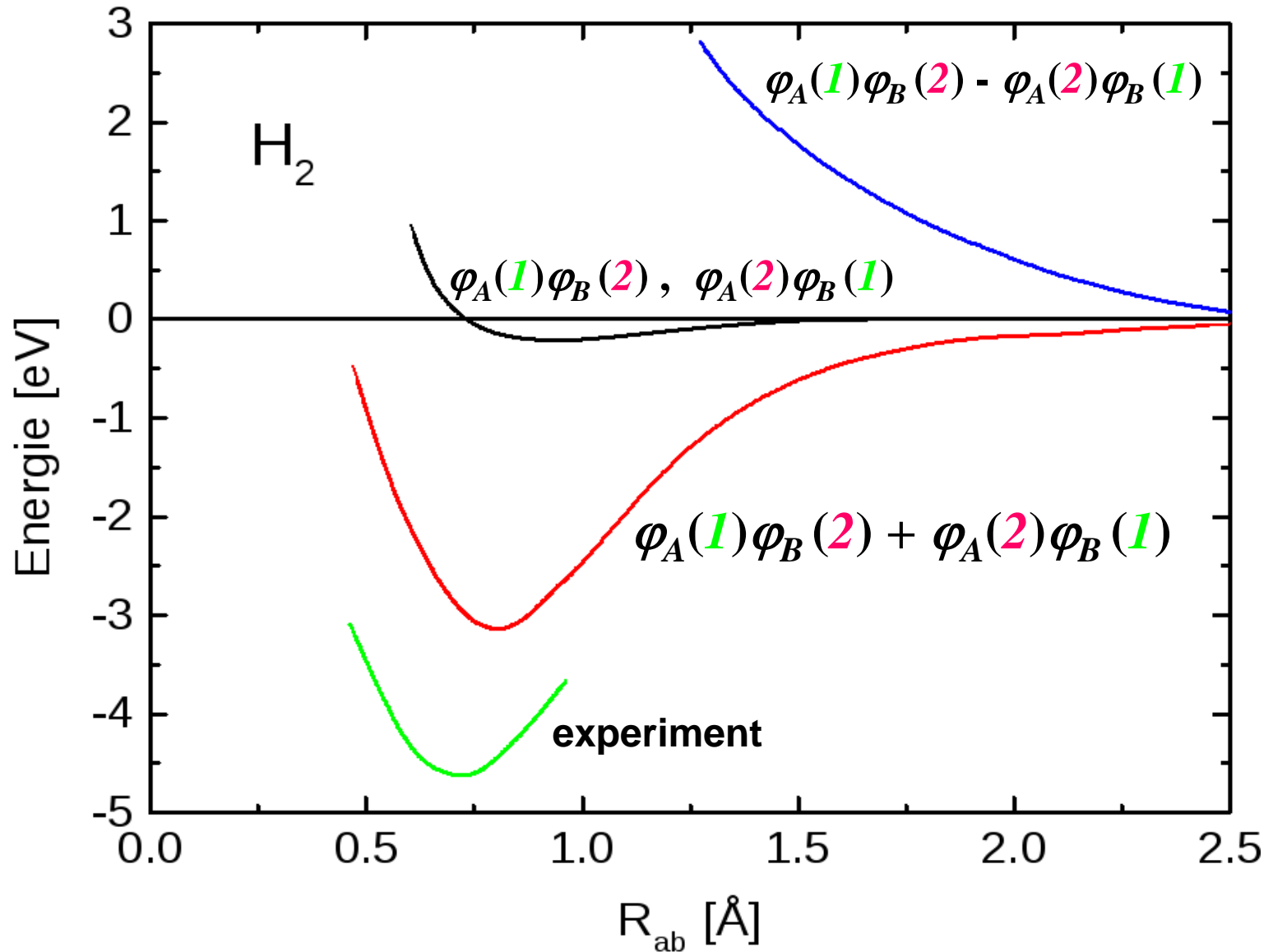
Repulsive interaction – due to the Pauli principle; the r^{-12} dependence is only empiric!

H₂ molecule – electron density,
antibonding orbital



H₂ molecule – electron density,
bonding orbital





Lattice energy

Potential energy of a lattice $U_B = \frac{1}{2} \sum_{j \neq k} u(r_{jk})$

For the Lennard-Jones potential we get

$$U_B = 4u_L \frac{N}{2} \left[\left(\frac{r_L}{a} \right)^{12} S_{12} - \left(\frac{r_L}{a} \right)^6 S_6 \right]$$

The lattice sum

$$S_n = \sum_{k \neq 0} \left(\frac{1}{s_{0k}} \right)^n, s_{jk} = r_{jk}/a$$

a is the distance of nearest neighbors. From $\frac{\partial U_B}{\partial a} = 0$ we obtain a

Ionic bond

Empiric potential $u(r) = u_B \exp\left(-\frac{r}{r_B}\right) \frac{\pm Q^2}{4\pi\epsilon_0 r}$

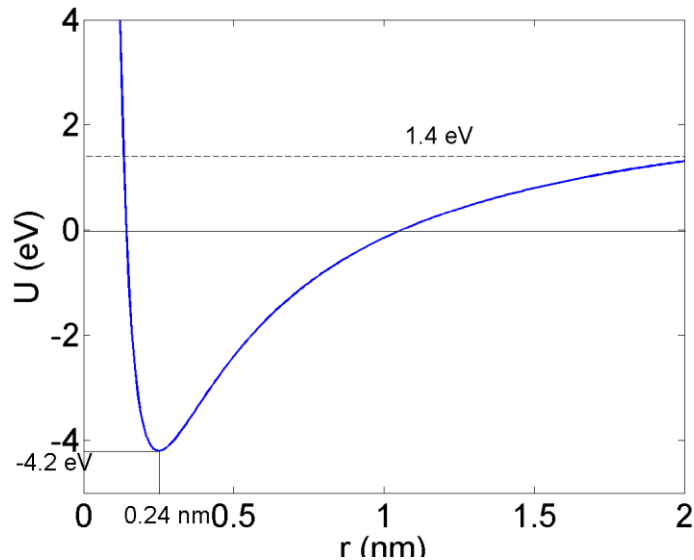
only for nearest neighbors

The lattice energy $U_B = \frac{N}{2} \left[z u_B \exp\left(-\frac{a}{r_B}\right) - \beta \frac{Q^2}{4\pi\epsilon_0 a} \right]$

The Madelung constant $\beta = - \sum_{k \neq 0} \frac{\text{sign}(Q_0 Q_k)}{s_{0k}}$

This sum is only conditionally convergent, i.e., its value depends on the summation order. The summation over expanding cubes converges to the correct value. In rocksalt lattice $\beta = \pm 3.495$

Cohesion energy $U_{coh} = U_{tot} - U_{gas}, U_{tot} = U_B + U_{kin}$



Energy of the molecule NaCl

Iont Cl^- je stabilnější než neutrální atom Cl. Připojením elektronu k atomu Cl se uvolní energie 3.7 eV (elektronová afinita). Energie potřebná k odtržení elektronu od neutrálního atomu Na a ke vzniku iontu Na^+ je 5.1 eV. Energie potřebná ke vzniku páru izolovaných iontů Na^+ a Cl^- je tedy 1.4 eV. Přiblížíme-li ionty k sobě, jejich energie klesá díky elektrostatické přitažlivé síle. Je-li vzdálenost iontů dostatečně malá, je celková energie molekuly Na^+Cl^- záporná a vzniká iontová vazba.

Iontová kohezní energie krystalu NaCl na jeden pár $\text{Na}^+ \text{Cl}^-$ je 7.8 eV, atomová kohezní energie na pár neutrálních atomů Na Cl je $7.8 - 5.1 + 3.6$ eV = +6.3 eV

Thermal expansion

For $T > 0$ K, the equilibrium value of a corresponds to the minimum of **free energy**

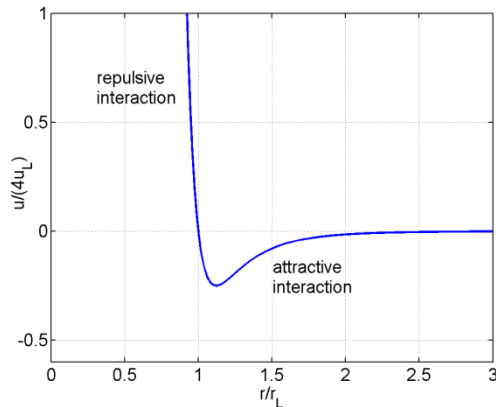
$$F = U - TS = U_B + F_{vib} \quad \left. \frac{\partial F}{\partial a} \right|_{eq} = 0$$

The vibration-induced part of the free energy follows from the Bose-Einstein statistics of phonons

$$F_{vib} = k_B T \sum_j \left[\frac{\hbar \omega_j}{2k_B T} + \ln \left(1 - \exp \left(-\frac{\hbar \omega_j}{k_B T} \right) \right) \right]$$

harmonic approximation: F_{vib} does not depend on a

anharmonicity: with increasing a the bonds get weaker $\Rightarrow \frac{\partial F_{vib}}{\partial a} < 0$



the Grüneisen constant

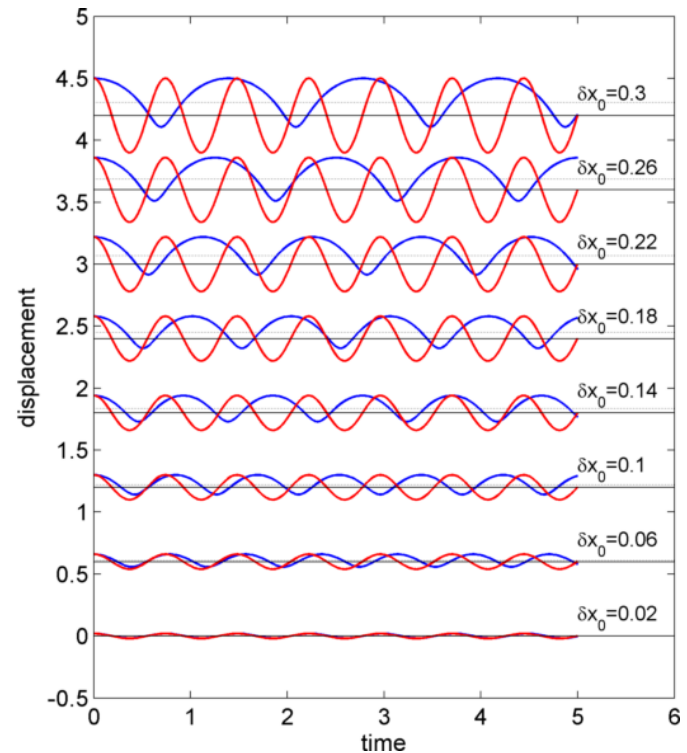
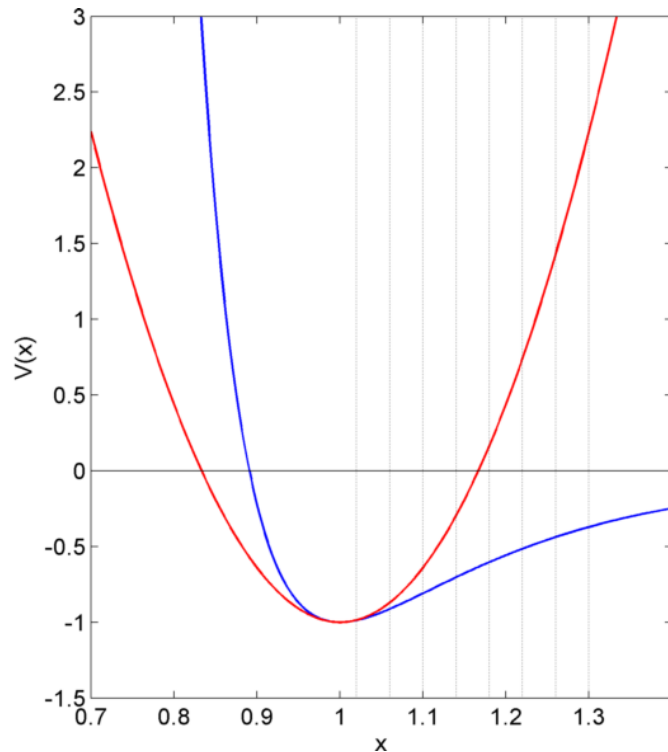
$$\gamma = \frac{\partial \ln \omega_j}{\partial V}$$

Simple example of a nonlinear oscillator: Lennard-Jones (LJ) potential

$$U(x) = U_0 \left[\left(\frac{x_0}{x} \right)^{12} - 2 \left(\frac{x_0}{x} \right)^6 \right]$$

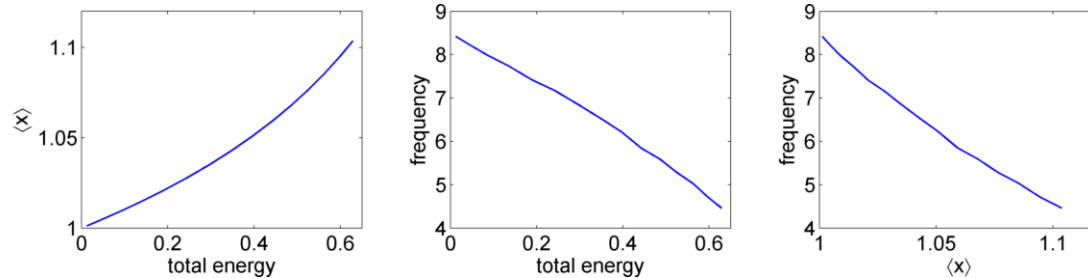
Equilibrium point is x_0 , $U(x_0) = -U_0$

Results of numerical simulations for $U_0 = 1$, $x_0 = 1$:



With increasing maximum displacement, i.e., with increasing total energy, the mean position x increases and the frequency decreases

With increasing temperature the mean inter-atomic distance increases \Rightarrow thermal dilatation



The coefficient of thermal dilatation is therefore connected with the decrease of the frequency of oscillations with increasing inter-atomic distance – Grüneisen parameter

$$\gamma = \frac{\alpha K_T}{C_V \rho} = -\frac{V}{\omega_0} \frac{\partial \omega_0}{\partial V} = -\frac{1}{2d} \frac{U'''(x_0)x_0^2 + (d-1)[U''(x_0)x_0 - U'(x_0)]}{U''(x_0)x_0 + (d-1)U'(x_0)}$$

α ...thermal dilatation coefficient

K_T ...isothermal bulk modulus

C_V ...heat capacity at constant volume V

d ...dimension of the system

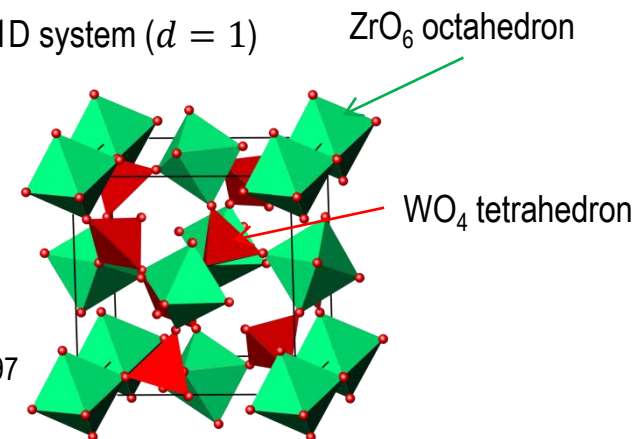
For the LJ potential: $U''(x_0) = 72 \frac{U_0}{x_0^2}$, $U'''(x_0) = -1512 \frac{U_0}{x_0^3} \Rightarrow \gamma = \frac{189}{19}$ for a 1D system ($d = 1$)

Negative thermal expansion materials: $U'''(x_0)x_0 > -(d-1)U''(x_0)$

Example: zirconium tungstate $Zr(WO_4)_2$, $\alpha \approx -7.2 \times 10^{-6} K^{-1}$

NTE is probably caused by correlated rotation of the ZrO_6 octahedra and WO_4 tetrahedra

<https://commons.wikimedia.org/w/index.php?curid=15786797>



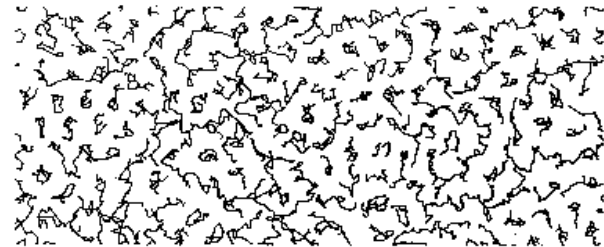
I.2. Crystal structure

gas phase



a

liquid phase



b

solid phase

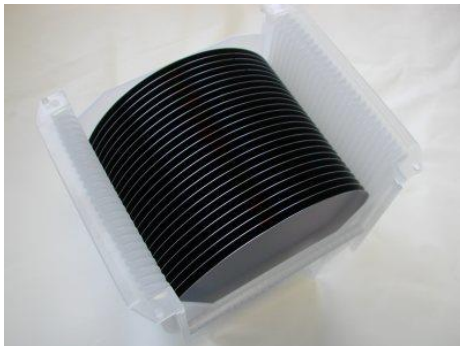


c

natural quartz crystals



Si ingots (single crystals)
(ON-Semi, Rožnov p. R.)

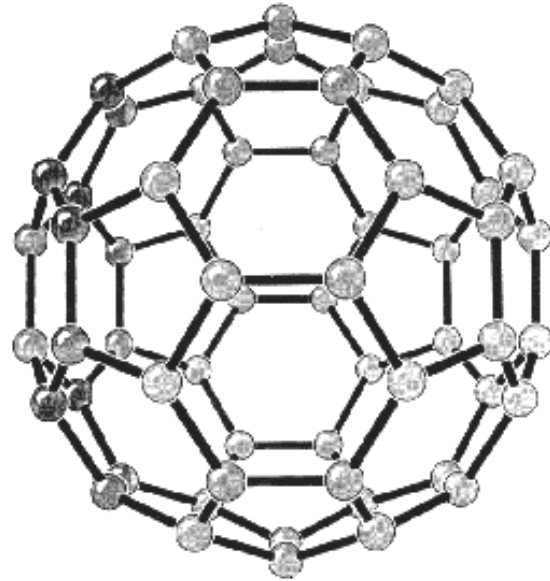


Polished surface of a Be ingot

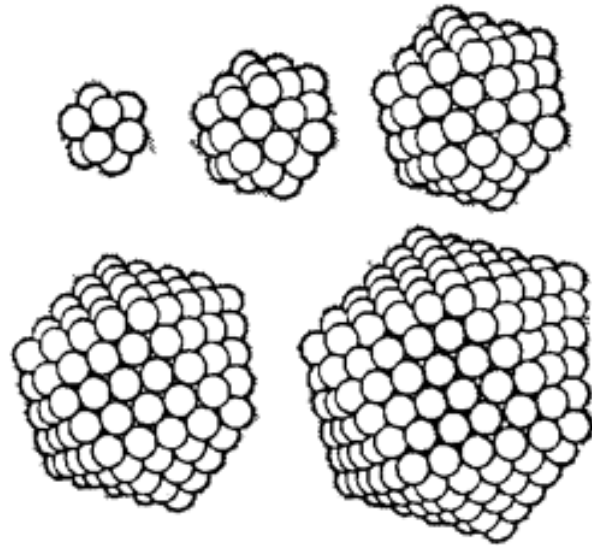


Nanocrystals – magic clusters:

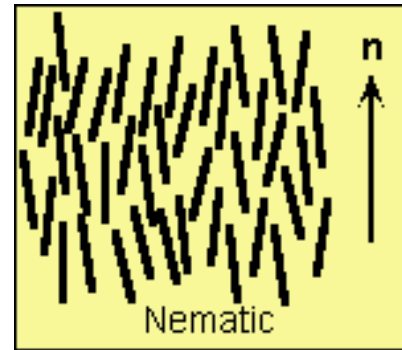
C_{60} fullerene



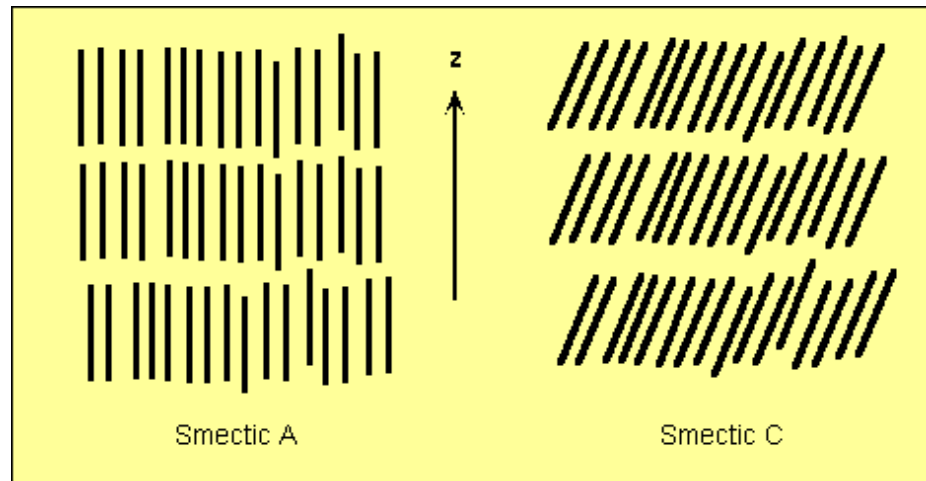
Magic clusters of Kr atoms with 13, 55, 147, 309, 561,... atoms.



nematic liquid crystals (orientational order of molecules)

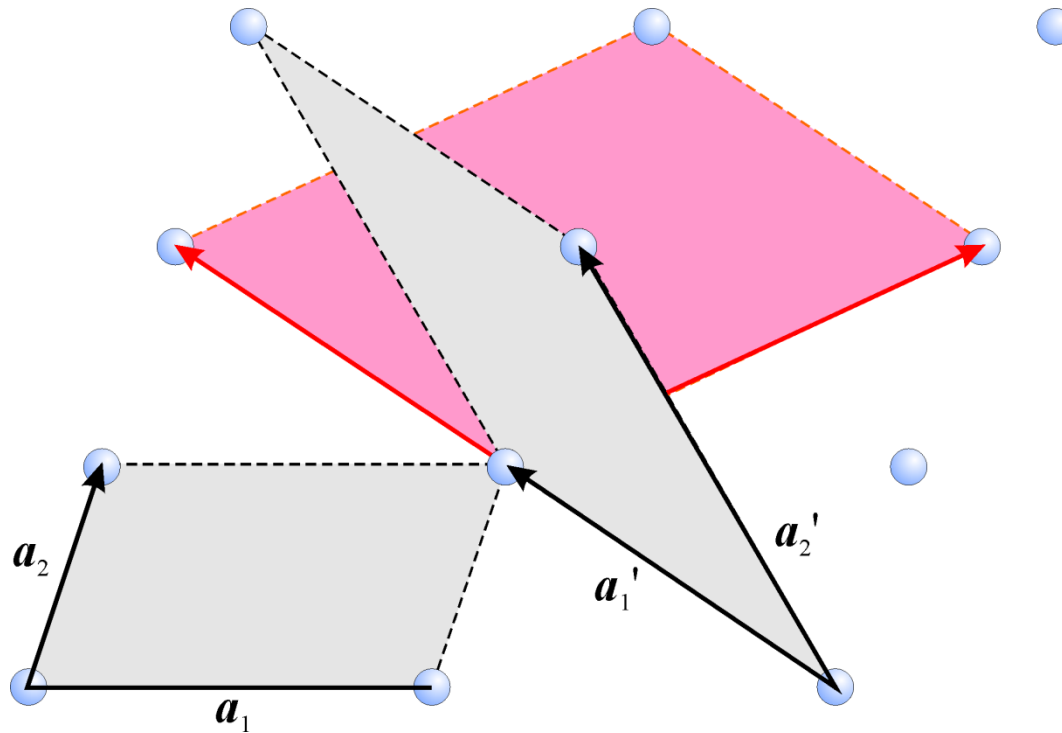


smectic liquid crystals (position order in one direction)



Primitive lattice (prostorová mřížka)

$$\mathbf{R}_n = n_1 \mathbf{a}_1 + n_2 \mathbf{a}_2 + n_3 \mathbf{a}_3, n_{1,2,3} \in \mathbb{Z}$$



All unit cells of the primitive lattice have the same volume

Symmetry properties of primitive lattices:

- translation symmetry
- point symmetry
 - inversion
 - mirror symmetry
 - rotation symmetry

All the symmetry elements of a primitive lattice create the **space group** of the lattice

Two subgroups:

- translation group (generated by the vectors \mathbf{R}_n)
- point group

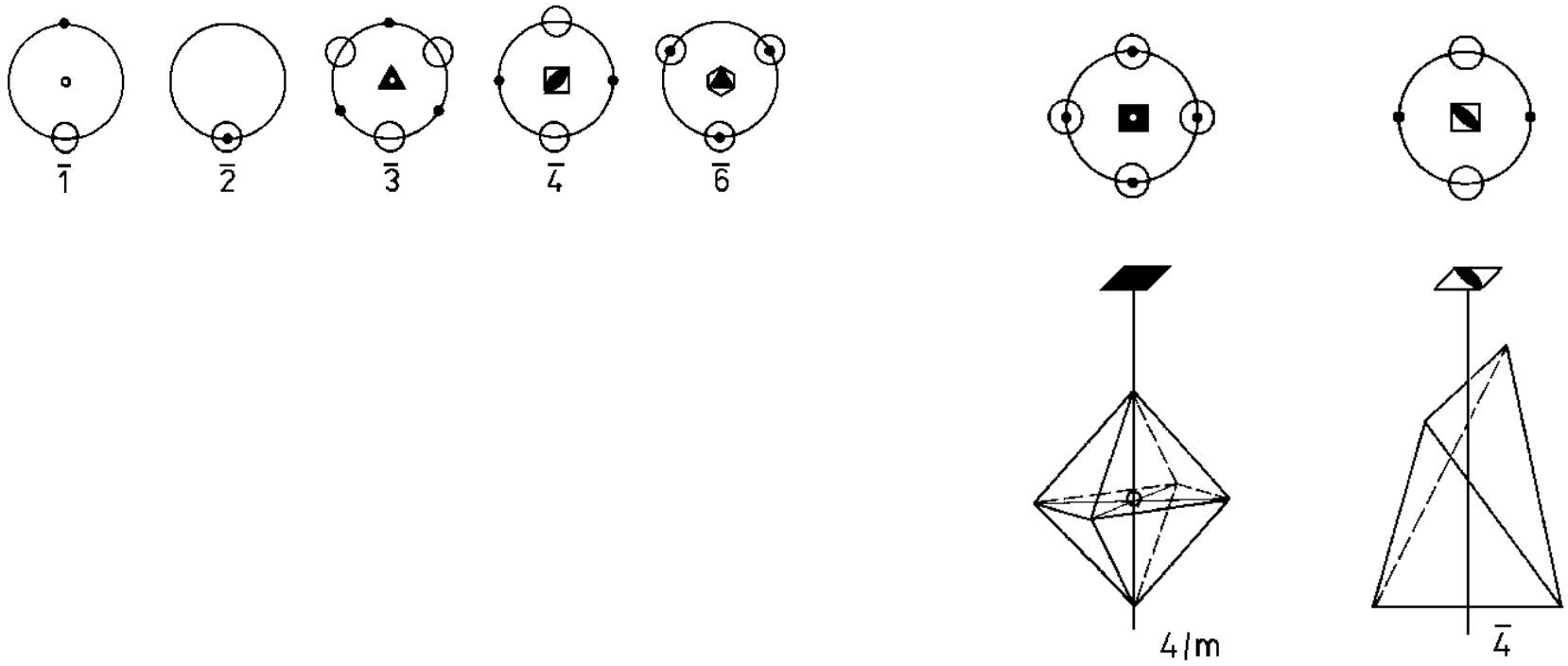
Examples of elements of point symmetry

1-fold, 2-fold, 3-fold, 4-fold and 6-fold rotation axis: 1,2,3,4,6

mirror plane: m

inversion: i

Combination of point symmetry operations – inversion axes



Standard (Schoenflies) notation:

E = Identity

C_n = rotation through $2\pi/n$

σ = reflection in a plane

σ_h = reflection in a "horizontal" plane

σ_v = reflection in a "vertical" plane

σ_d = reflection in a "diagonal" plane

i = inversion

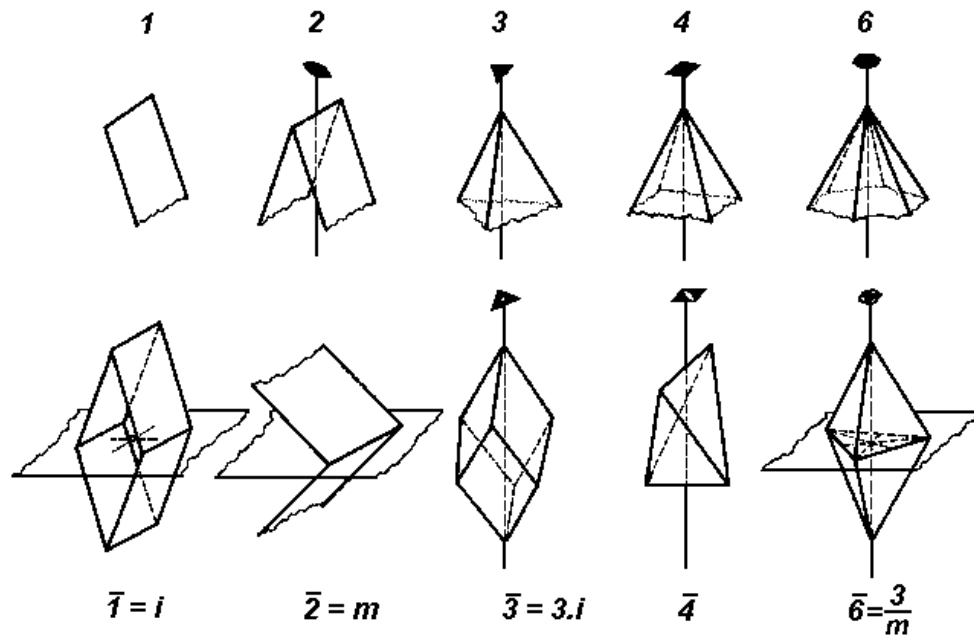
S_n = improper rotation through $2\pi/n$, which consists of a rotation by $2\pi/n$ followed by a reflection in a horizontal plane

$iC_n = \bar{n}$ compound rotation-inversion, which consists of a rotation followed by an inversion.

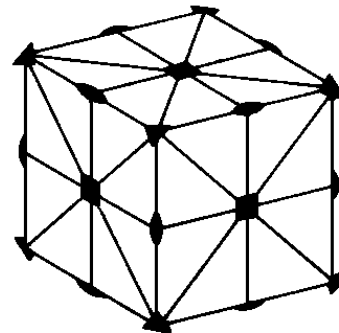
$$\bar{3} \equiv S_6 \equiv iC_3, \bar{6} \equiv S_3 \equiv iC_6$$

	Schoenflies	Hermann-Mauguin
rotation	C_n	n
rotation-inversion	iC_n	\bar{n}
mirror plane	σ	m
horizontal reflection plane \perp to n – fold axes	σ_h	n/m
n – fold axes in vertical reflection plane	σ_v	nm
two non – equivalent vertical reflection planes	$\sigma_{v'}$	nmm

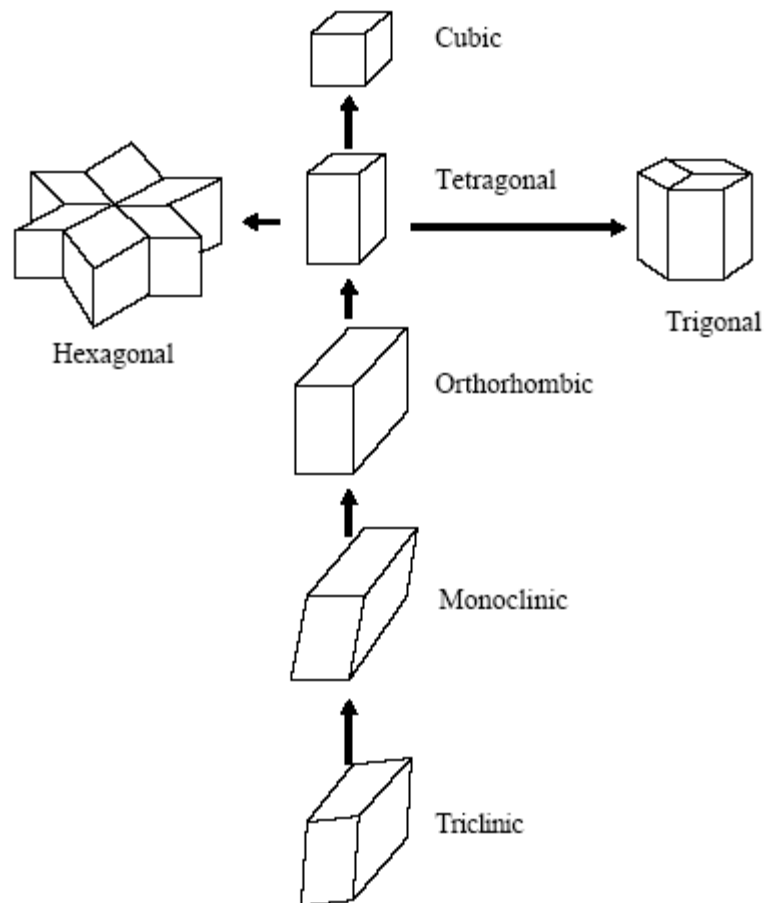
Proper Rotations		Improper Rotations	
International	Schoenflies	International	Schoenflies
1	C_1	$\bar{1}$	S_2
2	C_2	$\bar{2} \equiv m$	σ
3	C_3	$\bar{3}$	S_6^{-1}
3_2	C_3^{-1}	$\bar{3}_2$	S_6
4	C_4	$\bar{4}$	S_4^{-1}
4_3	C_4^{-1}	$\bar{4}_3$	S_4
6	C_6	$\bar{6}$	S_3^{-1}
6_5	C_6^{-1}	$\bar{6}_5$	S_3



All point symmetries of a cube, the 3-fold axis is the inversion axis $\bar{3}$



7 point groups of primitive lattices exist **(the holoedric groups)**



Simple and centered lattices

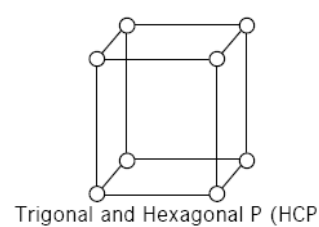
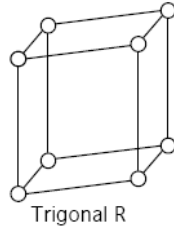
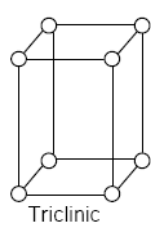
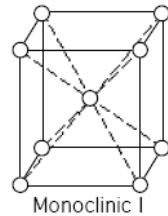
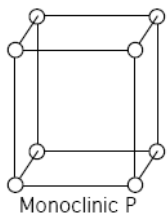
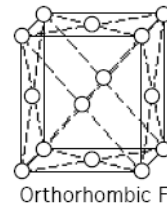
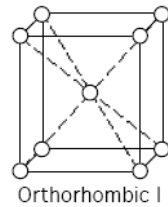
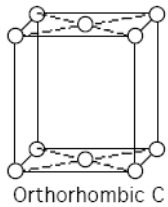
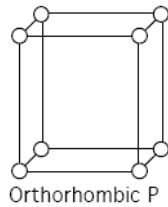
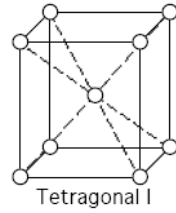
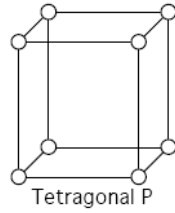
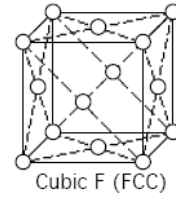
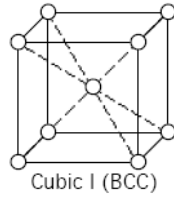
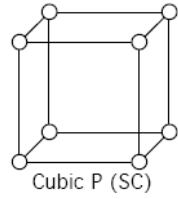
simple primitive lattice – a unit cell exists with a full point symmetry

centered primitive lattice – all unit cells have lower point symmetry than the full lattice

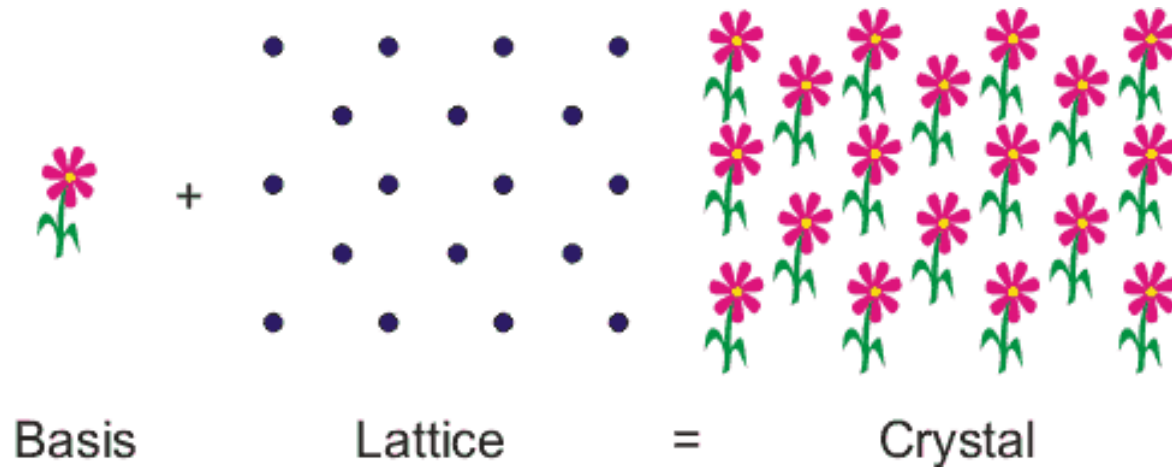
System	Angles and Dimensions	Lattices in System
Triclinic	$a \neq b \neq c, \alpha \neq \beta \neq \gamma$	P (primitive)
Monoclinic	$a \neq b \neq c, \alpha = \gamma = 90^\circ \neq \beta$	P (primitive) I (body centered)
Orthorhombic	$a \neq b \neq c, \alpha = \beta = \gamma = 90^\circ$	P (primitive) C (base centered) I (body centered) F (face centered)
Tetragonal	$a = b \neq c, \alpha = \beta = \gamma = 90^\circ$	P (primitive) I (body centered)
Cubic	$a = b = c, \alpha = \beta = \gamma = 90^\circ$	P (primitive) I (body centered) F (face centered)
Trigonal	$a = b = c, 120^\circ > \alpha = \beta = \gamma \neq 90^\circ$	R (rhombohedral primitive)
Hexagonal	$a = b \neq c, \alpha = \beta = 90^\circ, \gamma = 120^\circ$	R (rhombohedral primitive)

SYMMETRY ELEMENTS

System	Minimum symmetry elements
Cubic	Four 3-fold rotation axes
Tetragonal	One 4-fold rotation (or rotation - inversion) axis
Orthorhombic	Three perpendicular 2-fold rotation (or rotation - inversion) axes
Rhombohedral	One 3-fold rotation (or rotation - inversion) axis
Hexagonal	One 6-fold rotation (or rotation - inversion) axis
Monoclinic	One 2-fold rotation (or rotation - inversion) axis
Triclinic	None



Crystal lattice (crystal structure)



The point group of a crystal lattice is a subgroup of a holohedric group; 32 subgroups exist \Rightarrow 32 **crystallographic classes**

230 space groups of crystal lattices

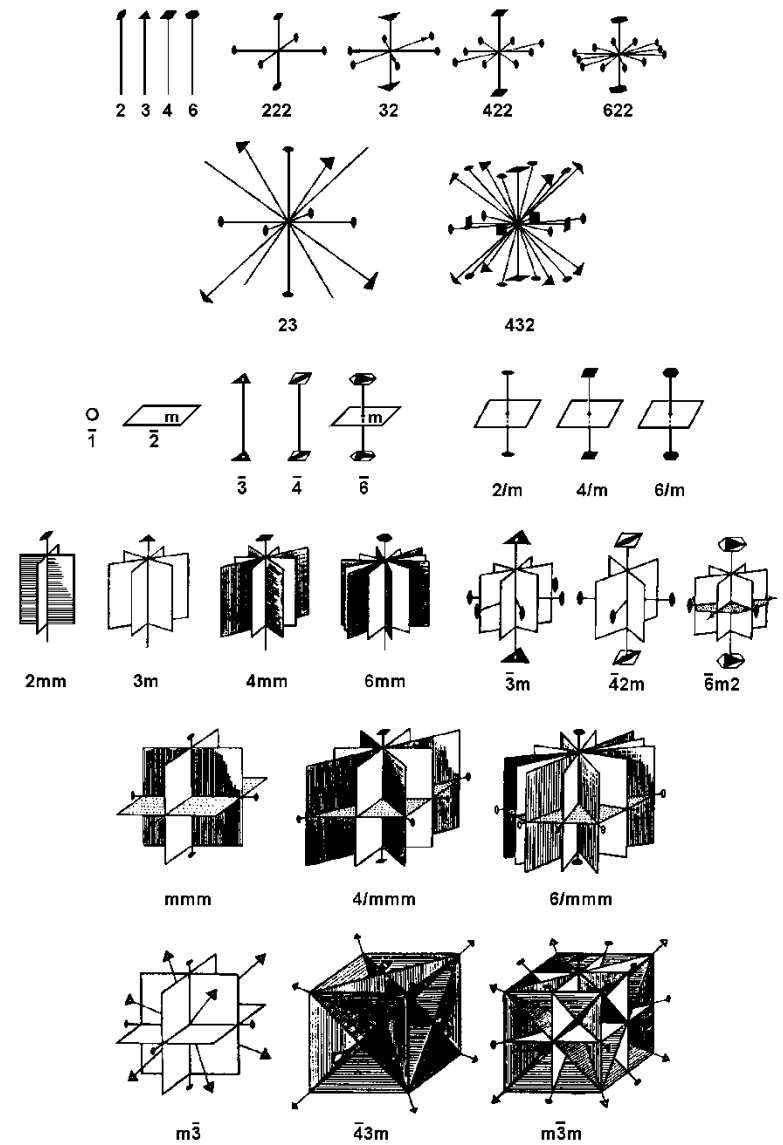
non-primitive symmetry operations:

- glide planes
- screw axes

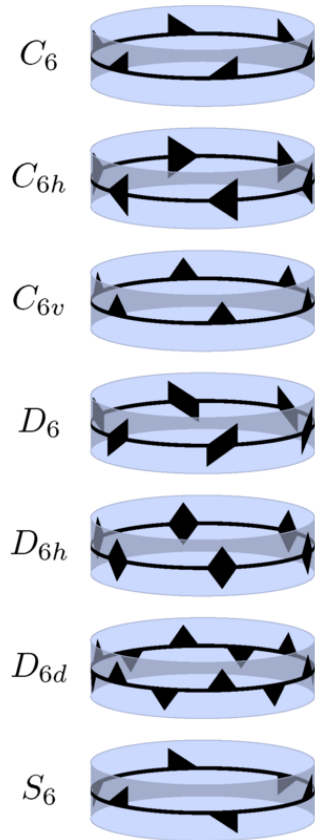
crystallography point groups

The 32 Point Groups and Their Symbols				
System	Schoenflies symbol	Hermann-Mauguin symbol		Examples
		Full	Abbreviated	
Triclinic	C_1	1	1	Al_2SiO_5
	$C_i, (S_2)$	$\bar{1}$	$\bar{1}$	
Monoclinic	$C_{2v}, (C_{1h}), (S_1)$	m	m	KNO_2
	C_2	2	2	
	C_{2h}	$2/m$	$2/m$	
Orthorhombic	C_{2v}	$2mm$	mm	I, Ga
	$D_2, (V)$	222	222	
	$D_{2h}, (V_h)$	$2/m 2/m 2/m$	mmm	
Tetragonal	S_4	$\bar{4}$	$\bar{4}$	CaWO_4
	C_4	4	4	
	C_{4h}	$4/m$	$4/m$	
	$D_{2d}, (V_d)$	$\bar{4}2m$	$\bar{4}2m$	
	C_{4v}	$4mm$	$4mm$	$\text{TiO}_2, \text{In}, \beta - \text{Sn}$
	D_4	422	42	
	D_{4h}	$4/m 2/m 2/m$	$4/mmm$	
Rhombohedral	C_3	3	3	AsI_3
	$C_{3i}, (S_6)$	$\bar{3}$	$\bar{3}$	FeTiO_3
	C_{3v}	$3m$	$3m$	Se Bi, As, Sb, Al_2O_3
	D_3	32	32	
	D_{3d}	$32/m$	$3m$	
Hexagonal	$C_{3h}, (S_3)$	6	6	ZnO, NiAs CeF_3 Mg, Zn, graphite
	C_6	6	6	
	C_{6h}	$6/m$	$6/m$	
	D_{3h}	$\bar{6}2m$	$\bar{6}2m$	
	C_{6v}	$6mm$	$6mm$	
	D_6	622	62	
	D_{6h}	$6/m 2/m 2/m$	$6/mmm$	
Cubic	T	23	23	NaClO_3
	T_h	$2/m\bar{3}$	$m\bar{3}$	FeS_2
	T_d	$\bar{4}3m$	$\bar{4}3m$	ZnS
	O	432	43	$\beta\text{-Mn}$
	O_h	$4/m \bar{3} 2/m$	$m\bar{3}m$	NaCl, diamond, Cu

32 point groups

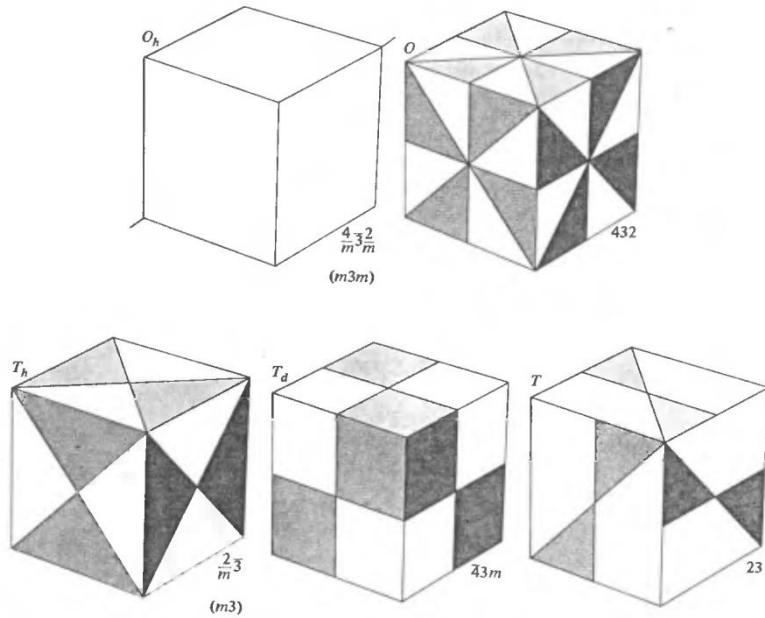


https://en.wikipedia.org/wiki/List_of_space_groups



THE NONCUBIC CRYSTALLOGRAPHIC POINT GROUPS^a

OBJECTS WITH THE SYMMETRY OF THE FIVE CUBIC CRYSTALLOGRAPHIC POINT GROUPS^a



SCHOENFLIES	HEXAGONAL	TETRAGONAL	TRIGONAL	ORTHO-RHOMBIC	MONOCLINIC	TRICLINIC	INTERNATIONAL
C_n	C_6 6	C_4 4	C_3 3		C_2 2	C_1 1	n
C_{nv}	C_{6v} $6mm$	C_{4v} $4mm$	C_{3v} $3m$	C_{2v} $2mm$			nmm (n even) nm (n odd)
C_{nh}	C_{6h} $6/m$	C_{4h} $4/m$			C_{2h} $2/m$		n/m
	C_{3h} $\bar{6}$				C_{1h} ($\bar{2}$) m		\bar{n}
S_n		S_4 $\bar{4}$	S_6 (C_{3i}) $\bar{3}$			S_2 (C_i) $\bar{1}$	
D_n	D_6 622	D_4 422	D_3 32	D_2 (V) 222			$n22'$ (n even) $n2$ (n odd)
D_{nh}	D_{6h} $6/mmm$	D_{4h} $4/mmm$		D_{2h} (mmm) (V_h) $2/mmm$			$\frac{n}{m} \frac{2}{m} \frac{2}{m}$ (n/mmm)
	D_{3h} $\bar{6}2m$						$\bar{n}2m$ (n even)
D_{nd}		D_{2d} (V_d) $42m$	D_{3d} ($\bar{3}m$) $\bar{3} \frac{2}{m}$				$\bar{n} \frac{2}{m}$ (n odd)

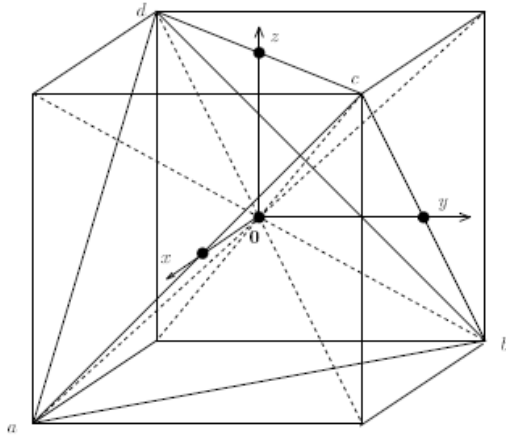


Figure 3.3: Schematic diagram for the symmetry operations of the group T_d .

Symmetry Operations of T_d

- Identity
- 8 C_3 about body diagonals corresponding to rotations of $\pm \frac{2\pi}{3}$
- 3 C_2 about x, y, z directions
- 6 S_4 about x, y, z corresponding to rotations of $\pm \frac{\pi}{2}$
- 6 σ_d planes that are diagonal reflection planes

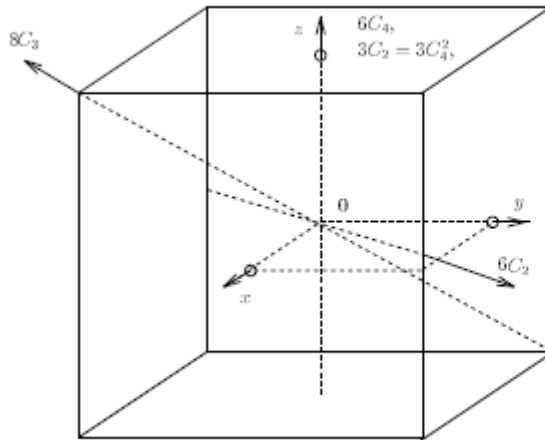
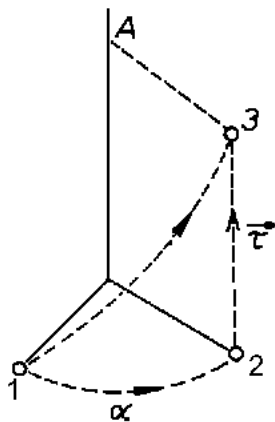


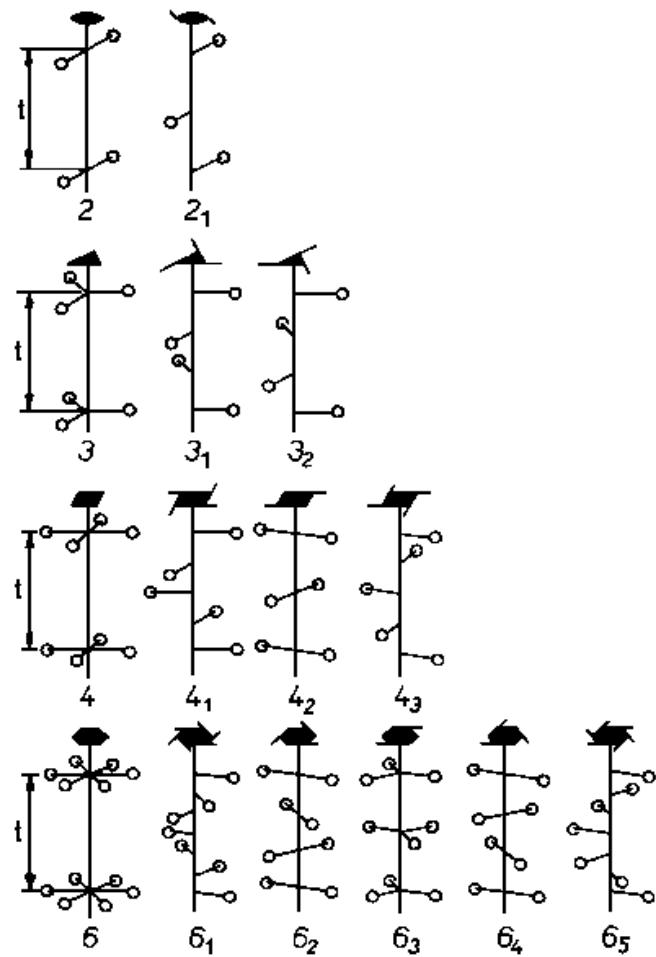
Figure 3.4: Schematic for the symmetry operations of the group O .

The symmetry operations are: E ; $8C_3$; $3C_2 = 3C_4^2$, $6C_2$ and $6C_4$. To get O_h we combine these 24 operations with inversion to give 48 operations in all.

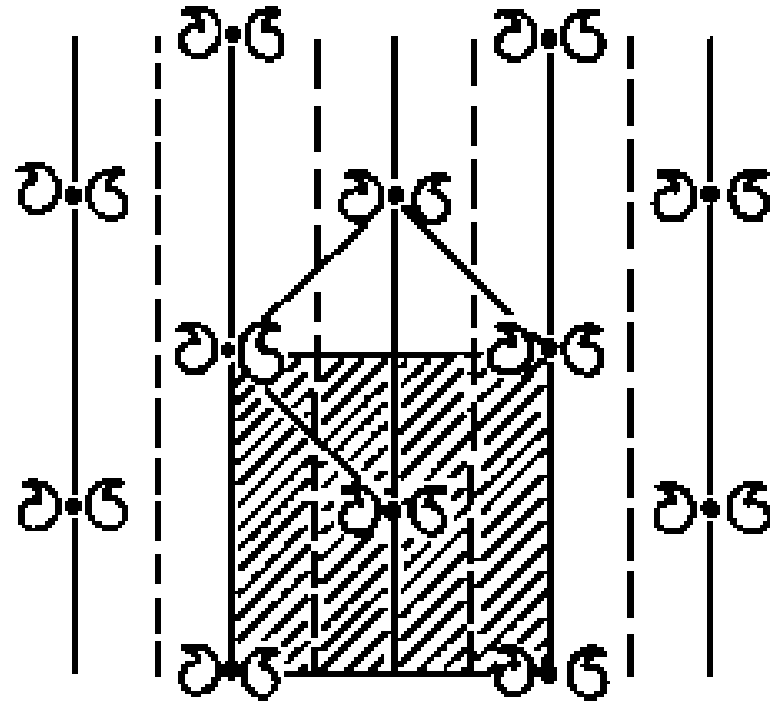
screw axis



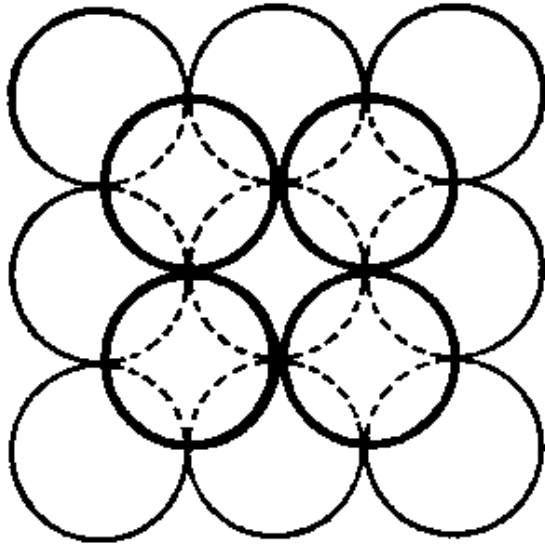
possible screw axes:



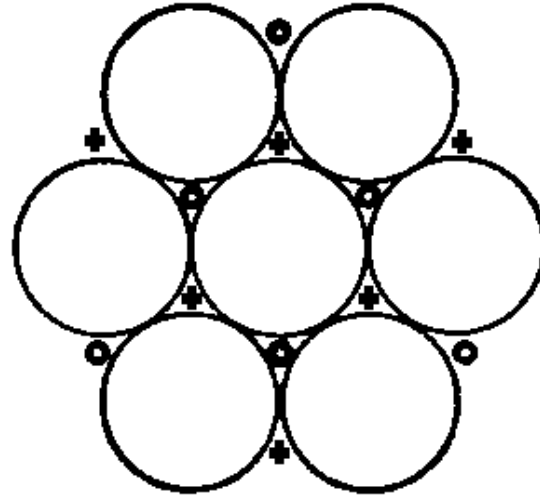
glide plane



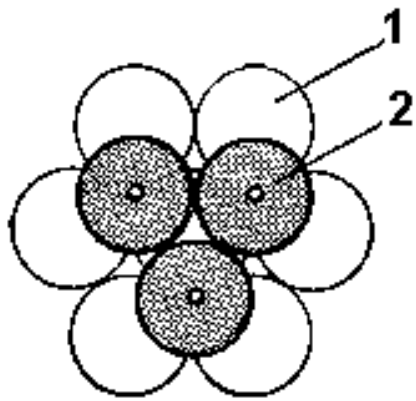
Close-packed structures



A

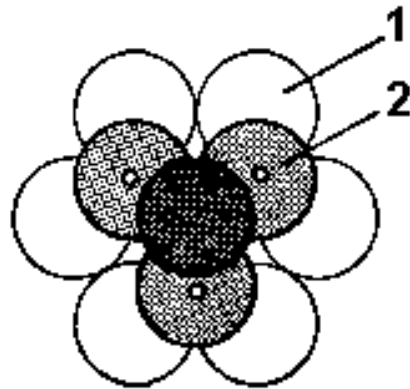


B



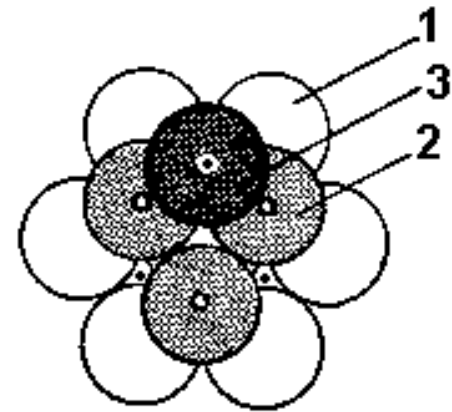
A

2nd layer



B

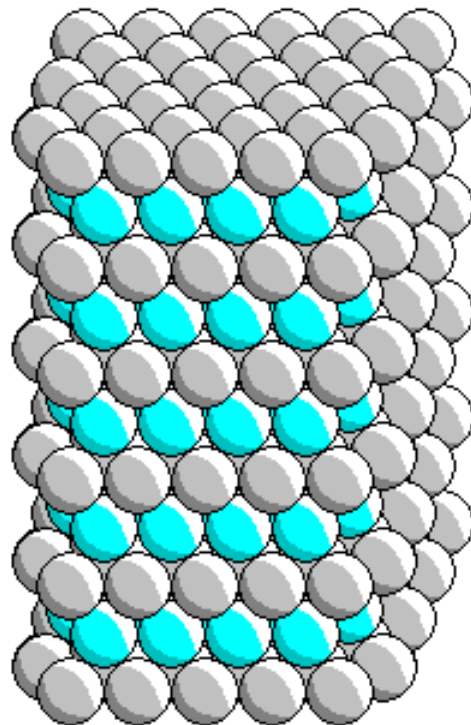
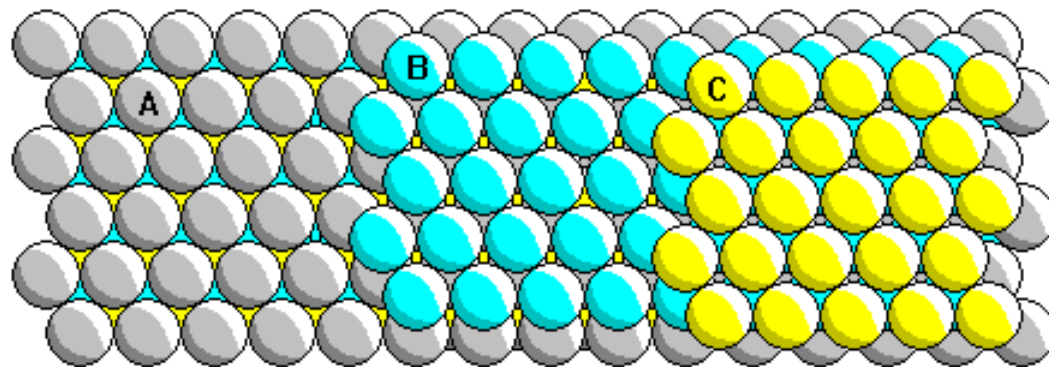
3rd layer, hcp stacking



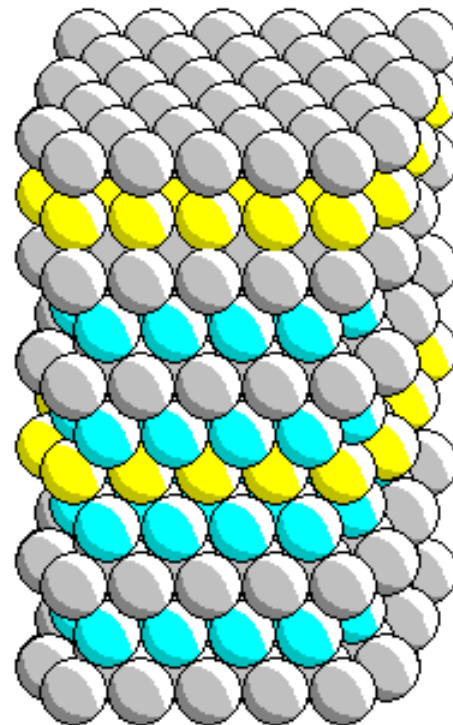
C

3rd layer, fcc stacking

hcp structure

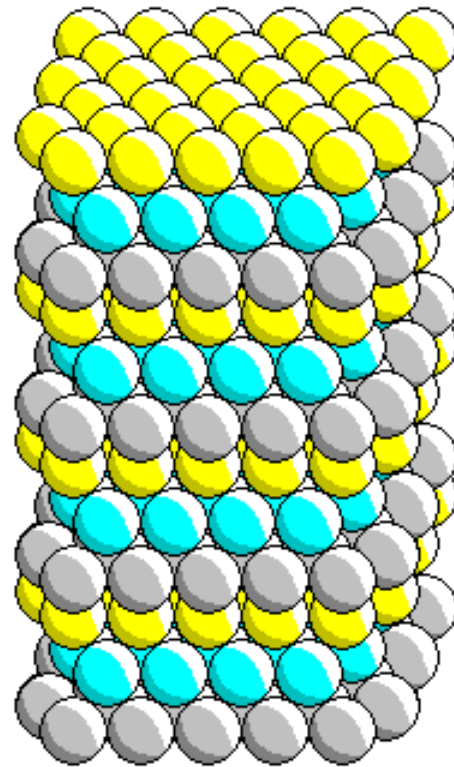
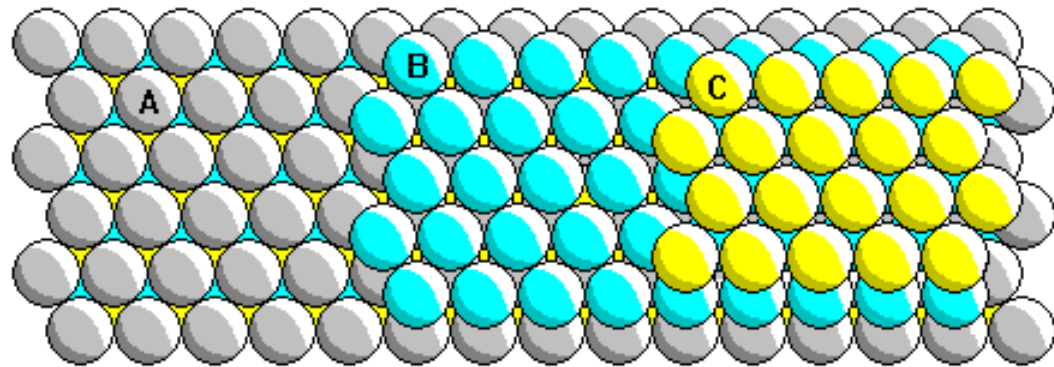


A
B
A
B
A
B
A
B
A
B
A

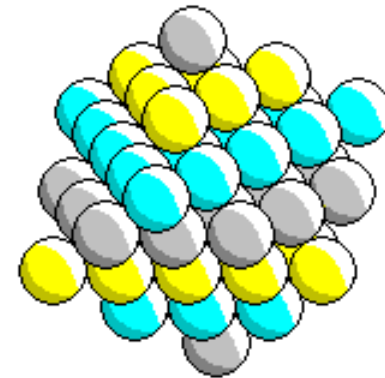


A
C
A
B
A
B
C
B
A
B
A

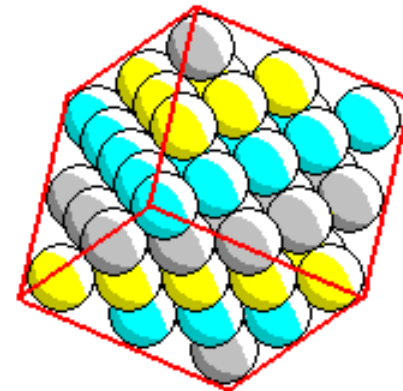
fcc structure

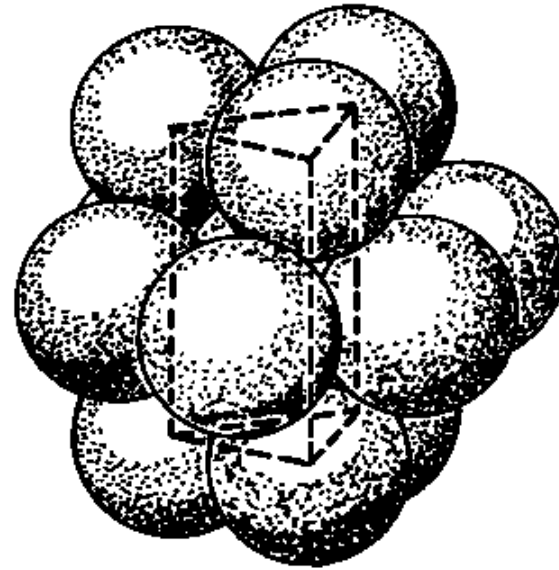


C
B
A
C
B
A
C
B
A
C
B
A



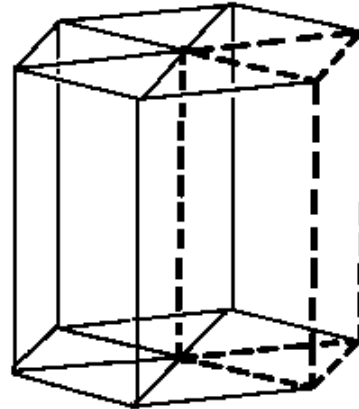
A
C
B
A
C
B
A
A
C
B
A
C
B
A



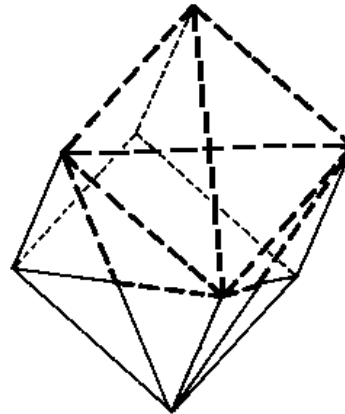
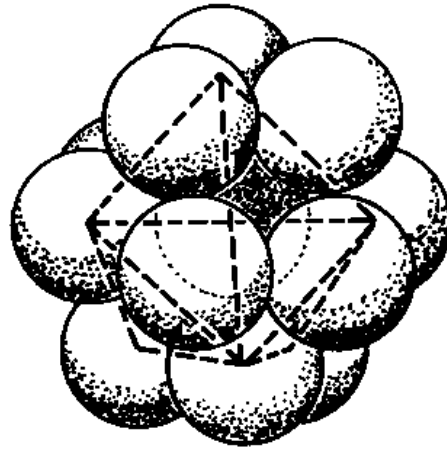


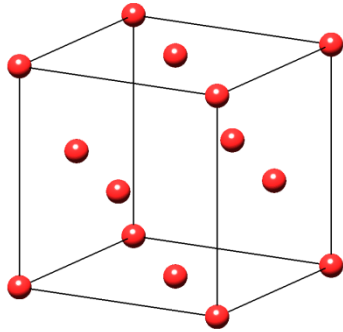
hcp stacking

$$\frac{c}{a} = \sqrt{\frac{8}{3}}$$

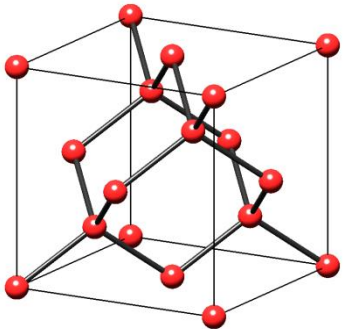


fcc stacking

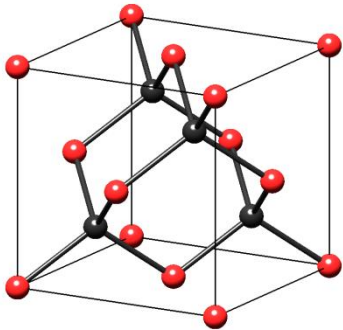




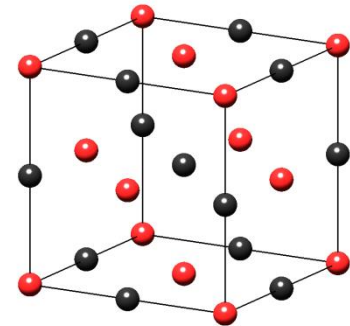
fcc primitive lattice, one atom in the lattice point (Al, for instance)

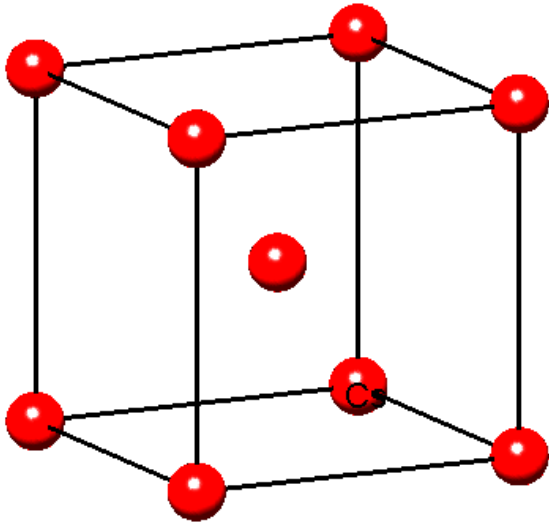


fcc primitive lattice, two identical atoms in the lattice point (Si, for instance)

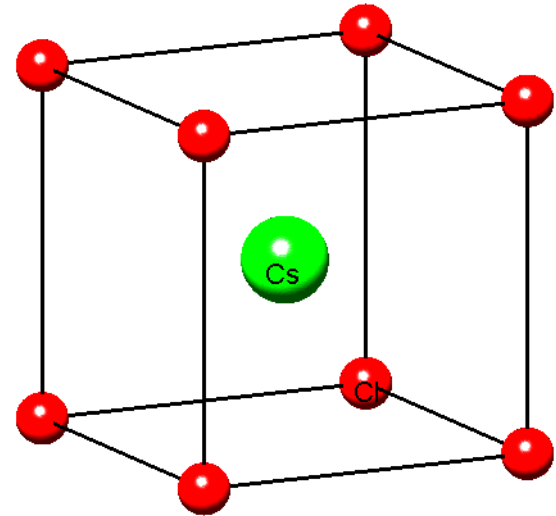


fcc primitive lattice, two different atoms in the lattice point (GaAs (left), NaCl (right))

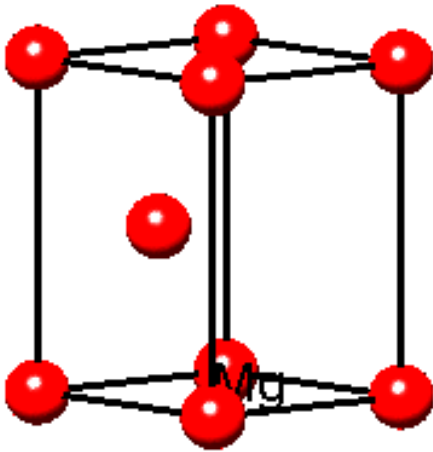




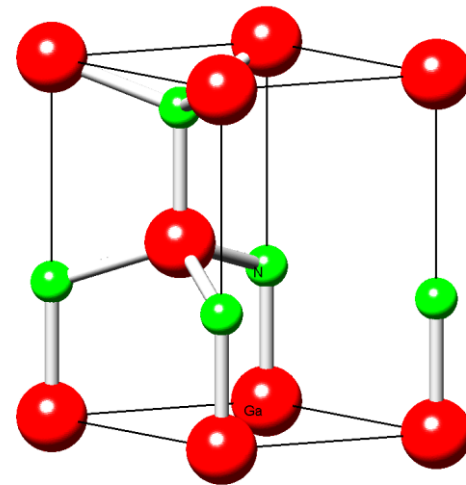
Cs (bcc lattice)



CsCl (simple cubic with a 2atom-base)

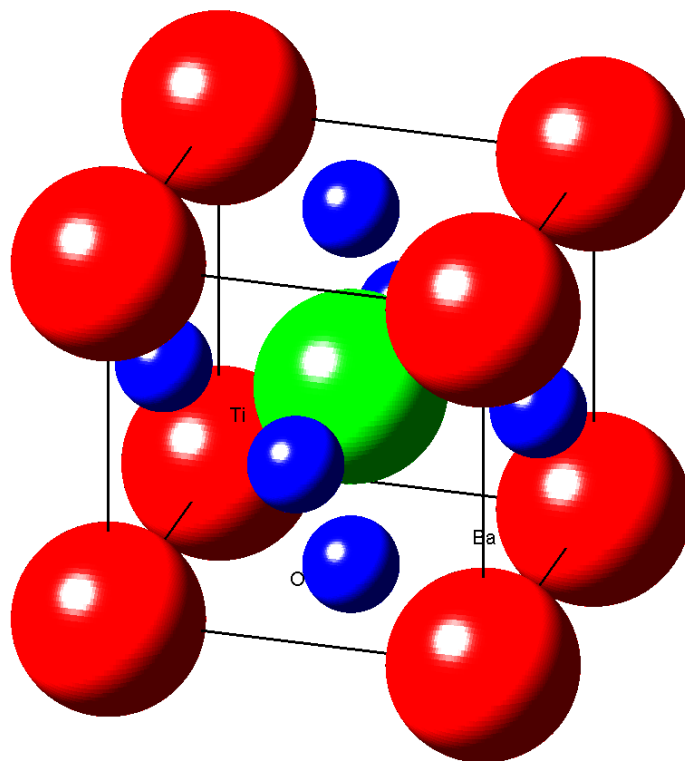


Mg (hcp lattice)

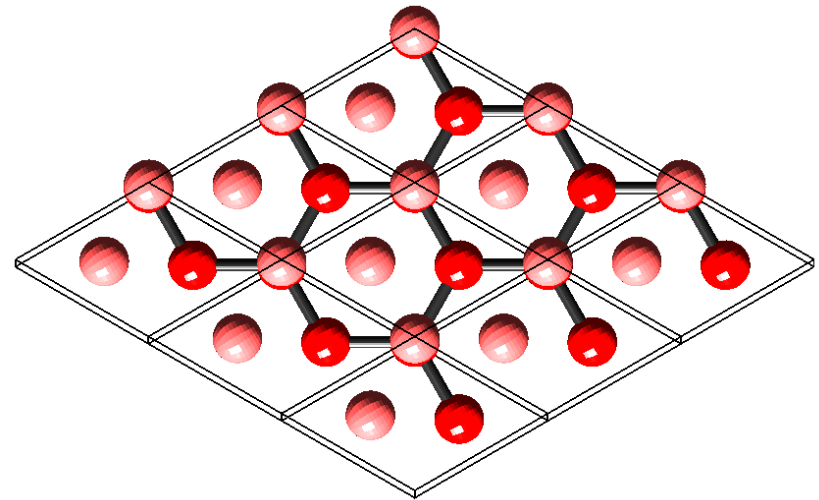
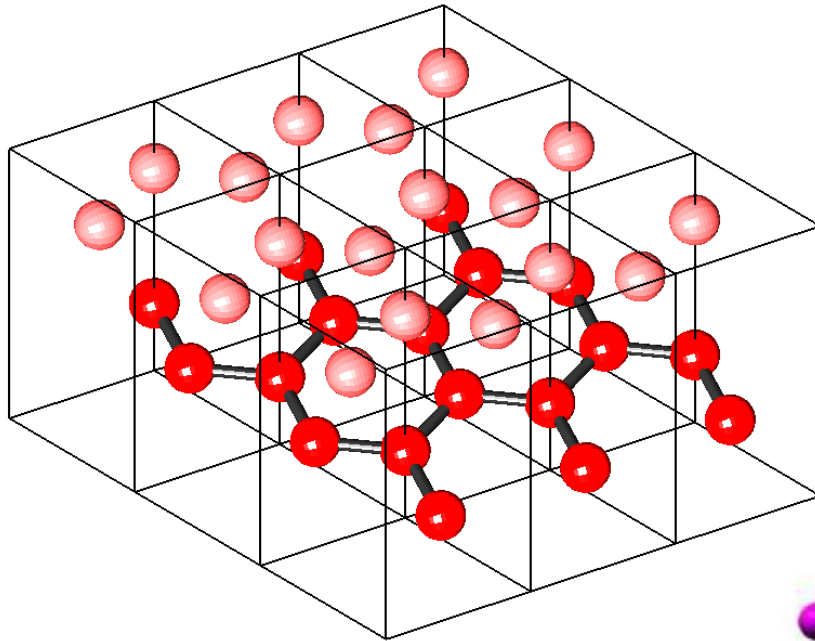


GaN (wurtzite = hcp with a 2atom base)

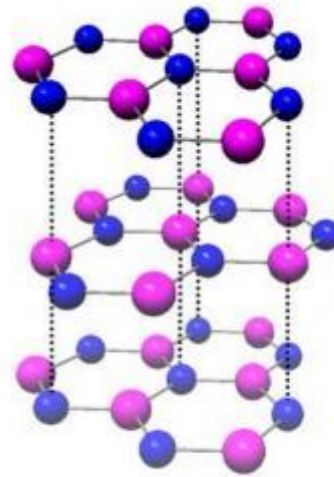
BaTiO₃ – perovskite structure (almost simple cubic)



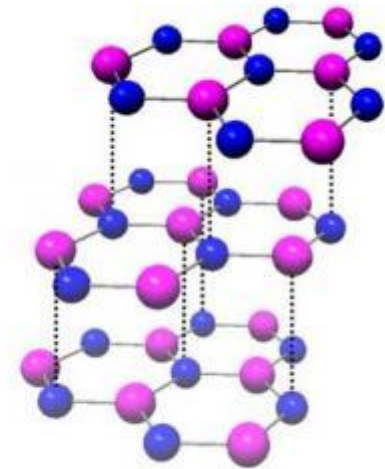
Graphite (graphene)



Bernal stacking (ABAB)

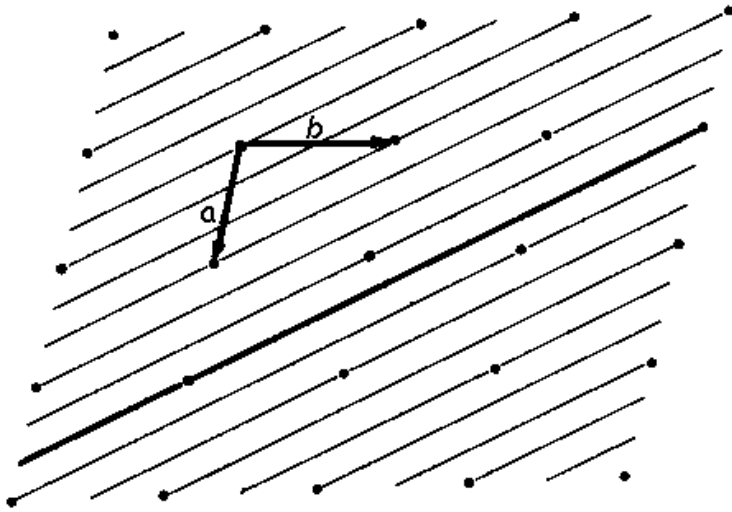


ABA



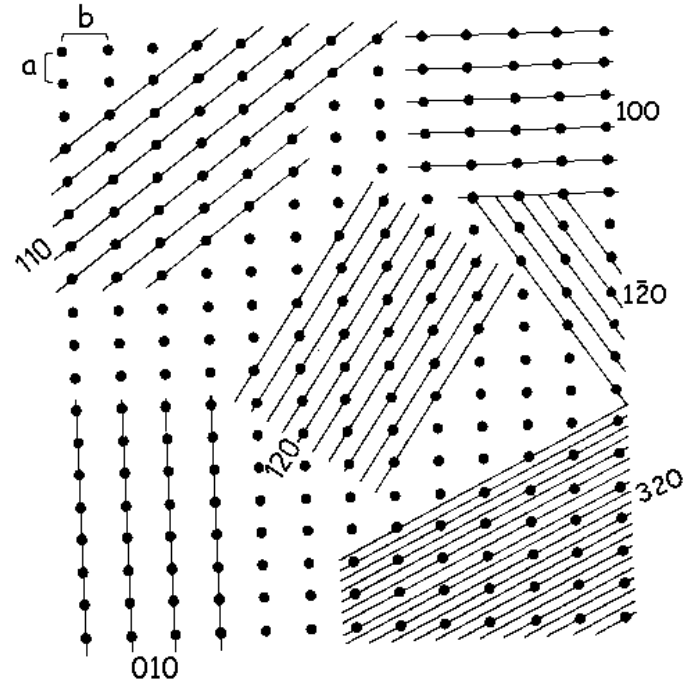
ABC

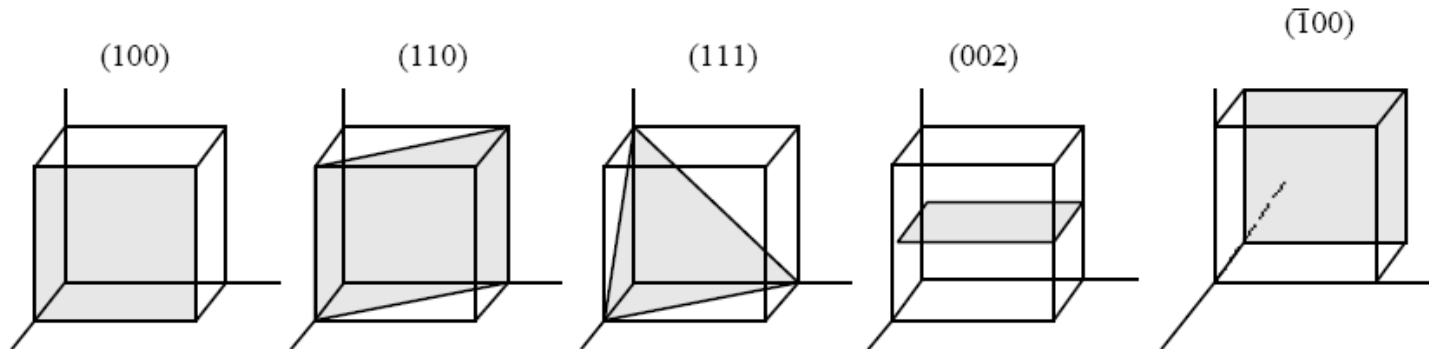
I.3. Crystallographic directions, crystallographic planes



$(hkl) \perp [hkl]$ only for cubic crystals!!!

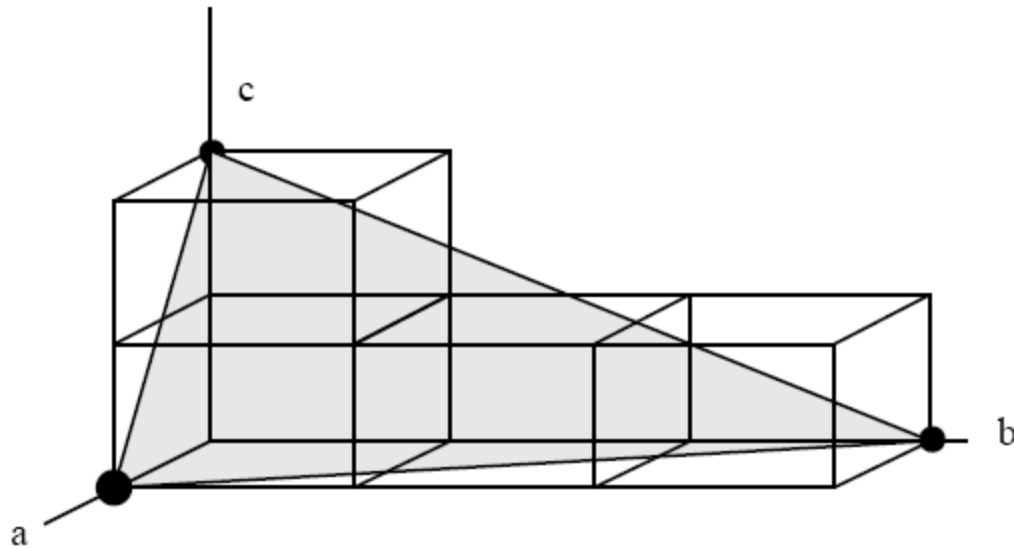
Miller indices





Note: (100) , $(\bar{1}00)$, (200) , (300) are parallel
 (111) , (222) , (333) are parallel
 (100) , (010) , (001) are orthogonal and in some crystal systems *may* be identical

Note: h, k and l are always integers



$$u'' = 1, v'' = 3, w'' = 2$$

$$h = 1/1 = 1$$

$$k = 1/3$$

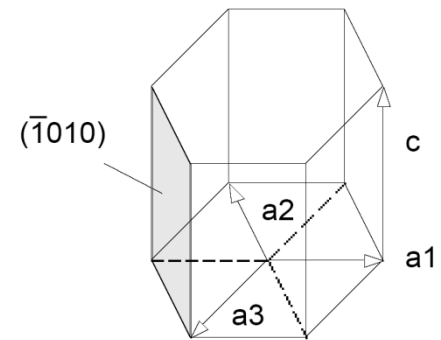
$$l = 1/2$$

$$(1 \ 1/3 \ 1/2) ?$$

Multiply by 6

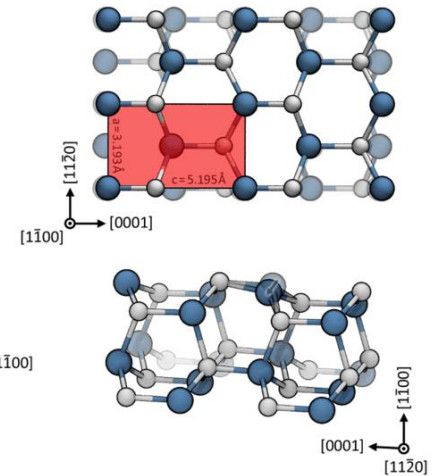
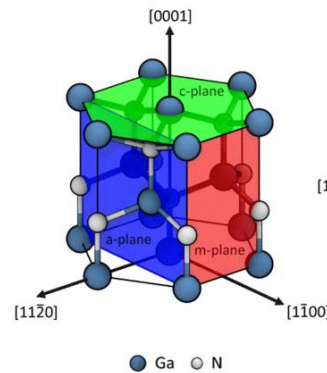
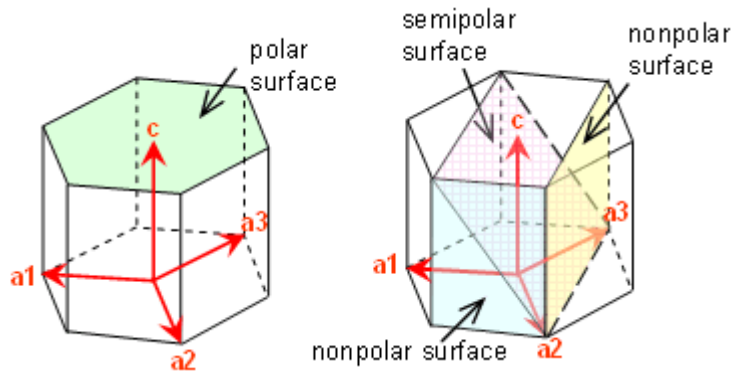
$$(623)$$

For hexagonal crystals, usually 4 Miller indices are used



The miller indices of crystallographic directions and planes are **always defined with respect to a simple lattice!!**

Example – GaN:



I.4. Reciprocal lattice

Reciprocal lattice is a primitive lattice, the basis vectors of which are

$$\mathbf{a}_i \cdot \mathbf{b}_j = 2\pi\delta_{ij}$$

$$\hat{\mathbf{A}} = \begin{pmatrix} a_{1x} & a_{1y} & a_{1z} \\ a_{2x} & a_{2y} & a_{2z} \\ a_{3x} & a_{3y} & a_{3z} \end{pmatrix}$$

$$\hat{\mathbf{B}} = 2\pi(\hat{\mathbf{A}}^{-1})^T$$

Properties:

- lattice reciprocal to a reciprocal lattice is the original lattice
- primitive lattice and its reciprocal lattice belong to the same syngony
- $(hkl) \perp [hkl]^*$ always!
- $V^* = 8\pi^3/V$
- the net plane distance $d_{hkl} = 2\pi/|h\mathbf{b}_1 + k\mathbf{b}_2 + l\mathbf{b}_3|$

A mathematical discursion – periodic functions in 3D

Periodic function in 3D primitive lattice

$$f(\mathbf{r}) = f(\mathbf{r} + \mathbf{R}), \mathbf{R} = n_1 \mathbf{a}_1 + n_2 \mathbf{a}_2 + n_3 \mathbf{a}_3, n_{1,2,3} \in \mathbb{Z}$$

can be expressed by a Fourier series in reciprocal lattice

$$f(\mathbf{r}) = \sum_{\mathbf{g}} f_{\mathbf{g}} e^{i\mathbf{g} \cdot \mathbf{r}}, f_{\mathbf{g}} = \frac{1}{V_c} \int_{V_c} d^3 \mathbf{r} f(\mathbf{r}) e^{-i\mathbf{g} \cdot \mathbf{r}}$$

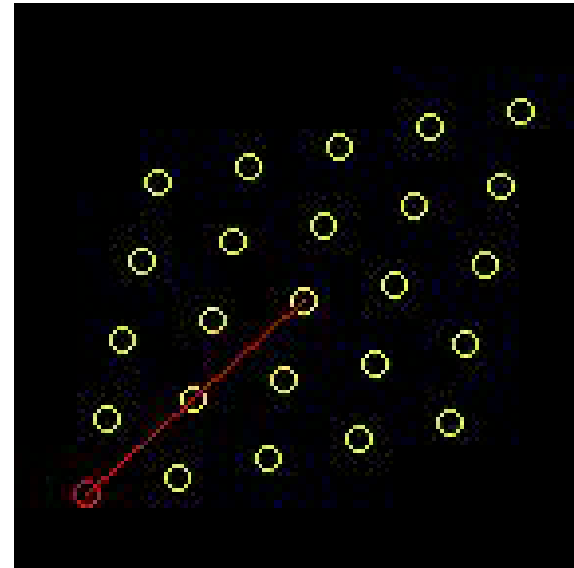
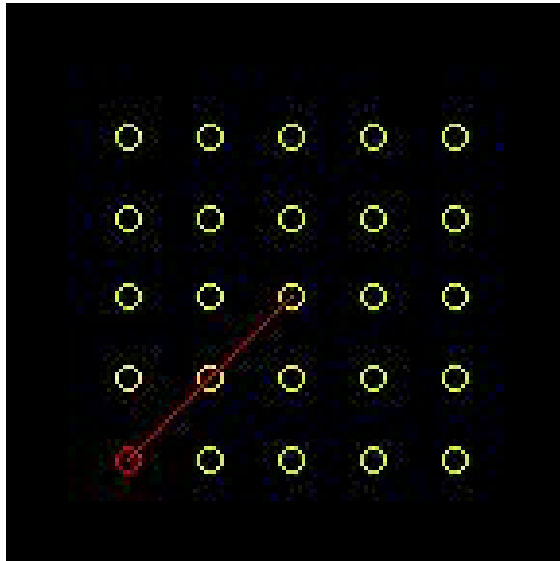
Special cases:

$$f(\mathbf{r}) = \sum_{\mathbf{R}} v(\mathbf{r} - \mathbf{R}), v \in L_2 \Rightarrow f_{\mathbf{g}} = \frac{1}{V_c} \int_{E_3} d^3 \mathbf{r} v(\mathbf{r}) e^{-i\mathbf{g} \cdot \mathbf{r}}$$

$$f(\mathbf{r}) = \sum_{\mathbf{R}} \delta^{(3)}(\mathbf{r} - \mathbf{R}) \Rightarrow f_{\mathbf{g}} = \frac{1}{V_c} \Rightarrow \sum_{\mathbf{g}} e^{i\mathbf{g} \cdot \mathbf{r}} = V_c \sum_{\mathbf{R}} \delta^{(3)}(\mathbf{r} - \mathbf{R})$$

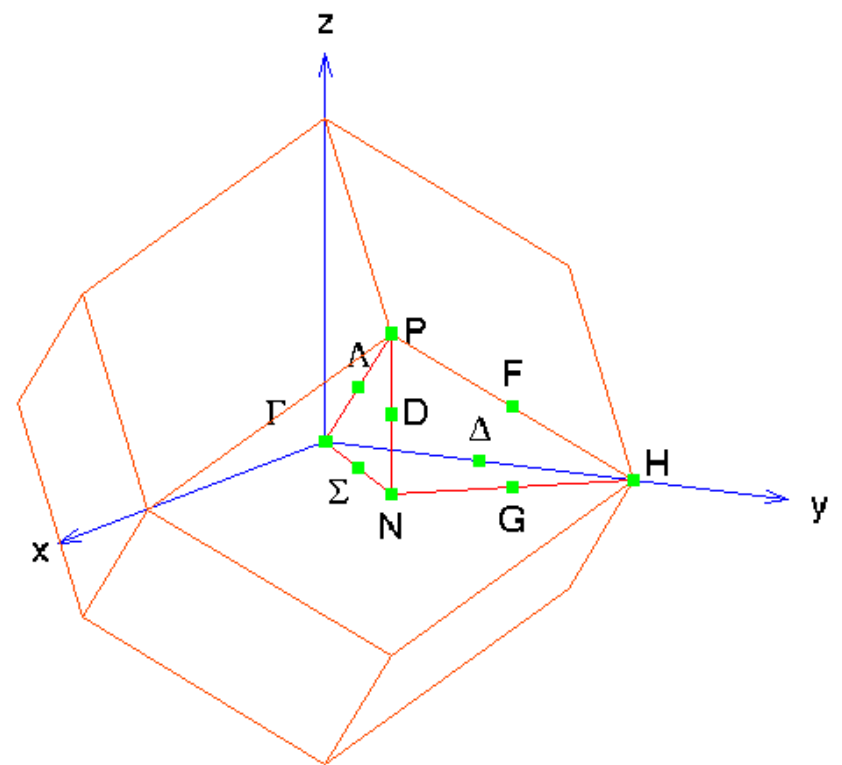
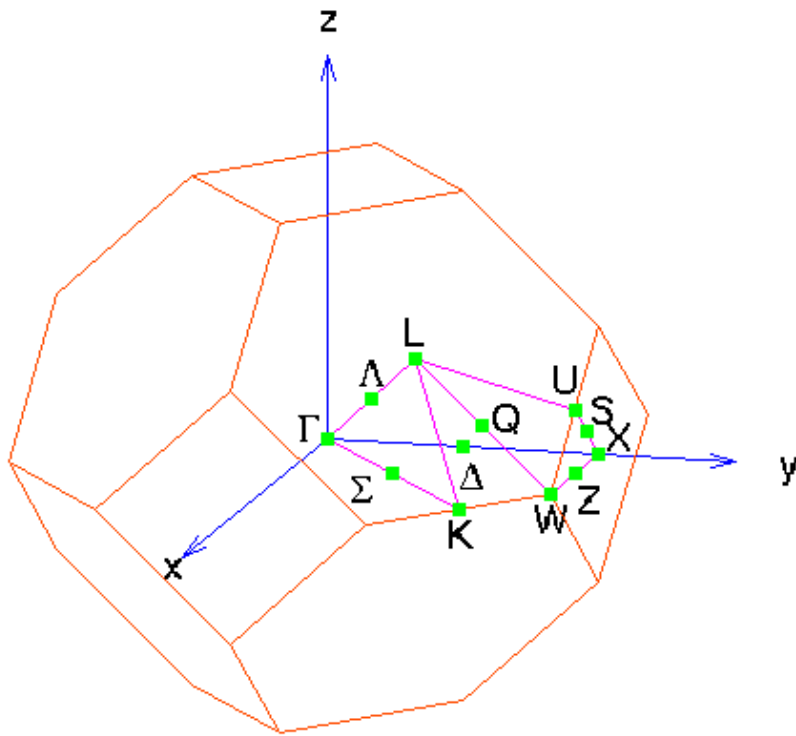
1.5. Brillouin zones

2D reciprocal lattices:



Reciprocal lattice to a fcc lattice, the 1st Brillouin zone

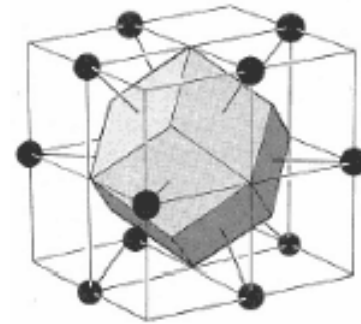
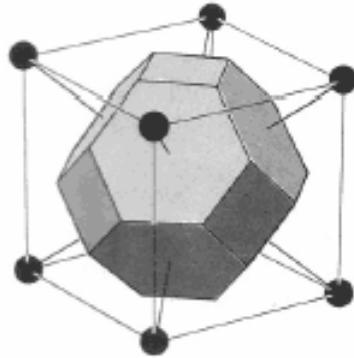
Reciprocal lattice to a bcc lattice, the 1st Brillouin zone



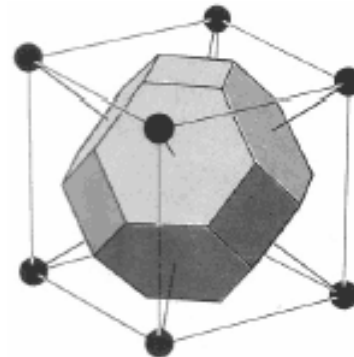
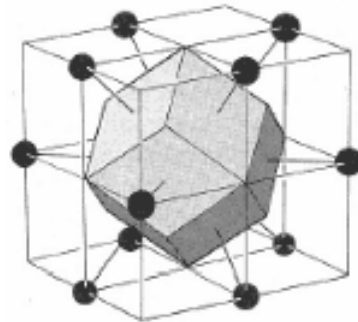
real space

reciprocal space

bcc

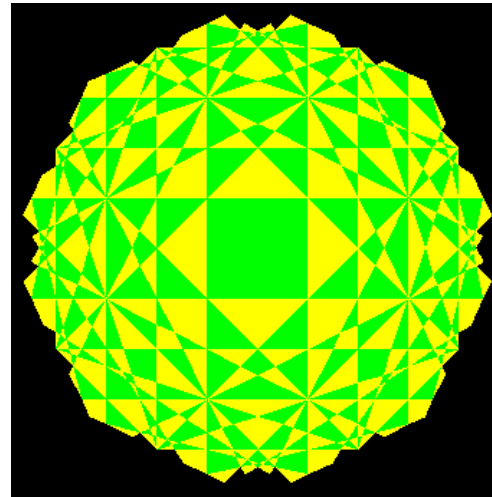


fcc

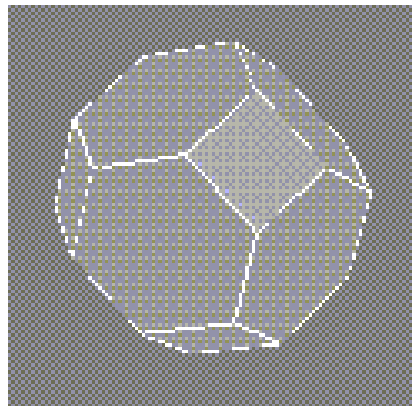


Higher Brillouin zones:

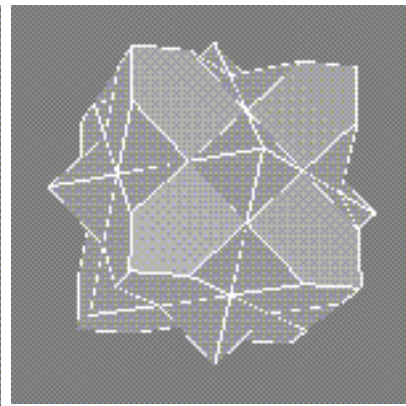
2D square lattice:



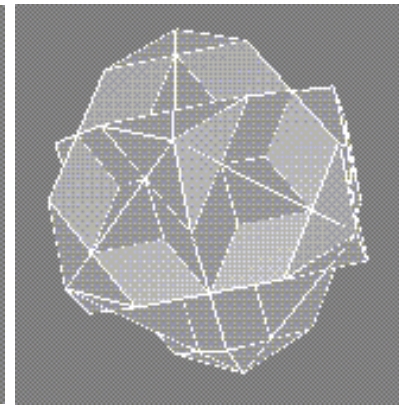
fcc lattice:



1st zone



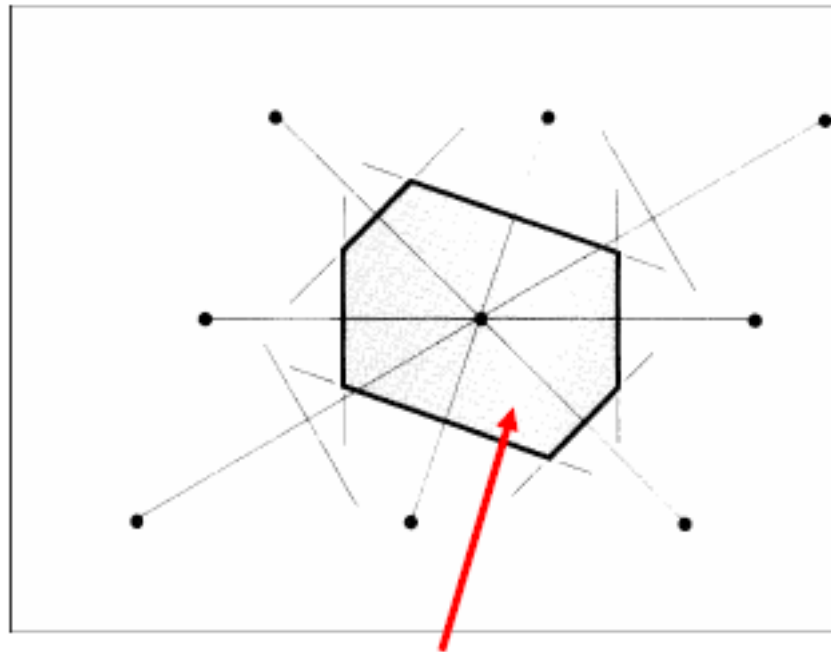
2nd zone



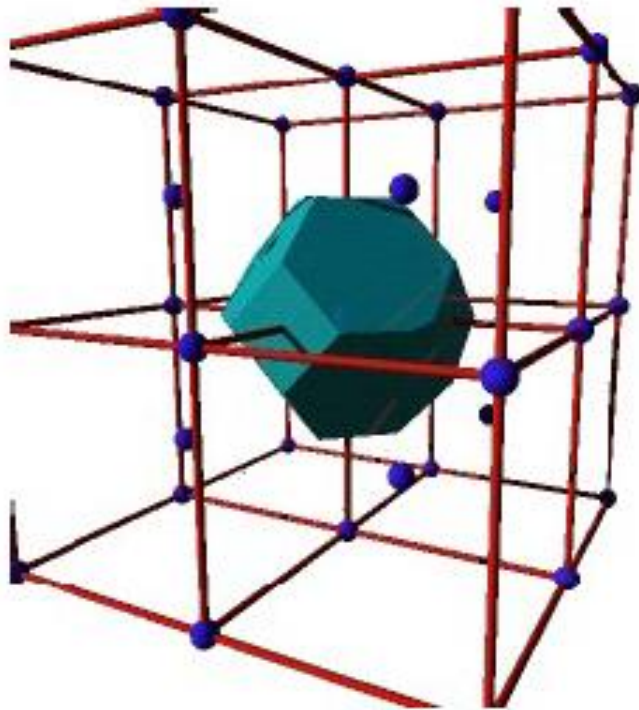
3rd zone

The Wigner-Seitz cell

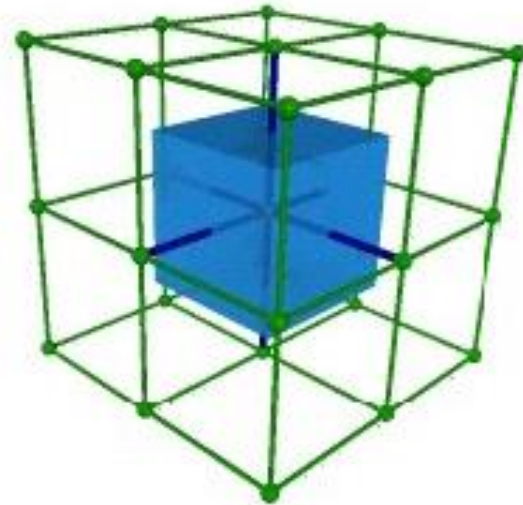
The 1st Brillouin zone is the Wigner-Seitz cell of the reciprocal lattice



Wigner-Seitz cell

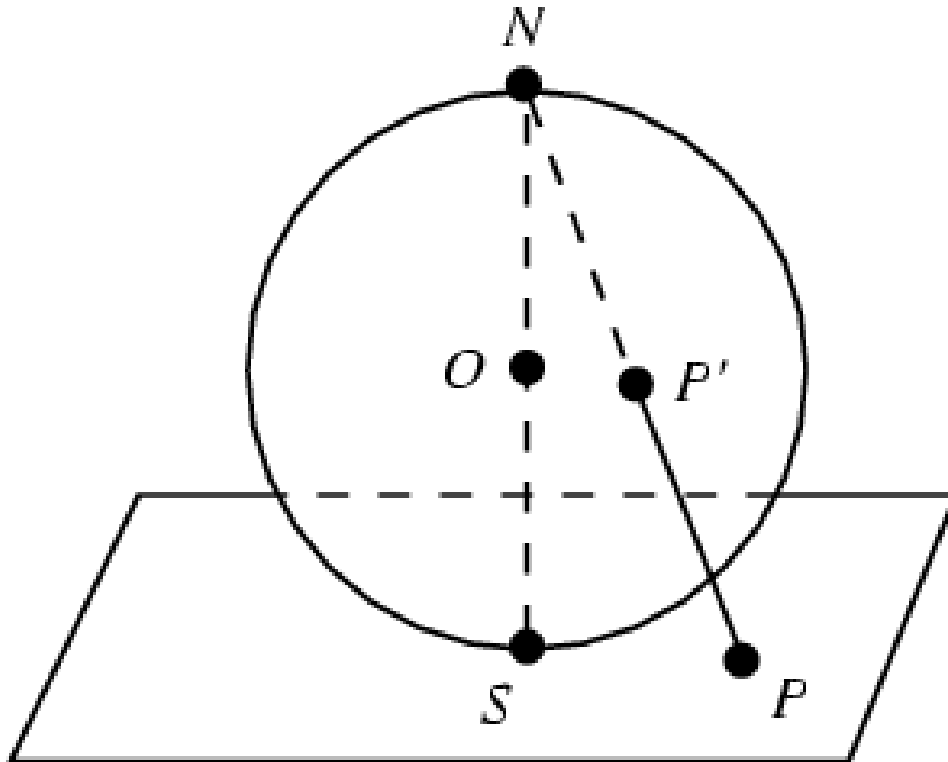


BCC lattice

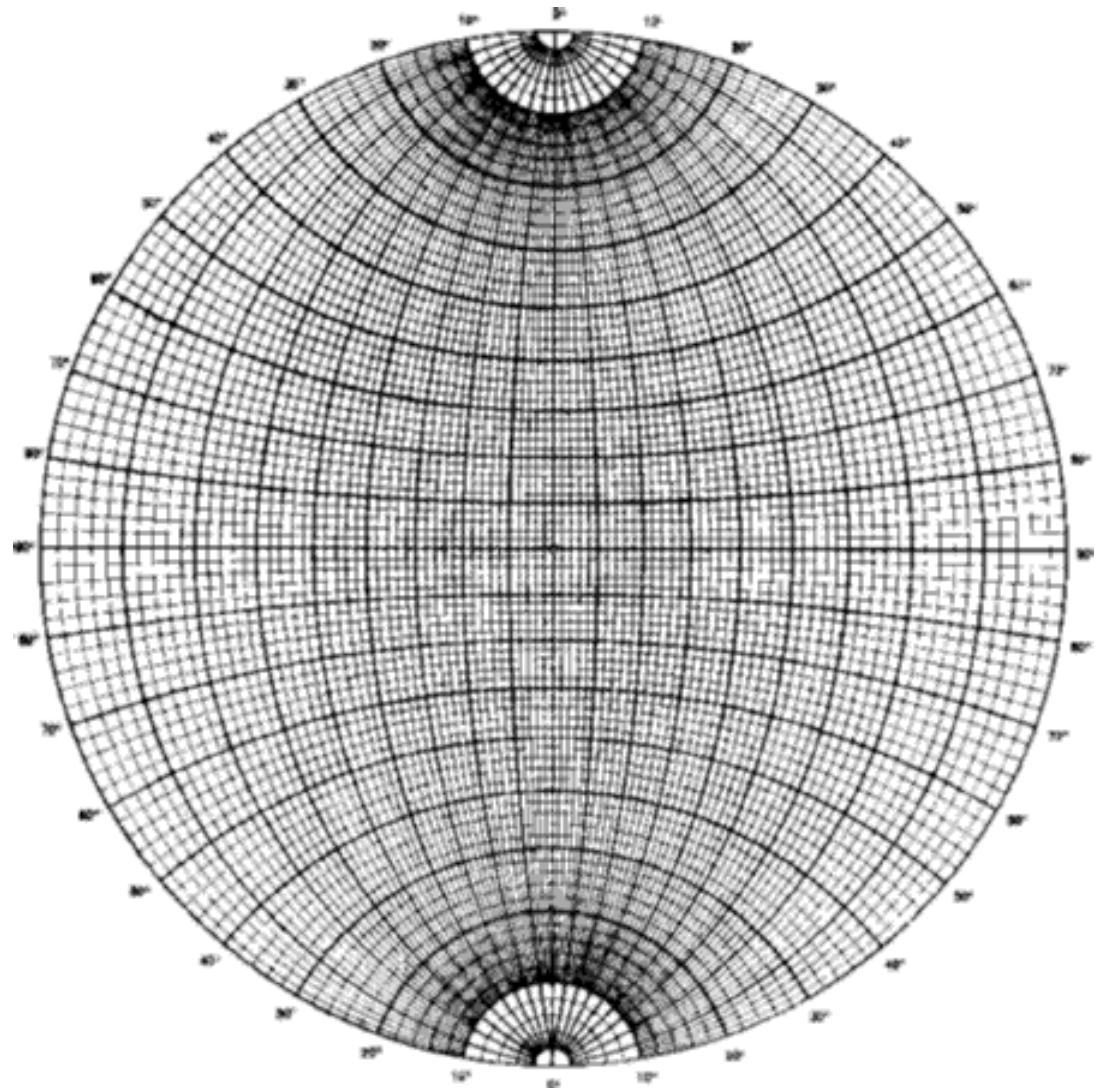


Simple cubic lattice

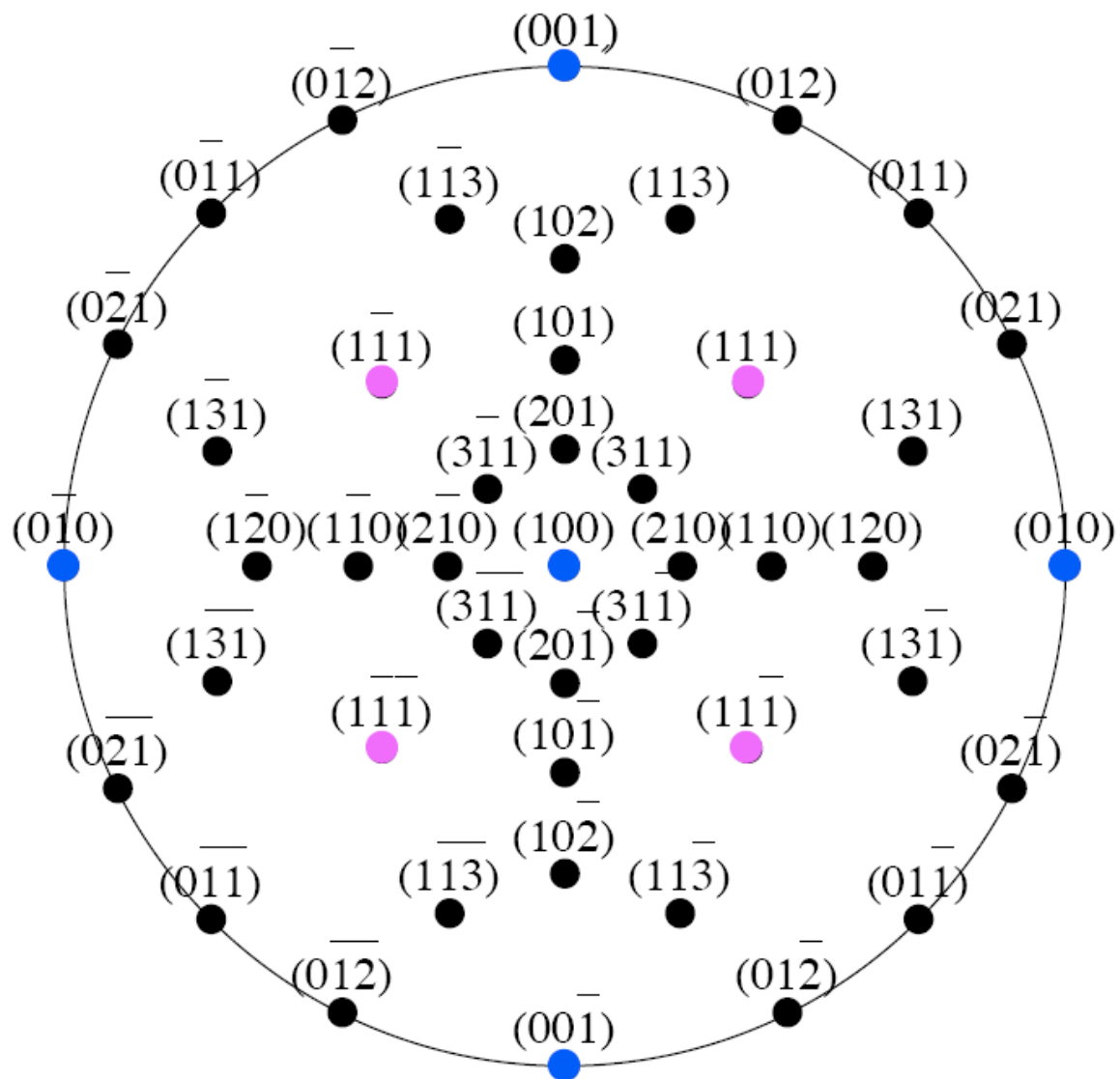
I.6. Stereographic projection



The Wulff chart



Standard projection of a cubic
crystal, surface (100)

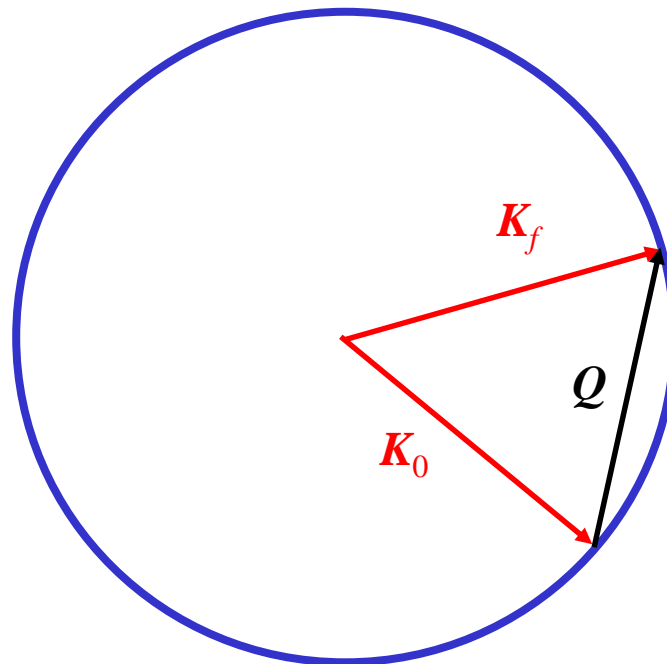


I.7. Elements of x-ray diffraction

Assumptions:

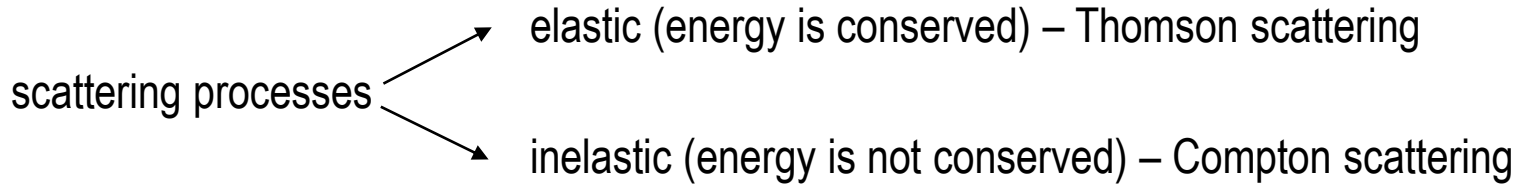
- elastic scattering $\Rightarrow \mathcal{E}_i = \mathcal{E}_f, |\mathbf{K}_i| = |\mathbf{K}_f|$
- kinematical scattering \Rightarrow 1st Born approximation
- far-field limit \Rightarrow Fraunhofer approximation:

$$\frac{e^{iK|\mathbf{R}-\mathbf{r}|}}{|\mathbf{R}-\mathbf{r}|} \approx \frac{e^{iK|\mathbf{R}|}}{|\mathbf{R}|} e^{-i\mathbf{K}_f \cdot \mathbf{r}}, \mathbf{K}_f = K \frac{\mathbf{R}}{|\mathbf{R}|}$$



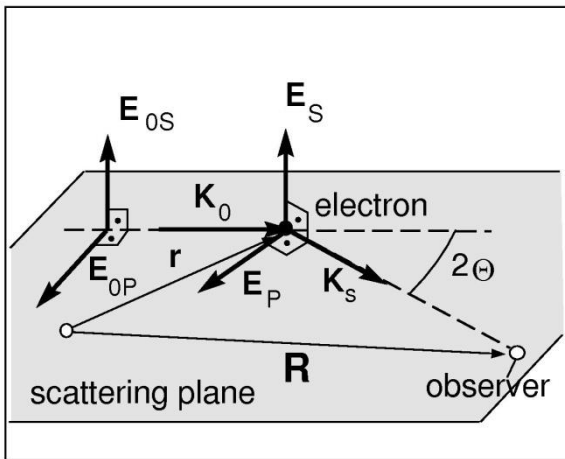
$$\mathbf{Q} = \mathbf{K}_f - \mathbf{K}_0$$

Scattering of x-rays by a free electron



From a quantum description it follows that scattering of x-rays from free electrons is **always inelastic**. Elastic scattering from a free electron exists only in a classical limit (classical electrodynamics)

Elastic (Thomson) scattering



The primary wave is plane and monochromatic:

$$\mathbf{E}_0(\mathbf{r}, t) = \mathbf{E}_0 e^{-i(\omega t - \mathbf{K}_0 \cdot \mathbf{r})}$$

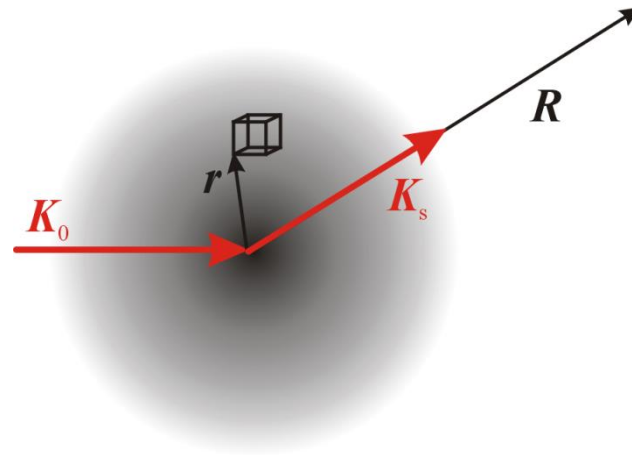
The scattered wave is spherical and monochromatic with the same frequency:

$$E(\mathbf{R}, t) = -\frac{r_{el}}{|\mathbf{R} - \mathbf{r}|} \sin \varphi [E_0(\mathbf{r}, t)]_{delayed}$$

$$E(\mathbf{R}, t) = -E_0 \frac{r_{el}}{|\mathbf{R} - \mathbf{r}|} \sin \varphi e^{-i(\omega t - \mathbf{K}_0 \cdot \mathbf{r})} e^{iK|\mathbf{R} - \mathbf{r}|}$$

$$\sin \varphi = C = \begin{cases} 1 & \text{in S polarization} \\ \cos 2\Theta & \text{in P polarization} \end{cases}$$

Scattering from a single atom



$$E(\mathbf{R}) = -E_0 C r_{el} \int d^3 \mathbf{r} \frac{\rho(\mathbf{r})}{|\mathbf{R} - \mathbf{r}|} e^{i\mathbf{K}_0 \cdot \mathbf{r}} e^{iK|\mathbf{R} - \mathbf{r}|} \approx -E_0 C r_{el} \frac{e^{iKR}}{R} \int d^3 \mathbf{r} \rho(\mathbf{r}) e^{i\mathbf{Q} \cdot \mathbf{r}}$$

Fourier transformation of the electron density of an atom – atomic form-factor

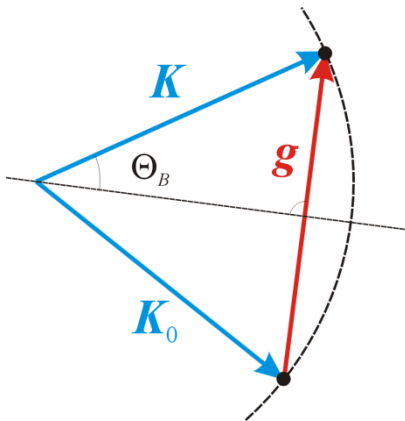
The scattered intensity is proportional to the Fourier transformation of the electron density:

$$E(\mathbf{Q}) = AE_0 \int d^3\mathbf{r} \rho(\mathbf{r}) e^{-i\mathbf{Q}\cdot\mathbf{r}}$$

$$\rho(\mathbf{r}) = \sum_{\mathbf{R}} \rho_c(\mathbf{r} - \mathbf{R}) \Omega(\mathbf{R})$$

$$E(\mathbf{Q}) = A \frac{E_0}{V_c} \underbrace{\rho_c^{FT}(\mathbf{Q})}_{\text{structure factor}} \underbrace{\sum_{\mathbf{g}} \Omega^{FT}(\mathbf{Q} - \mathbf{g})}_{\text{geometrical factor}}$$

Maximum of the geometrical factor is for $\mathbf{Q} = \mathbf{g}$



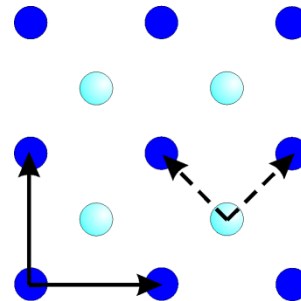
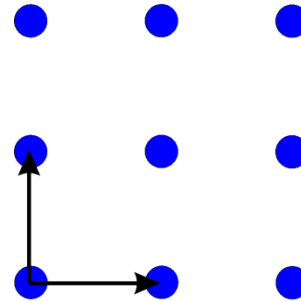
Bragg diffraction condition

$$|g| = 2K \sin \Theta_B \Rightarrow 2d_{hkl} \sin \Theta_B = \lambda$$

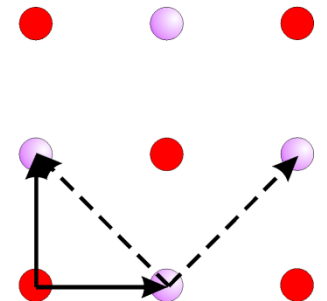
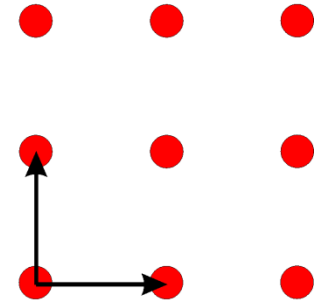
Structure factor of simple and centered 2D square lattices, forbidden diffractions

bravais.exe

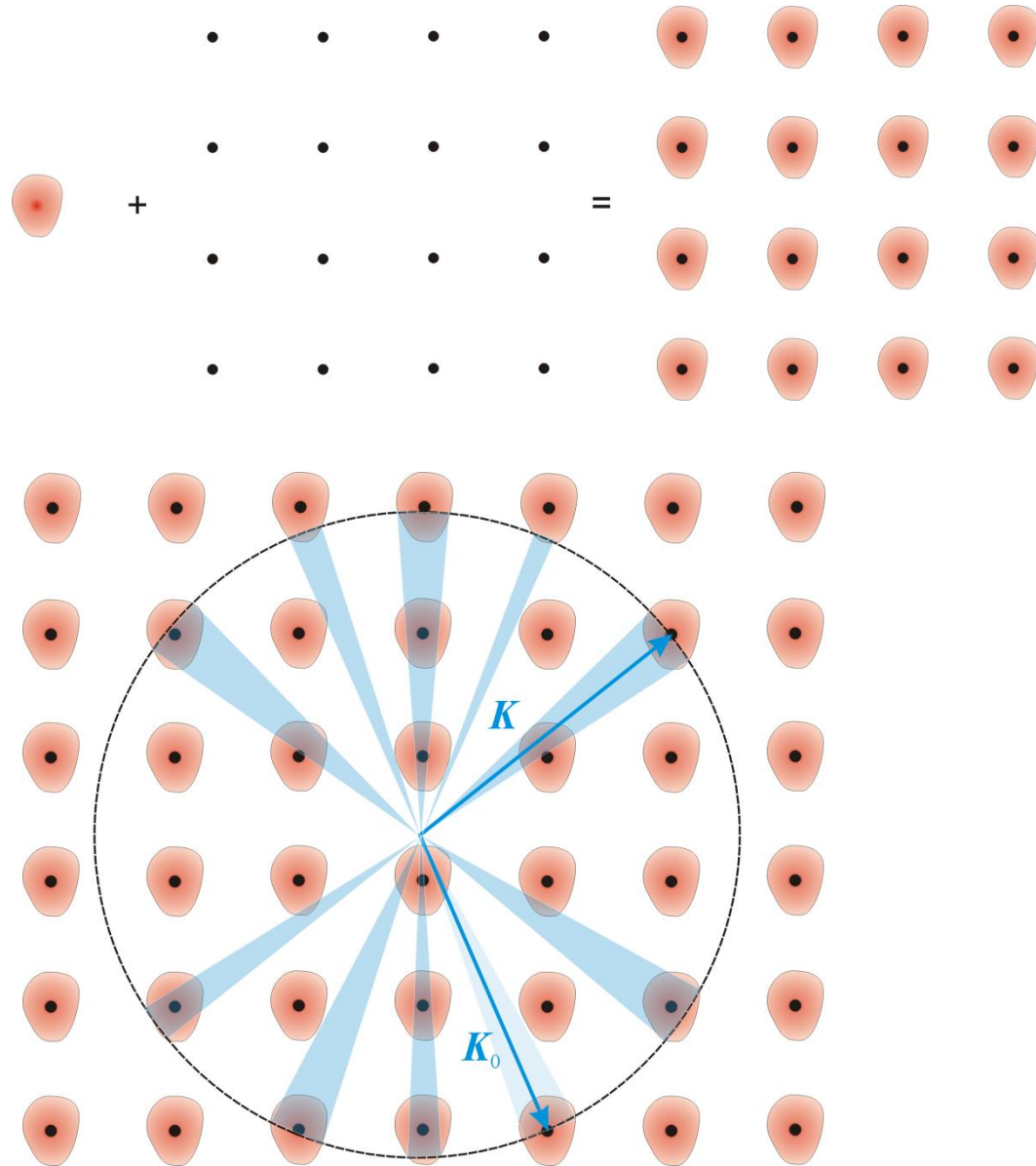
direct lattice



reciprocal lattice



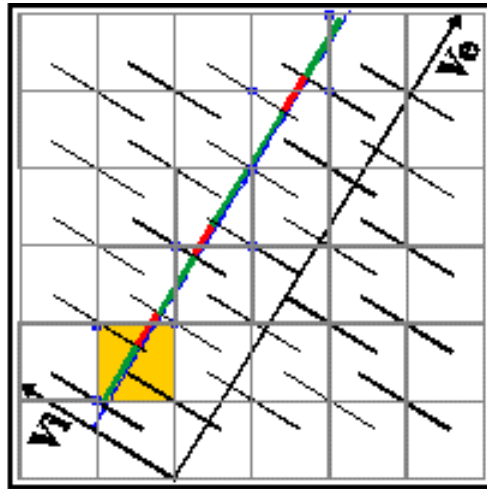
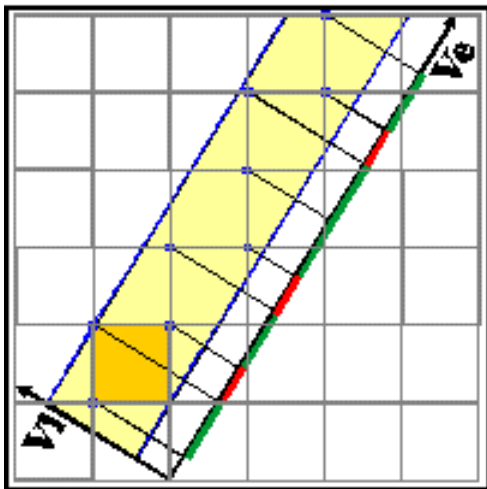
The Ewald construction



1.8 Quasicrystals

Structures with a perfect long-range order but no translational symmetry
Description projection from a 5 or 6-dimensional primitive lattice to 3D space

Example – 1D quasiperiodic Fibonacci chain



quasiperiodic sequence of L and S segments

<http://www.jcrystal.com/steffenweber/JAVA/jfibo/jfibo.html>

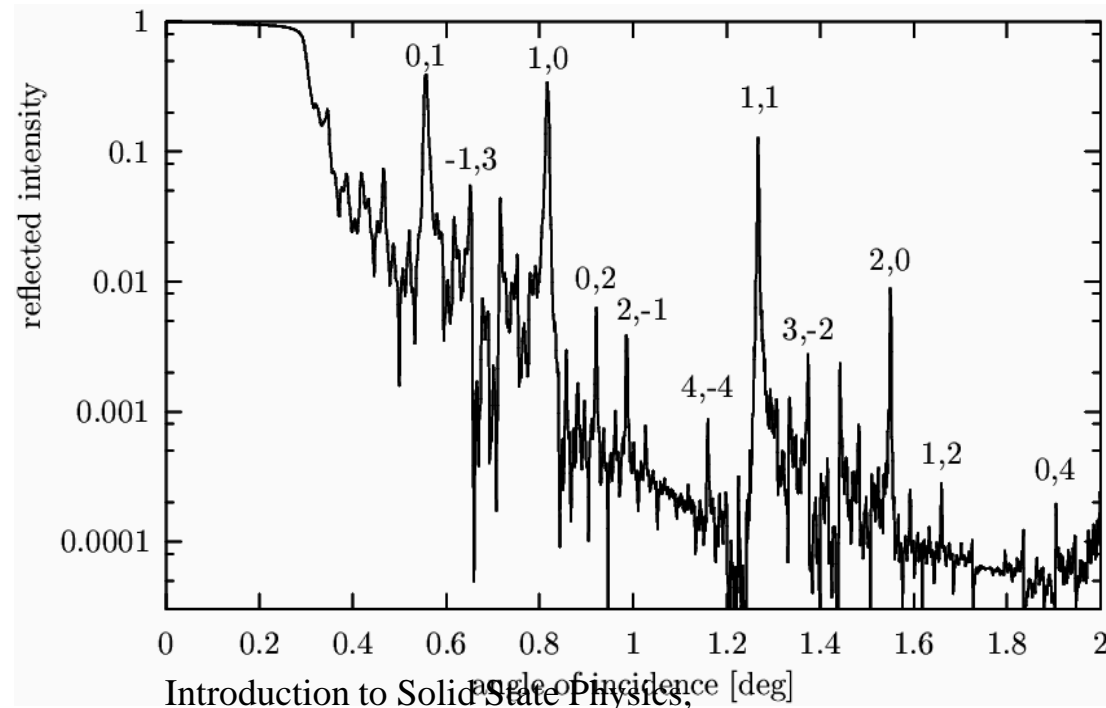
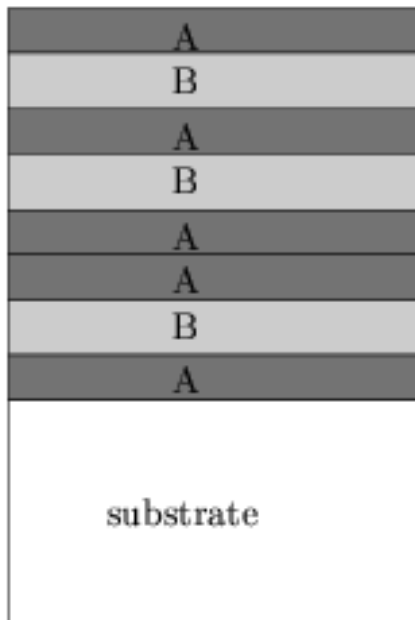
Fibonacci multilayer: F = ABAABABAABAAB...

Peak positions: the golden mean $\tau = \frac{\sqrt{5}-1}{2} \approx 0.618$

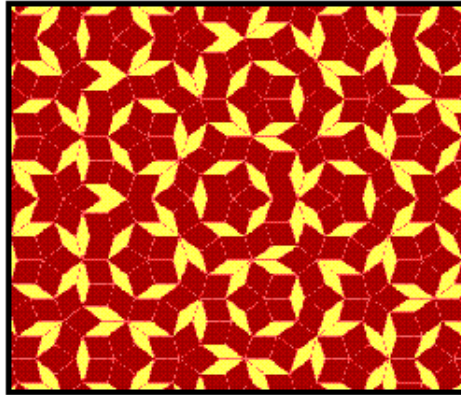
$$Q_{z,pq}^{\text{kinematical}} = \frac{2\pi}{t_A + \tau t_B} (p + q\tau) = \langle q_z \rangle_{pq}^{\text{(SRA)}}$$

Self-similarity: $(p + q\tau) \cdot \tau = p\tau + q\tau^2 = q + (p - q) \cdot \tau$

GaAs/AIAs Fibonacci multilayer (superlattice) structure and X-ray reflectivity



Penrose tilings

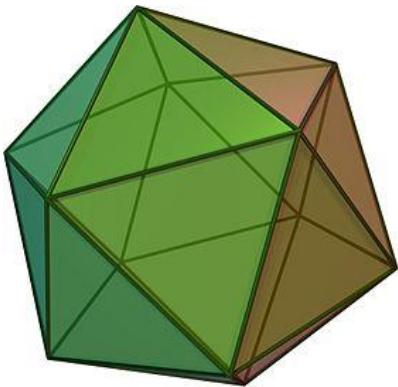


two types of tiles, no translational periodicity, selfsimilarity

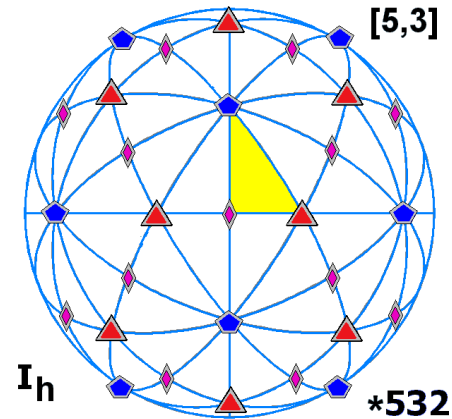
<http://www.jcrystal.com/steffenweber/JAVA/jtiling/jtiling.html>

Types of QCs:

- quasiperiodic in 2 dimensions (octagonal, decagonal, dodecagonal)
- quasiperiodic in 3 dimensions (icosahedral)
- incommensurately modulated structures



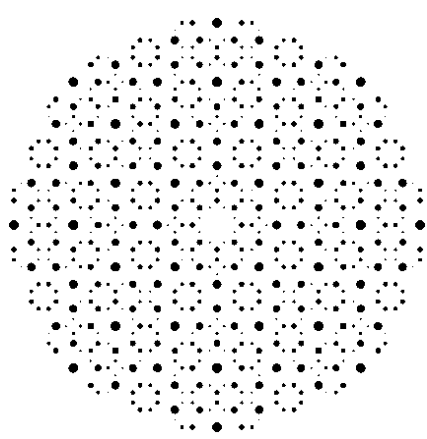
Icosahedral point group I_h



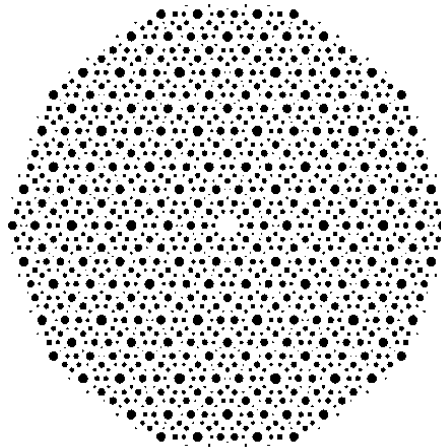
Regular icosahedron (dvacetistěn)

Public Domain, <https://commons.wikimedia.org/w/index.php?curid=642240>

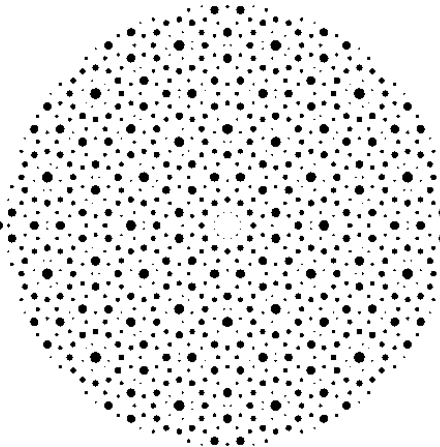
Fourier transformation of the atomic positions (x-ray diffraction)



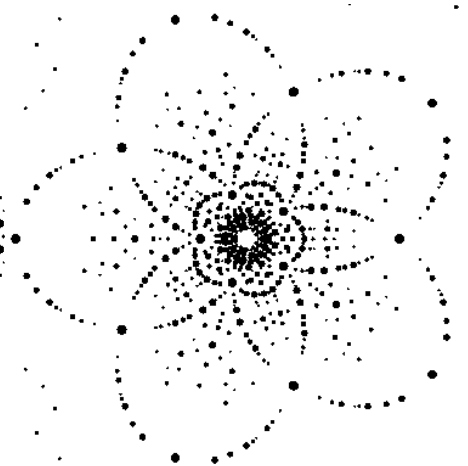
octagonal



decagonal

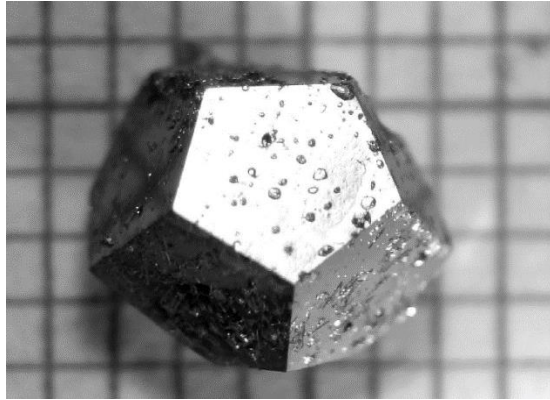


dodecagonal

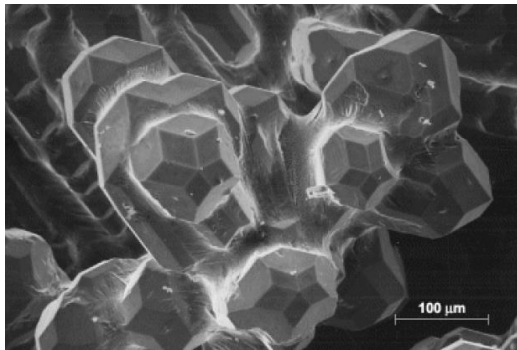


icosahedral

Examples of icosahedral quasicrystals



Single-grain sample of a quasicrystalline compound AlPdRe
<http://www.stanford.edu/group/fisher/research/quasicrystals.html>



Quasicrystal of an AlCuFe alloy displaying an external form consistent with their icosahedral symmetry
<http://www.answers.com/topic/quasicrystal>

The electron density can be expressed as the Fourier sum:

$$\rho(\mathbf{r}) = \frac{1}{V_c} \sum_{\mathbf{g}} \rho_{\mathbf{g}} e^{i\mathbf{g}\cdot\mathbf{r}}$$

In a usual crystal:

$$\mathbf{g} = g_1 \mathbf{b}_1 + g_2 \mathbf{b}_2 + g_3 \mathbf{b}_3, \quad g_{1,2,3} \in \mathbb{N}$$

In an icosahedral quasicrystal:

$$\tilde{\mathbf{g}} = \sum_{n=1}^6 g_n \tilde{\mathbf{b}}_n, \quad g_n \in \mathbb{N}, \quad \tilde{\mathbf{g}}, \tilde{\mathbf{b}}_n \in E_6^*$$

\mathbf{g} is obtained from $\tilde{\mathbf{g}}$ by projection into E_3^* , all possible \mathbf{g} 's fill densely the reciprocal space E_3^*

III. RESPONSE OF A CONDENSED BODY TO AN EXTERNAL IMPULSE

III.1. General description – Kramers Kronig relation

External force: $F(t)$ (we neglect the space variables, we assume a scalar force)

Reaction of the system: $x(t)$

We assume a linear response:

$$x(t) = \int_{-\infty}^t dt' \alpha(t - t') F(t') = \int_{-\infty}^{\infty} dt' \alpha(t - t') F(t') \text{ if } \alpha(\tau) = 0 \text{ for } \tau < 0$$

After Fourier transformation

$$x(\omega) = \alpha(\omega) F(\omega)$$

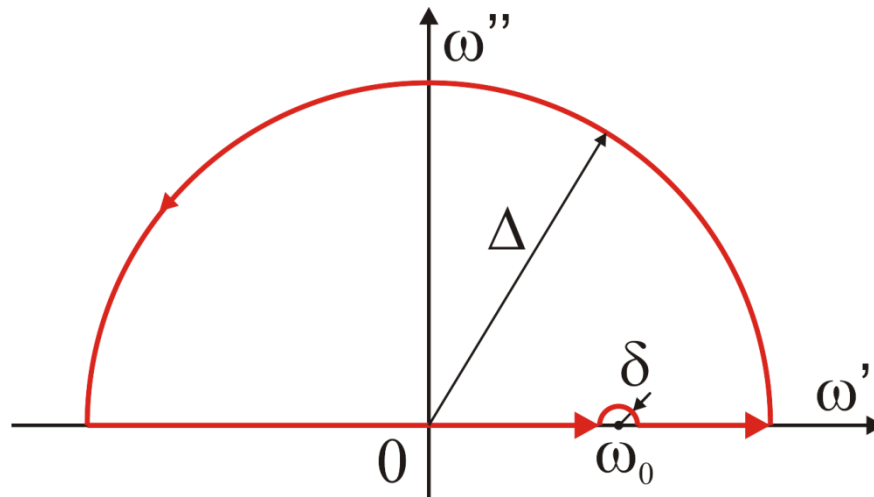
The functions $x(t)$, $F(t)$ are real, function $\alpha(\omega)$ is a complex function of a complex variable ω :

$$\alpha(\omega) = \int_0^{\infty} dt \alpha(t) e^{i\omega' t} e^{-\omega'' t}, \omega = \omega' + i\omega''$$

$\alpha(\omega)$ is analytic for $\omega'' \geq 0$. The singularities of $\alpha(\omega)$ exist only in the lower half-plane $\omega < 0$. Let us consider the function

$$\frac{\alpha(\omega)}{\omega - \omega_0}$$

This function is analytic in the upper half-plane except for $\omega = \omega_0$, where it has a singularity. Let us integrate this function over a closed loop



Inside this loop, the function is analytic, thus the integral is zero:

$$0 = \oint d\omega \frac{\alpha(\omega)}{\omega - \omega_0} = \int_{-\Delta}^{\omega_0 - \delta} d\omega \frac{\alpha(\omega)}{\omega - \omega_0} + i \int_{\pi}^0 d\varphi \alpha(\omega_0 + \delta e^{i\varphi}) + \int_{\omega_0 + \delta}^{\Delta} d\omega \frac{\alpha(\omega)}{\omega - \omega_0} + i \int_0^{\pi} d\varphi \alpha(\omega_0 + \Delta e^{i\varphi})$$

Now we perform the limits $\lim_{\delta \rightarrow 0^+} \lim_{\Delta \rightarrow +\infty}$ and we obtain

$$i\pi\alpha(\omega_0) = P \int_{-\infty}^{\infty} d\omega \frac{\alpha(\omega)}{\omega - \omega_0} = \lim_{\delta \rightarrow 0^+} \left[\int_{-\infty}^{\omega_0 - \delta} d\omega \frac{\alpha(\omega)}{\omega - \omega_0} + \int_{\omega_0 + \delta}^{\infty} d\omega \frac{\alpha(\omega)}{\omega - \omega_0} \right]$$

The Kramers-Kronig relations are

$$\alpha'(\omega_0) = \frac{1}{\pi} P \int_{-\infty}^{\infty} d\omega \frac{\alpha''(\omega)}{\omega - \omega_0}, \alpha''(\omega_0) = -\frac{1}{\pi} P \int_{-\infty}^{\infty} d\omega \frac{\alpha'(\omega)}{\omega - \omega_0}$$

Example: orientation polarization

$$\alpha(\omega) = \frac{\alpha_0}{1 - i\omega\tau} \Rightarrow \alpha'(\omega) = \frac{\alpha_0}{1 + (\omega\tau)^2}, \alpha''(\omega) = \frac{\omega\tau\alpha_0}{1 + (\omega\tau)^2}$$

singularity in $\omega = -i/\tau$

Example: atomic polarization

$$\alpha(\omega) = \frac{Ze^2}{m(\omega_0^2 - \omega^2 - i\gamma\omega)} \Rightarrow$$
$$\alpha'(\omega) = \frac{Ze^2(\omega_0^2 - \omega^2)}{m[(\omega_0^2 - \omega^2)^2 + (\gamma\omega)^2]}, \alpha''(\omega) = \frac{Ze^2\gamma\omega}{m[(\omega_0^2 - \omega^2)^2 + (\gamma\omega)^2]}$$

Singularities in $\omega = -i\frac{\gamma}{2} \pm \sqrt{\omega_0^2 - \left(\frac{\gamma}{2}\right)^2}$

III.2. Response to an electric field

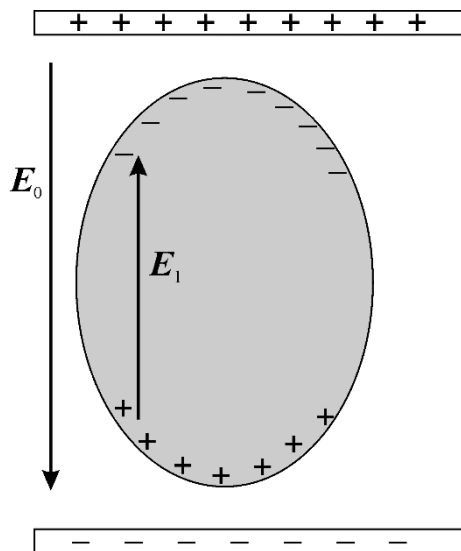
Summary of basic quantities

Polarization $\mathbf{P} = \frac{1}{V} \sum_j \mathbf{p}_j = \epsilon_0 \chi \mathbf{E}$

\mathbf{E} is the macroscopic field in the sample

Relative permittivity (dielectric constant) $\epsilon = 1 + \chi$

The connection of \mathbf{E} with the external field \mathbf{E}_0 :



$$\mathbf{E} = \mathbf{E}_0 + \mathbf{E}_1$$

$$E_{1j} = \frac{1}{\epsilon_0} N_{jk} P_k, j, k = x, y, z$$

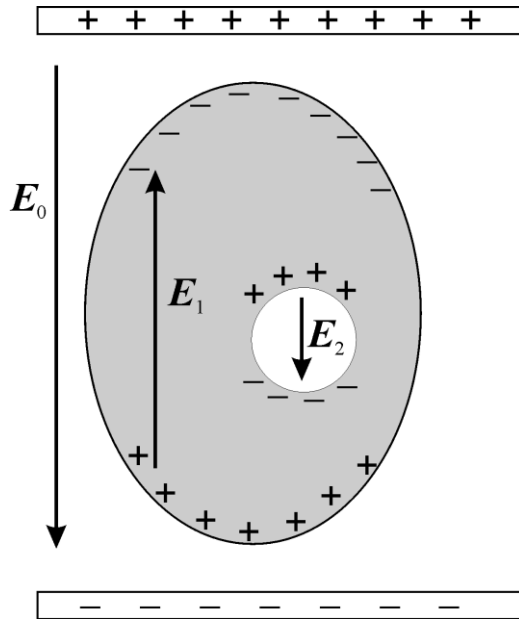
Depolarization factors:

sphere: $N_{jk} = -\frac{1}{3} \delta_{jk}$

flat disc: $\hat{\mathbf{N}} = \begin{pmatrix} -1 & 0 & 0 \\ 0 & 0 & 0 \\ 0 & 0 & 0 \end{pmatrix}$

The local field acting on an atom \mathbf{E}_L : $\mathbf{p} = \alpha \mathbf{E}_L$

The Lorentz formula for the local field:



$$\mathbf{E}_L = \mathbf{E}_0 + \mathbf{E}_1 + \mathbf{E}_2 + \mathbf{E}_3$$

$$\mathbf{E}_3 = 0 \text{ (symmetry)}, \mathbf{E}_2 = \frac{\mathbf{P}}{3\epsilon_0}$$

$$\mathbf{E}_L = \mathbf{E} + \frac{\mathbf{P}}{3\epsilon_0}$$

The Clausius-Mossotti relation (called Lorentz-Lorenz formula if we replace $\epsilon(\omega)$ by $n^2(\omega)$) [Ludvig Lorentz, Hendrik Lorentz]

$$\frac{\epsilon - 1}{\epsilon + 2} = \alpha \frac{N}{3\epsilon_0}$$

Electric displacement $\mathbf{D} = \epsilon_0 \mathbf{E} + \mathbf{P} = \epsilon \epsilon_0 \mathbf{E}$

Polarizability α is a microscopic quantity. Its value depends on the polarization mechanism.

Possible polarization mechanisms:

1. Orientation polarization
2. Ionic (displacement) polarization
3. Atomic polarization

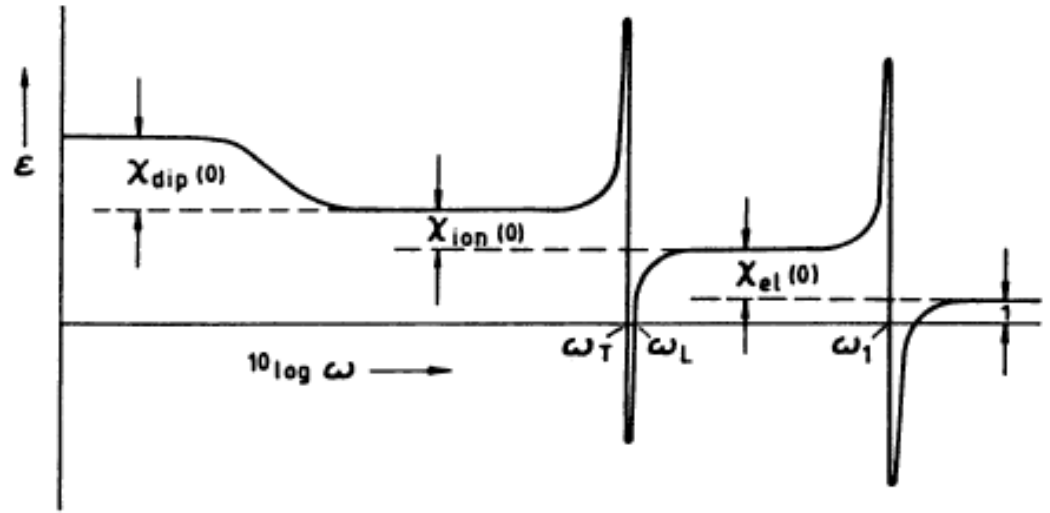
Orientation polarization

Orientation of **permanent** electric moments in an external field. Let us assume that a molecule has a permanent dipole moment \mathbf{p} . The interaction energy with the local field \mathbf{E}_L is

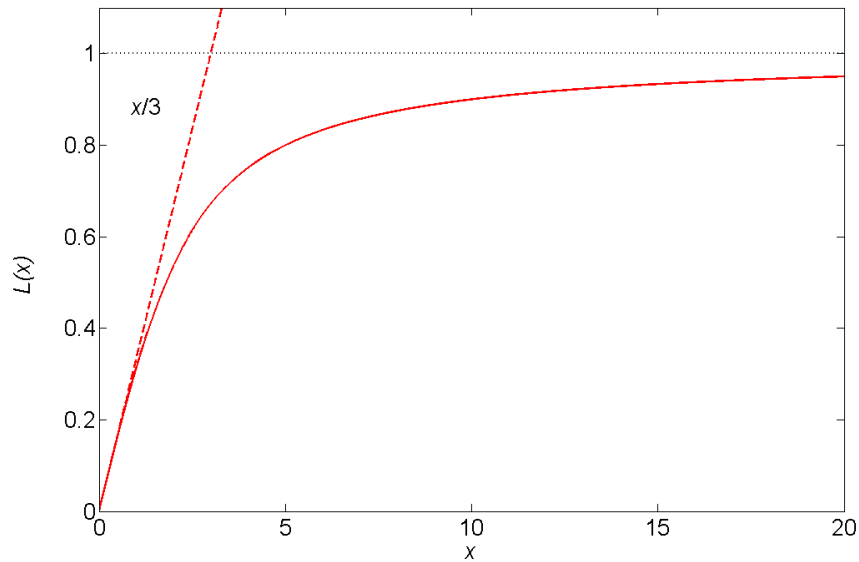
$$\mathcal{E} = -\mathbf{p} \cdot \mathbf{E}_L$$

Let us consider a system of non-interacting permanent dipoles. The mean value of the component of \mathbf{p} parallel to \mathbf{E}_L is

$$\langle p_{\parallel} \rangle = \frac{\int d^2\mathbf{p}^0 p_{\parallel} e^{p_{\parallel} E_L / (k_B T)}}{\int d^2\mathbf{p}^0 e^{p_{\parallel} E_L / (k_B T)}} = \frac{\int_0^{2\pi} d\varphi \int_0^{\pi} d\vartheta \sin \vartheta p \cos \vartheta e^{p_{\parallel} E_L \cos \vartheta / (k_B T)}}{\int_0^{2\pi} d\varphi \int_0^{\pi} d\vartheta \sin \vartheta e^{p_{\parallel} E_L \cos \vartheta / (k_B T)}} = p \mathcal{L} \left(\frac{p E_L}{k_B T} \right)$$



where $\mathcal{L}(x) = \coth x - \frac{1}{x}$ is the Langevin function



Typical values: $p \approx 10^{-29}$ Cm (displacement of 1e by 0.6 Å)

$E_L \approx 10^7$ V/m or smaller

at room temperature $x \approx 0.02$ and we can replace the Langevin function by $\mathcal{L}(x) \approx x/3$ and

$$\langle p_{\parallel} \rangle \approx \frac{p^2 E_L}{3k_B T} \Rightarrow \alpha \approx \frac{p^2}{3k_B T} \quad \text{Roughly, } \frac{\alpha}{4\pi\epsilon_0} \approx 10^{-28} \text{ m}^3$$

For such large polarizabilities the Clausius-Mossotti relation is not correct. From this relation it follows:

$$\varepsilon = \frac{2 \frac{N\alpha}{\varepsilon_0} + 3}{3 - \frac{N\alpha}{\varepsilon_0}}$$

Example: liquid water $p \approx 0.62 \times 10^{-29} \text{Cm}$, $N \approx 4 \times 10^{28} \text{m}^{-3}$ therefore $\frac{N\alpha}{\varepsilon_0} \approx 12$
 $\varepsilon \approx 80$
 at 300K. Thus, a negative value of ε follows. Experimental value

The Lorentz formula for the local field is not valid for a material with polar molecules

Response of a system of polar molecules to a time-dependent electric field

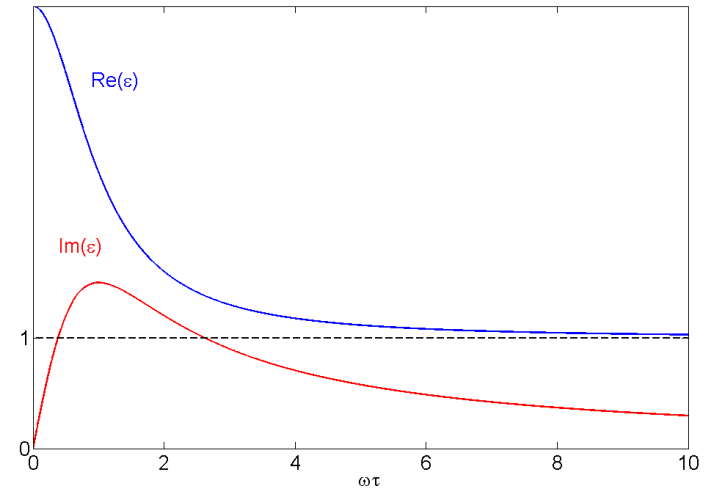
Debye relaxation equation: $\frac{d\mathbf{P}}{dt} = \frac{1}{\tau} (\langle \mathbf{P} \rangle - \mathbf{P})$

The time-averaged value of the polarization $\langle \mathbf{P} \rangle = \chi(0)\varepsilon_0 \mathbf{E}$, $\chi(0) = \chi(\omega = 0)$

For a monochromatic primary wave $\mathbf{E}(t) = \mathbf{E}_0 e^{-i\omega t}$ we assume $\mathbf{P} \sim e^{-i\omega t}$ and the stationary

solution is $\mathbf{P}(t) = \frac{\varepsilon_0 \chi(0)}{1 - i\omega\tau} \mathbf{E}_0 e^{-i\omega t} \Rightarrow \varepsilon(\omega) = 1 + \frac{\chi(0)}{1 - i\omega\tau}$

from the simple model:



experimental results (water):

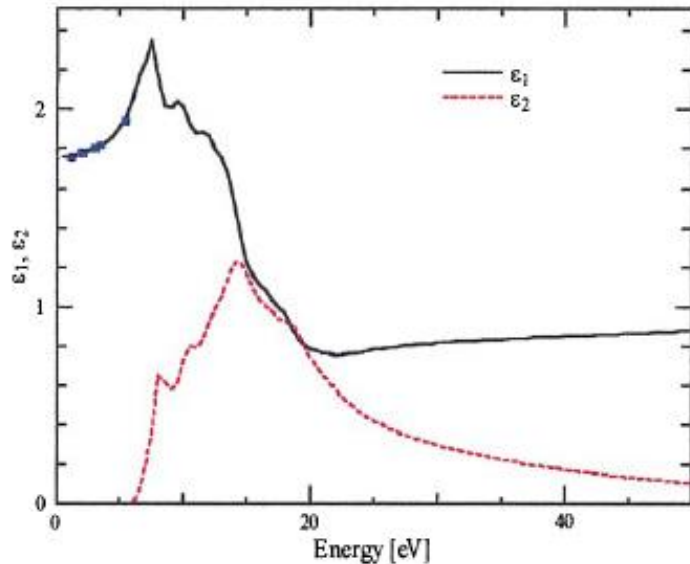


Fig. 2. Real (ϵ_1) and imaginary (ϵ_2) parts of the dielectric function of liquid water from the present work. Closed squares: ϵ_1 was calculated from the index of refraction.

PNAS

Proceedings of the National Academy of Sciences of the United States of America www.pnas.org

The complete optical spectrum of liquid water measured by inelastic x-ray scattering

Hisashi Hayashi, Noboru Watanabe, Yasuo Udagawa, and C.-C. Kao

PNAS 2000;97:6264-6266; originally published online May 30, 2000;
doi:10.1073/pnas.110572097

Displacement polarization – see Chap. V

Atomic polarization

Exact calculation – quantum mechanical perturbation method, here only a simple classical model: Z electrons are uniformly distributed in a sphere of radius r , x is a displacement of the nucleus from the centre of the sphere. The restoring electric field generated by the electrons is

$$E = -\frac{Ze\left(\frac{x}{r}\right)^3}{4\pi\epsilon_0 x^2} = -\frac{Ze}{4\pi\epsilon_0 r^3} x$$

The applied field E_L is balanced by E

$$x = \frac{4\pi\epsilon_0 r^3}{Ze} E_L \Rightarrow p = Zex = 4\pi\epsilon_0 r^3 E_L$$

atomic polarizability $\frac{\alpha}{4\pi\epsilon_0} = r^3 \approx 10^{-30} \text{m}^3$

by approx. two orders smaller than the orientation polarizability

TABLE III. Comparison of electronic polarizabilities, α_m of the alkali-halides, taken from Table I, with $\alpha_A + \alpha_H$, taken from Table II, (a) for $\lambda = D$; (b) for $\lambda = \infty$. First line α_m . Second line $\alpha_A + \alpha_H$. All values are in Å^3 .

	F	Cl	Br	I
		(a) $\lambda = D$		
Li	0.920	2.980	4.159	6.248
	0.673	2.989	4.187	6.459
Na	1.186	3.360	4.560	6.721
	1.053	3.368	4.566	6.839
K	1.966	4.272	5.508	7.790
	1.981	4.297	5.495	7.767
Rb	2.572	4.856	6.147	8.532
	2.623	4.939	6.137	8.409
Cs	3.664	6.419	7.497	9.952
	3.979	6.295	7.493	9.765

measured
simulated

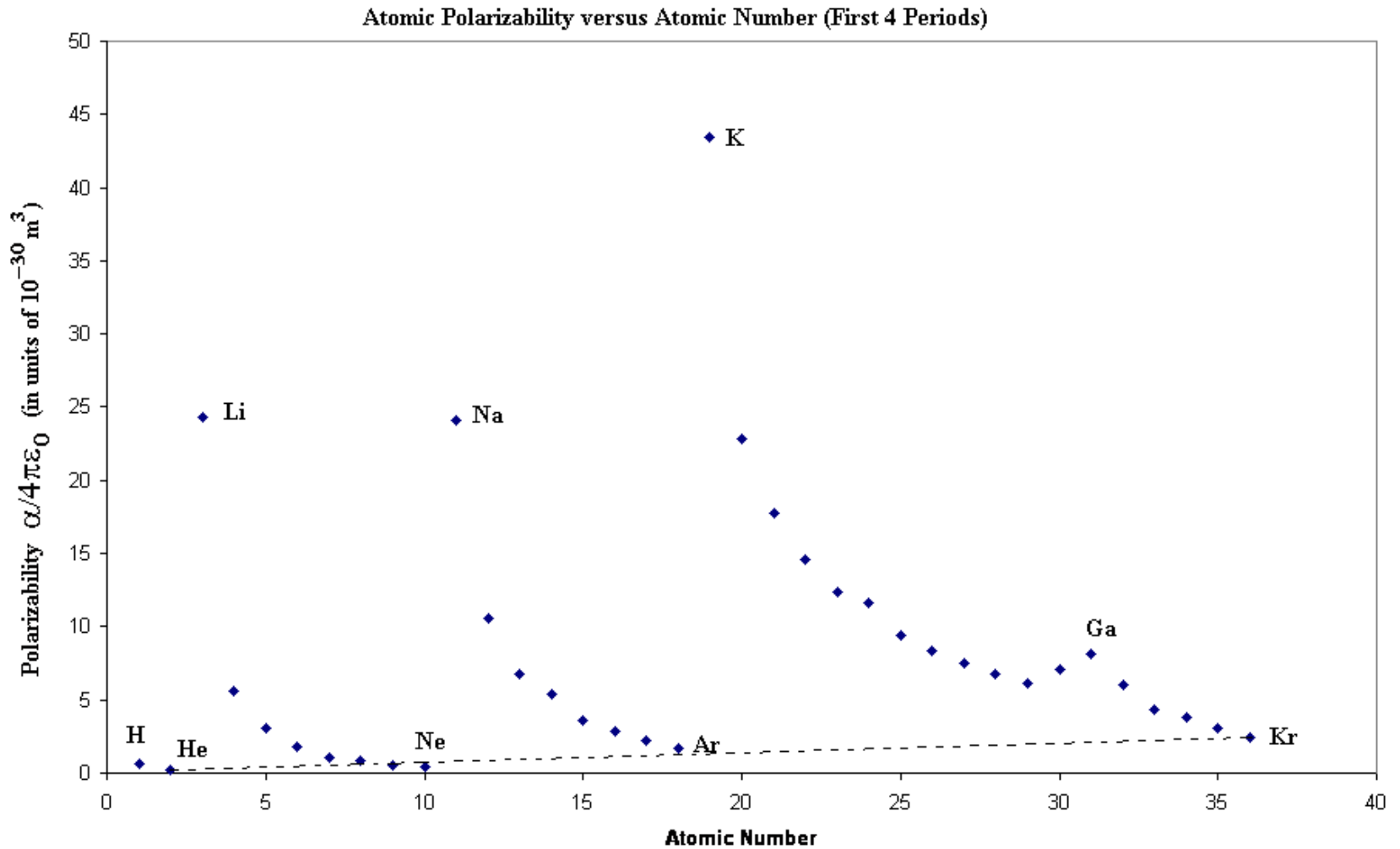
Electronic Polarizabilities of Ions in Crystals*

JACK R. TESSMAN† AND A. H. KAHN, *Department of Physics, University of California, Berkeley, California*

AND

WILLIAM SHOCKLEY, *Bell Telephone Laboratories, Murray Hill, New Jersey*

(Received August 10, 1953)



Response of a system of non-interacting atoms to a time-dependent electric field

The equation of movement of the sphere filled with electrons with respect to an immobile nucleus:

$$Zm\ddot{x} + Zm\gamma\dot{x} + \frac{Z^2e^2}{4\pi\epsilon_0r^3}x = ZeE_0e^{-i\omega t}$$

Stationary solution

$$\mathbf{x} = \frac{e}{m(\omega_0^2 - \omega^2 - i\omega\gamma)} \mathbf{E}_0 e^{-i\omega t}$$

Resonance frequency

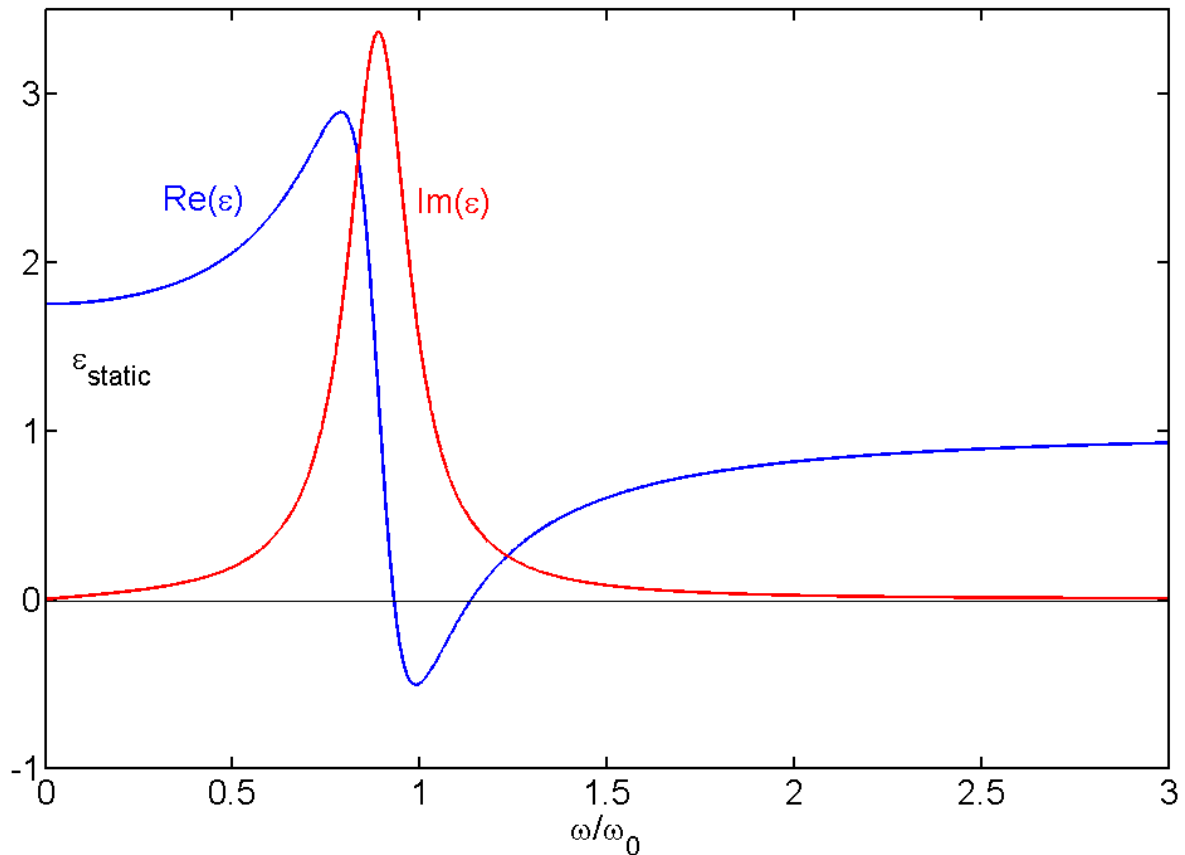
$$\omega_0 = \left(\frac{Ze^2}{4\pi\epsilon_0r^3m} \right)^{1/2}$$

Polarizability

$$\alpha = \frac{Ze^2}{m(\omega_0^2 - \omega^2 - i\omega\gamma)}$$

Permittivity

$$\epsilon = \frac{2\frac{N\alpha}{\epsilon_0} + 3}{3 - \frac{N\alpha}{\epsilon_0}} \quad \text{its static value:} \quad \epsilon(0) = \frac{8\pi r^3 N + 3}{3 - 4\pi r^3 N}$$



More in the lecture on optical properties of solid, the Lorentz formula:

$$n^2(\omega) = [n_r(\omega) + ik(\omega)]^2 = 1 + \chi(\omega) = 1 + \sum_j \frac{f_j \omega_{pj}^2}{\omega_{0j}^2 - i\omega\gamma_j - \omega^2}$$

Combination of the Lorentz model with the Lorentz-Lorenz formula

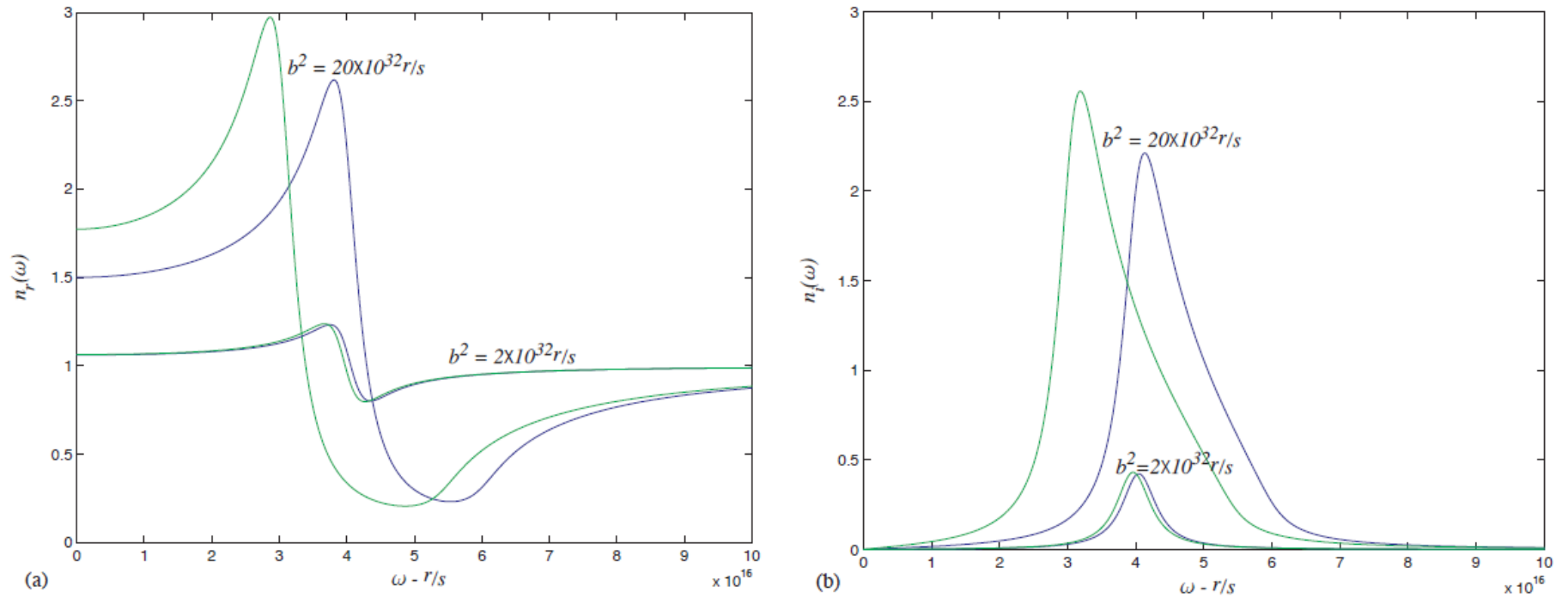


Fig. 1. Angular frequency dependence of the real (a) and imaginary (b) parts of the complex index of refraction for a Lorentz model dielectric with (green curves) and without (blue curves) the Lorentz-Lorenz formula for two different values of the material plasma frequency.

K. E. Oughstun and N. A. Cartwright, Optics Express 11, 1541 (2003)

IV. MEAN-FIELD THEORY

IV. 3. Spontaneous ordering of electric moments - Ferroelectric state

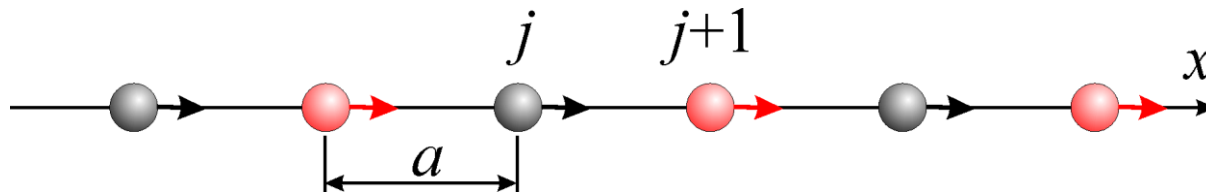
Is a spontaneous polarization possible?

We have found

$$\mathbf{P} = \varepsilon_0 \chi \mathbf{E} = \mathbf{E} \frac{N\alpha}{1 - \frac{N\alpha}{3\varepsilon_0}}$$

Thus, if $N\alpha = 3\varepsilon_0$ we obtain $\mathbf{P} \neq 0$ for $\mathbf{E} = 0$

Another hypothetic example – an 1D chain of ions with alternating charges



Equation of motion:

$$m_j \frac{d^2 u_j}{dt^2} = K(u_{j+1} + u_{j-1} - 2u_j) + \sum_{n < j} \frac{Q_j Q_n}{4\pi\epsilon_0(x_j - x_n)^2} - \sum_{n > j} \frac{Q_j Q_n}{4\pi\epsilon_0(x_j - x_n)^2}$$

$$m_j \frac{d^2 u_j}{dt^2} \approx K(u_{j+1} + u_{j-1} - 2u_j) - \frac{1}{2\pi\epsilon_0 a^3} \left[\sum_{n < j} \frac{Q_j Q_n (u_n - u_j)}{(n - j)^3} - \sum_{n > j} \frac{Q_j Q_n (u_n - u_j)}{(n - j)^3} \right]$$

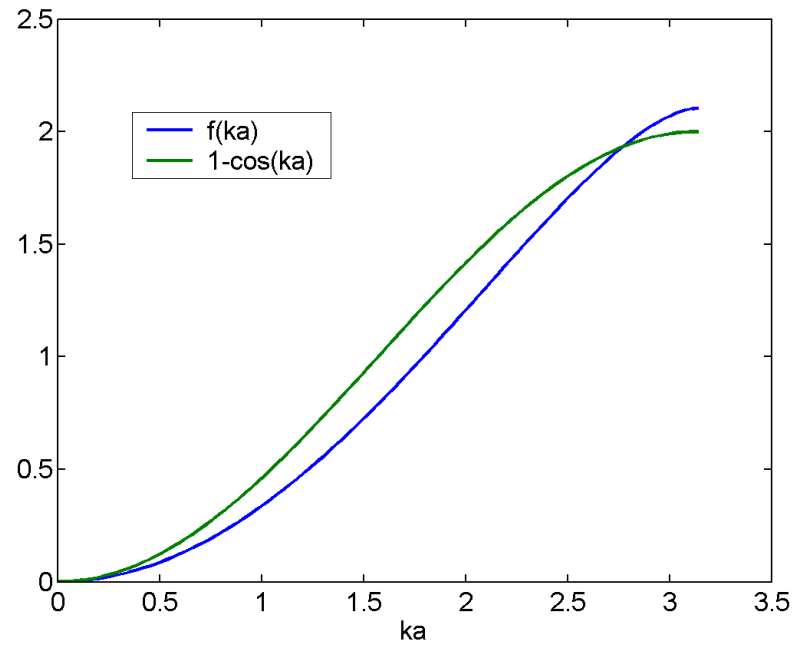
We assume a solution in the form of a plane wave

$$u_j \sim e^{-i(\omega t - jka)}$$

and we obtain the dispersion relation

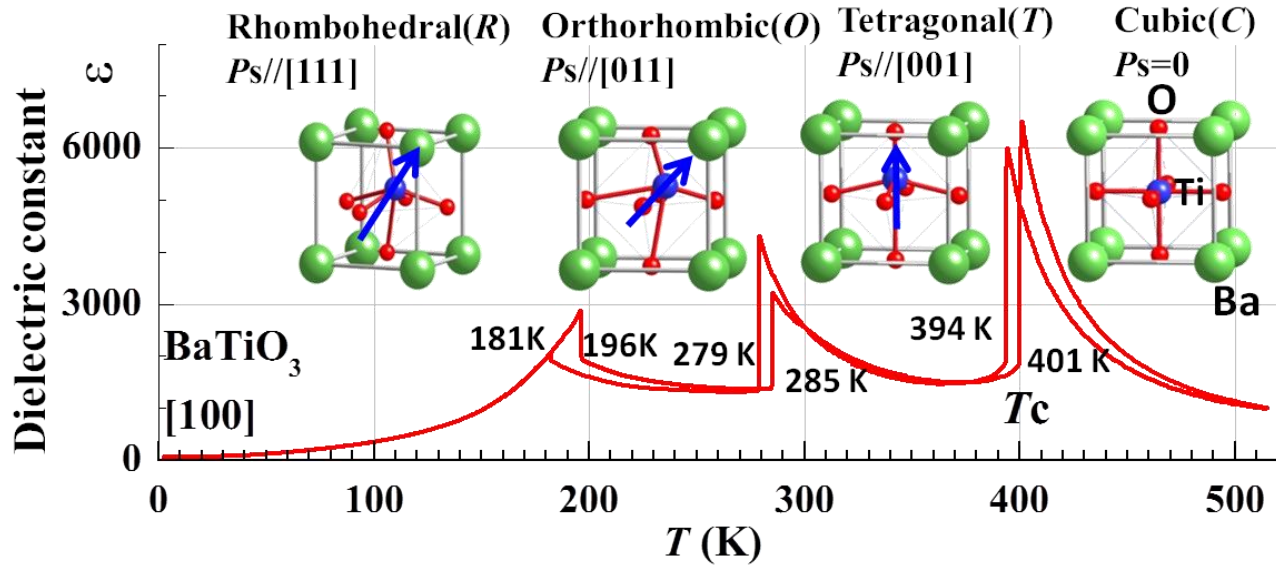
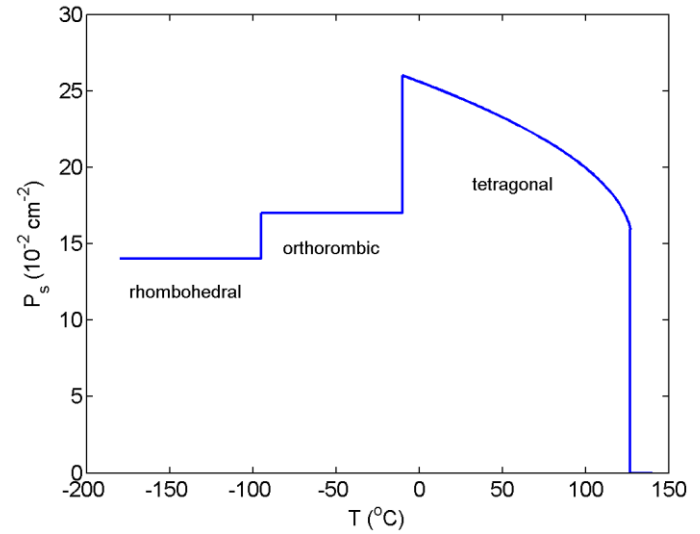
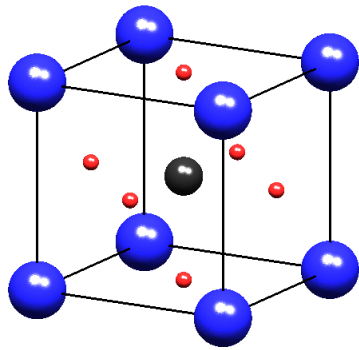
$$m\omega^2 = 2K[1 - \cos(ka)] + 2A \sum_{j=1}^{\infty} (-1)^j \frac{1 - \cos(jka)}{j^3}, \quad A = \frac{e^2}{2\pi\epsilon_0 a^3}$$

A wave vector k exists, for which $\omega = 0$ – a weak phonon \Rightarrow spontaneous polarization

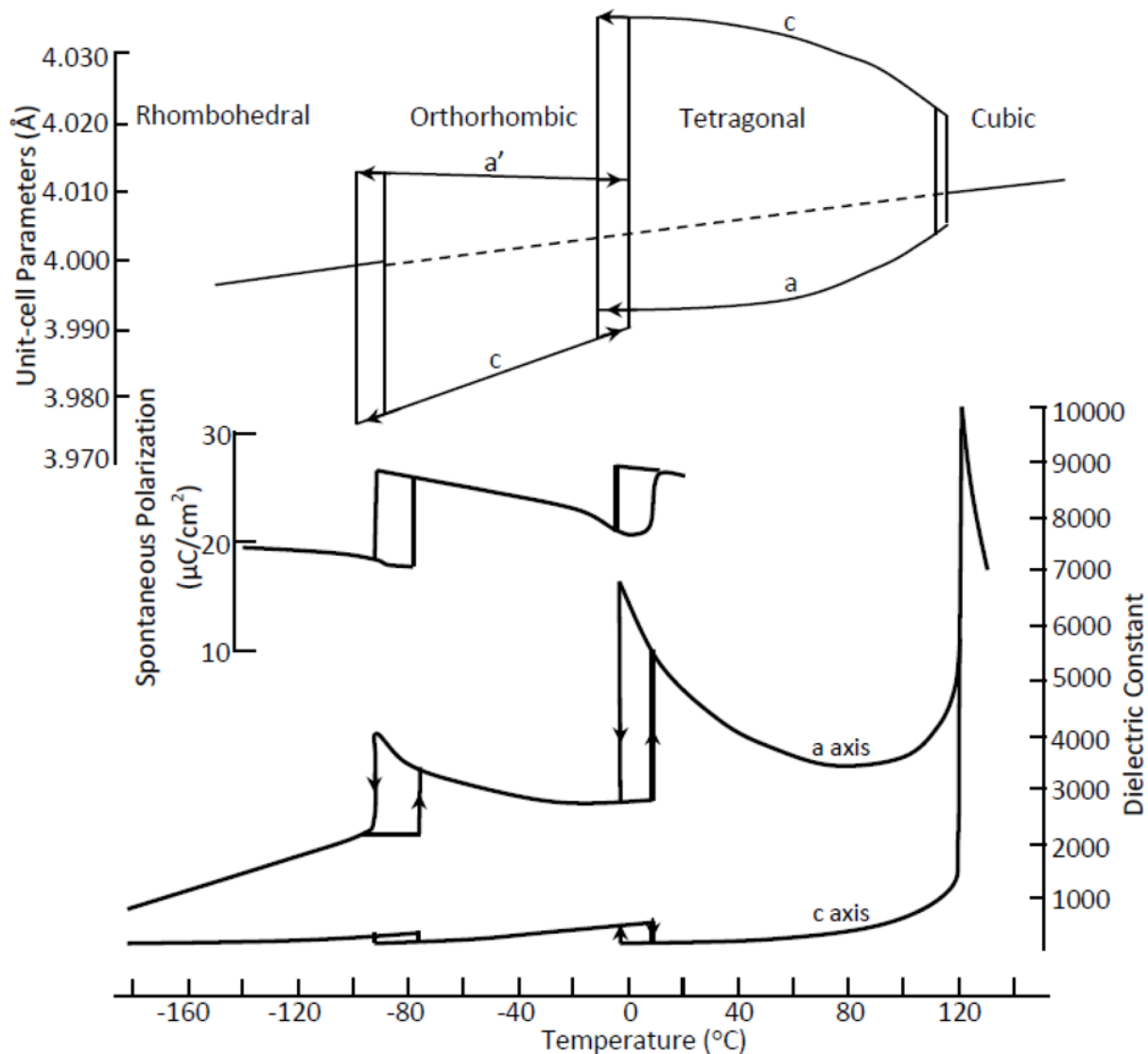


$$f(x) = \sum_{j=1}^{\infty} (-1)^j \frac{\cos(jx) - 1}{j^3}$$

The most common ferroelectric material – BaTiO₃



Lattice parameters and permittivity of BaTiO₃



The Landau theory of phase transitions

Variables: P (polarization), T
Helmholtz free energy $F(P, T)$

The equilibrium condition $\left. \frac{\partial F}{\partial P} \right|_{eq} = 0$

Due to the inversion symmetry

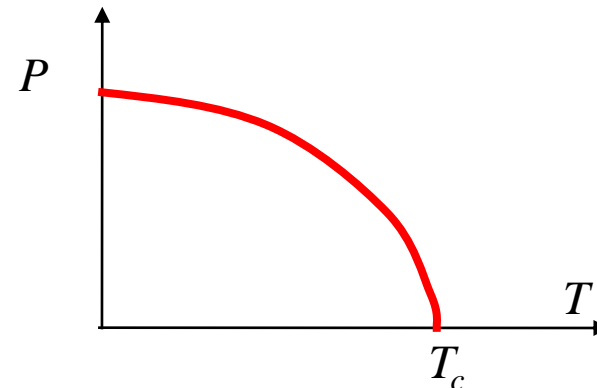
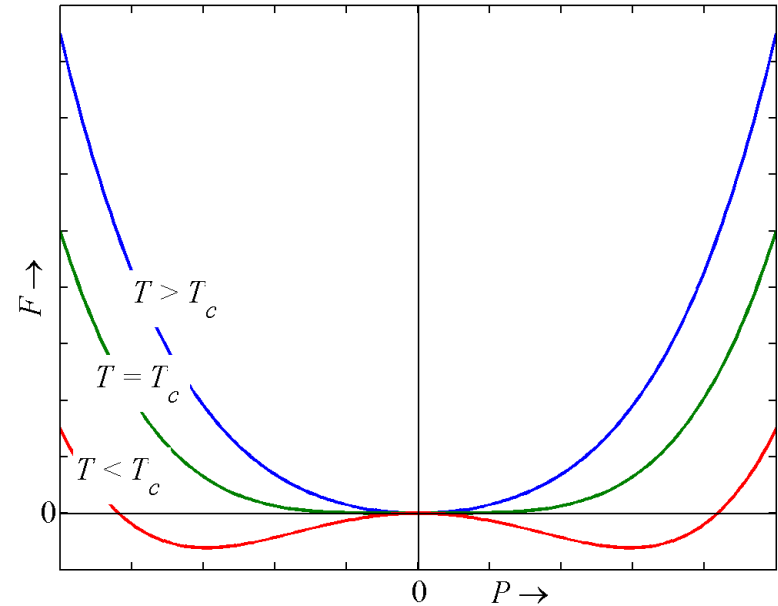
$$F(P, T) = F(0, T) + c_2 P^2 + c_4 P^4 + c_6 P^6 + \dots$$

$$c_2 = b(T - T_c)$$

Spontaneous polarization

$$P_s \equiv P_{eq} = \sqrt{b \frac{T_c - T}{2c_4}}$$

up to P^4 , $c_4 > 0$:



Gibbs free energy with an external electric field:

$$\Phi = F - EP = F(0, T) + c_2 P^2 + c_4 P^4 + c_6 P^6 + \dots - EP$$

$$\left. \frac{\partial \Phi}{\partial P} \right|_{eq} = 0 \Rightarrow E = 2b(T - T_c)P_{eq} + 4c_4 P_{eq}^3$$

Dielectric susceptibility:

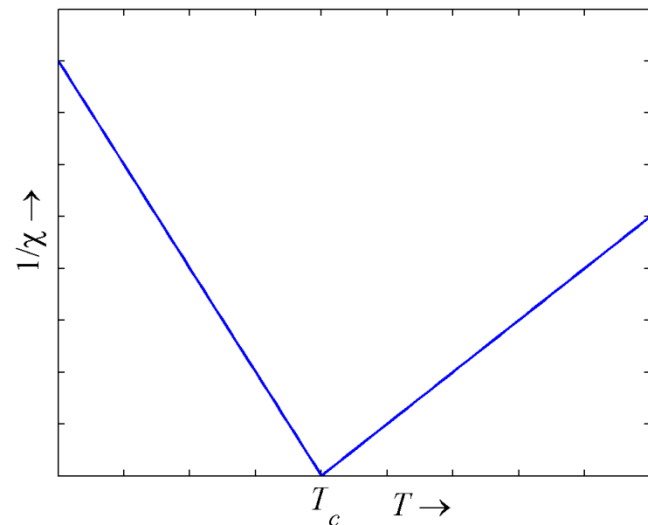
$$\frac{1}{\epsilon_0 \chi} = \left. \frac{\partial E}{\partial P} \right|_{E=0} = 2b(T - T_c) + 12c_4 P_{eq}^2$$

Therefore:

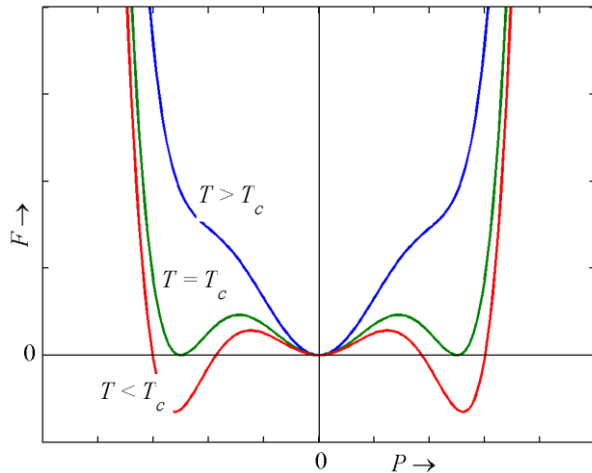
$$T > T_c: \chi = \frac{1}{\epsilon_0} \frac{1}{2b(T - T_c)}$$

$$T < T_c: \chi = \frac{1}{\epsilon_0} \frac{1}{4b(T_c - T)}$$

Phase transition of the 2nd order



Up to P^6 , $c_4 < 0, c_6 > 0$:



$$\left. \frac{\partial F}{\partial P} \right|_{eq} = 0 = 2b(T - T^*)P + 4c_4P^3 + 6c_6P^5$$

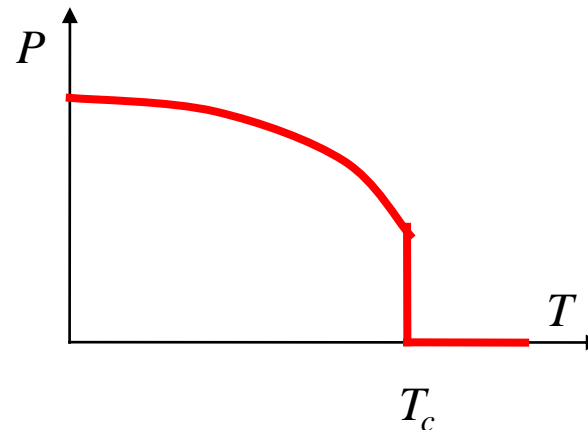
$$\Rightarrow P_{eq}^2 = \frac{1}{3c_6} \left[-c_4 \pm \sqrt{c_4^2 - 3c_6b(T - T^*)} \right]$$

The critical temperature:

$$T_c = T^* + \frac{c_4^2}{3bc_6}$$

Phase transition of the 1st order

χ does not diverge at T_c



Gibbs free energy with an external electric field:

$$\Phi = F - EP = F(0, T) + c_2 P^2 + c_4 P^4 + c_6 P^6 + \dots - EP$$

$$\left. \frac{\partial \Phi}{\partial P} \right|_{eq} = 0 \Rightarrow E = 2b(T - T^*)P_{eq} + 4c_4 P_{eq}^3 + 6c_6 P_{eq}^5$$

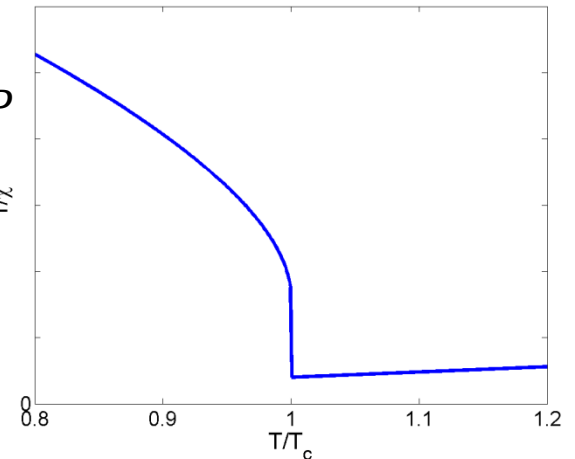
Dielectric susceptibility:

$$\frac{1}{\epsilon_0 \chi} = \left. \frac{\partial E}{\partial P} \right|_{E=0} = 2b(T - T^*) + 12c_4 P_{eq}^2 + 30c_6 P_{eq}^4$$

Therefore:

$$T > T_c: \chi = \frac{1}{\epsilon_0} \frac{1}{2b(T - T^*)}$$

$$T < T_c: \chi = \frac{1}{\epsilon_0} \frac{1}{8b \left[T^* - T + \frac{2c_4^2}{3bc_6} + \frac{c_4^2}{bc_6} \sqrt{1 - \frac{3bc_6}{c_4^2} (T - T^*)} \right]}$$

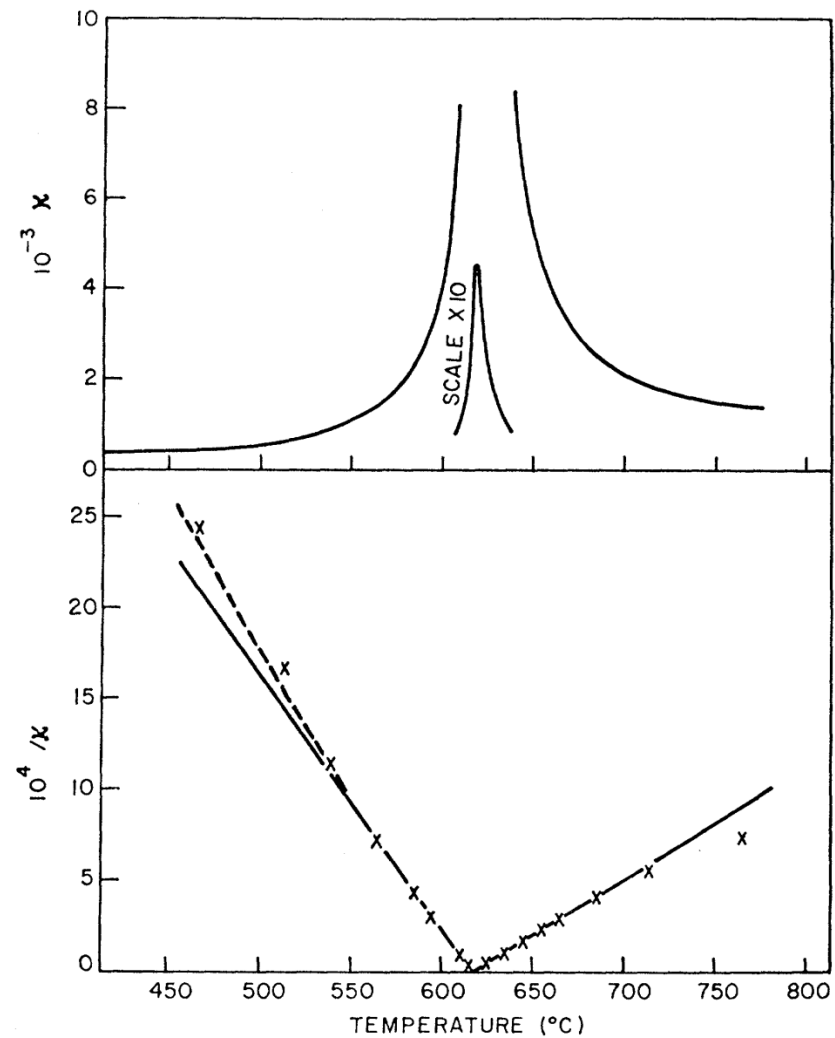


**Dielectric, Thermal, and Pyroelectric Properties of
Ferroelectric LiTaO₃**

A. M. GLASS

Bell Telephone Laboratories, Murray Hill, New Jersey

(Received 4 March 1968)

FIG. 3. Temperature variation of dielectric constant κ and κ^{-1} for LiTaO₃.

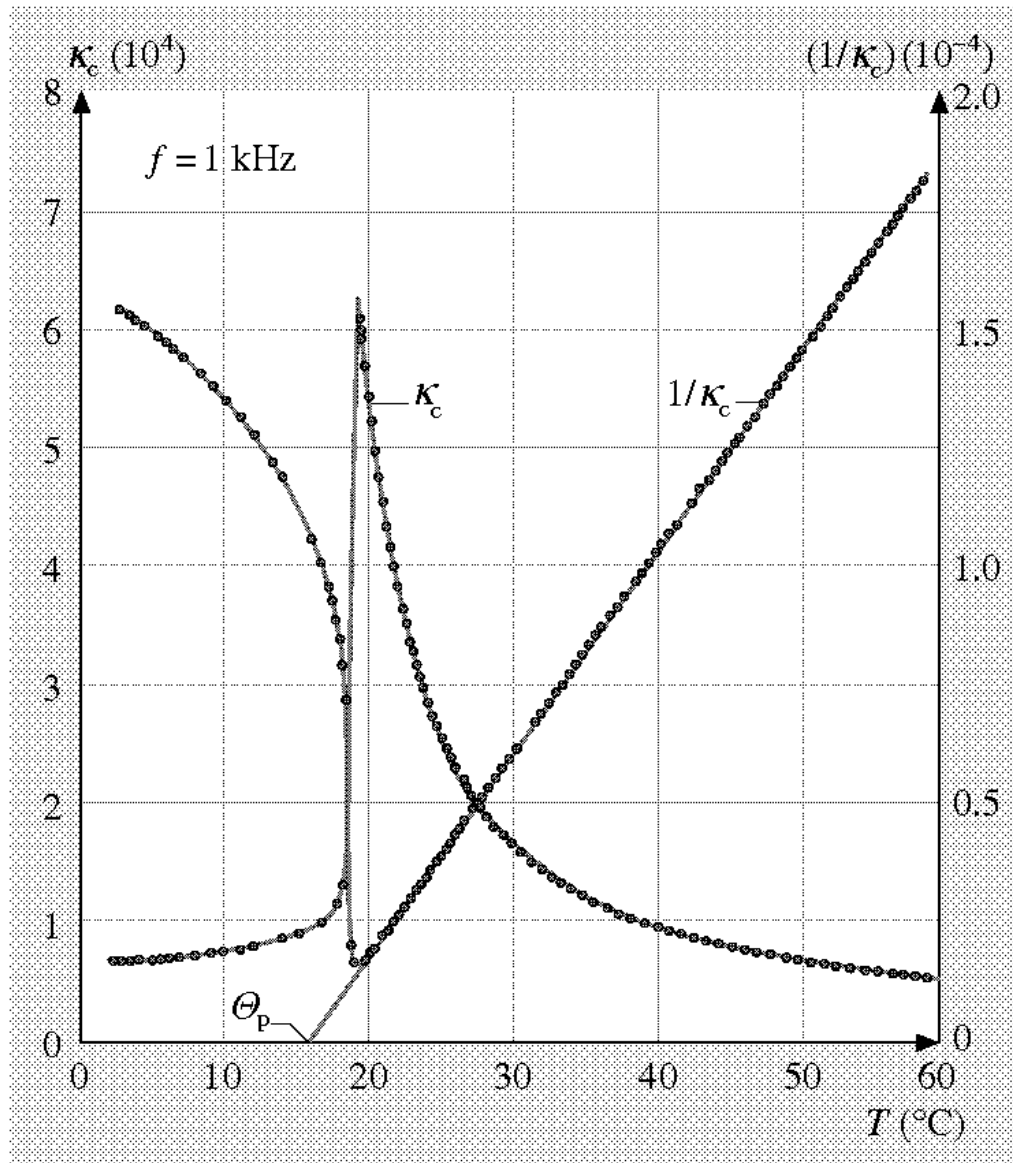
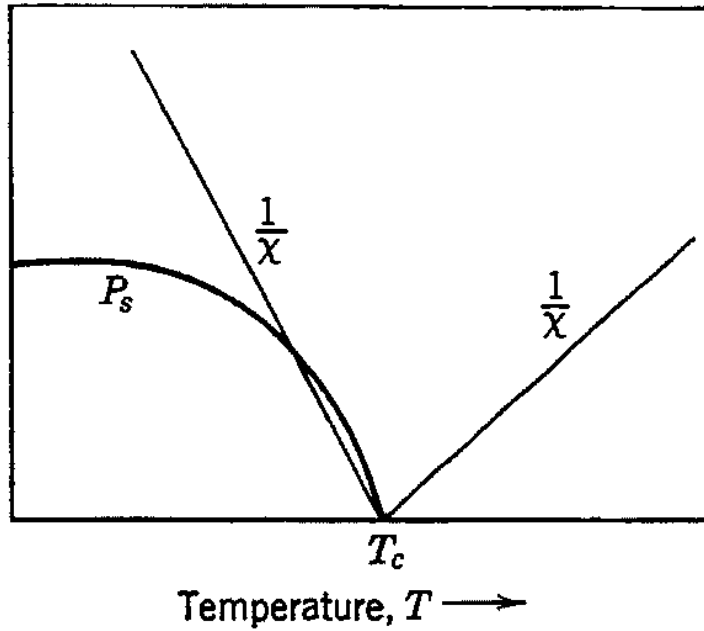
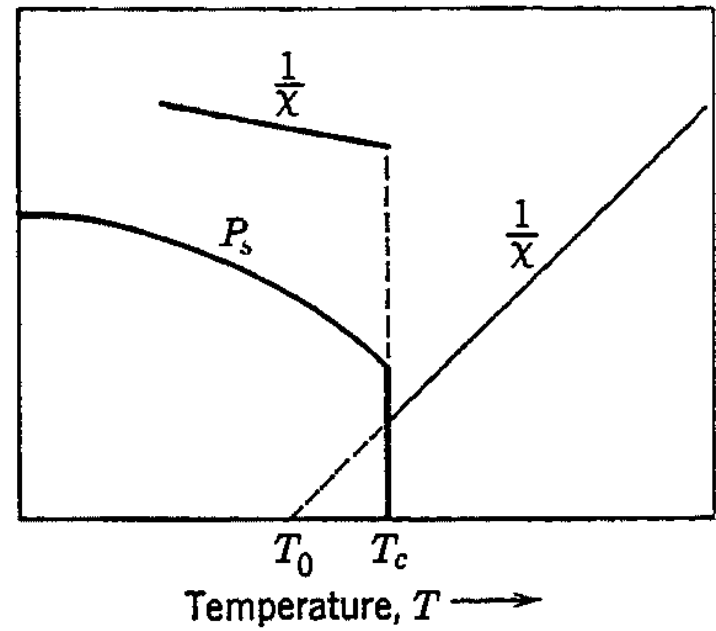


Fig. 4.5-47 SbSI. κ_c and $1/\kappa_c$ versus T



Phase transition of the 2nd order



Phase transition of the 1st order

III. RESPONSE OF A CONDENSED BODY TO AN EXTERNAL IMPULSE

III. 4. Response to an external magnetic field

Basic quantities

Magnetic moment of a current I in a loop with the area S :

$$\mathbf{m} = IS = -\frac{e}{T}\pi R^2 = -e\frac{\mathbf{b}}{2m_e}, \mathbf{b} = m_e\mathbf{v} \times R$$

magnetic dipole moment induced by an orbital moment of electron: $m_L = -\frac{e\hbar}{2m_e}L$

magnetic dipole moment induced by a spin moment of electron: $\mathbf{m}_S = -g_0\mu_B\mathbf{S}$

the Bohr magneton: $\mu_B = \frac{e\hbar}{2m_e} \approx 9.724 \times 10^{-24} \text{J/T} \approx 5.788 \times 10^{-5} \text{eV/T}$

electron g-factor: $g_0 \approx 2.0023 \approx 2$

Macroscopic quantities:

$$\text{Magnetization} \quad \mathbf{M} = \frac{1}{V} \sum_j \mathbf{m}_j$$

$$\text{Susceptibility:} \quad \mathbf{M} = \chi \mathbf{H}, \chi = \frac{\partial M}{\partial H}$$

$$\text{Magnetic induction:} \quad \mathbf{B} = \mu_0(\mathbf{H} + \mathbf{M}) = \mu \mathbf{H}, \mu = \mu_0(1 + \chi)$$

$$\text{Statistical average:} \quad \langle M \rangle = \frac{\sum_n M_n e^{-\mathcal{E}_n/(k_B T)}}{\sum_n e^{-\mathcal{E}_n/(k_B T)}}, M_n = -\frac{1}{V} \frac{\partial \mathcal{E}_n}{\partial B}$$

$$\text{Free energy:} \quad Z = e^{-F/(k_B T)} = \sum_n e^{-\mathcal{E}_n/(k_B T)}$$

$$\text{Susceptibility again:} \quad \chi = \frac{\partial \langle M \rangle}{\partial H} = \mu_0 \frac{\partial \langle M \rangle}{\partial B} = -\mu_0 \frac{\partial^2 F}{\partial B^2}$$

Comment: CGS units:

magnetic induction \mathbf{B} (magnetic flux density): SI: 1 Tesla (T) = $\text{kg s}^{-2} \text{A}^{-1}$
CGS: 1 Gauss (G) = 10^{-4} T

magnetic intensity \mathbf{H} : SI: 1 A/m
CGS: 1 Oersted (Oe) = $10^3/4\pi$ A/m = 79.5775 A/m

Interaction of electrons with an external magnetic field

Non-relativistic Hamiltonian of a free electron without spin in an external magnetic field

$$\hat{H} = \frac{1}{2m_e} (\hat{\mathbf{p}} + e\mathbf{A})^2 \quad (\text{electron charge is } -e)$$

The vector potential of the field is \mathbf{A} : $\mathbf{B} = \text{rot}\mathbf{A}, \text{div}\mathbf{A} = 0$

We can choose $\mathbf{A} = -\frac{1}{2}(\mathbf{r} \times \mathbf{B})$

The spin term in the Hamiltonian: $\hat{H}_S = -\mathbf{m}_S \cdot \mathbf{B}$

We obtain for the Hamiltonian

$$\hat{H}_S = \frac{1}{2m_e} \sum_j \hat{\mathbf{p}}_j^2 + \mu_B (\hat{\mathbf{L}} + g_0 \hat{\mathbf{S}}) \cdot \mathbf{B} + \frac{e^2}{8m_e} B^2 \sum_j (\hat{x}_j^2 + \hat{y}_j^2)$$

Perturbation theory (up to the 2nd order and 2nd power of \mathbf{B}):

$$\Delta\mathcal{E}_n = \underbrace{\mu_B \mathbf{B} \cdot \langle n | \hat{\mathbf{L}} + g_0 \hat{\mathbf{S}} | n \rangle}_{\text{linear term}} + \underbrace{\frac{e^2}{8m_e} B^2 \langle n | \sum_j (\hat{x}_j^2 + \hat{y}_j^2) | n \rangle}_{\text{quadratic terms}} + \sum_{m \neq n} \frac{|\mu_B \mathbf{B} \cdot \langle n | \hat{\mathbf{L}} + g_0 \hat{\mathbf{S}} | m \rangle|^2}{\mathcal{E}_n - \mathcal{E}_m}$$

Langevin diamagnetism

Ions with fully occupied shells: $\hat{\mathbf{L}}|0\rangle = \hat{\mathbf{S}}|0\rangle = 0$ in the ground state

Energy shift of the ground state:

$$\Delta\mathcal{E}_0 = \frac{e^2}{8m_e} B^2 \langle 0 | \sum_j (\hat{x}_j^2 + \hat{y}_j^2) | 0 \rangle = \frac{e^2}{12m_e} B^2 \langle 0 | \sum_j \hat{r}_j^2 | 0 \rangle$$

Diamagnetic susceptibility: $\chi = -\frac{\mu_0 e^2 N}{6m_e V} Z \langle r^2 \rangle$

Properties:

- χ is a constant, independent of field strength;
- induced by the external field;
- always negative because of Lenz rule;
- always present in an external field, however often covered by the positive paramagnetic susceptibility;
- for atoms with closed shells, the Langevin diamagnetism is the only magnetism available;
- χ is proportional to the area of an atom, important for chemistry;
- all noble metal atoms are diamagnetic
- temperature independent.

Examples for Langevin Diamagnetism:

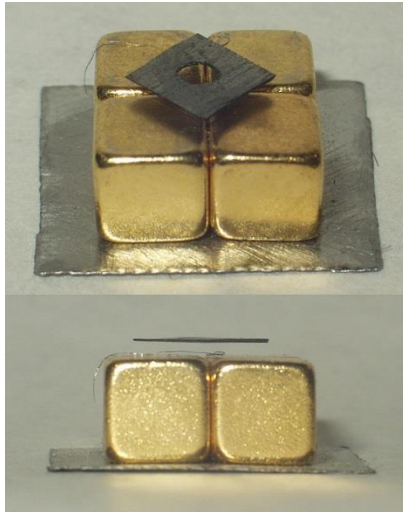
χ	
He	$-1.9 \times 10^{-6} \text{cm}^3/\text{mol}$
Xe	$-43 \times 10^{-6} \text{cm}^3/\text{mol}$
Bi	$-16 \times 10^{-6} \text{cm}^3/\text{g}$
Cu	$-1.06 \times 10^{-6} \text{cm}^3/\text{g}$
Ag	$-2.2 \times 10^{-6} \text{cm}^3/\text{g}$
Au	$-1.8 \times 10^{-6} \text{cm}^3/\text{g}$

The Langevin diamagnetism does not depend on temperature

Diamagnetic levitation – a diamagnetic material moves in an inhomogeneous magnetic field in the direction of negative gradient of B . The condition of levitation is

$$B \frac{dB}{dz} \geq \mu_0 \rho \frac{g}{\chi}$$

Water levitates at $B \frac{dB}{dz} \geq 1400 \text{ T}^2/\text{m}$, graphite levitates at $B \frac{dB}{dz} \geq 375 \text{ T}^2/\text{m}$



Pyrolytic graphite

By en:User:Splarka - English Wikipedia, Public Domain,
<https://commons.wikimedia.org/w/index.php?curid=1004783>

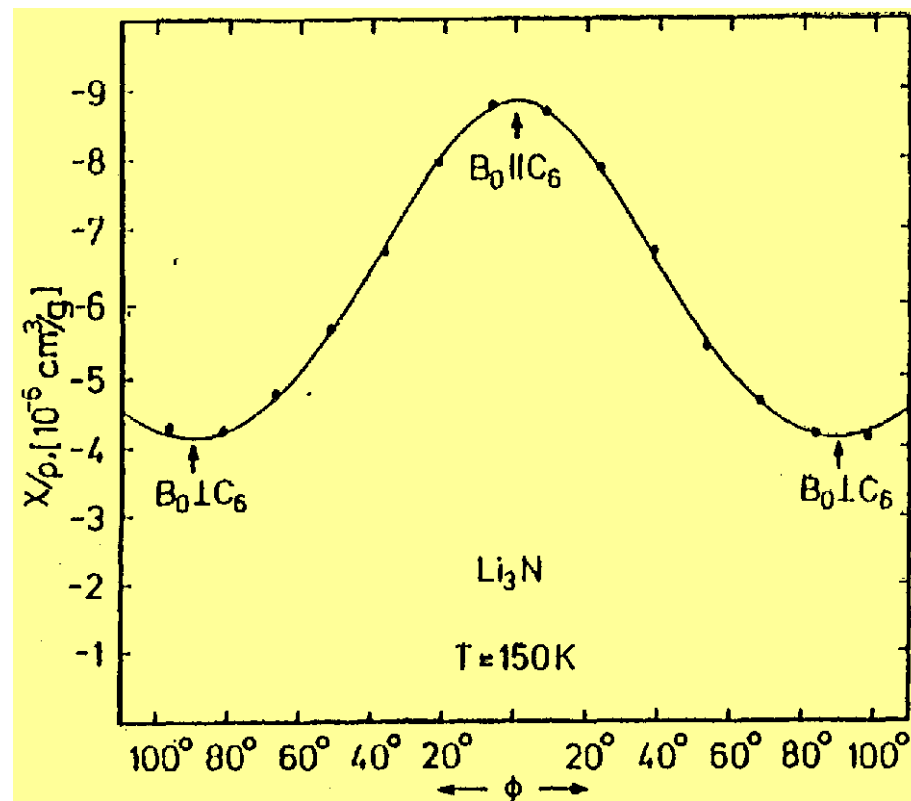
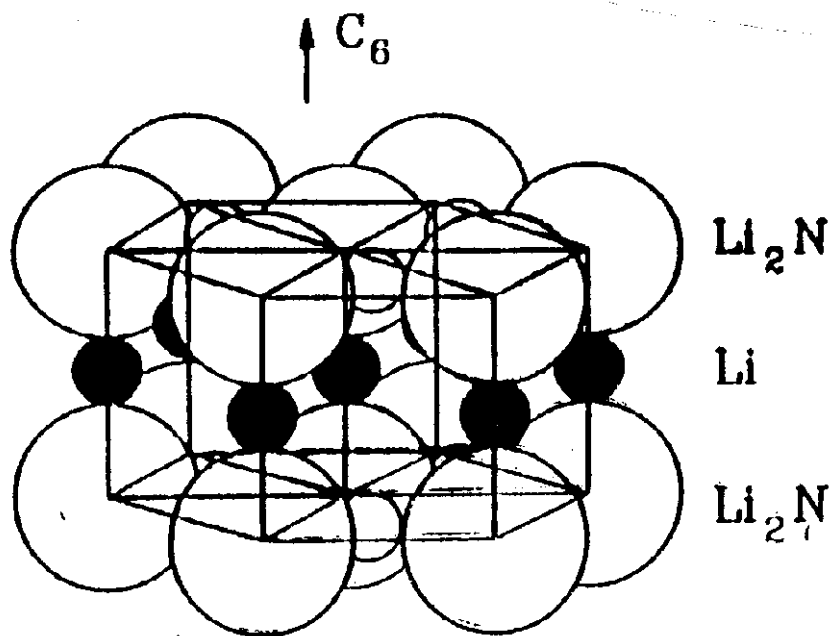


A live frog levitates inside a 32 mm diameter vertical bore of a solenoid in a magnetic field of about 16 T

By Lijnis Nelemans - English Wikipedia, CC BY-SA 3.0,
<https://commons.wikimedia.org/w/index.php?curid=1004796>

Diamagnetism can exhibit spatial anisotropy in crystals

Example: Li_3N



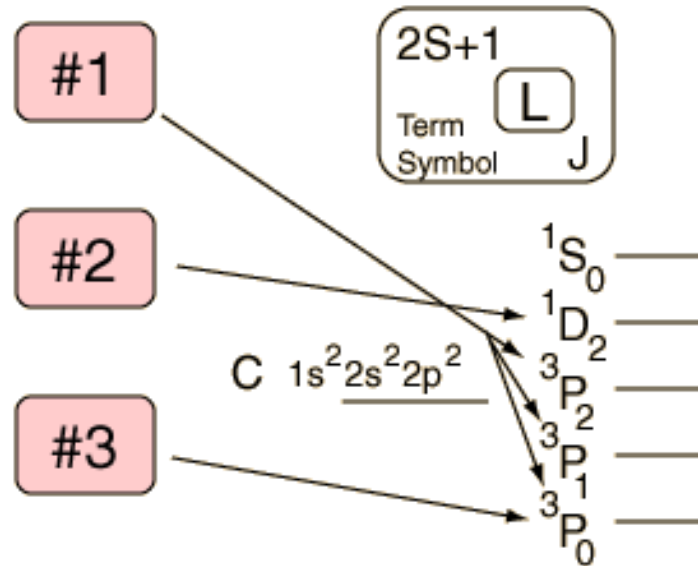
Ground state of an ion with a partially occupied shell

orbital quantum number l of the electrons in the partially occupied shell, the maximum possible number of electrons in the shell is $n = 2(2l + 1)$

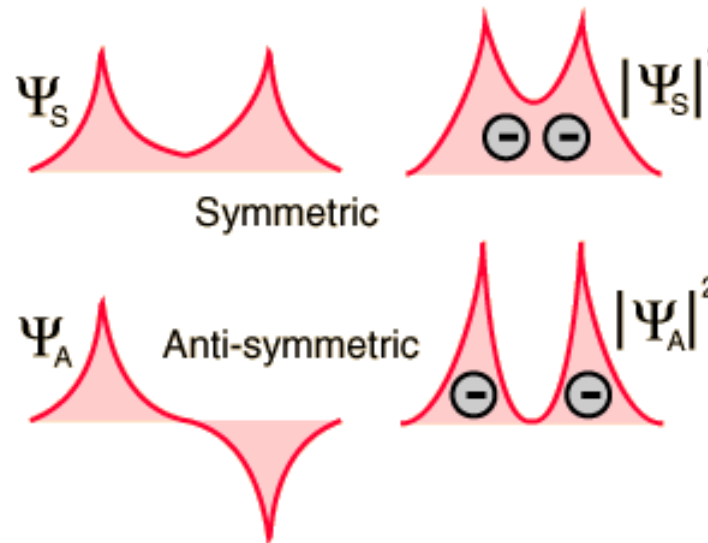
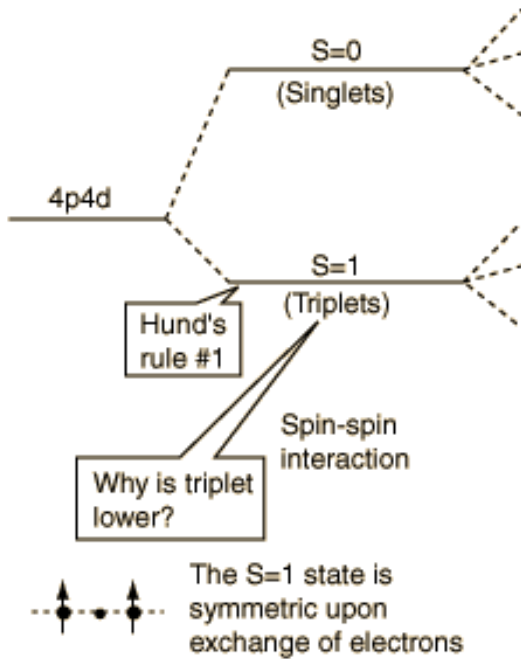
The degeneracy of the state with n electrons in the shell is removed by the LS-coupling. The state of the shell is described by the quantum numbers

$$L, L_z, S, S_z, \text{ where } \hat{J} = \hat{L} + \hat{S}, \hat{S} = \sum_j \hat{s}_j, \hat{L} = \sum_j \hat{l}_j$$

The Hund rules:



1. The term with the maximum multiplicity lies lowest in energy $\Rightarrow S$ has a maximum possible value



Electrons have greater probability of being close to each other.

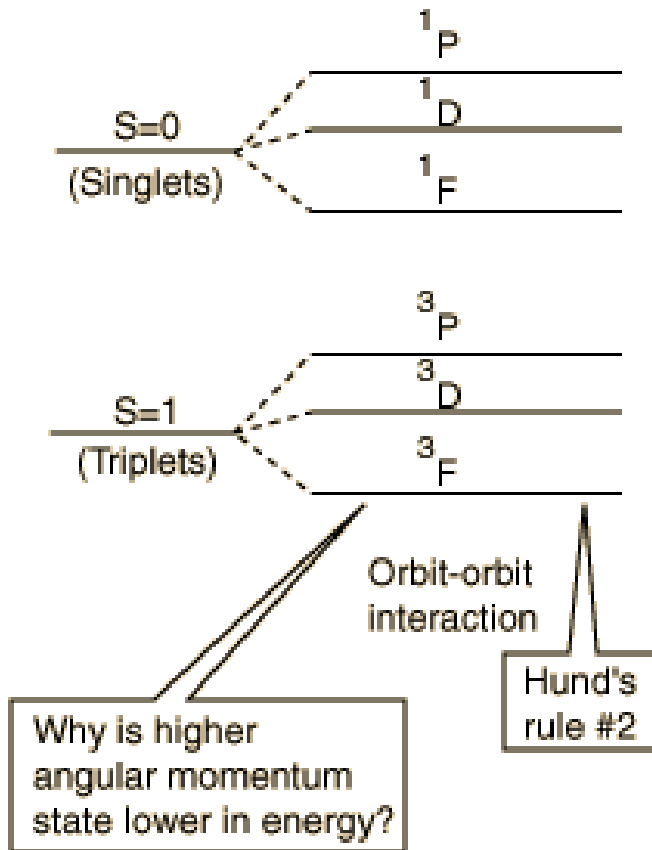
Higher energy associated with S = 0

Probability must go to zero at origin since Y changes sign, so less opportunity for electrons to be close together.

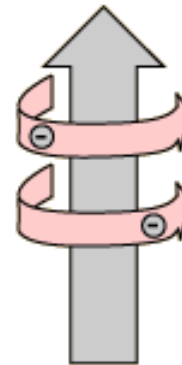
Lower energy associated with S = 1

Since $\Psi_{\text{spin}} \Psi_{\text{space}}$ must be anti-symmetric, then Ψ_{space} must be anti-symmetric to obey the Pauli exclusion principle.

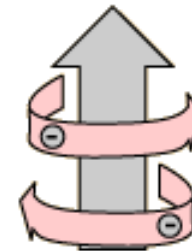
2. For a given multiplicity, the term with the largest value of L lies lowest in energy.



High L , electrons orbiting same direction to add to L value.

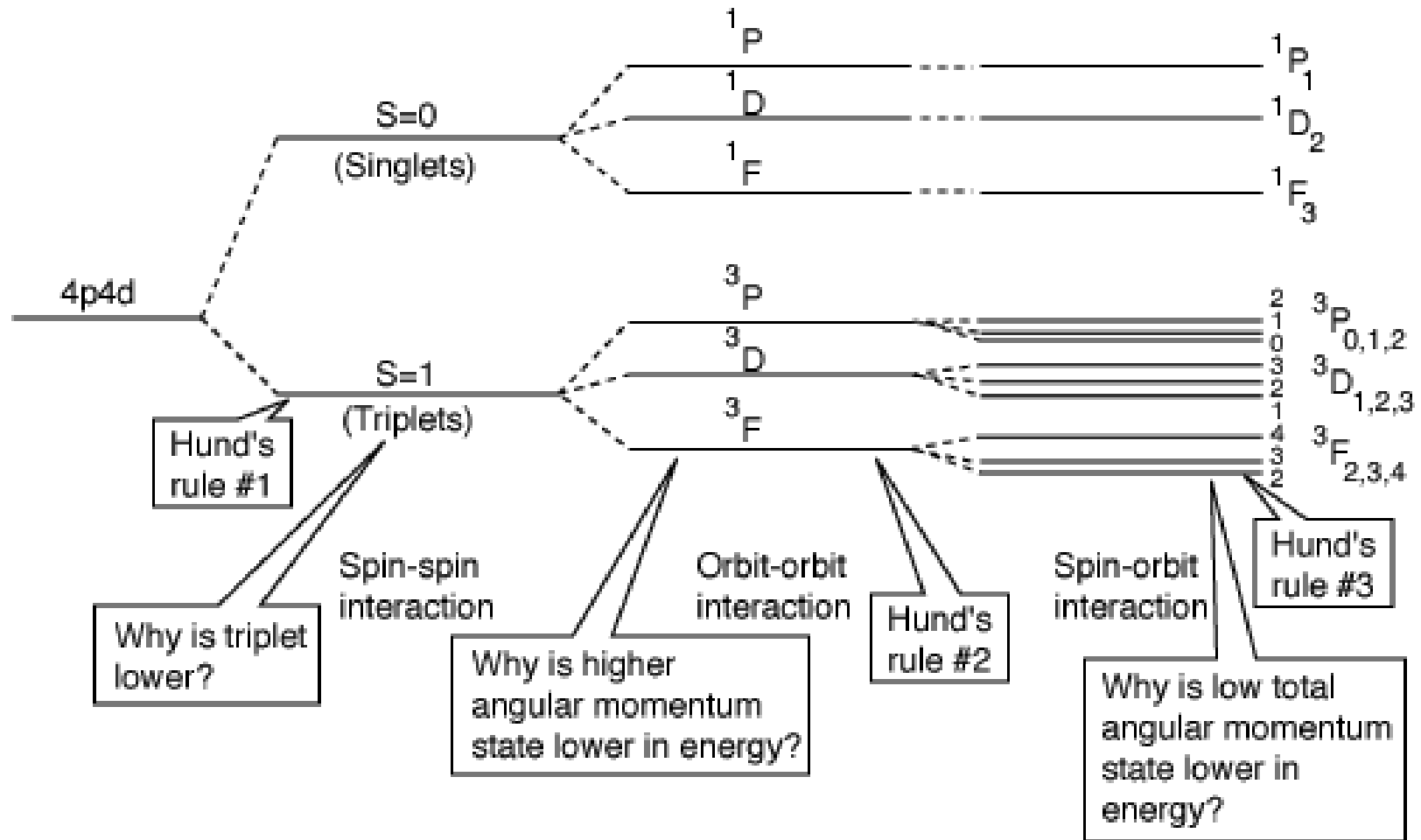


Low L , some electrons orbiting in opposite direction to reduce the L value.



For large L value, some or all of the electrons are orbiting in the same direction. That implies that they can stay a larger distance apart on the average since they could conceivably always be on the opposite side of the nucleus. For low L value, some electrons must orbit in the opposite direction and therefore pass close to each other once per orbit, leading to a smaller average separation of electrons and therefore a higher energy.

3. For atoms with less than half-filled shells, the level with the lowest value of J lies lowest in energy.



Elements by Orbital
Only the first 36 elements are shown

Sequence with which the orbitals fill with electrons

$1s$	H $1s^1$	$1s$	1
	He $1s^2$	$1s$	1 1
$2s$	Li $1s^2 2s^1$	$2s$	1
	Be $1s^2 2s^2$	$2s$	1 1
$2p$	B $1s^2 2s^2 2p_x^1$	$2p$	x y z
	C $1s^2 2s^2 2p_x^1 2p_y^1$	$2p$	1 1
	N $1s^2 2s^2 2p_x^1 2p_y^1 2p_z^1$	$2p$	1 1 1
	O $1s^2 2s^2 2p_x^2 2p_y^1 2p_z^1$	$2p$	1 1 1
	F $1s^2 2s^2 2p_x^2 2p_y^2 2p_z^1$	$2p$	1 1 1
	Ne $1s^2 2s^2 2p_x^2 2p_y^2 2p_z^2$	$2p$	1 1 1
$3s$	Na [Ne] $3s^1$	$3s$	1
	Mg [Ne] $3s^2$	$3s$	1 1
$3p$	Al [Ne] $3s^2 3p^1$	$3p$	x y z
	Si [Ne] $3s^2 3p^2$	$3p$	1 1
	P [Ne] $3s^2 3p^3$	$3p$	1 1 1
	S [Ne] $3s^2 3p^4$	$3p$	1 1 1
	Cl [Ne] $3s^2 3p^5$	$3p$	1 1 1
	Ar [Ne] $3s^2 3p^6$	$3p$	1 1 1
$4s$	K [Ar] $4s^1$	$4s$	1
	Ca [Ar] $4s^2$	$4s$	1 1
$3d$	Sc [Ar] $3d^1 4s^2$	$3d$	1
	Ti [Ar] $3d^2 4s^2$	$3d$	1 1
	V [Ar] $3d^3 4s^2$	$3d$	1 1 1
	Cr [Ar] $3d^5 4s^1$	$3d$	1 1 1 1 1
	Mn [Ar] $3d^5 4s^2$	$3d$	1 1 1 1 1
	Fe [Ar] $3d^6 4s^2$	$3d$	1 1 1 1 1
	Co [Ar] $3d^7 4s^2$	$3d$	1 1 1 1 1
	Ni [Ar] $3d^8 4s^2$	$3d$	1 1 1 1 1
	Cu [Ar] $3d^{10} 4s^1$	$3d$	1 1 1 1 1
	Zn [Ar] $3d^{10} 4s^2$	$3d$	1 1 1 1 1
$4p$	Ga [Ar] $3d^{10} 4s^2 4p^1$	$4p$	1
	Ge [Ar] $3d^{10} 4s^2 4p^2$	$4p$	1 1
	As [Ar] $3d^{10} 4s^2 4p^3$	$4p$	1 1 1
	Se [Ar] $3d^{10} 4s^2 4p^4$	$4p$	1 1 1
	Br [Ar] $3d^{10} 4s^2 4p^5$	$4p$	1 1 1
	Kr [Ar] $3d^{10} 4s^2 4p^6$	$4p$	1 1 1

<i>d</i> -shell ($l = 2$)										
n	$l_z = 2,$	1,	0,	-1,	-2	S	$L = \sum l_z $	J	SYMBOL	
1	↓					1/2	2	3/2	} $J = L - S $	${}^2D_{3/2}$
2	↓	↓				1	3	2		3F_2
3	↓	↓	↓			3/2	3	3/2		${}^4F_{3/2}$
4	↓	↓	↓	↓		2	2	0		5D_0
5	↓	↓	↓	↓	↓	5/2	0	5/2		${}^6S_{5/2}$
6	↑↓	↑	↑	↑	↑	2	2	4	} $J = L + S$	5D_4
7	↑↓	↑↓	↑	↑	↑	3/2	3	9/2		${}^4F_{9/2}$
8	↑↓	↑↓	↑↓	↑	↑	1	3	4		3F_4
9	↑↓	↑↓	↑↓	↑↓	↑	1/2	2	5/2		${}^2D_{5/2}$
10	↑↓	↑↓	↑↓	↑↓	↑↓	0	0	0		1S_0

<i>f</i> -shell (<i>l</i> = 3)												
<i>n</i>	<i>l_z</i> = 3,	2,	1,	0,	-1,	-2,	-3	<i>S</i>	<i>L</i> = Σ <i>l_z</i>	<i>J</i>		
1	↓							1/2	3	5/2	} <i>J</i> = <i>L</i> - <i>S</i>	² <i>F</i> _{5/2}
2	↓	↓						1	5	4		³ <i>H</i> ₄
3	↓	↓	↓					3/2	6	9/2		⁴ <i>I</i> _{9/2}
4	↓	↓	↓	↓				2	6	4		⁵ <i>I</i> ₄
5	↓	↓	↓	↓	↓			5/2	5	5/2		⁶ <i>H</i> _{5/2}
6	↓	↓	↓	↓	↓	↓		3	3	0		⁷ <i>F</i> ₀
7	↓	↓	↓	↓	↓	↓	↓	7/2	0	7/2		⁸ <i>S</i> _{7/2}
8	↑↓	↑	↑	↑	↑	↑	↑	3	3	6	} <i>J</i> = <i>L</i> + <i>S</i>	⁷ <i>F</i> ₆
9	↑↓	↑↓	↑	↑	↑	↑	↑	5/2	5	15/2		⁶ <i>H</i> _{15/2}
10	↑↓	↑↓	↑↓	↑	↑	↑	↑	2	6	8		⁵ <i>I</i> ₈
11	↑↓	↑↓	↑↓	↑↓	↑	↑	↑	3/2	6	15/2		⁴ <i>I</i> _{15/2}
12	↑↓	↑↓	↑↓	↑↓	↑↓	↑	↑	1	5	6		³ <i>H</i> ₆
13	↑↓	↑↓	↑↓	↑↓	↑↓	↑↓	↑	1/2	3	7/2		² <i>F</i> _{7/2}
14	↑↓	↑↓	↑↓	↑↓	↑↓	↑↓	↑↓	0	0	0		¹ <i>S</i> ₀

Magnetic moments of ions with partially filled shells

1. Let $J = 0$:

$$\text{Then } \langle 0 | \hat{L}_z + g_0 \hat{S}_z | 0 \rangle = 0$$

If we suppose that only the ground state is occupied, we obtain

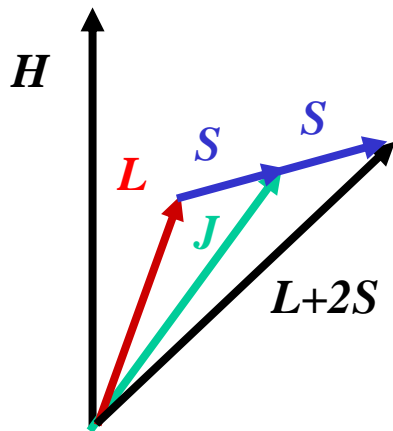
$$\chi = \chi_{dia} + 2\mu_B^2 \frac{N}{V} \sum_n \frac{|\langle n | \hat{L}_z + g_0 \hat{S}_z | 0 \rangle|^2}{\epsilon_n - \epsilon_0}$$

negative
positive

van Vleck paramagnetism (a weak effect)

2. Let $J \neq 0$:

Complication!!!!



m i.e. $J+S$ will precess fast about J , and J will precess much slower about H . Thus, for magnetism only the time average component of the magnetisation m_{\parallel} parallel to J counts.

Wigner-Eckart theorem:

$$\langle JLSJ_z | \hat{L}_z + g_0 \hat{S}_z | JLSJ_z' \rangle = g(J, L, S) J_z \delta_{J_z J_z'}$$

Landé factor

$$g(J, L, S) = 1 + \frac{J(J+1) - L(L+1) + S(S+1)}{2J(J+1)}$$

The full magnetic moment of the shell is $\hat{\mathbf{m}} = -\mu_B (\hat{\mathbf{L}} + g_0 \hat{\mathbf{S}})$

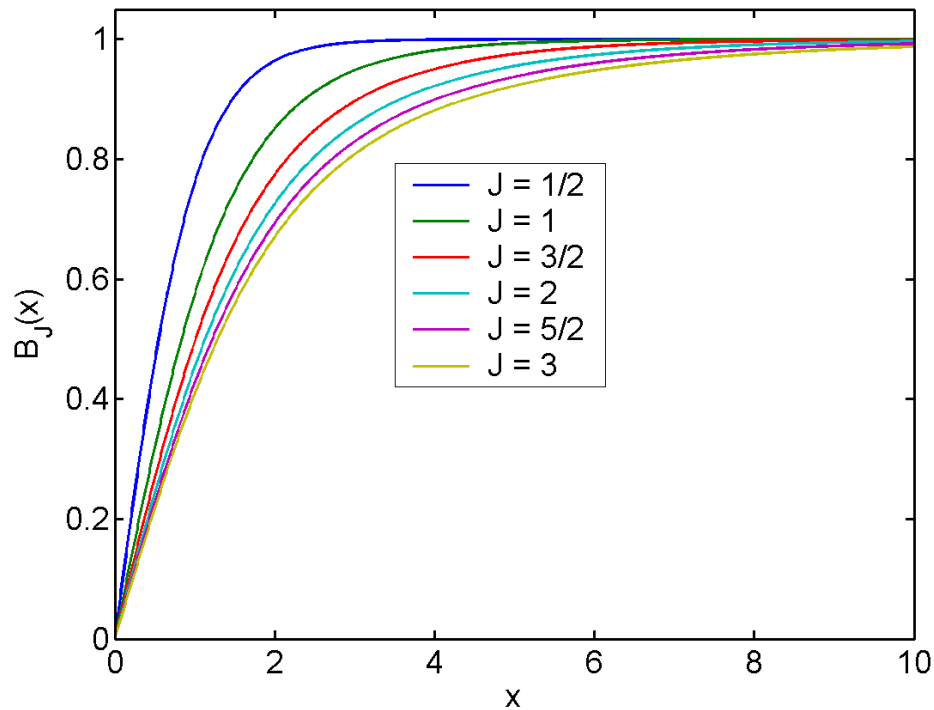
Its component parallel to \mathbf{J} is $\hat{\mathbf{m}}_{\parallel} = -g\mu_B \hat{\mathbf{J}}$

The potential energy of the shell in an external magnetic field $\mathcal{E} = g\mu_B B J_z$

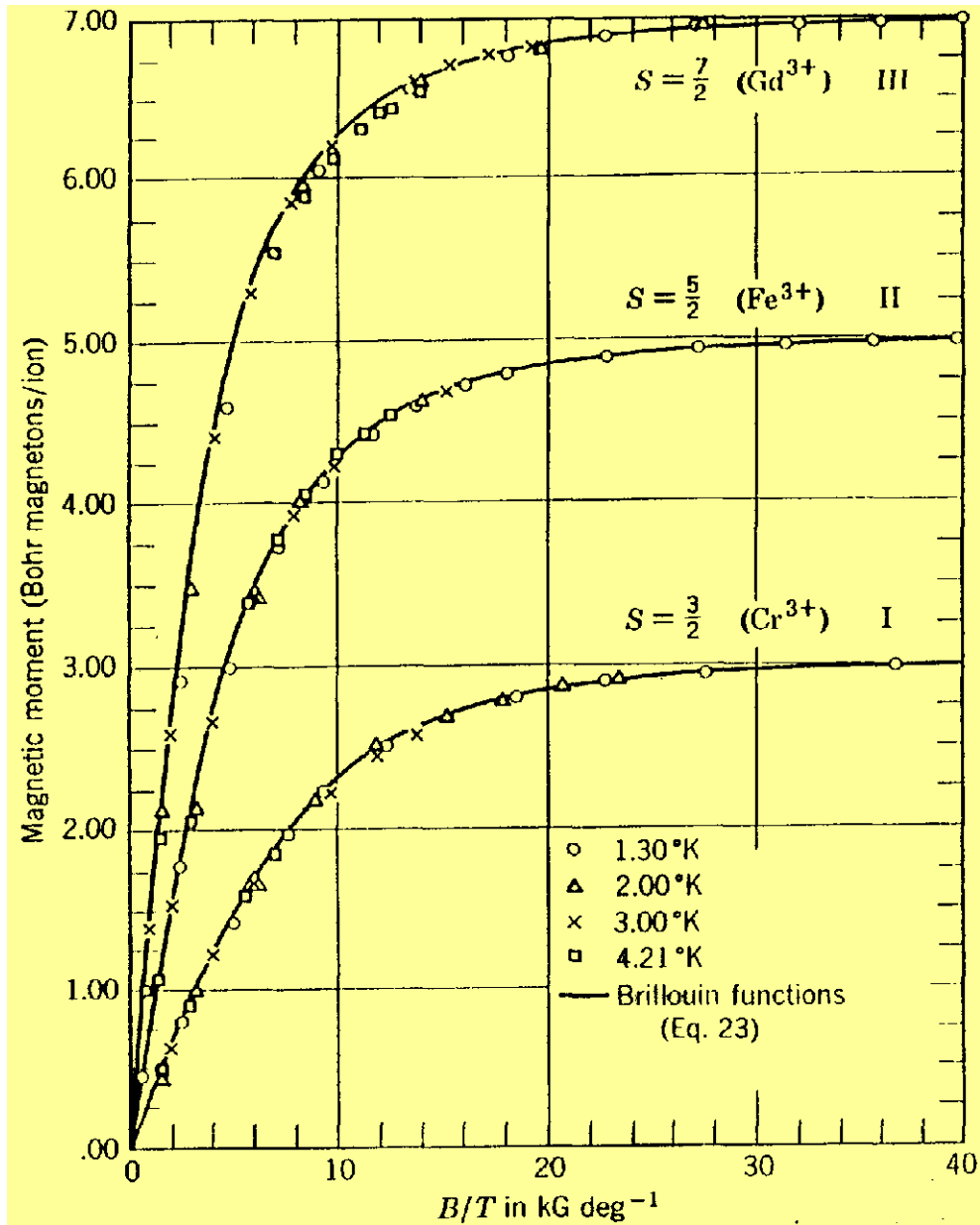
Paramagnetic susceptibility

$$e^{-F/(k_B T)} = \sum_{J_z=-J}^J e^{-g\mu_B J_z/(k_B T)}, M = -\frac{N}{V} \frac{\partial F}{\partial B} = \frac{N}{V} g\mu_B J B_J \left(\frac{g\mu_B J B}{k_B T} \right)$$

The Brillouin function $B_J(x) = \frac{2J+1}{2J} \coth\left(\frac{2J+1}{2J}x\right) - \frac{1}{2J} \coth\left(\frac{1}{2J}x\right)$



Examples



Asymptotic behaviour:

saturated value: $T \rightarrow 0$ or $B \rightarrow \infty: M \rightarrow \frac{N}{V} g\mu_B J$

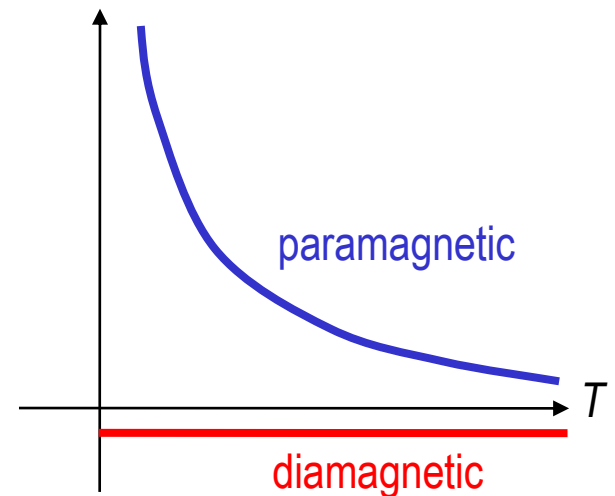
small arguments of the Brillouin function:

$$T \rightarrow \infty \text{ or } B \rightarrow 0: M \rightarrow \frac{N}{V} (g\mu_B)^2 \frac{J(J+1)}{3k_B T} B$$

Paramagnetic susceptibility:

$$\chi = \frac{N}{V} \mu_0 (g\mu_B)^2 \frac{J(J+1)}{3k_B T} = \frac{C}{T}$$

The Curie law



Magnetic moments of ions in a condensed system

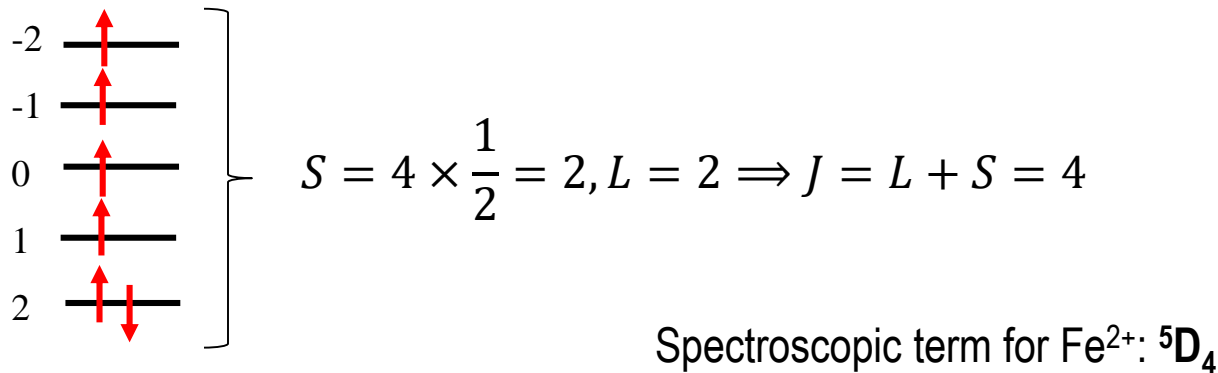
The Curie law

$$\chi = \frac{N}{V} \mu_0 \frac{(\mu_B p_{eff})^2}{3k_B T}$$

3d ions:

Example: FeCl_2 with ionicity Fe^{2+} : Atomic Fe has the electronic configuration $3d^6 4s^2$, in the compound the configuration is $3d^6$, i.e. the 6 electrons in the d-shell are left.

Level scheme for the d-shell according to Hund's rule:



Expected g_j value:
$$g = 1 + \frac{4 \times 5 + 2 \times 3 - 2 \times 3}{2 \times 4 \times 5} = \frac{3}{2}$$

from which we calculate the effective moment $p_{eff} = \frac{3}{2} \sqrt{20} \approx 6.7$

Considering only $J = S$, then $p_{eff} = 4.9$.

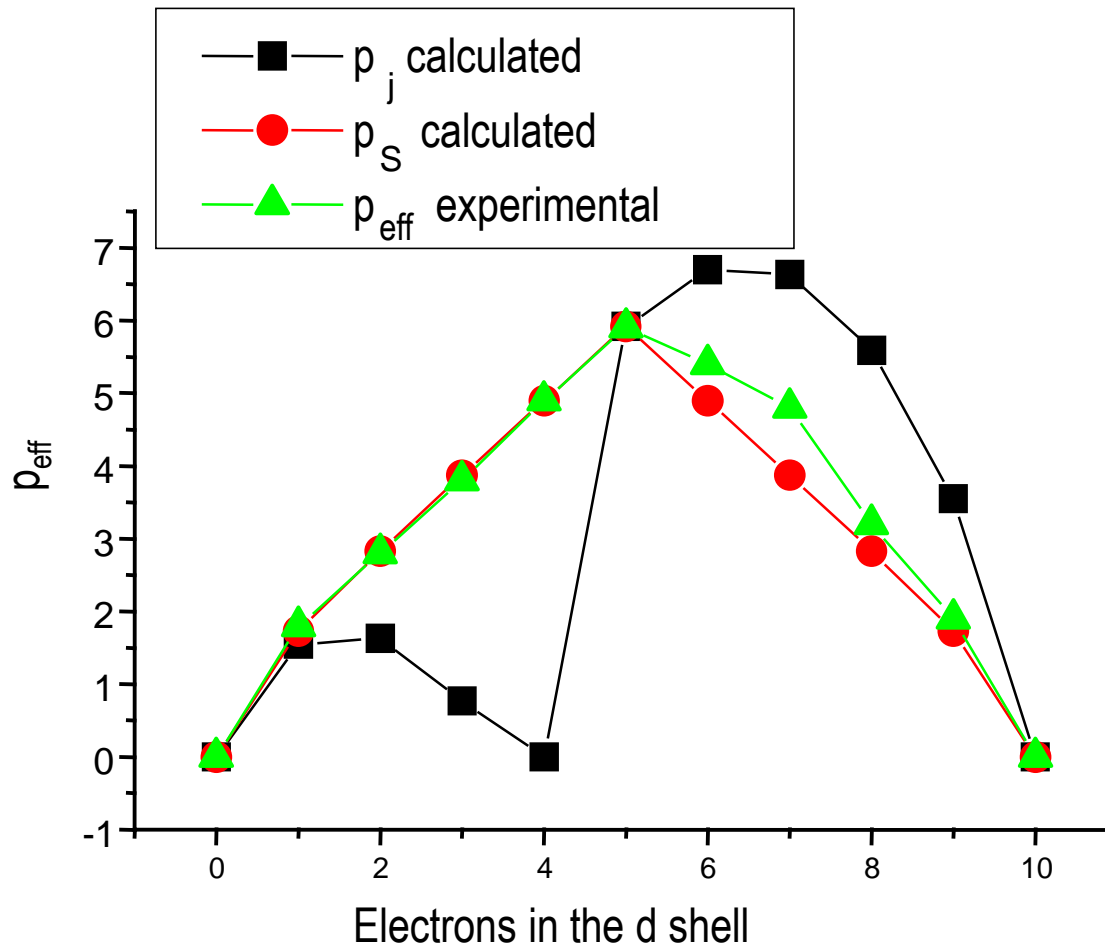
Experimental value: $p_{eff} = 5.4$
 \Rightarrow closer to $J = S$ than to $J = L+S$

In most cases of transition metal ions, the orbital moment appears to be quenched.

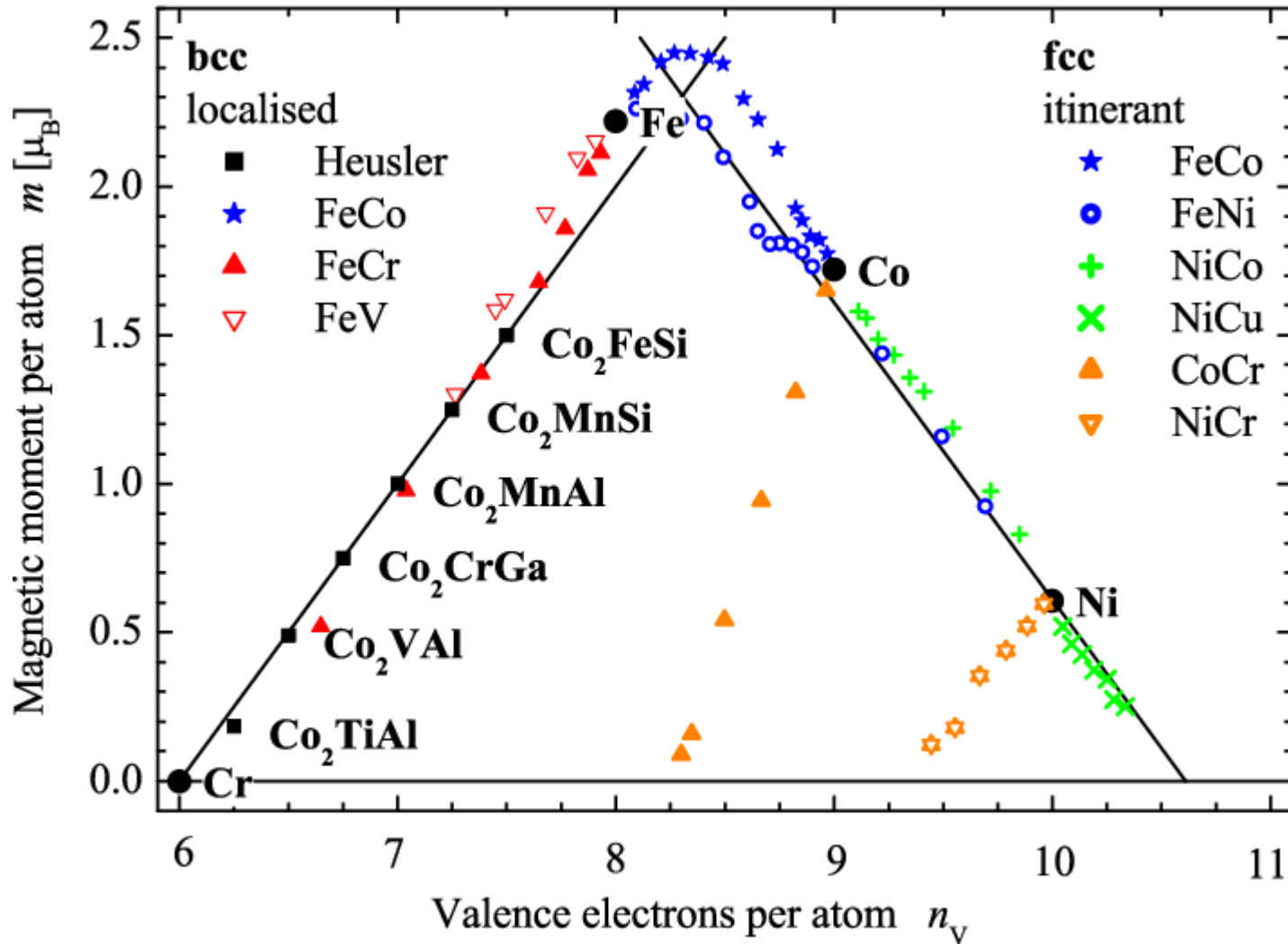
CALCULATED AND MEASURED EFFECTIVE MAGNETON NUMBERS p FOR THE IRON ($3d$) GROUP IONS^a

ELEMENT (AND IONIZATION)	BASIC ELECTRON CONFIGURATION	GROUND- STATE TERM	CALCULATED ^b p		MEASURED ^c p
			$(J = S)$	$(J = L \pm S)$	
Ti ³⁺	$3d^1$	${}^2D_{3/2}$	1.73	1.55	—
V ⁴⁺	$3d^1$	${}^2D_{3/2}$	1.73	1.55	1.8
V ³⁺	$3d^2$	3F_2	2.83	1.63	2.8
V ²⁺	$3d^3$	${}^4F_{3/2}$	3.87	0.77	3.8
Cr ³⁺	$3d^3$	${}^4F_{3/2}$	3.87	0.77	3.7
Mn ⁴⁺	$3d^3$	${}^4F_{3/2}$	3.87	0.77	4.0
Cr ²⁺	$3d^4$	5D_0	4.90	0	4.8
Mn ³⁺	$3d^4$	5D_0	4.90	0	5.0
Mn ²⁺	$3d^5$	${}^6S_{5/2}$	5.92	5.92	5.9
Fe ³⁺	$3d^5$	${}^6S_{5/2}$	5.92	5.92	5.9
Fe ²⁺	$3d^6$	5D_4	4.90	6.70	5.4
Co ²⁺	$3d^7$	${}^4F_{9/2}$	3.87	6.54	4.8
Ni ²⁺	$3d^8$	3F_4	2.83	5.59	3.2
Cu ²⁺	$3d^9$	${}^2D_{5/2}$	1.73	3.55	1.9

Magnetic moments of 3d transition metal ions as a function of electrons in the d shell

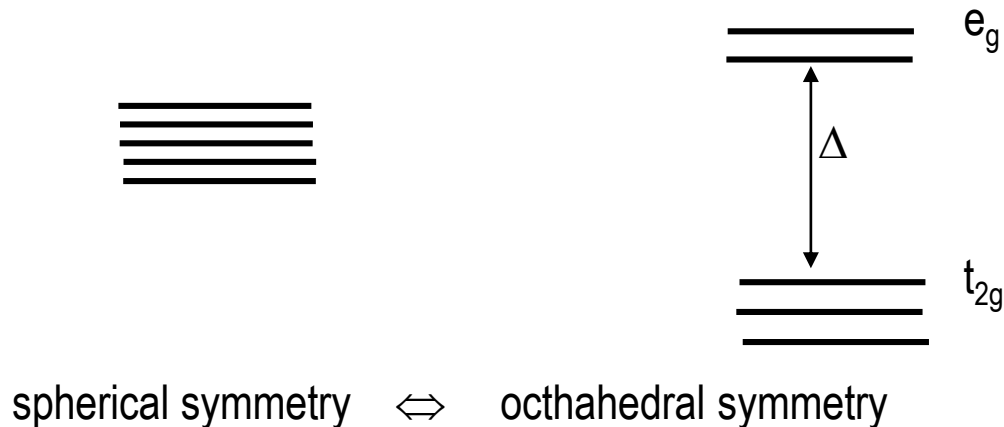


Example of the Slater-Pauling curve



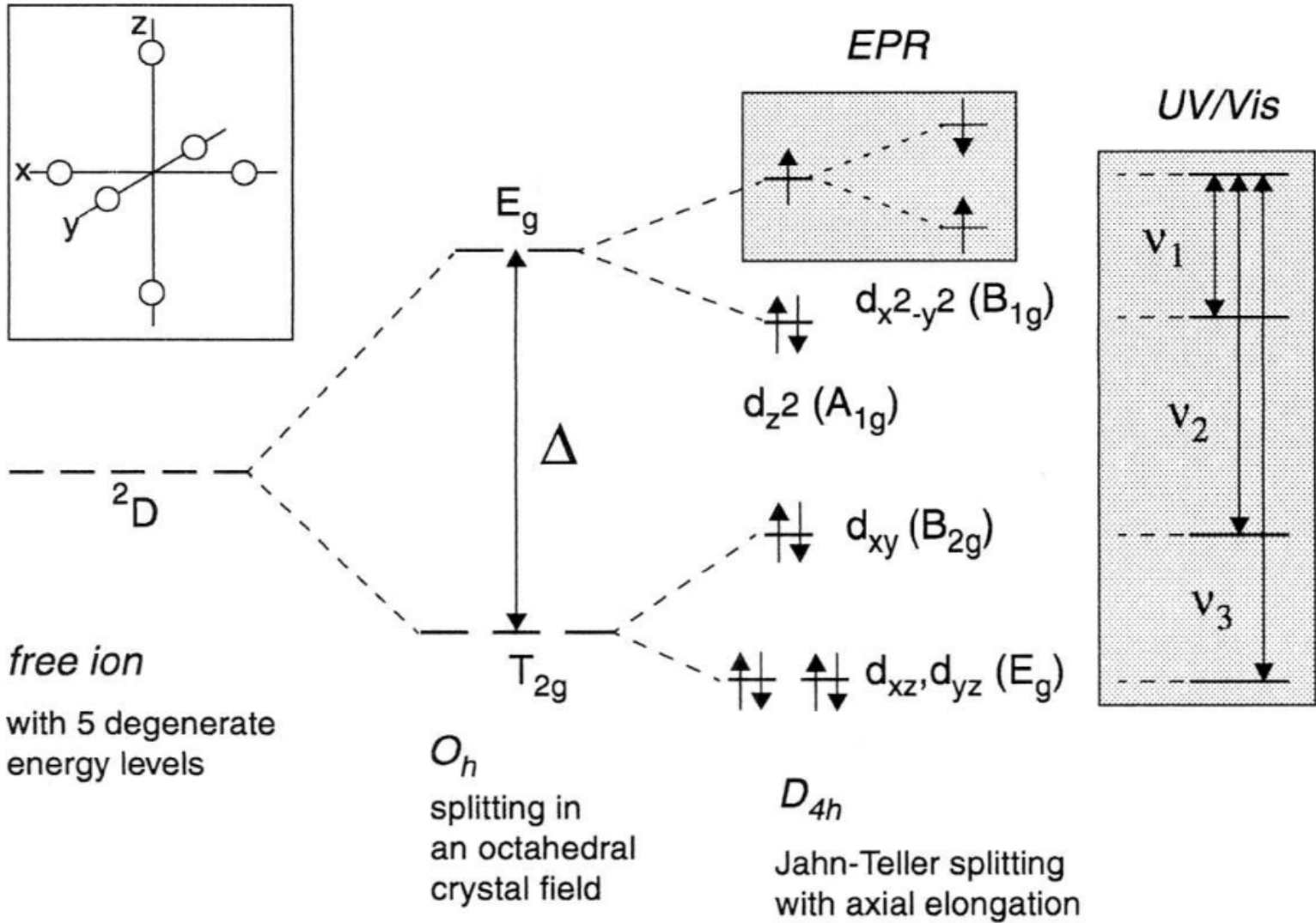
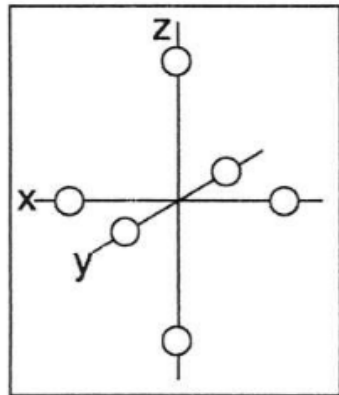
What is the reason for orbital quenching in transition metal ions?

- 3d electrons take part in chemical binding (i.e. FeCl_2 , FeF_3);
- The 3d electrons are subject to strong crystal electric fields (CEF) of the neighbouring ions;
- The CEF lifts the $2L+1$ degeneracy of the d^n - electrons;
- Lifting of degeneracy leads to an energy splitting of the d-shell:



Δ is the CEF splitting between orbitals of different symmetry; Orbital angular moments of non-degenerate levels have no fixed phase relationship;

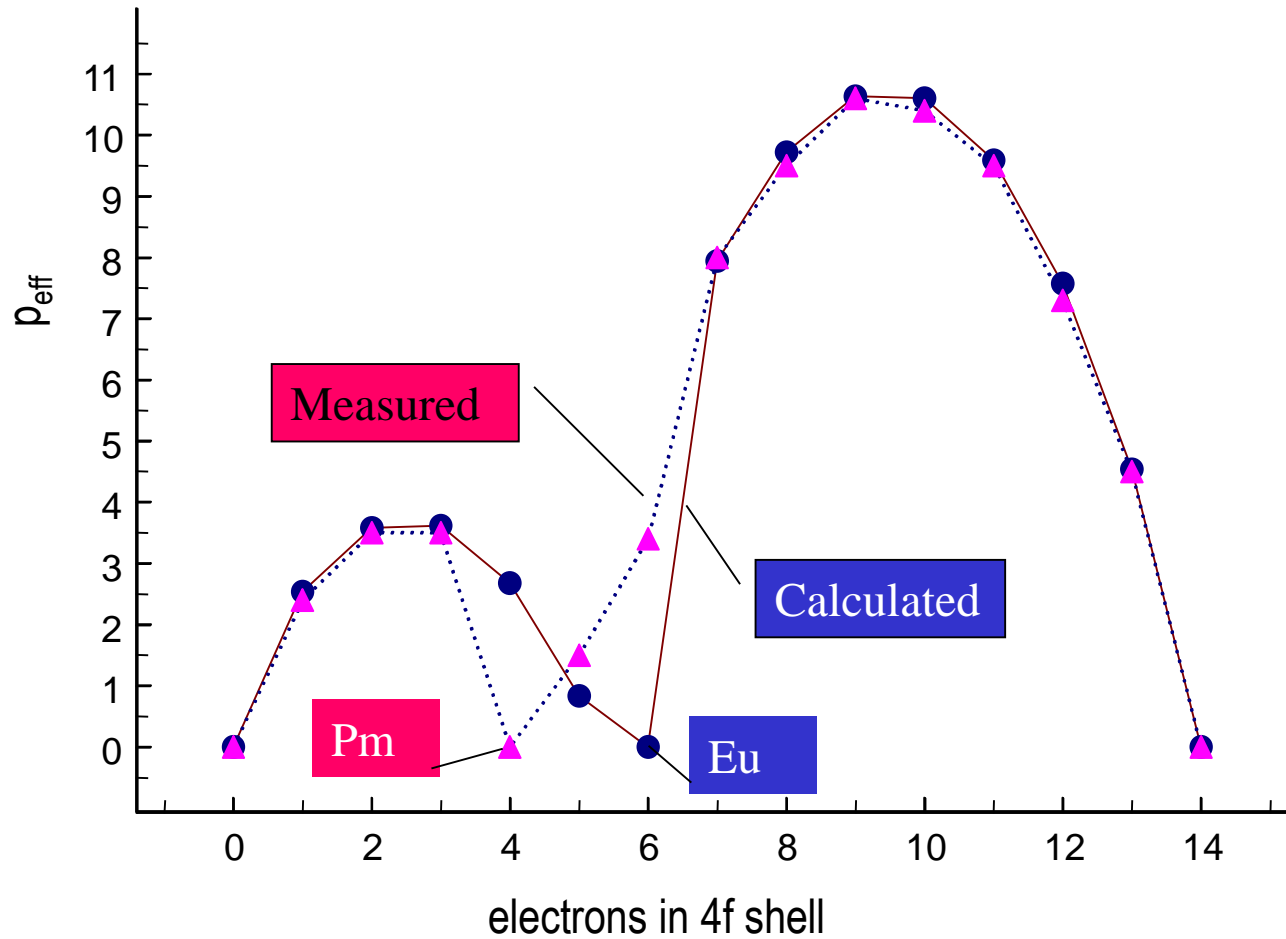
The time average expectation value for the orbital moments is then $\langle L \rangle = 0$; L is not a good quantum number.



CALCULATED AND MEASURED EFFECTIVE MAGNETON NUMBERS p FOR RARE EARTH IONS^a

ELEMENT (TRIPLY IONIZED)	BASIC ELECTRON CONFIGURATION	GROUND-STATE TERM	CALCULATED ^b p	MEASURED ^c p
La	$4f^0$	1S	0.00	diamagnetic
Ce	$4f^1$	$^2F_{5/2}$	2.54	2.4
Pr	$4f^2$	3H_4	3.58	3.5
Nd	$4f^3$	$^4I_{9/2}$	3.62	3.5
Pm	$4f^4$	5I_4	2.68	—
Sm	$4f^5$	$^6H_{5/2}$	0.84	1.5
Eu	$4f^6$	7F_0	0.00	3.4
Gd	$4f^7$	$^8S_{7/2}$	7.94	8.0
Tb	$4f^8$	7F_6	9.72	9.5
Dy	$4f^9$	$^6H_{15/2}$	10.63	10.6
Ho	$4f^{10}$	5I_8	10.60	10.4
Er	$4f^{11}$	$^4I_{15/2}$	9.59	9.5
Tm	$4f^{12}$	3H_6	7.57	7.3
Yb	$4f^{13}$	$^2F_{7/2}$	4.54	4.5
Lu	$4f^{14}$	1S	0.00	diamagnetic

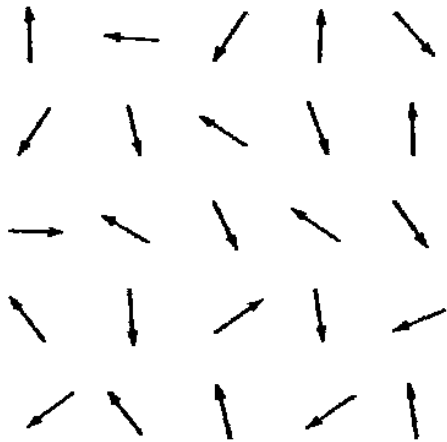
Effective magnetic moments of rare metal ions



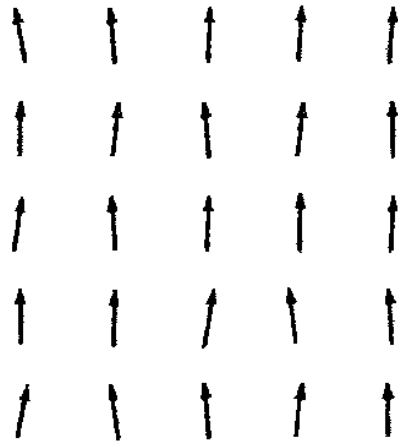
IV. MEAN FIELD THEORY

IV.4. Spontaneous ordering of magnetic moments

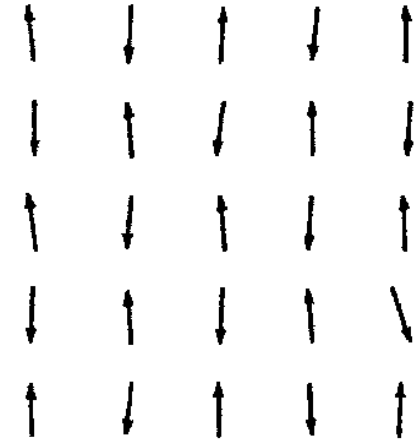
Types of the magnetic ordering:



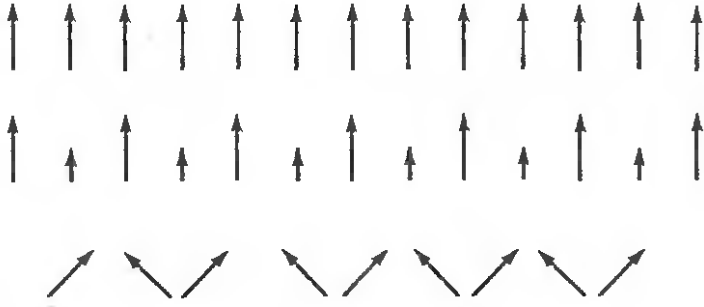
paramagnetic



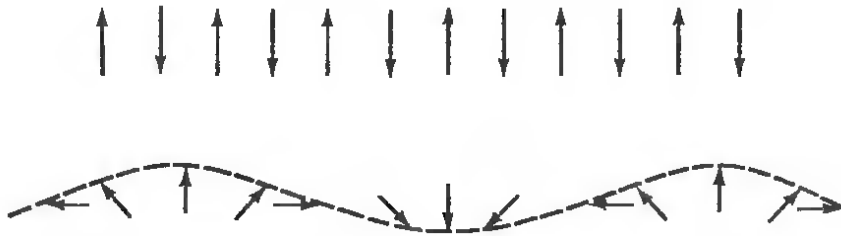
ferromagnetic



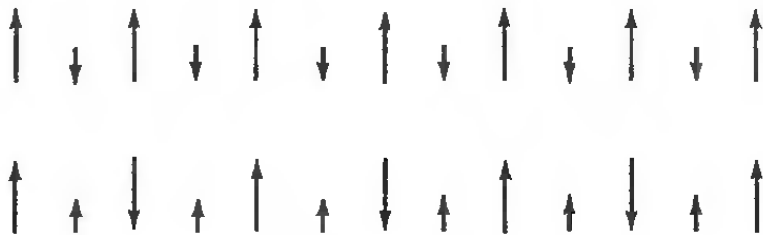
antiferromagnetic



some types of the ferromagnetic ordering



some types of the antiferromagnetic ordering



some types of the ferrimagnetic ordering

SELECTED FERROMAGNETS, WITH CRITICAL TEMPERATURES T_c AND SATURATION MAGNETIZATION M_0

MATERIAL	T_c (K)	M_0 (gauss) ^a
Fe	1043	1752
Co	1388	1446
Ni	627	510
Gd	293	1980
Dy	85	3000
CrBr ₃	37	270
Au ₂ MnAl	200	323
Cu ₂ MnAl	630	726
Cu ₂ MnIn	500	613
EuO	77	1910
EuS	16.5	1184
MnAs	318	870
MnBi	670	675
GdCl ₃	2.2	550

^a At $T = 0$ (K).

Source: F. Keffer, *Handbuch der Physik*, vol. 18, pt. 2, Springer, New York, 1966; P. Heller, *Rep. Progr. Phys.*, 30, (pt. II), 731 (1967).

SELECTED ANTIFERROMAGNETS, WITH CRITICAL TEMPERATURES T_c

MATERIAL	T_c (K)	MATERIAL	T_c (K)
MnO	122	KCoF ₃	125
FeO (wüstite)	198	MnF ₂	67.34
CoO	291	FeF ₂	78.4
NiO	600	CoF ₂	37.7
RbMnF ₃	54.5	MnCl ₂	2
KFeF ₃	115	VS	1040
KMnF ₃	88.3	Cr	311

Source: F. Keffer, *Handbuch der Physik*, vol. 18, pt. 2, Springer, New York, 1966.

SELECTED FERRIMAGNETS, WITH CRITICAL TEMPERATURES T_c AND SATURATION MAGNETIZATION M_0

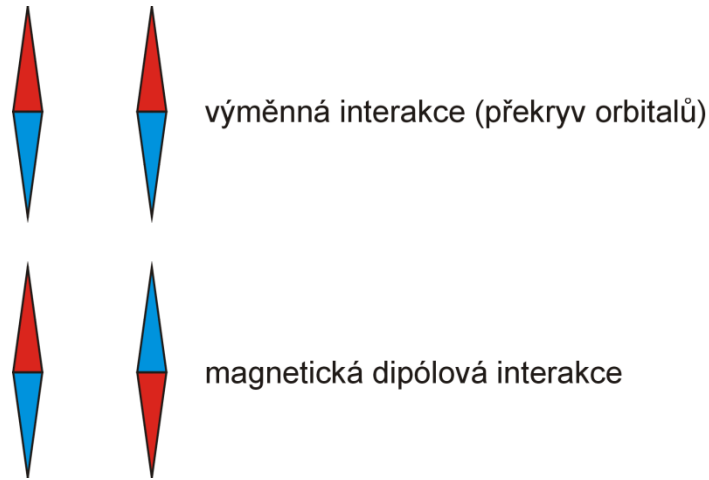
MATERIAL	T_c (K)	M_0 (gauss) ^a
Fe ₃ O ₄ (magnetite)	858	510
CoFe ₂ O ₄	793	475
NiFe ₂ O ₄	858	300
CuFe ₂ O ₄	728	160
MnFe ₂ O ₄	573	560
Y ₃ Fe ₅ O ₁₂ (YIG)	560	195

^a At $T = 0$ (K).

Source: F. Keffer, *Handbuch der Physik*, vol. 18, pt. 2, Springer, New York, 1966.

Hematite Fe₂O₃ is a weak antiferromagnetic below 250K, canted antiferromagnetic (or weakly ferromagnetic) between 250K and 948K, above 948K paramagnetic

The reason of the ordering cannot be the magnetic dipole interaction – too weak!!



Exchange interaction can explain the ordering

We assume a 2-electron system, we neglect the spin-dependence of the hamiltonian. The non-perturbed hamiltonian is

$$\hat{H}\psi(\mathbf{r}_1, \mathbf{r}_2) = \left[-\frac{\hbar^2}{2m} (\Delta_1 + \Delta_2) + V(\mathbf{r}_1, \mathbf{r}_2) \right] \psi(\mathbf{r}_1, \mathbf{r}_2) = E\psi(\mathbf{r}_1, \mathbf{r}_2)$$

The wave function (with spin variables)

$$\Psi(\mathbf{r}_1, s_1, \mathbf{r}_2, s_2) = \psi(\mathbf{r}_1, \mathbf{r}_2)\chi(s_1, s_2)$$

The non-perturbed hamiltonian

$$\hat{H}_0 = -\frac{\hbar^2}{2m}(\nabla_1^2 + \nabla_2^2) + V(\mathbf{r}_1) + V(\mathbf{r}_2)$$

Perturbance

$$\hat{H}' = \frac{e^2}{4\pi\epsilon_0|\mathbf{r}_1 - \mathbf{r}_2|}$$

We consider two one-electron eigenstates of \mathbf{H}_0 :

$$\hat{H}_0\psi_j(\mathbf{r}) = E_j\psi_j(\mathbf{r}), j = a, b$$

The energy level is 4 times degenerated. We choose the following eigenfunctions:

$$S = 0, S_z = 0: \Psi_S = \frac{1}{2}[\psi_a(\mathbf{r}_1)\psi_b(\mathbf{r}_2) + \psi_a(\mathbf{r}_2)\psi_b(\mathbf{r}_1)][\alpha(s_1)\beta(s_2) - \alpha(s_2)\beta(s_1)]$$

$$S = 1, S_z = 1: \Psi_{T1} = \frac{1}{\sqrt{2}}[\psi_a(\mathbf{r}_1)\psi_b(\mathbf{r}_2) - \psi_a(\mathbf{r}_2)\psi_b(\mathbf{r}_1)]\alpha(s_1)\alpha(s_2)$$

$$S = 1, S_z = 0: \Psi_{T2} = \frac{1}{2}[\psi_a(\mathbf{r}_1)\psi_b(\mathbf{r}_2) - \psi_a(\mathbf{r}_2)\psi_b(\mathbf{r}_1)][\alpha(s_1)\beta(s_2) + \alpha(s_2)\beta(s_1)]$$

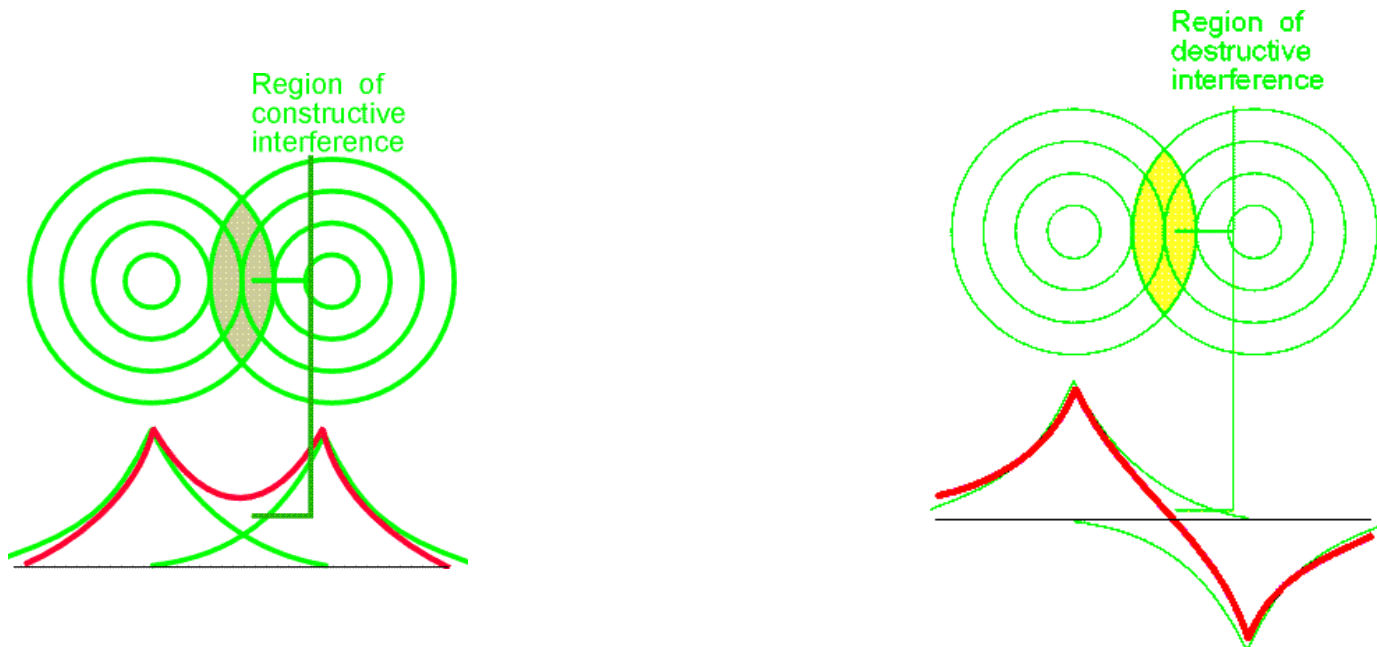
$$S = 1, S_z = -1: \Psi_{T3} = \frac{1}{\sqrt{2}}[\psi_a(\mathbf{r}_1)\psi_b(\mathbf{r}_2) - \psi_a(\mathbf{r}_2)\psi_b(\mathbf{r}_1)]\beta(s_1)\beta(s_2)$$

The 1st iteration, perturbation theory – shifts of the energies:

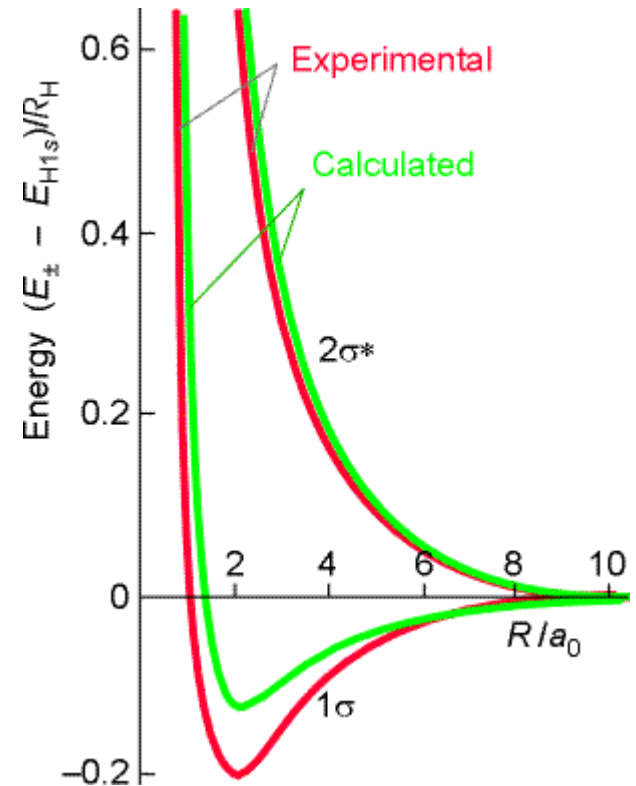
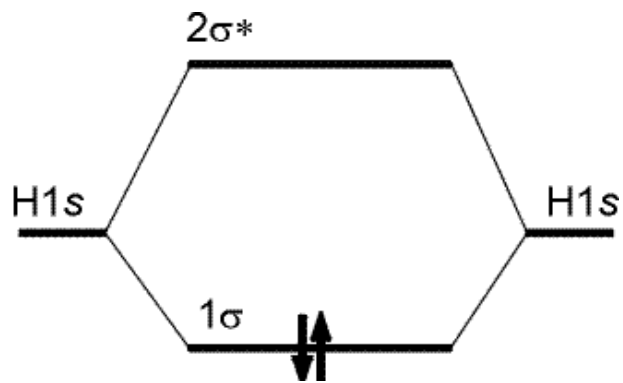
$$E_T = \langle \Psi_{Tj} | \hat{H}' | \Psi_{Tj} \rangle = E_1 - J, j = 1, 2, 3, E_S = \langle \Psi_S | \hat{H}' | \Psi_S \rangle = E_1 + J$$

$$E_1 = \int d^3 r_1 \int d^3 r_2 |\psi_a(r_1)|^2 \hat{H}' |\psi_b(r_2)|^2, J = \int d^3 r_1 \int d^3 r_2 \psi_a(r_1)^* \psi_b(r_1) \hat{H}' \psi_b(r_2)^* \psi_a(r_2)$$

J is the exchange integral. From one 4times degenerated level, one non-degenerated (singlet) and one 3times degenerated (triplet).

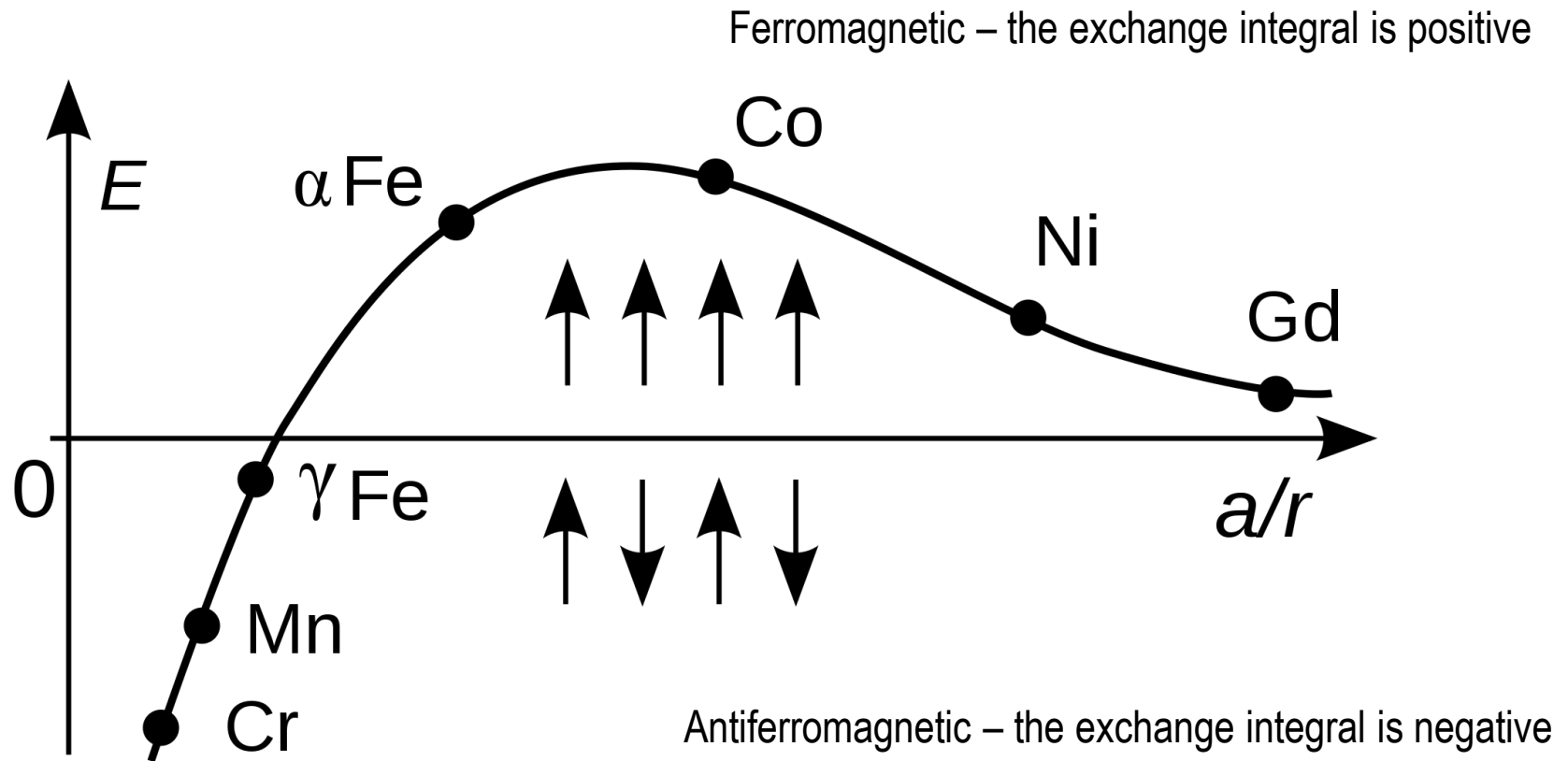


Numerical calculations: H₂ molecule



the singlet state has lower energy than the triplet \Rightarrow the singlet state (antiferromagnetic) is bonding, the triplet state (ferromagnetic) is antibonding

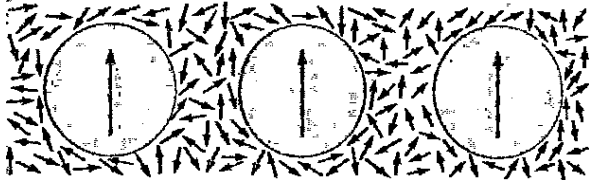
Bethe-Slater curve – the dependence of the exchange integral on the interatomic distance for 3d metals



By Zureks - Own work, CC0, <https://commons.wikimedia.org/w/index.php?curid=9788329>

Direct exchange – important in 3d metals

Indirect exchange: mediated by the spins of conduction electrons – important in 4f metals

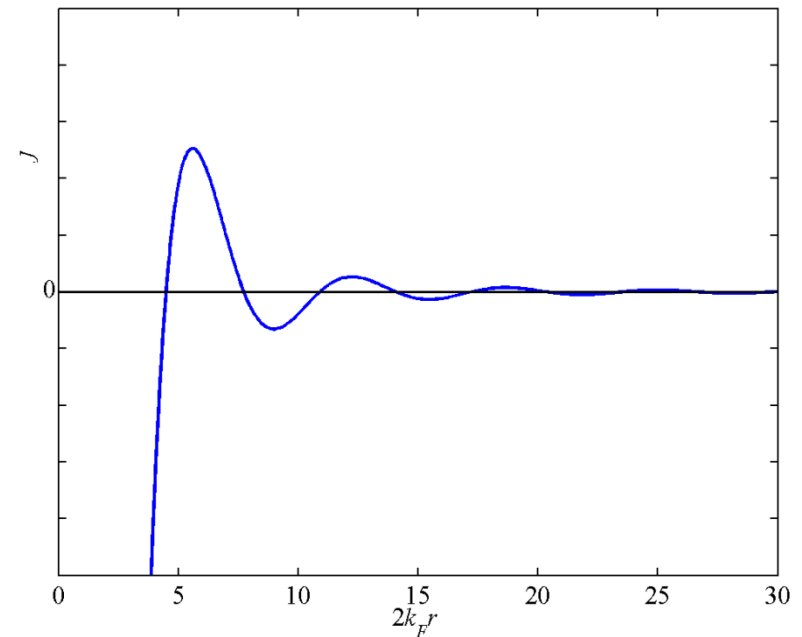


RKKY interaction (*Ruderman-Kittel-Kasuya-Yosida*)

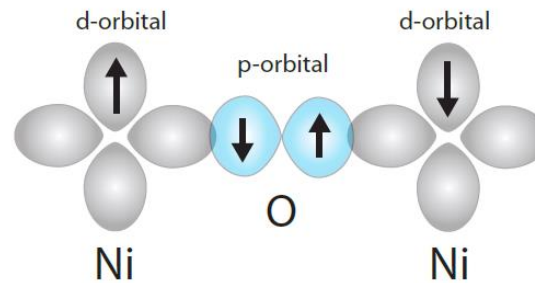
$$J_{\text{RKKY}} \propto \frac{2k_F r \sin(2k_F r) - \cos(2k_F r)}{(2k_F r)^4}$$

If $J > 0$, prefer triplet state or FM

If $J < 0$, prefer singlet state or AF

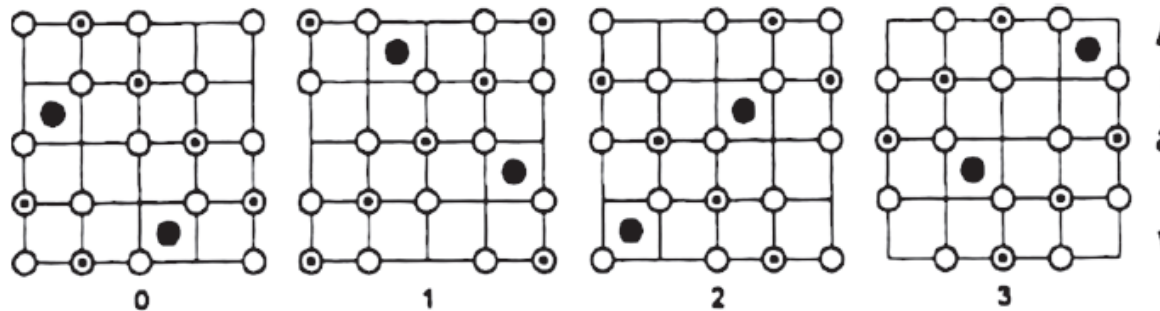
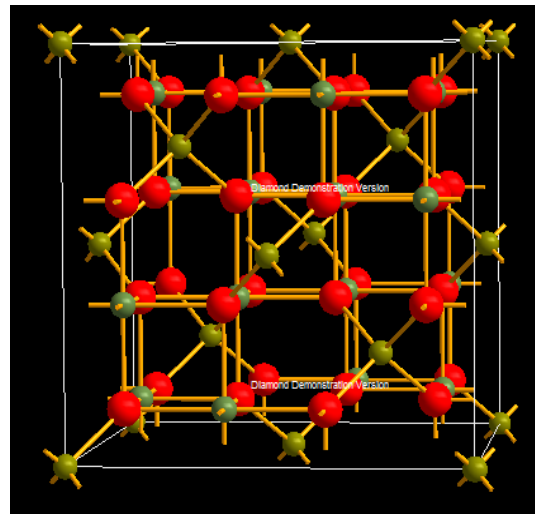
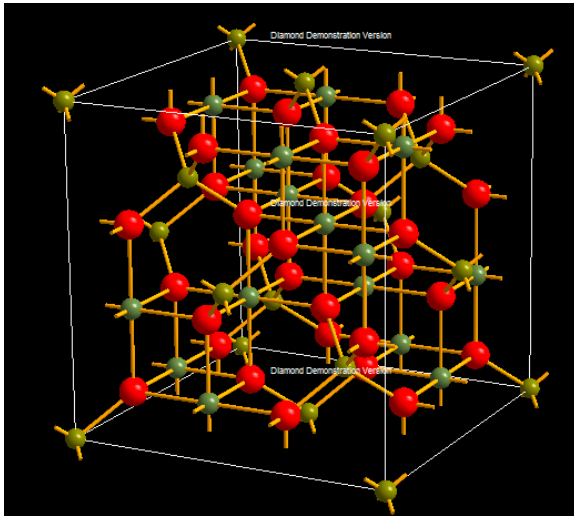


Super-exchange interaction:



Ferrimagnetism:

Typical example – $\text{Fe}_3\text{O}_4 \equiv (\text{Fe}^{2+}\text{O})(\text{Fe}^{3+}_2\text{O}_3)$
 Magnetite crystal structure (inverse spinel)



Layers at heights 0, $a/4$, $a/2$, $3a/4$

● A At height $a/8$ above layer
 ○ O^{2-} ⊙ B

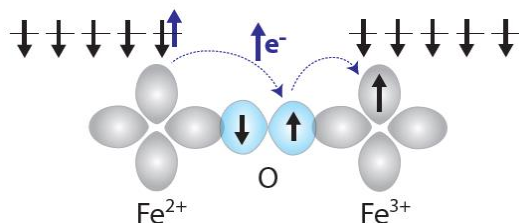
A ...tetrahedral sites
 B ...octahedral sites

The Fe^{2+} ion ($3d^6$) has $m = 4\mu_B$ while the Fe^{3+} ion ($3d^5$) has $m = 5\mu_B$

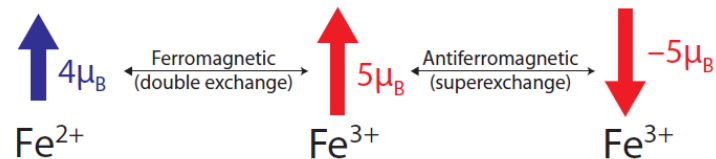
The B-O-B bond angle is 90 deg, the A-O-A angle is 80 deg and the A-O-B angle is 125 deg. The super-exchange interaction is therefore strongest across the A-O-B bond, so that magnetic moments on A sites anti-align with those on the B sites.

There are two principal arrangements of the 8 divalent and 16 trivalent metal ions onto the 8 tetrahedral A sites and 16 octahedral B sites of the spinel structure. The first, called normal spinel has divalent metal ions on A sites and trivalent ions on B sites. This is sometimes written $(\text{M}^{2+})[\text{M}^{3+}]_2\text{O}_4$, where the brackets indicate the A() and B[] sites. Inverse spinel has half the trivalent ions on A sites, the other half on B sites, and all the divalent ions also on B sites. This can be written as $(\text{M}^{3+})_2[\text{M}^{2+}\text{M}^{3+}]\text{O}_4$. Most simple ferrites (such as Fe_3O_4) have this inverse spinel structure. In this case, the anti-ferromagnetic superexchange interaction between ions on sites A and B is such that the magnetic moments of the trivalent ions (e.g. Fe^{3+}) anti-align.

Ferromagnetic double exchange interaction



Resulting spin alignment



The Heisenberg spin hamiltonian

Phenomenologically constructed operator acting on the spin wave function having the same eigenvalues and eigenfunctions as the full hamiltonian.

Let us assume a 2-spin systems with the effective spin operators \hat{S}_1, \hat{S}_2

The following formulas hold:

$$\hat{S}_j^2 \chi_j(s_j) = S_j(S_j + 1) \chi_j(s_j) = \frac{3}{4} \chi_j(s_j), \quad \text{since } S_{1,2} = \frac{1}{2}$$

$$\hat{S}^2 \chi(s_1, s_2) = (\hat{S}_1 + \hat{S}_2)^2 \chi(s_1, s_2) = \left(\frac{3}{2} + 2\mathbf{S}_1 \cdot \mathbf{S}_2 \right) \chi(s_1, s_2)$$

Therefore,
$$\hat{S}_1 \cdot \hat{S}_2 \chi = -\frac{3}{4} \chi (S = 0), \quad \hat{S}_1 \cdot \hat{S}_2 \chi = +\frac{1}{4} \chi (S = 1)$$

We define
$$\hat{H}_S = \frac{1}{4}(E_S + 3E_T) - (E_S - E_T) \hat{S}_1 \cdot \hat{S}_2 = \text{const} - 2J \hat{S}_1 \cdot \hat{S}_2$$

and
$$\hat{H}_S \chi(S = 0) = E_S \chi(S = 0), \quad \hat{H}_S \chi(S = 1) = E_T \chi(S = 1)$$

The Heisenberg hamiltonian for a spin system
$$\hat{H}_S = -\sum_{i \neq j} J_{ij} \hat{S}_i \cdot \hat{S}_j$$

With an external magnetic field:
$$\hat{H}_S = -\sum_{i \neq j} J_{ij} \hat{S}_i \cdot \hat{S}_j - g\mu_B \sum_j \mathbf{B} \cdot \hat{S}_j$$

The Weiss theory of molecular field

The terms in the Heisenberg hamiltonian containing $\mathbf{S}(\mathbf{R})$:

$$\Delta \hat{H}_S = -\hat{\mathbf{S}}(\mathbf{R}) \cdot \left[\sum_{R' \neq R} J(\mathbf{R} - \mathbf{R}') \hat{\mathbf{S}}(\mathbf{R}') + g\mu_B \mathbf{B} \right] \approx -g\mu_B \hat{\mathbf{S}}(\mathbf{R}) \cdot \mathbf{B}_{\text{eff}}$$

The mean-field approximation: we replace $\mathbf{S}(\mathbf{R}')$ by its average value – we neglect fluctuations. On the spin in point \mathbf{R} , the following effective field is acting

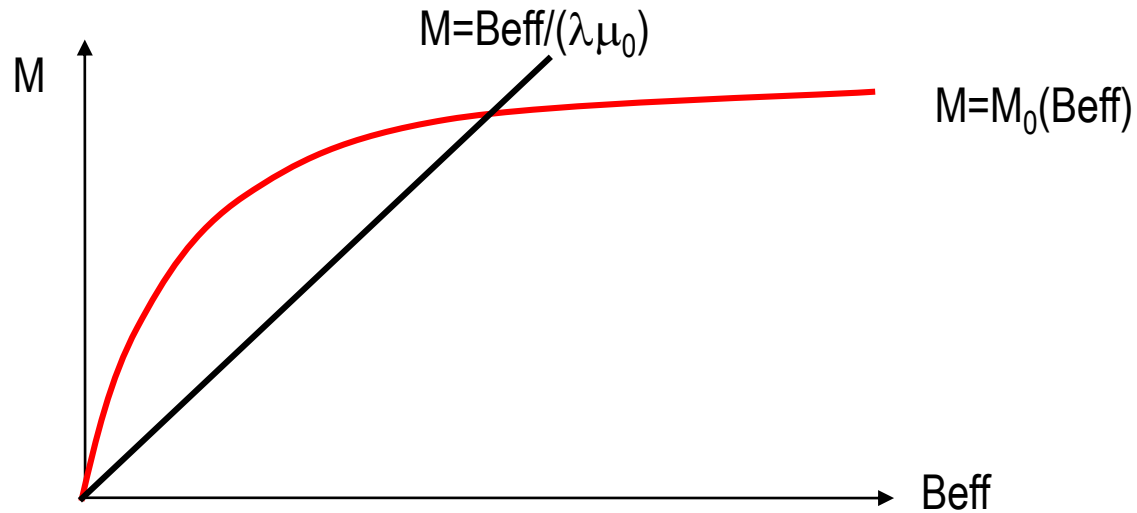
$$\mathbf{B}_{\text{eff}} = \mathbf{B} + \frac{1}{g\mu_B} \sum_{R' \neq R} J(\mathbf{R} - \mathbf{R}') \langle \hat{\mathbf{S}}(\mathbf{R}') \rangle$$

where $\langle \hat{\mathbf{S}} \rangle = \frac{V}{N} \frac{M}{g\mu_B}$ We obtain $\mathbf{B}_{\text{eff}} = \mathbf{B} + \lambda \mu_0 \mathbf{M}$ $\lambda = \frac{V}{N} \frac{\sum_{\mathbf{R} \neq 0} J(\mathbf{R})}{\mu_0 (g\mu_B)^2}$

Equation for the spontaneous magnetization $M = M_0 \left(\frac{\lambda \mu_0 M}{T} \right)$

where $M_0(B/T) = \frac{N}{V} g\mu_B S B_J \left(\frac{g\mu_B S B}{k_B T} \right)$

Numerical solution:



A non-zero solution exists if

$$\left. \frac{\partial M_0}{\partial B_{\text{eff}}} \right|_0 = \frac{1}{\mu_0} \left. \frac{\partial M_0}{\partial H_{\text{eff}}} \right|_0 = \frac{1}{\mu_0} \chi_0 = \frac{1}{\mu_0} \frac{C}{T} \geq \frac{1}{\lambda \mu_0}$$

$$T \leq T_c = \lambda C$$

The critical (Curie) temperature:

$$T_c = \frac{N}{V} \mu_0 \frac{(g\mu_B)^2}{3k_B} S(S+1)\lambda = \frac{S(S+1)}{3k_B} \sum_{R \neq 0} J(\mathbf{R})$$

For $T > T_c$ we define the susceptibility

$$\chi = \frac{\partial M}{\partial H} = \frac{\partial M}{\partial H_{\text{eff}}} \frac{\partial H_{\text{eff}}}{\partial H} = \chi_0 (1 + \lambda \chi) \Rightarrow \chi = \frac{\chi_0}{1 - \lambda \chi_0}$$

Since $\chi_0 = \frac{C}{T}$

we obtain $\chi = \frac{C}{T - T_c}$

The Curie-Weiss law

Numerical example:

$L=0, J=S=1/2, g=2$:

$$T_c = \frac{\lambda N \mu_0 \mu_B^2}{V k_B} = \lambda C$$

if $N/V \approx 9.10^{28} \text{ m}^{-3}$, we obtain $C \approx 1\text{K}$, $\lambda \approx 1000$

The exchange integral: $\sum J \approx zJ$ and we obtain $J \approx 0.03 \text{ eV}$

Spontaneous magnetization for $T < T_c$:

for small x , the Brillouin function behaves as $B_J(x) \approx Ax - Bx^3$

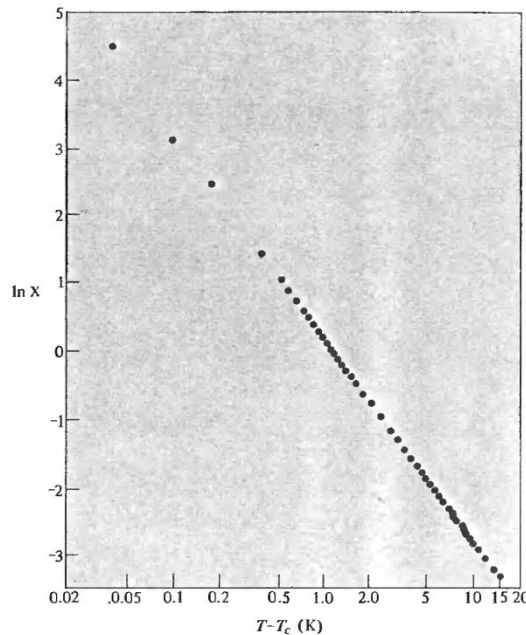
From
$$M = M_0 \left(\frac{\lambda \mu_0 M}{T} \right)$$

we obtain $M \propto (T_c - T)^{1/2}$

Experimental values for all materials: $M \propto (T_c - T)^\beta$, $\beta \approx 0.35$

Susceptibility above T_c : the mean field theory predicts $\chi \propto (T - T_c)^{-1}$

Experiment (Fe+0.16%W):

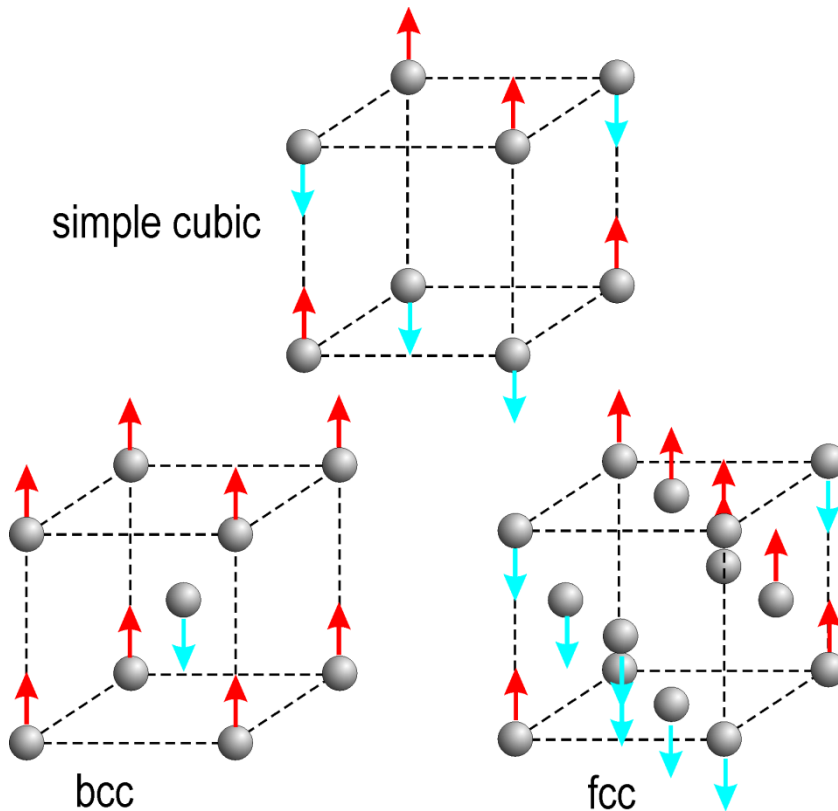


$$\chi \propto (T - T_c)^{-\gamma}, \gamma \approx 1.33$$

Critical fluctuations at T_c are important!

Mean field theory for antiferromagnets – the Néel model

Possible cubic antiferromagnetic structures:



complication in case of fcc:
the orientations of spins in a given
coordination sphere is not constant!

Two sublattices with opposite spins:

$$\mathbf{B}_{\text{eff}}^A = \mu_0 (\mathbf{H} - \lambda \mathbf{M}_B), \mathbf{B}_{\text{eff}}^B = \mu_0 (\mathbf{H} - \lambda \mathbf{M}_A)$$

Mean-field approach:

$$M_A = M_0 \left(\frac{B_{\text{eff}}^A}{T} \right), M_B = M_0 \left(\frac{B_{\text{eff}}^B}{T} \right)$$

high temperatures:

$$M_A = \frac{CB_{\text{eff}}^A}{2T\mu_0}, M_B = \frac{CB_{\text{eff}}^B}{2T\mu_0}$$

and hence

$$M_A + \frac{\lambda C}{2T} M_B = \frac{C}{2T} H$$

$$M_B + \frac{\lambda C}{2T} M_A = \frac{C}{2T} H$$

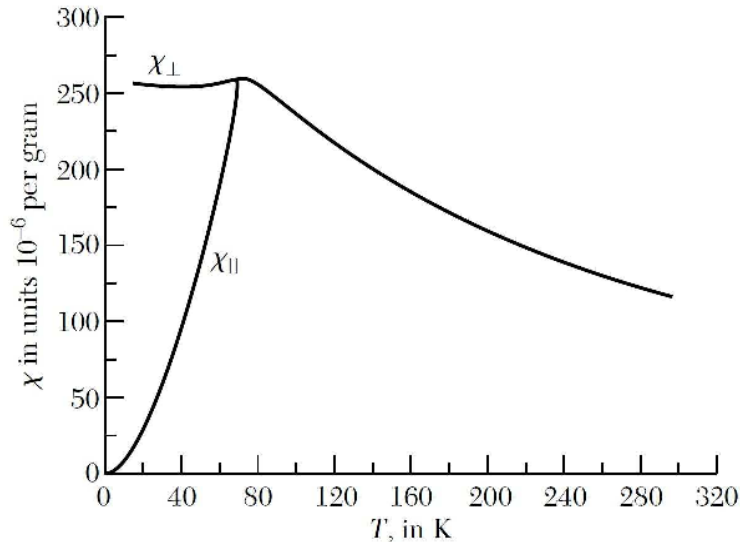
$$M = M_A + M_B = \frac{C}{T + \lambda C/2} H, \chi = \frac{M}{H} = \frac{C}{T + T_N}$$

Spontaneous magnetization follows from the equation analogous to the ferromagnetic case:

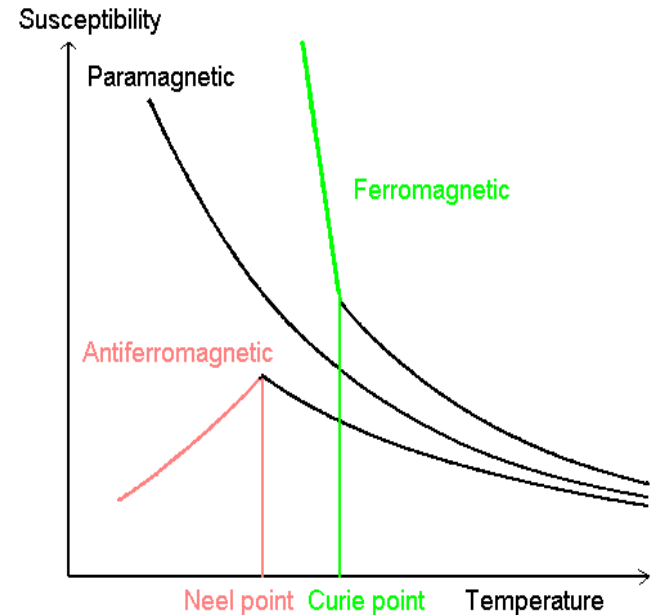
$$M_A = M_0 \left(\frac{\mu_0 \lambda M_A}{T} \right), M_B = M_0 \left(\frac{\mu_0 \lambda M_B}{T} \right)$$

since $M_A = -M_B$.

susceptibility below and above the Neel temperature:



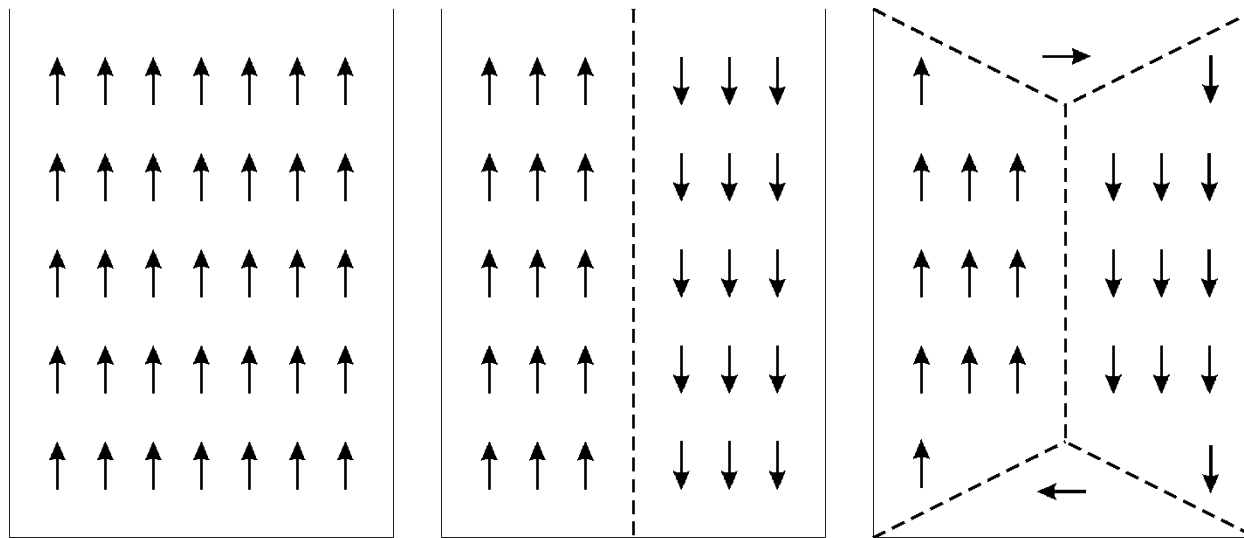
Susceptibility of MnF_2



Ferromagnetic domains

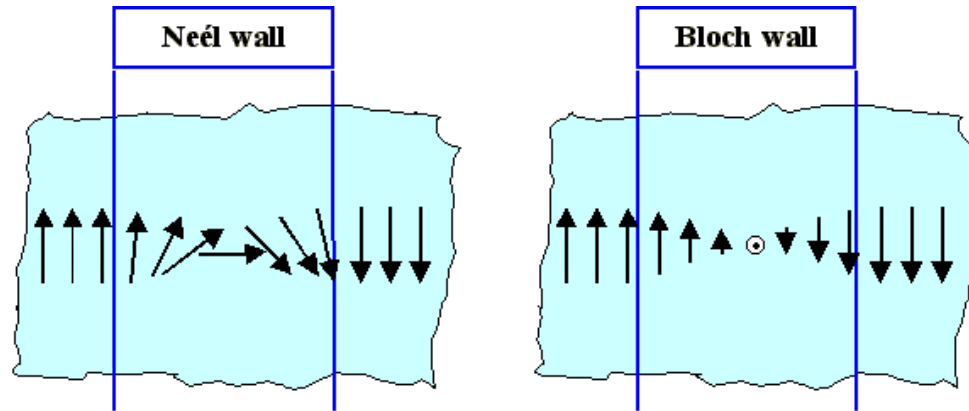
Exchange interaction \Rightarrow parallel ordering of spins

Dipole interaction \Rightarrow antiparallel ordering of spins



decreasing the dipole exchange energy

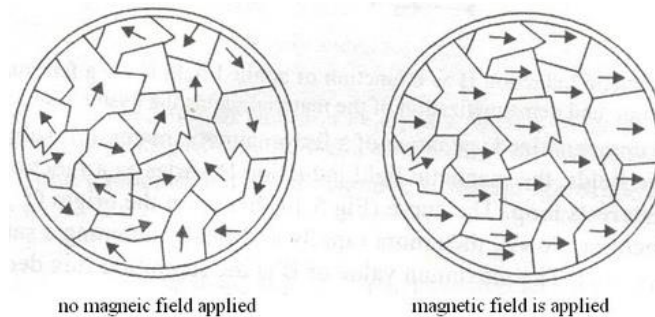
Structure of a domain wall



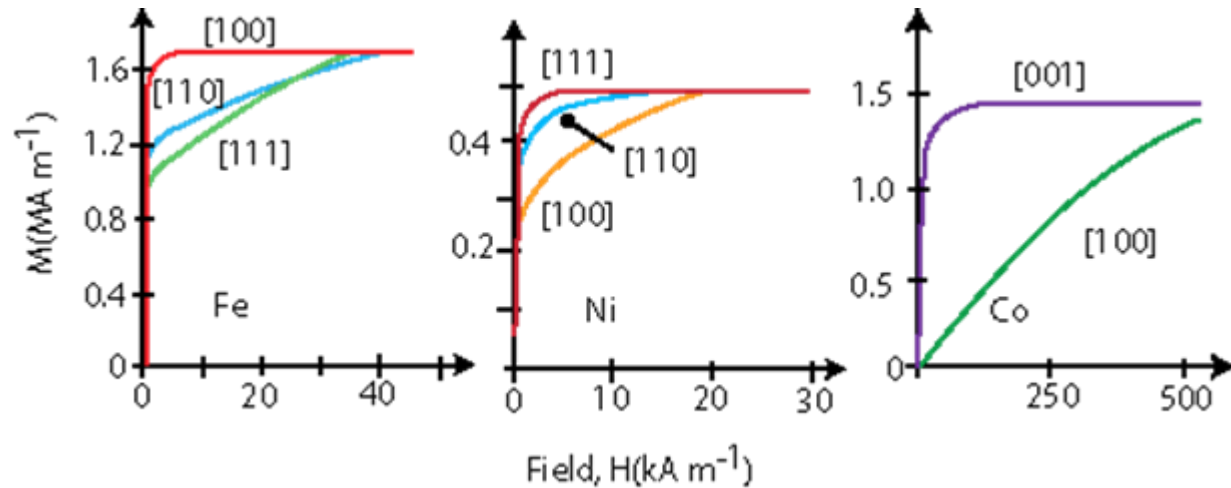
such a wall costs less energy than an abrupt wall

Energy of an abrupt wall per spin pair $\propto JS^2$

Energy of a wall with the thickness of n spins $\propto nJS^2 \cos(\pi/n) \approx JS^2(n - \pi^2/(2n))$



Magnetic anisotropy



Magnetisation of Fe, Ni and Co single crystals along different crystallographic directions. For a sufficiently large magnetising field, the saturation magnetisation M_s is always reached, however this occurs for a much smaller field when oriented along the $\langle 100 \rangle$ direction for Fe, Co, or $\langle 111 \rangle$ direction in Ni (easy axis).

Magnetisation anisotropy energy for cubic crystals

$$E = K_1(\alpha_1^2\alpha_2^2 + \alpha_2^2\alpha_3^2 + \alpha_3^2\alpha_1^2) + K_2\alpha_1^2\alpha_2^2\alpha_3^2 + \dots$$

Where $\alpha_{1,2,3}$ are the direction cosines between the magnetisation vector \mathbf{M} and the $\langle 100 \rangle$ crystallographic axes

Something about multiferroics:

Multiferroics and magnetoelectrics: thin films and nanostructures

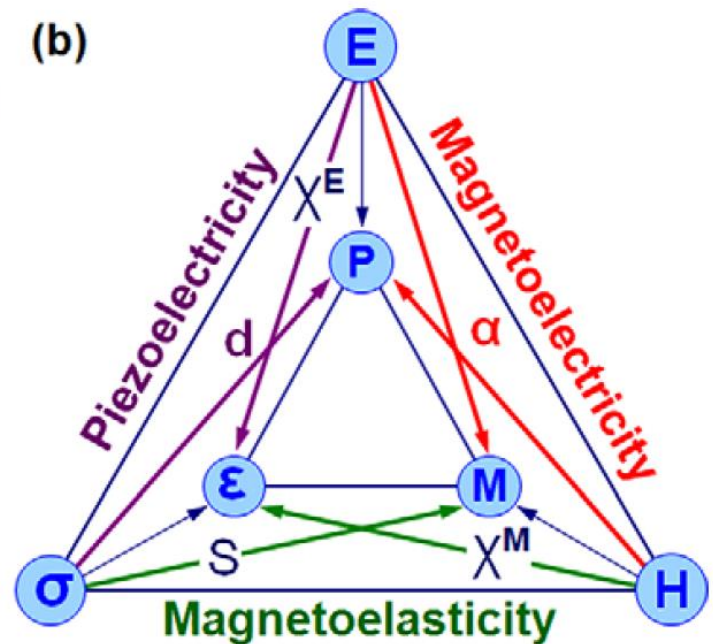
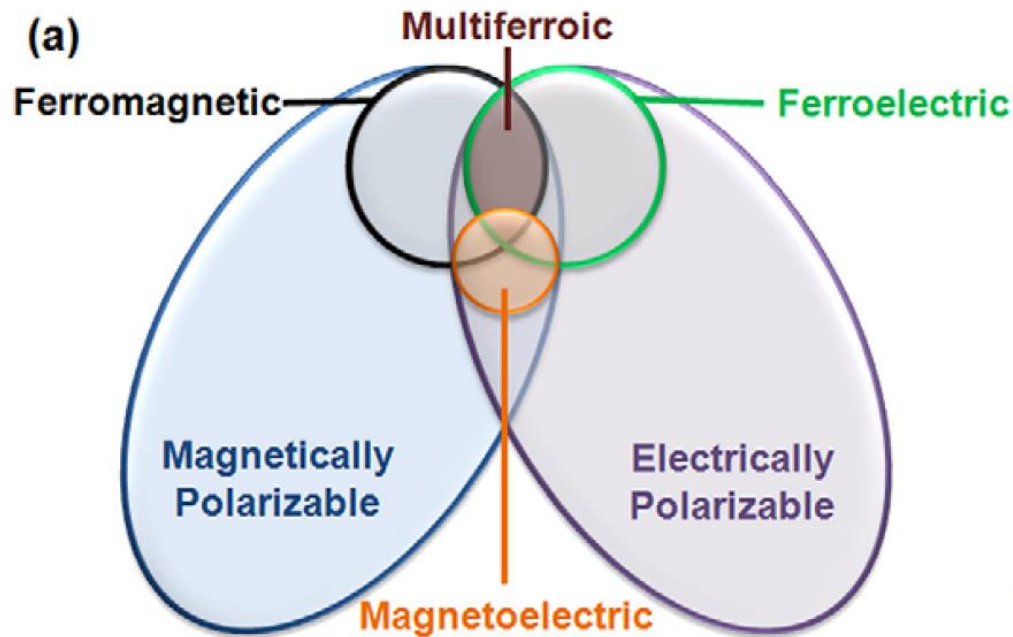
L W Martin, S P Crane, Y-H Chu, M B Holcomb, M Gajek,
M Huijben, C-H Yang, N Balke and R Ramesh

Department of Materials Science and Engineering, University of California, Berkeley,
CA 94720, USA.

Department of Physics, University of California, Berkeley, CA 94720, USA

and

Materials Sciences Division, Lawrence Berkeley National Laboratory, Berkeley,
CA 94720, USA



Free energy:

$$F(\mathbf{E}, \mathbf{H}) = F_0 - P_i^S E_i - M_i^S H_i - \frac{1}{2} \epsilon_0 \epsilon_{ij} E_i E_j - \frac{1}{2} \mu_0 \mu_{ij} H_i H_j - \frac{1}{2} \beta_{ijk} E_i H_j H_k - \frac{1}{2} \gamma_{ijk} H_i E_j E_k - \dots \quad (1)$$

with \vec{E} and \vec{H} as the electric field and magnetic field respectively. Differentiation leads to the constitutive order parameters polarization

$$P_i(\vec{E}, \vec{H}) = -\frac{\partial F}{\partial E_i} = P_i^S + \epsilon_0 \epsilon_{ij} E_j + \alpha_{ij} H_j + \frac{1}{2} \beta_{ijk} H_j H_k + \gamma_{ijk} H_i E_j + \dots \quad (2)$$

high-order terms

and magnetization

$$M_i(\vec{E}, \vec{H}) = -\frac{\partial F}{\partial H_i} = M_i^S + \mu_0 \mu_{ij} H_j + \alpha_{ij} E_i + \beta_{ijk} E_i H_j + \frac{1}{2} \gamma_{ijk} E_j E_k + \dots \quad (3)$$

linear magnetoelectric effect

However: $\alpha_{ij}^2 < \chi_{ii}^s \chi_{ii}^m$ i.e., the magnetoelectric effect can only be large in ferroelectric and ferromagnetic materials

Typical multiferroic material

Multiferroic BiFeO₃ films: domain structure and polarization dynamics

F. Zavaliche , S. Y. Yang , T. Zhao , Y. H. Chu , M. P. Cruz , C. B. Eom & R. Ramesh

To cite this article: F. Zavaliche , S. Y. Yang , T. Zhao , Y. H. Chu , M. P. Cruz , C. B. Eom & R. Ramesh (2006) Multiferroic BiFeO₃ films: domain structure and polarization dynamics, Phase Transitions, 79:12, 991-1017, DOI: [10.1080/01411590601067144](https://doi.org/10.1080/01411590601067144)

To link to this article: <https://doi.org/10.1080/01411590601067144>

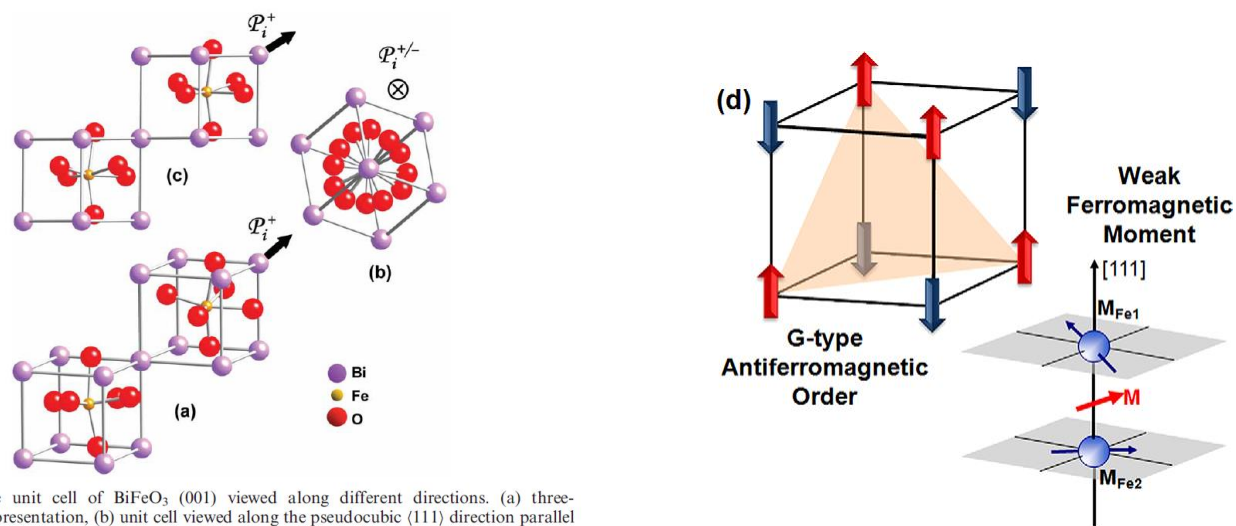


Figure 1. The unit cell of BiFeO₃ (001) viewed along different directions. (a) three-dimensional representation, (b) unit cell viewed along the pseudocubic (111) direction parallel with the Fe displacement (polarization axis), (c) a view along a pseudocubic (110) axis perpendicular to the polarization direction.

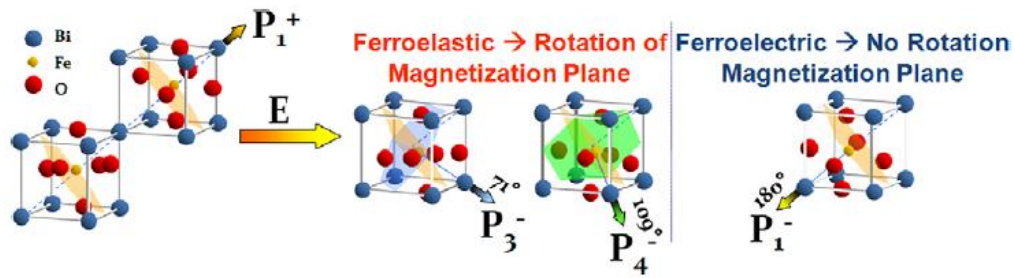
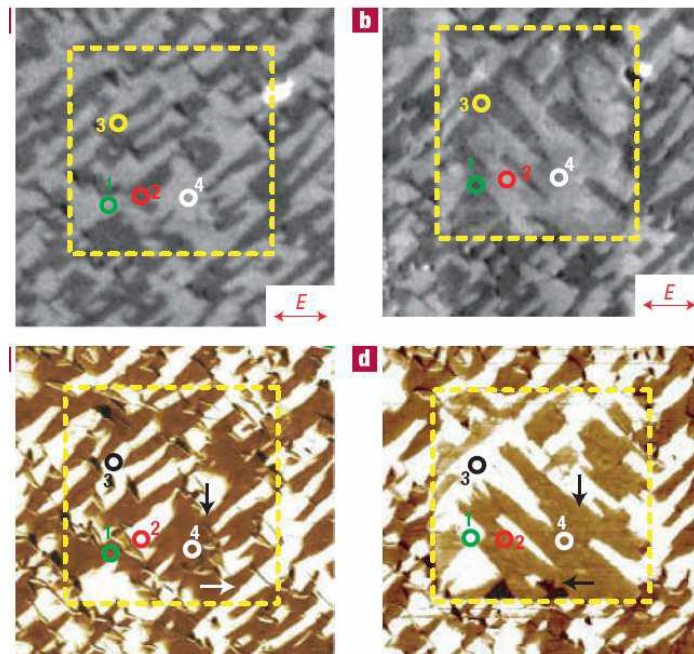
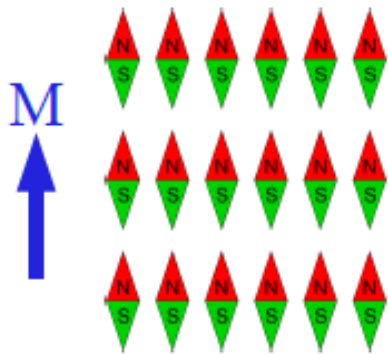


Figure 3. Schematic illustration of coupling between ferroelectricity and antiferromagnetism in BiFeO_3 . Upon electrically switching BiFeO_3 by the appropriate ferroelastic switching events (i.e., 71° and 109° changes in polarization) a corresponding change in the nature of antiferromagnetism is observed.

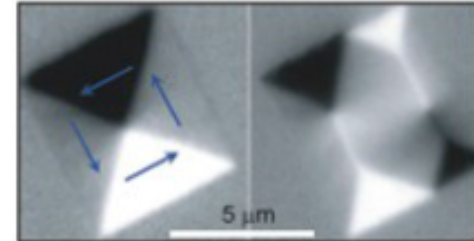


Magneto-electric multiferroics = ferromagnetic + ferroelectric

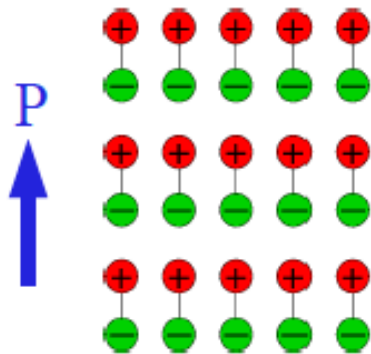
• Ferromagnetic:



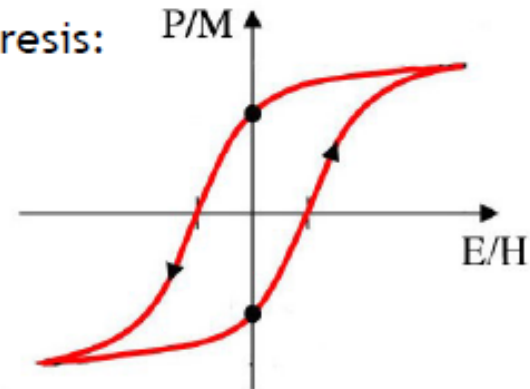
• Domains:



• Ferroelectric:



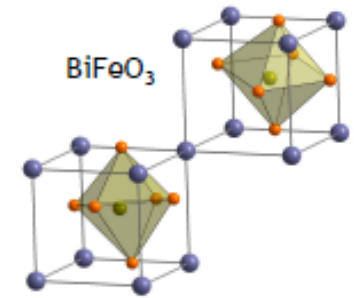
• Hysteresis:



Non-volatile data-storage!

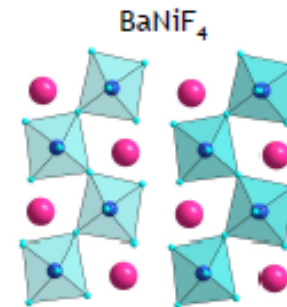
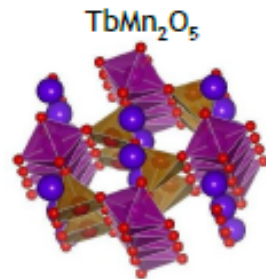
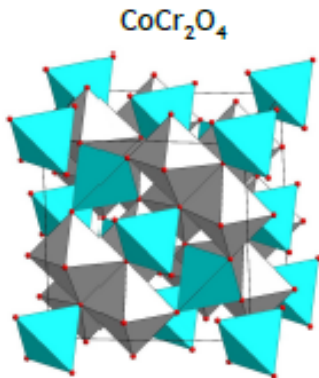
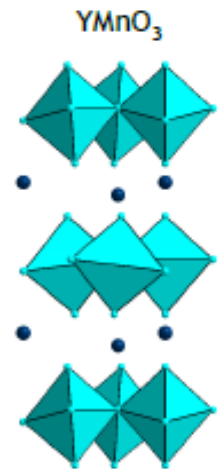
1) Ferroelectricity independent of magnetism

- Boracites: $\text{Ni}_3\text{B}_7\text{O}_{13}\text{I}$, $\text{Ni}_3\text{B}_7\text{O}_{13}\text{Cl}$, $\text{Co}_3\text{B}_7\text{O}_{13}\text{I}$, ...
- “Doped” multiferroics: $\text{Pb}(\text{Fe}_{2/3}\text{W}_{1/3})\text{O}_3$, $\text{Pb}(\text{Fe}_{1/2}\text{Nb}_{1/2})\text{O}_3$, ...
- “Lone pair” ferroelectrics: BiFeO_3 , BiMnO_3 , ...
- “Geometric” ferroelectrics
 - proper: BaMF_4 ($M=\text{Mn, Fe, Co, Ni}$)
 - improper: YMnO_3 , HoMnO_3 , ... (hexagonal manganites)



2) Ferroelectricity induced by ...

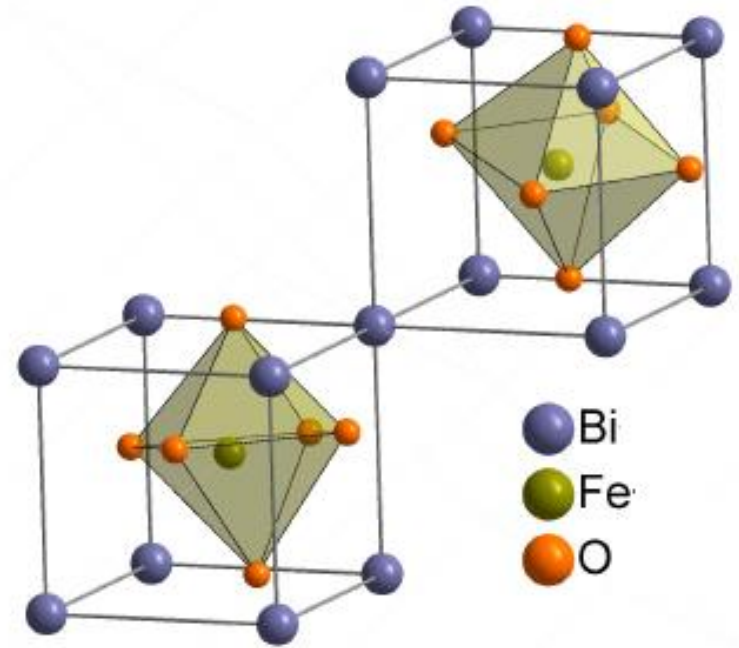
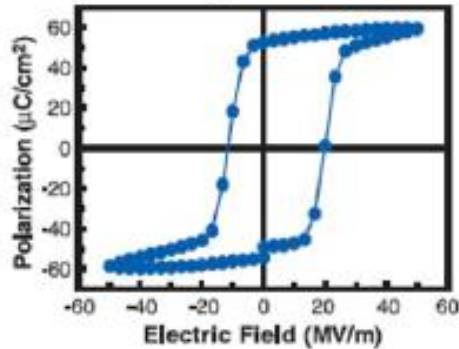
- ...magnetic order: TbMnO_3 , TbMn_2O_5 , $\text{Ni}_3\text{V}_2\text{O}_8$, CuFeO_2 , CoCr_2O_4 , ...
- ...charge order”: LuFe_2O_4 , $\text{Pr}_{1-x}\text{Ca}_x\text{MnO}_3$ (?)



One multiferroic is not necessarily equal to another multiferroic !

Epitaxial BiFeO₃ Multiferroic Thin Film Heterostructures

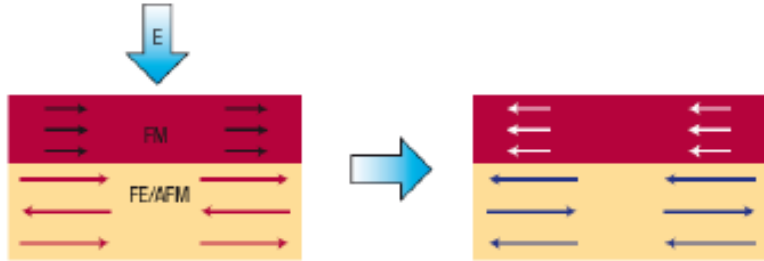
J. Wang,¹ J. B. Neaton,^{2†} H. Zheng,^{1†} V. Nagarajan,¹ S. B. Ogale,³
 B. Liu,¹ D. Viehland,⁴ V. Vaithyanathan,⁵ D. G. Schlom,⁵
 U. V. Waghmare,⁶ N. A. Spaldin,⁷ K. M. Rabe,²
 M. Wuttig,¹ R. Ramesh^{3*}



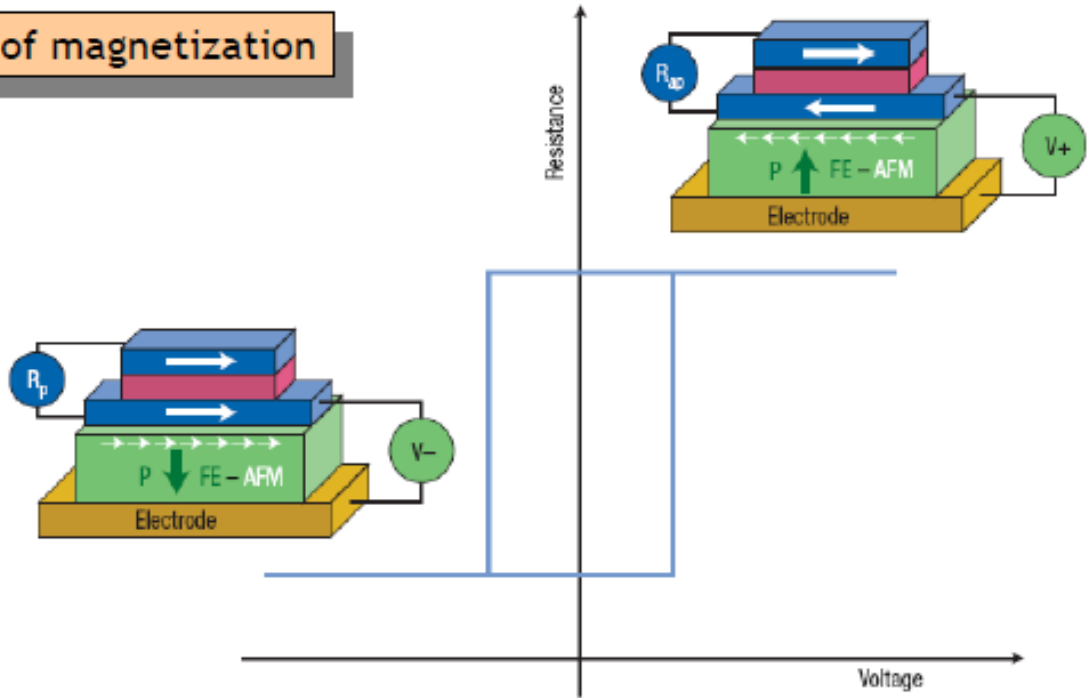
- ferroelectric below $T_E \approx 1100$ K
- antiferromagnetic below $T_M \approx 600$ K
- Controversial results about the “spontaneous polarization”:
 1970: $P = 6 \mu\text{C}/\text{cm}^2$ (single crystals)
 Teague et al., Solid State Comm. 8, 1073
 2003: $P = 60 \mu\text{C}/\text{cm}^2$ (thin films) Wang et al., Science 299, 1719

Large P : Effect of strain, defects, impurity phases, ... ???

Exchange bias coupling to a ferromagnet:



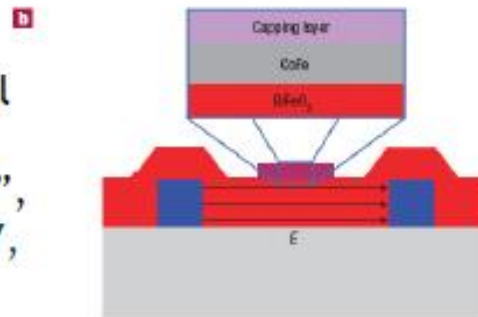
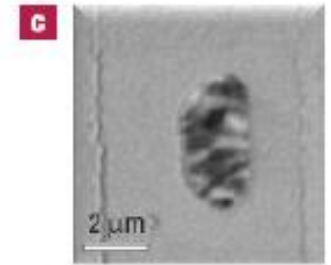
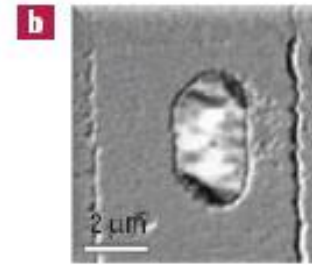
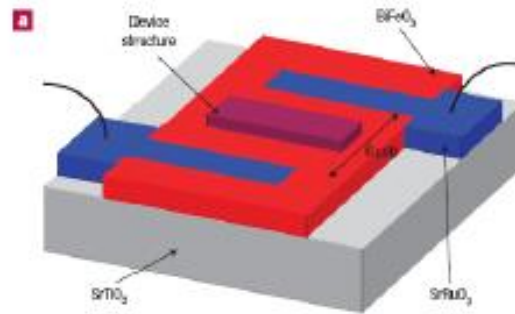
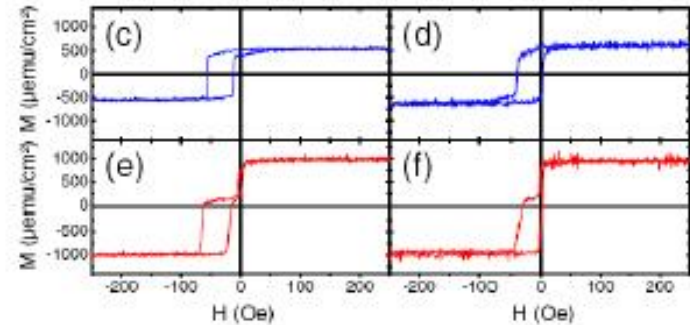
→ effective electric-field switching of magnetization



Magnetoelectric RA M

Bibes/Barthelemy, Nature Materials 7, 425 (2008)

Exchange bias demonstrated recently for $\text{BiFeO}_3/\text{CoFeB}$ heterostructures:
 Bea et al., PRL 100, 017204 (2008)

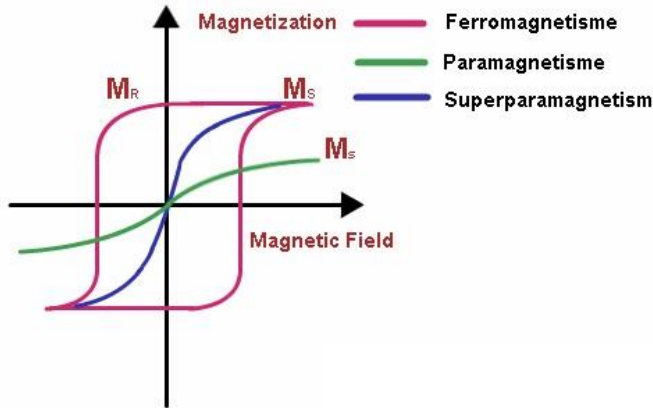


“Electric field control of local ferromagnetism using a magnetoelectric multiferroic”,
 Chu et al., Nature Materials 7, 478 (2008)

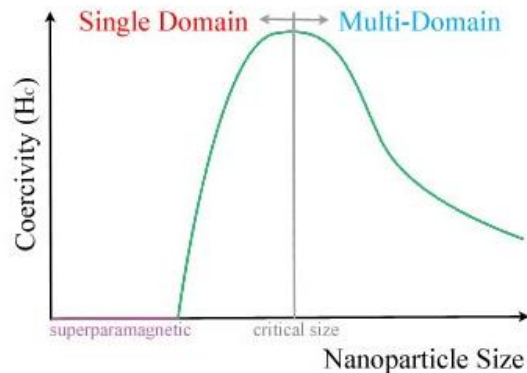
Magnetic nanoparticles

The magnetic properties are affected by size and magnetic anisotropy

Assembly of magnetic clusters (each comprised of many ferromagnetically aligned elemental moments) acting independently – **Superparamagnetic material**



The transition between the superparamagnetic and ferromagnetic states depends on the cluster size



Relaxation theory:

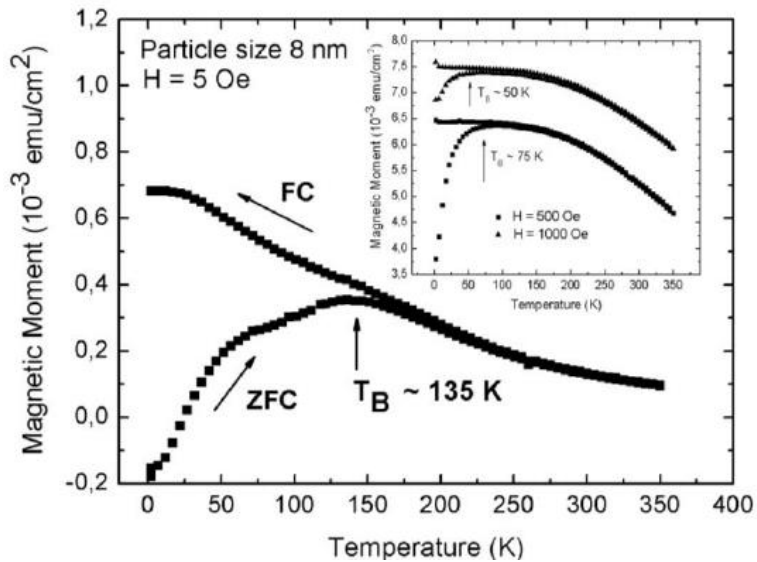
In a nanoparticle, the magnetic moment has usually only two stable orientations antiparallel to each other, separated by an energy barrier. The stable orientations define the magnetic easy axis of the nanoparticle. At finite temperature, there is a finite probability for the magnetization to flip and reverse its direction. The mean time between two flips is called the Néel relaxation time

$$\tau = \tau_0 \exp\left(\frac{KV}{k_B T}\right)$$

V is the particle volume and K is the magnetic anisotropy energy density. Let us assume that the measurement takes time τ_m . If $\tau \ll \tau_m$ the particle will flip many times during the measurement and in zero field the average moment is zero \Rightarrow superparamagnetic state. If $\tau \gg \tau_m$ the particle will not flip \Rightarrow blocked state.

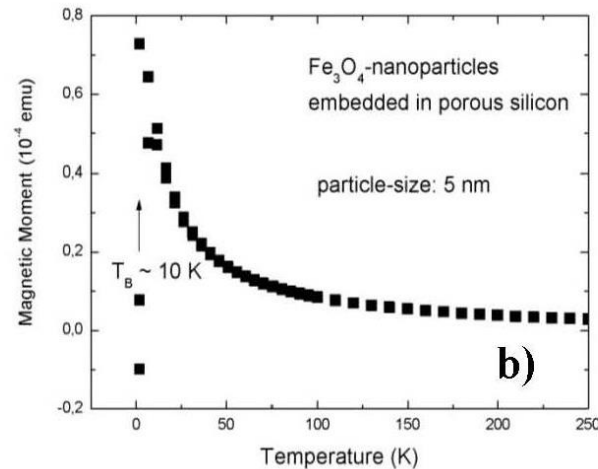
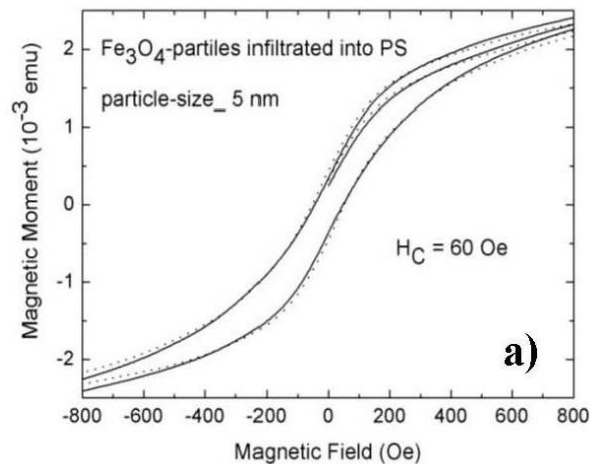
In a usual experiment τ_m is constant and temperature is varied. The sample transforms from the blocked state to a paramagnetic state at the blocking temperature T_B , in which $\tau = \tau_m$

$$T_B = \frac{KV}{k_B \ln\left(\frac{\tau_m}{\tau_0}\right)}$$



Zero field cooled (ZFC)/field cooled (FC) measurements of Fe₃O₄ particles infiltrated into porous silicon, carried out at a small applied magnetic field of 5 Oe and in a temperature range of between 4 K and 360 K. The blocking temperature (maximum peak of the ZFC-branch) at 135 K indicates dipolar coupling between the particles. Inset: Shift of TB towards lower temperatures with increasing applied magnetic field from about 135 K (H = 5 Oe) to 75 K (H = 500 Oe) and 50 K (H = 1,000 Oe)

Petra Granitzer and Klemens Rumpf: *Magnetic Nanoparticles Embedded in a Silicon Matrix*, Materials 2011, 4, 908-928; doi:10.3390/ma4050908

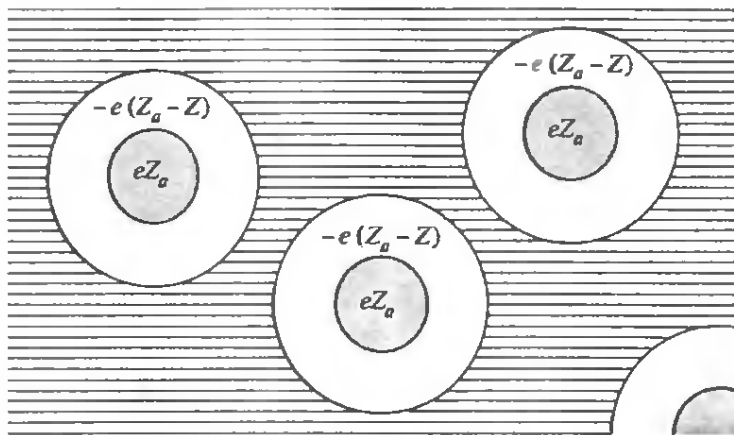


Magnetization of porous silicon (pore-diameter ~50 nm, pore-distance ~50 nm) with embedded magnetite nanoparticles of 5 nm in size. This sample exhibits no magnetic anisotropy between the two magnetization directions perpendicular (full line) and parallel (dotted line) to the surface; (b) Zero field/field cooled magnetization of porous silicon with the same morphology with infiltrated 5 nm magnetite nanoparticles shows a blocking temperature (TB) of about 10 K

V. CHARGE CARRIERS, ELECTRIC CURRENTS

V.1. Electrons in metals

The Drude model



Density of the electron gas

$$n = N_A Z \frac{\rho_m}{A}$$

$$n \approx 10^{22} \div 10^{23} \text{ cm}^{-3}$$

Density of an ideal gas at room temperature

$$n = N_A / V_A \approx 2.7 \times 10^{19} \text{ cm}^{-3}$$

The mean distance between the electrons – the radius of an equivalent sphere

$$\frac{4}{3} \pi r_s^3 = \frac{1}{n}$$

FREE ELECTRON DENSITIES OF SELECTED METALLIC ELEMENTS^a

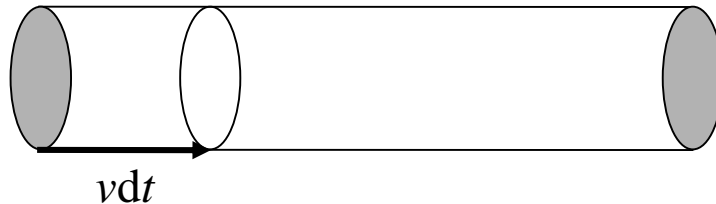
ELEMENT	Z	n ($10^{22}/\text{cm}^3$)	$r_s(\text{\AA})$	r_s/a_0
Li (78 K)	1	4.70	1.72	3.25
Na (5 K)	1	2.65	2.08	3.93
K (5 K)	1	1.40	2.57	4.86
Rb (5 K)	1	1.15	2.75	5.20
Cs (5 K)	1	0.91	2.98	5.62
Cu	1	8.47	1.41	2.67
Ag	1	5.86	1.60	3.02
Au	1	5.90	1.59	3.01
Be	2	24.7	0.99	1.87
Mg	2	8.61	1.41	2.66
Ca	2	4.61	1.73	3.27
Sr	2	3.55	1.89	3.57
Ba	2	3.15	1.96	3.71
Nb	1	5.56	1.63	3.07
Fe	2	17.0	1.12	2.12
Mn (α)	2	16.5	1.13	2.14
Zn	2	13.2	1.22	2.30
Cd	2	9.27	1.37	2.59
Hg (78 K)	2	8.65	1.40	2.65
Al	3	18.1	1.10	2.07
Ga	3	15.4	1.16	2.19
In	3	11.5	1.27	2.41
Tl	3	10.5	1.31	2.48
Sn	4	14.8	1.17	2.22
Pb	4	13.2	1.22	2.30
Bi	5	14.1	1.19	2.25
Sb	5	16.5	1.13	2.14

The basic assumptions:

1. The electrons in the gas are **free** \Rightarrow no forces act on the electrons between the collisions (we neglect the electrostatic interaction with the ions)
2. The electrons in the gas are **independent** \Rightarrow we neglect the electron-electron interactions
3. The collisions of the electrons are instantaneous events altering abruptly the electron velocities; the velocity after collision does not depend on the velocity before it
4. The electron gas is in a thermodynamic equilibrium with its surroundings; the distribution of the velocities of electrons obeys the Maxwell-Boltzmann statistics (classical statistic)

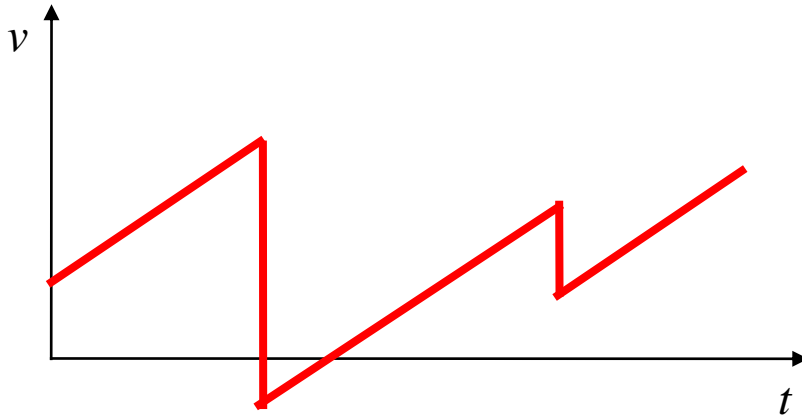
The probability that an electron experiences a collision in time dt is dt/τ
 τ is the **relaxation time**

DC electrical conductivity of a metal



$$\mathbf{j} = -nev$$

Time-averaged velocity of an electron in an external electric field



$$\mathbf{v} = v_0 - \frac{e\mathbf{E}}{m}t, \langle \mathbf{v} \rangle = -\frac{e\mathbf{E}}{m}\tau$$

The Ohm law in a differential form:

$$\mathbf{j} = \sigma\mathbf{E}, \sigma = \frac{ne^2\tau}{m}$$

Electron mobility:

$$\langle \mathbf{v} \rangle = \mu\mathbf{E}, \mu = -\frac{e\tau}{m}$$

Mean free path $l = \tau\sqrt{\langle v^2 \rangle}$

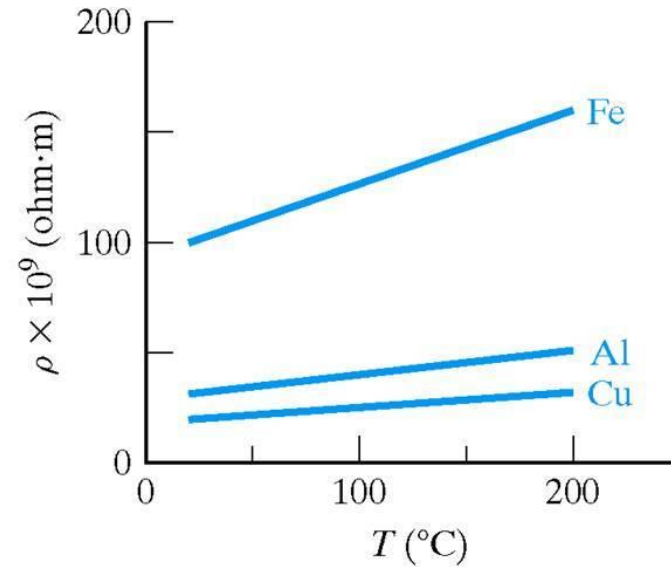
ELECTRICAL RESISTIVITIES OF SELECTED ELEMENTS^a

ELEMENT	77 K	273 K	373 K	$\frac{(\rho/T)_{373\text{ K}}}{(\rho/T)_{273\text{ K}}}$
Li	1.04	8.55	12.4	1.06
Na	0.8	4.2	Melted	
K	1.38	6.1	Melted	
Rb	2.2	11.0	Melted	
Cs	4.5	18.8	Melted	
Cu	0.2	1.56	2.24	1.05
Ag	0.3	1.51	2.13	1.03
Au	0.5	2.04	2.84	1.02
Be		2.8	5.3	1.39
Mg	0.62	3.9	5.6	1.05
Ca		3.43	5.0	1.07
Sr	7	23		
Ba	17	60		
Nb	3.0	15.2	19.2	0.92
Fe	0.66	8.9	14.7	1.21
Zn	1.1	5.5	7.8	1.04
Cd	1.6	6.8		
Hg	5.8	Melted	Melted	
Al	0.3	2.45	3.55	1.06
Ga	2.75	13.6	Melted	
In	1.8	8.0	12.1	1.11
Tl	3.7	15	22.8	1.11
Sn	2.1	10.6	15.8	1.09
Pb	4.7	19.0	27.0	1.04
Bi	35	107	156	1.07
Sb	8	39	59	1.11

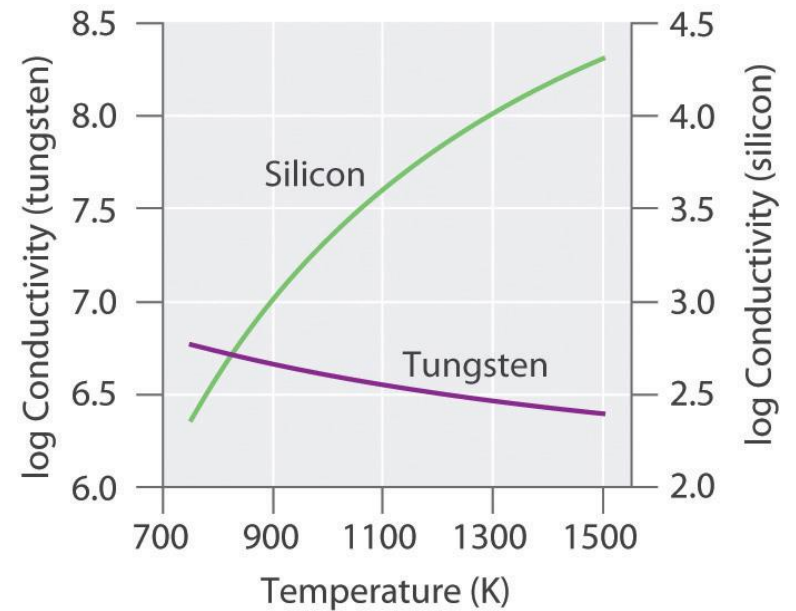
DRUDE RELAXATION TIMES IN UNITS OF 10^{-14} SECOND^a

ELEMENT	77 K	273 K	373 K
Li	7.3	0.88	0.61
Na	17	3.2	
K	18	4.1	
Rb	14	2.8	
Cs	8.6	2.1	
Cu	21	2.7	1.9
Ag	20	4.0	2.8
Au	12	3.0	2.1
Be		0.51	0.27
Mg	6.7	1.1	0.74
Ca		2.2	1.5
Sr	1.4	0.44	
Ba	0.66	0.19	
Nb	2.1	0.42	0.33
Fe	3.2	0.24	0.14
Zn	2.4	0.49	0.34
Cd	2.4	0.56	
Hg	0.71		
Al	6.5	0.80	0.55
Ga	0.84	0.17	
In	1.7	0.38	0.25
Tl	0.91	0.22	0.15
Sn	1.1	0.23	0.15
Pb	0.57	0.14	0.099
Bi	0.072	0.023	0.016
Sb	0.27	0.055	0.036

Temperature dependences of the resistivity of metals



Temperature dependence of the conductivity of a metal and a semiconductor



Time-evolution of the averaged electron momentum $\mathbf{p} = m\langle \mathbf{v} \rangle$

$$\mathbf{p}(t + dt) = [\mathbf{p}(t) + \mathbf{F}dt] \left(1 - \frac{dt}{\tau} \right) + \frac{dt}{\tau} \cdot 0$$

$$\frac{d\mathbf{p}}{dt} = -\frac{\mathbf{p}}{\tau} + \mathbf{F}$$

Thermal conductivity of an electron gas

The Wiedemann-Franz Law

$$L = \frac{\kappa}{\sigma T} = \text{const}$$

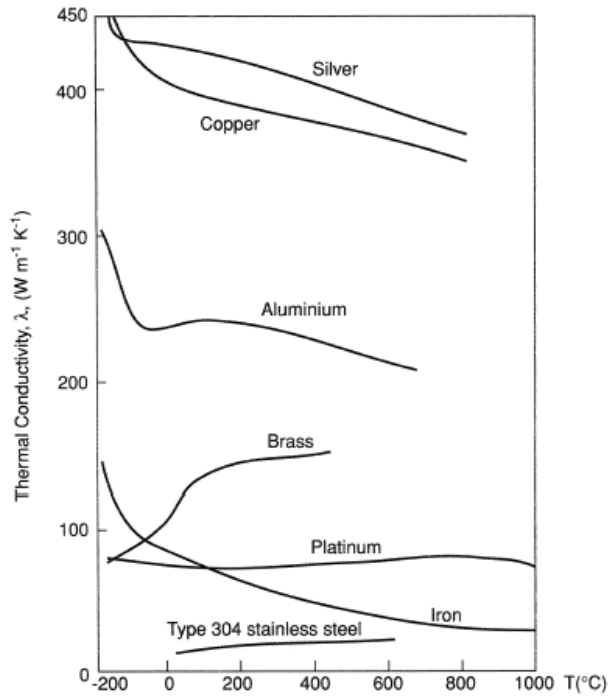
L is the Lorenz number

EXPERIMENTAL THERMAL CONDUCTIVITIES AND LORENZ NUMBERS OF SELECTED METALS

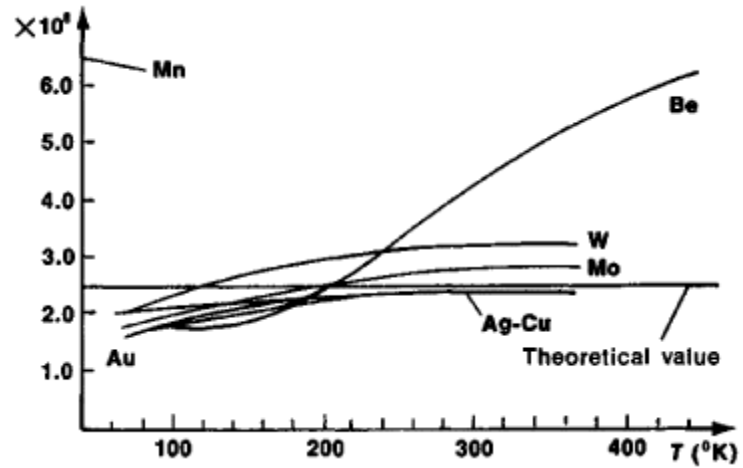
ELEMENT	273 K		373 K	
	κ (watt/cm-K)	$\kappa/\sigma T$ (watt-ohm/K ²)	κ (watt/cm-K)	$\kappa/\sigma T$ (watt-ohm/K ²)
Li	0.71	2.22×10^{-8}	0.73	2.43×10^{-8}
Na	1.38	2.12		
K	1.0	2.23		
Rb	0.6	2.42		
Cu	3.85	2.20	3.82	2.29
Ag	4.18	2.31	4.17	2.38
Au	3.1	2.32	3.1	2.36
Be	2.3	2.36	1.7	2.42
Mg	1.5	2.14	1.5	2.25
Nb	0.52	2.90	0.54	2.78
Fe	0.80	2.61	0.73	2.88
Zn	1.13	2.28	1.1	2.30

The temperature dependences

Thermal conductivity



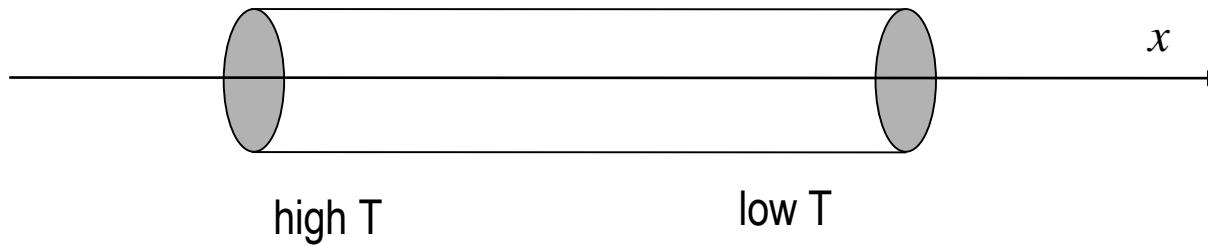
Lorenz number



This law was explained within the Drude model:

The density of the heat flow $\mathbf{j}_Q = -\kappa \nabla T$

The one-dimensional model:



$$j_Q \approx \frac{1}{2} n v [\mathcal{E}(T(x - v\tau)) - \mathcal{E}(T(x + v\tau))]$$

$$j_Q \approx -n v^2 \tau \frac{d\mathcal{E}}{dT} \frac{dT}{dx}$$

since $\langle v_x^2 \rangle = \langle v_y^2 \rangle = \langle v_z^2 \rangle = \frac{1}{3} \langle v^2 \rangle$, $n \frac{d\mathcal{E}}{dT} = c_V$ we obtain in 3D: $j_Q = -\frac{1}{3} v^2 \tau c_V \nabla T$, $\kappa = \frac{1}{3} v^2 \tau c_V$

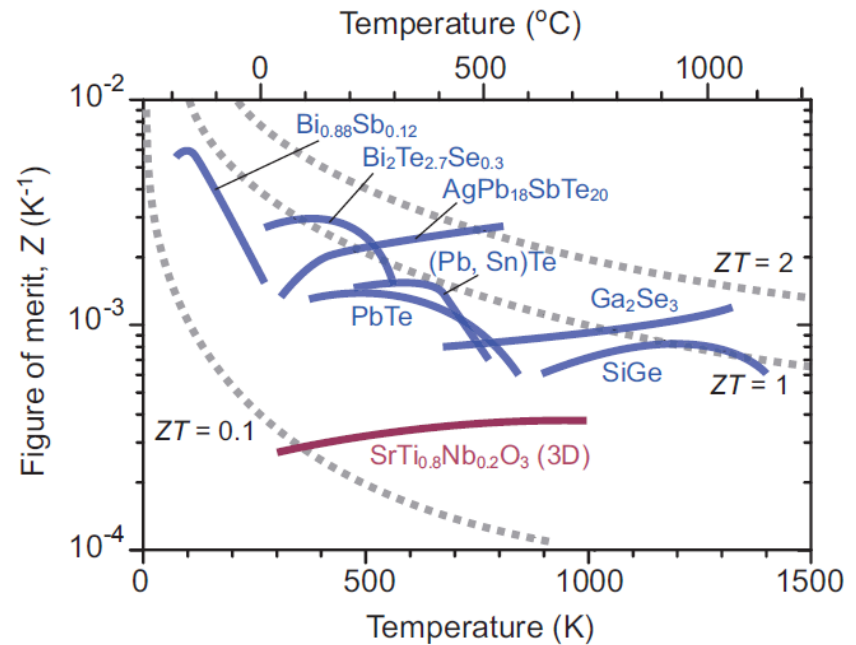
since $c_V = \frac{3}{2}nk_B$ and $\frac{1}{2}mv^2 = \frac{3}{2}k_B T$ we obtain

$$L = \frac{\kappa}{\sigma T} = \frac{3}{2} \left(\frac{k_B}{e} \right)^2 \approx 1.11 \times 10^{-8} \text{ W}\Omega/\text{K}^2 \quad \text{factor 2 is missing!!!}$$

Thermoelectric figure of merit: $ZT = S^2/L = TS^2\sigma/\kappa$

Including the lattice

$$ZT = \frac{S^2 T \sigma_{el}}{\kappa_{el} + \kappa_{latt}} = \frac{S^2}{L \left(1 + \frac{\kappa_{latt}}{\kappa_{el}} \right)}$$



From H. Ohta, Materials Today **10**, 44 (2007)

AC conductivity of a metal – optical properties of an electron gas

$$\mathbf{E}(t) = \text{Re}(\mathbf{E}(\omega)e^{-i\omega t})$$

We suppose the solution of the time-evolution equation for \mathbf{p} in the form $\mathbf{p}(t) = \text{Re}(\mathbf{p}(\omega)e^{-i\omega t})$

(the Fourier transformation of the equation)
$$-i\omega\mathbf{p}(\omega) = -\frac{\mathbf{p}(\omega)}{\tau} - e\mathbf{E}(\omega)$$

If $\mathbf{j}(t) = \text{Re}(\mathbf{j}(\omega)e^{-i\omega t})$ we obtain
$$\mathbf{j}(\omega) = \sigma(\omega)\mathbf{E}(\omega), \quad \sigma(\omega) = \frac{\sigma_0}{1-i\omega\tau}, \quad \sigma_0 = \frac{ne^2\tau}{m}$$

But:

- can we neglect the magnetic force? Yes, since $F_{\text{mag}} / F_{\text{el}} \approx v / c$
- can we neglect the space inhomogeneity of the electric field? Only if $l \ll \lambda$. If this is not fulfilled, a non-local approach must be used

The Maxwell equations:
$$\text{rot}\mathbf{E} = -\frac{\partial\mathbf{B}}{\partial t}, \quad \text{rot}\mathbf{H} = \frac{\partial\mathbf{D}}{\partial t} + \mathbf{j}, \quad \text{div}\mathbf{D} = \rho, \quad \text{div}\mathbf{B} = 0, \quad \mathbf{B} = \mu_0\mathbf{H}, \quad \mathbf{D} = \epsilon_0\epsilon\mathbf{E}$$

Two models:

1. electrons in vacuum: $\epsilon = 1, \sigma \neq 0$
$$-\Delta\mathbf{E}(\omega) = \frac{\omega^2}{c^2}\mathbf{E}(\omega) + i\omega\mu_0\sigma\mathbf{E}(\omega)$$
2. a homogeneous continuum without free charges: $\epsilon > 1, \sigma = 0$
$$-\Delta\mathbf{E}(\omega) = \frac{\omega^2}{c^2}\epsilon(\omega)\mathbf{E}(\omega)$$

Thus:
$$\epsilon(\omega) = 1 + i\frac{\sigma(\omega)}{\omega\epsilon_0} \Rightarrow \epsilon(\omega) = 1 + \frac{i}{\omega\epsilon_0} \frac{\sigma_0}{1-i\omega\tau}$$

The plasma frequency: $\omega_p = \sqrt{\frac{ne^2}{\epsilon_0 m}}$

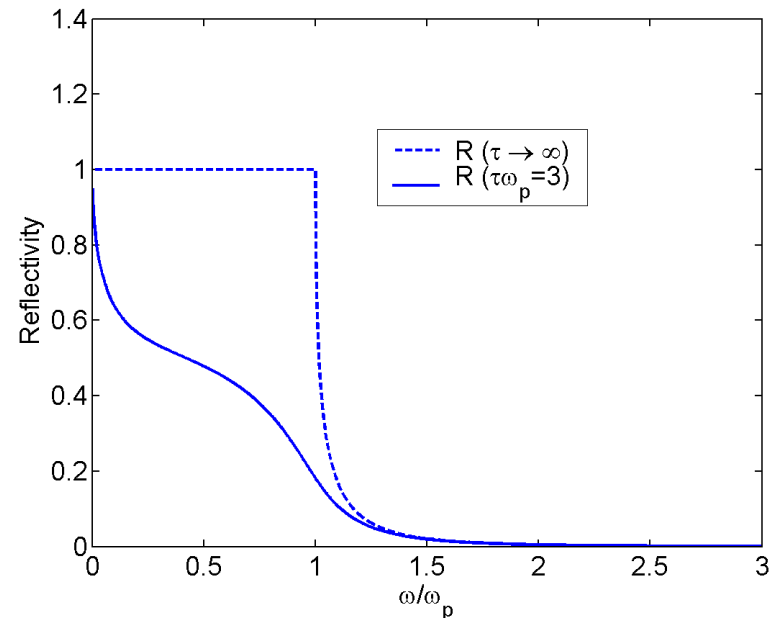
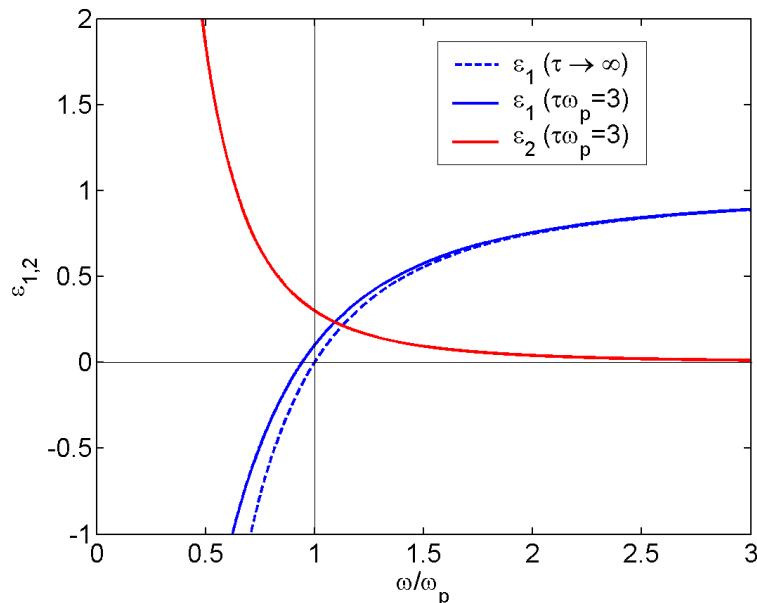
$$\epsilon(\omega) = 1 - \frac{\omega_p^2 \tau^2}{1 + \omega^2 \tau^2} + i \frac{\omega_p^2 \tau}{\omega(1 + \omega^2 \tau^2)}$$

Long relaxation times:

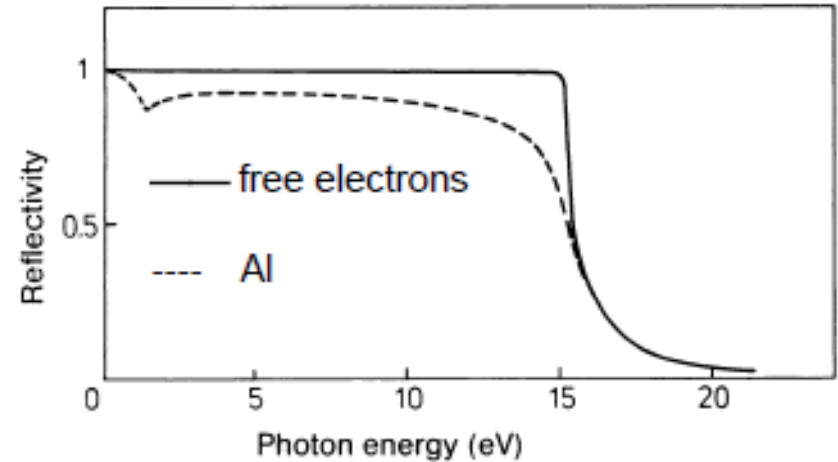
$$\epsilon(\omega) \rightarrow 1 - \frac{\omega_p^2}{\omega^2}$$

normal-incidence reflectivity

$$R(\omega) = \left| \frac{\sqrt{\epsilon(\omega)} - 1}{\sqrt{\epsilon(\omega)} + 1} \right|^2$$



Metal	Valency	N (10^{28} m^{-3})	$\omega_p/2\pi$ (10^{15} Hz)	λ_p (nm)
Li (77 K)	1	4.70	1.95	154
Na (5 K)	1	2.65	1.46	205
K (5 K)	1	1.40	1.06	282
Rb (5 K)	1	1.15	0.96	312
Cs (5 K)	1	0.91	0.86	350
Cu	1	8.47	2.61	115
Ag	1	5.86	2.17	138
Au	1	5.90	2.18	138
Be	2	24.7	4.46	67
Mg	2	8.61	2.63	114
Ca	2	4.61	1.93	156
Al	3	18.1	3.82	79



The plasma frequency is the frequency of free oscillations of the electron gas

Continuity equation $\text{div } \mathbf{j} = -\frac{\partial \rho}{\partial t} \Rightarrow \text{div } \mathbf{j}(\omega) = i\omega\rho(\omega)$

The Gauss law: $\text{div } \mathbf{E} = \frac{\rho}{\epsilon_0} \Rightarrow \text{div } \mathbf{j}(\omega) = \frac{\rho\sigma(\omega)}{\epsilon_0}$

The frequency of the charge eigenoscillations is

$$1 + i \frac{\sigma(\omega)}{\omega\epsilon_0} = 0 \Rightarrow \omega = \omega_p \text{ (for } \tau \rightarrow \infty \text{)}$$

Simple interpretation of the plasma frequency

The force from the cations acting on a single free electron

$$\mathbf{F} = -\mathbf{x} \frac{ne^2}{\epsilon_0}$$

Equation of movement of the electron

$$m \frac{d^2 x}{dt^2} + \frac{ne^2}{\epsilon_0} x = 0$$

The resonance frequency

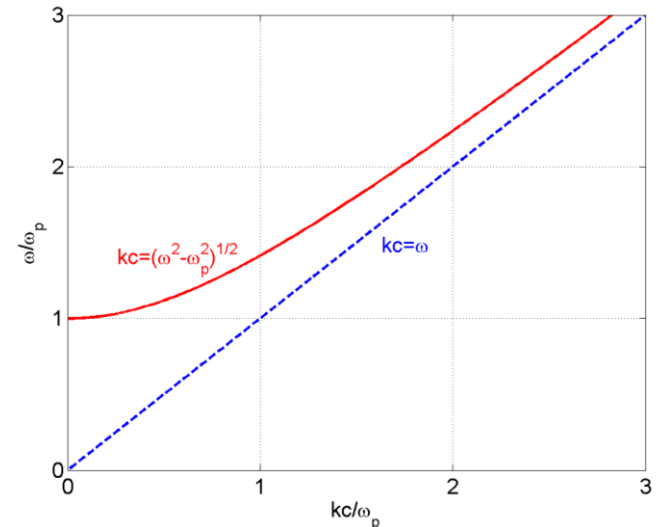
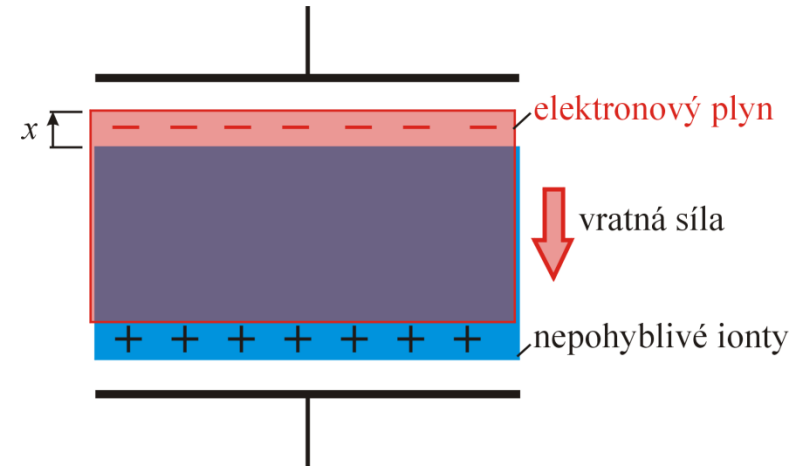
$$\omega_p = \sqrt{\frac{ne^2}{m\epsilon_0}} \Rightarrow \omega_p \propto \sqrt{n}$$

The dispersion relation for the electromagnetic field in the electron gas

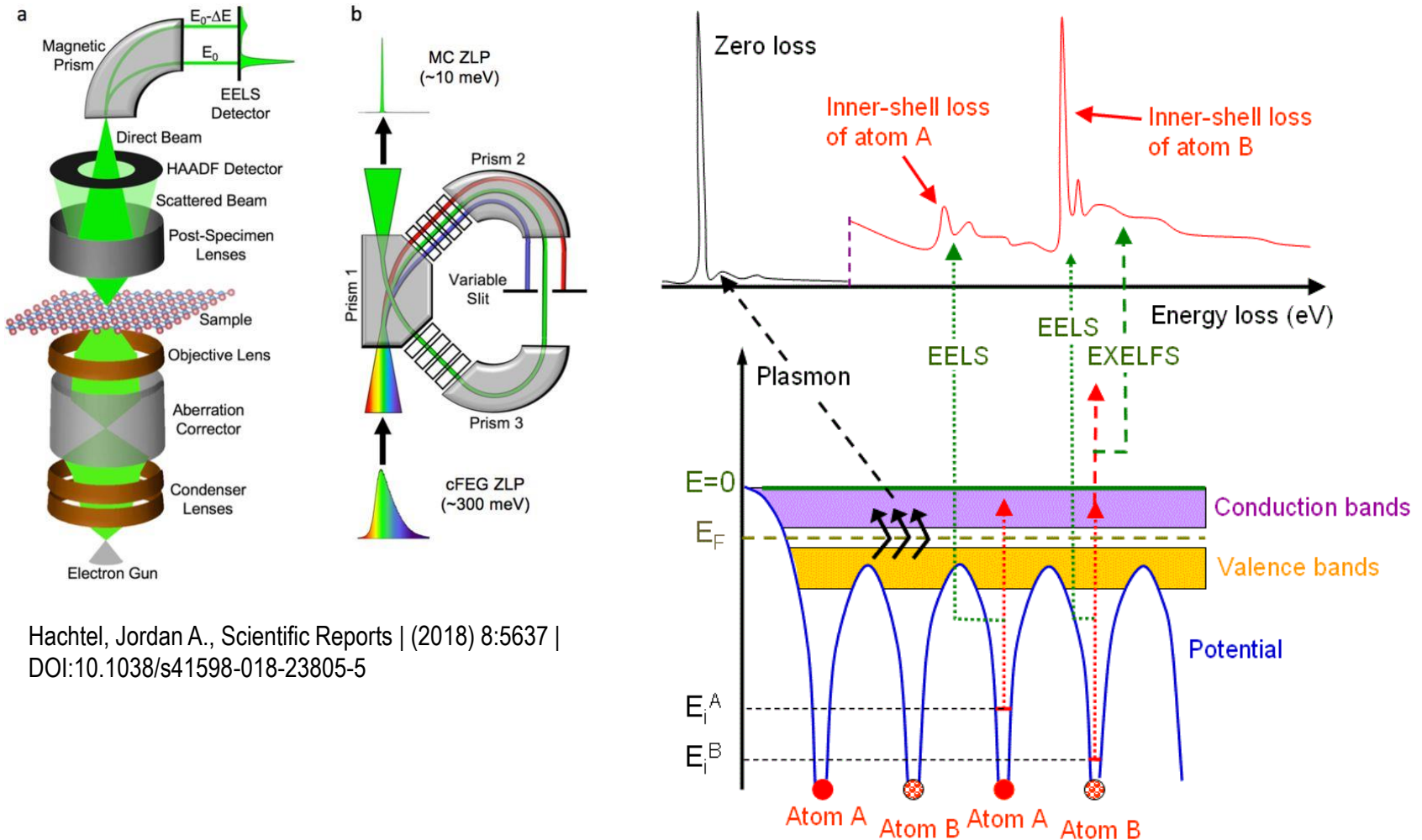
$$\epsilon(\omega) = \frac{c^2 k^2}{\omega^2} = 1 - \frac{\omega_p^2}{\omega^2}$$

$$c^2 k^2 = \omega^2 - \omega_p^2$$

An evanescent wave for $\omega < \omega_p$



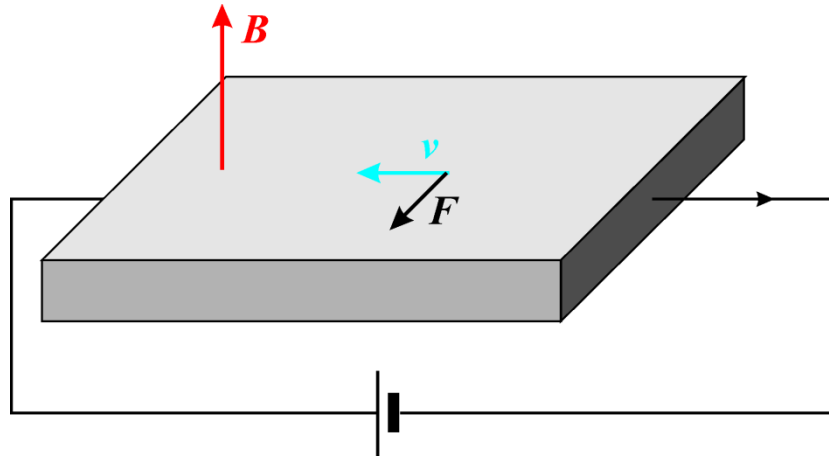
Electron energy loss spectroscopy



Hachtel, Jordan A., Scientific Reports | (2018) 8:5637 | DOI:10.1038/s41598-018-23805-5

<http://www.globalsino.com/EM/page4780.html>

Classical Hall effect



$$eE_H = F = eBv, j = nev \Rightarrow E_H = RjB, R = -\frac{1}{ne}$$

using the equation of movement $\frac{d\mathbf{p}}{dt} = -\frac{\mathbf{p}}{\tau} + \mathbf{F}$ $\mathbf{F} = -e\mathbf{E} - e\frac{\mathbf{p}}{m} \times \mathbf{B}$

Stationary state: $\frac{dp_x}{dt} = 0, p_y = 0$ We obtain $E_y = -\frac{j_x B}{ne} = Rj_x B$

The sign of the Hall constant R depends on the sign of the charge carriers

HALL COEFFICIENTS OF SELECTED ELEMENTS
IN MODERATE TO HIGH FIELDS^a

METAL	VALENCE	$-1/R_H nec$
Li	1	0.8
Na	1	1.2
K	1	1.1
Rb	1	1.0
Cs	1	0.9
Cu	1	1.5
Ag	1	1.3
Au	1	1.5
Be	2	-0.2
Mg	2	-0.4
In	3	-0.3
Al	3	-0.3

Electric conductivity is a tensor

$$j_m = \sigma_{mn} E_n$$

$$\frac{v_x}{\tau} - \omega_c v_y = -\frac{e}{m} E_x$$

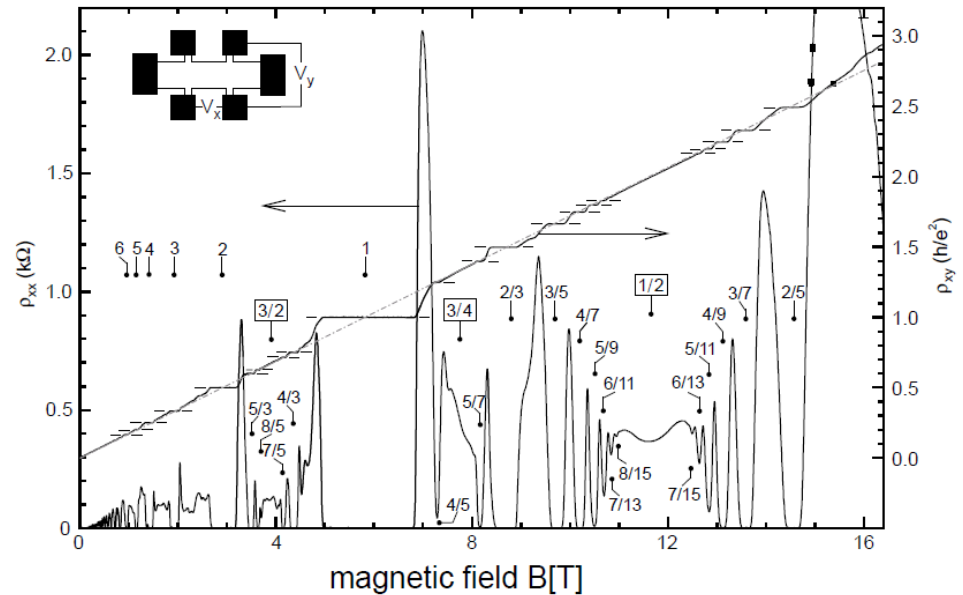
where $\omega_c = \frac{eB}{m}$

$$\frac{v_y}{\tau} + \omega_c v_x = -\frac{e}{m} E_y$$

$$\frac{v_z}{\tau} = -\frac{e}{m} E_z$$

Then $\sigma_{xx} = \sigma_{yy} = \frac{\sigma_0}{1 + (\omega_c \tau)^2}$, $\sigma_{xy} = -\sigma_{yx} = \frac{\sigma_0 \omega_c \tau}{1 + (\omega_c \tau)^2}$, $\sigma_{zz} = \sigma_0$

The longitudinal conductivity is independent from the field \mathbf{B} , however it has been discovered in 1930's that above a critical field B_c oscillations in σ_{xx} appear in 2D systems – Shubnikov deHaas effect (SdH). Stair-case dependence of the Hall resistance $r_H = r_{xy} = U_H / I$ on B in 2D systems is explained by the quantum Hall effect (QHE)



The Sommerfeld model

Obvious discrepancy: the Wiedemann-Franz law can be explained withing the Drude model (except the factor 2) but the thermal capacity for one electron ($3/2 k_B$) is too high!!

Explanation: Fermi-Dirac statistics instead of the classical Maxwell-Boltzmann statistics
all the other assumptions of the Drude model are still valid

The ground state of an electron gas

Independent and free electrons \Rightarrow an one-electron problem

$$-\frac{\hbar^2}{2m} \nabla^2 \psi(\mathbf{r}) = E \psi(\mathbf{r})$$

How to choose the boundary conditions? We do not consider the surfaces, we investigate only the bulk properties. Therefore we choose periodic Born-von Kármán boundary conditions

$$\psi(x, y, z) = \psi(x + L, y, z) = \psi(x, y + L, z) = \psi(x, y, z + L)$$

plane-wave solution $\psi_{\mathbf{k}}(\mathbf{r}) = \frac{1}{\sqrt{V}} e^{i\mathbf{k}\cdot\mathbf{r}}$ $V = L^3$ is the volume of the Born-von Kármán region

From the boundary conditions, the possible values of \mathbf{k} follow:

$$k_{x,y,z} = \frac{2\pi}{L} n_{x,y,z}, n_{x,y,z} \text{ are integers}$$

The one-electron eigenstates create a simple cubic lattice in reciprocal space with the lattice parameter $2\pi/L$

The energy eigenvalues $E_{\mathbf{k}} = \frac{\hbar^2 k^2}{2m}$

The functions $\psi_{\mathbf{k}}(\mathbf{r})$ are the eigenfunctions of velocity and momentum with the eigenvalues

$$\mathbf{v}_{\mathbf{k}} = \frac{\hbar\mathbf{k}}{m}, \mathbf{p}_{\mathbf{k}} = \hbar\mathbf{k}$$

In the ground state, all the single-electron states with lowest possible energy are occupied by 2 electrons with opposite spins. The occupied states occur in a sphere, the radius of which is the length of the wave vector of the highest-energy occupied state (the Fermi radius)

$$N = 2 \cdot \frac{\frac{4}{3} \pi k_F^3}{\left(\frac{2\pi}{L}\right)^3} \Rightarrow k_F = (3\pi^2 n)^{1/3}$$

or $k_F = \frac{(9\pi/4)^{1/3}}{r_s} \approx \frac{1.92}{r_s}$ k_F is in the order of few \AA^{-1}

The Fermi energy: $E_F = \frac{\hbar^2 k_F^2}{2m} \approx \frac{50.1 \text{ eV}}{\left(\frac{r_s}{a_B}\right)^2}$

The Fermi velocity: $v_F = \frac{\hbar k_F}{m} \approx \frac{4.2 \times 10^6 \text{ m/s}}{\frac{r_s}{a_B}}$ For room temperature: $v_F \gg \sqrt{\frac{3k_B T}{m}}$

The Fermi temperature: $E_F = k_B T_F \approx \frac{58.2 \times 10^4 \text{ K}}{\left(r_s / a_B\right)^2}$

FERMI ENERGIES, FERMI TEMPERATURES, FERMI WAVE VECTORS, AND FERMI VELOCITIES FOR REPRESENTATIVE METALS^a

ELEMENT	r_s/a_0	ϵ_F	T_F	k_F	v_F
Li	3.25	4.74 eV	5.51×10^4 K	1.12×10^8 cm ⁻¹	1.29×10^8 cm/sec
Na	3.93	3.24	3.77	0.92	1.07
K	4.86	2.12	2.46	0.75	0.86
Rb	5.20	1.85	2.15	0.70	0.81
Cs	5.62	1.59	1.84	0.65	0.75
Cu	2.67	7.00	8.16	1.36	1.57
Ag	3.02	5.49	6.38	1.20	1.39
Au	3.01	5.53	6.42	1.21	1.40
Be	1.87	14.3	16.6	1.94	2.25
Mg	2.66	7.08	8.23	1.36	1.58
Ca	3.27	4.69	5.44	1.11	1.28
Sr	3.57	3.93	4.57	1.02	1.18
Ba	3.71	3.64	4.23	0.98	1.13
Nb	3.07	5.32	6.18	1.18	1.37
Fe	2.12	11.1	13.0	1.71	1.98
Mn	2.14	10.9	12.7	1.70	1.96
Zn	2.30	9.47	11.0	1.58	1.83
Cd	2.59	7.47	8.68	1.40	1.62
Hg	2.65	7.13	8.29	1.37	1.58
Al	2.07	11.7	13.6	1.75	2.03
Ga	2.19	10.4	12.1	1.66	1.92
In	2.41	8.63	10.0	1.51	1.74
Tl	2.48	8.15	9.46	1.46	1.69
Sn	2.22	10.2	11.8	1.64	1.90
Pb	2.30	9.47	11.0	1.58	1.83
Bi	2.25	9.90	11.5	1.61	1.87
Sb	2.14	10.9	12.7	1.70	1.96

The total energy of the ground state of the electron gas is

$$E = 2 \sum_{k < k_F} \frac{\hbar^2 k^2}{2m} \approx 2 \int_{k < k_F} d^3 \mathbf{k} \left(\frac{L}{2\pi} \right)^3 \frac{\hbar^2 k^2}{2m} = V \frac{\hbar^2 k_F^5}{10\pi^2 m}$$

Mean energy per one electron is

$$E / N = \frac{3}{5} \mathcal{E}_F$$

In the Drude model we obtained

$$E / N = \frac{3}{2} k_B T \ll \frac{3}{5} k_B T_F$$

States of an electron gas at $T > 0K$

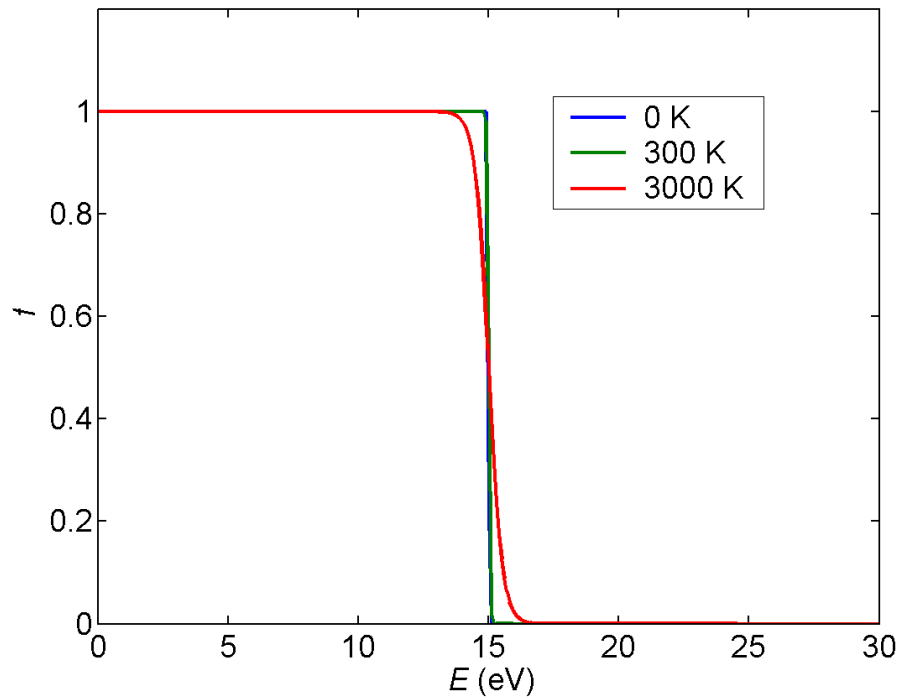
The Fermi-Dirac statistics:

Probability of finding an electron in an one-electron state i of a N -electron system at temperature T :

$$f_i = \frac{1}{e^{(E_i - \mu)/k_B T} + 1}$$

The chemical potential follows from the normalization condition:

$$\sum_i f_i = N$$



For $T \rightarrow 0$ we obtain $f_{\mathbf{k}} = \begin{cases} 1 & \text{for } \mathcal{E}_{\mathbf{k}} < \mu \\ 0 & \text{for } \mathcal{E}_{\mathbf{k}} > \mu \end{cases}$ thus $\lim_{T \rightarrow 0} \mu = \mathcal{E}_F$

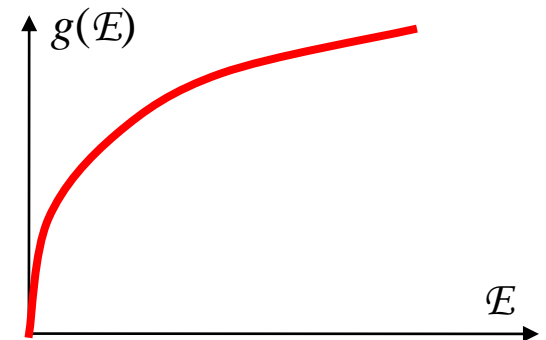
Let us calculate again the total energy of an electron gas

$$E = 2 \sum_{\mathbf{k}} f_{\mathbf{k}} \mathcal{E}_{\mathbf{k}} \approx \frac{V}{4\pi^3} \int d^3 \mathbf{k} f_{\mathbf{k}} \mathcal{E}_{\mathbf{k}}$$

Since $f(\mathbf{k}) = f(\mathcal{E}(\mathbf{k}))$ $E = V \int_0^{\infty} d\mathcal{E} g(\mathcal{E}) f(\mathcal{E}) \mathcal{E}$

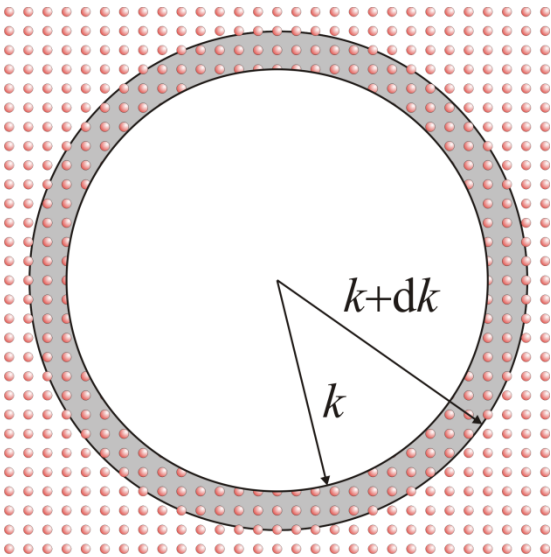
where $g(E) = \frac{m}{(\pi \hbar)^2} \sqrt{\frac{2mE}{\hbar^2}} = \frac{3}{2} \frac{n}{E_F} \left(\frac{E}{E_F}\right)^{1/2}$ is the energy density of one-electron states

$$g(E) = \frac{\text{number of states with the energies } \mathcal{E} \in \langle \mathcal{E}, \mathcal{E} + d\mathcal{E} \rangle}{V d\mathcal{E}}$$

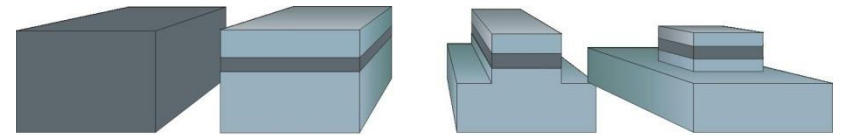


Two-dimensional electron gas:

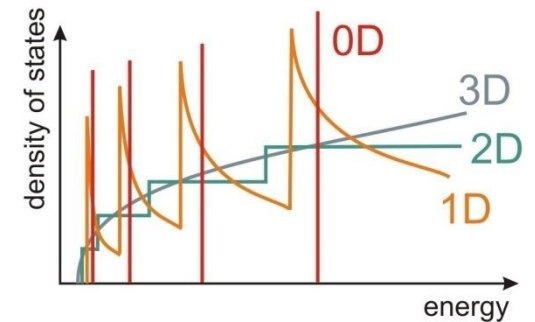
How many one-electron states have the energy between E and $E+dE$?



$$dN = 2 \frac{2\pi k dk}{(2\pi/L)^2} = \frac{mL^2}{\pi\hbar^2} dE \Rightarrow g(E) = \frac{1}{L^2} \frac{dN}{dE} = \frac{m}{\pi\hbar^2} = \text{const.}$$



low dimensional structures



One-dimensional electron gas:

$$dN = 2 \frac{2dk}{(2\pi/L)} = L \frac{\sqrt{2m}}{\pi\hbar\sqrt{E}} dE \Rightarrow g(E) = \frac{1}{L} \frac{dN}{dE} = \frac{\sqrt{2m}}{\pi\hbar\sqrt{E}}$$

Back to the calculation of the total energy in a 3D gas:

normalization:
$$n = \frac{N}{V} = \int_0^{\infty} d\mathcal{E} g(\mathcal{E}) f(\mathcal{E})$$

The integrals for E and n can be calculated only numerically. If the temperature is not too high, one obtains:

$$u = \frac{E}{V} \approx \frac{3}{5} n \mathcal{E}_F + \frac{\pi^2}{6} (k_B T)^2 g(\mathcal{E}_F),$$
$$\mu \approx \mathcal{E}_F \left[1 - \frac{1}{3} \left(\frac{\pi k_B T}{2 \mathcal{E}_F} \right)^2 \right]$$

specific heat of the electron gas is

$$c_V = \left(\frac{\partial u}{\partial T} \right)_n = \frac{\pi^2}{2} \frac{k_B T}{\mathcal{E}_F} n k_B = \gamma T, \quad \gamma = \frac{1}{3} (\pi k_B)^2 g(\mathcal{E}_F) \sim m^*$$

within the Drude model

$$c_V^{\text{Drude}} = \frac{3}{2} n k_B \gg c_V$$

**SOME ROUGH EXPERIMENTAL VALUES FOR THE COEFFICIENT
OF THE LINEAR TERM IN T OF THE MOLAR SPECIFIC HEATS
OF METALS, AND THE VALUES GIVEN BY SIMPLE FREE
ELECTRON THEORY**

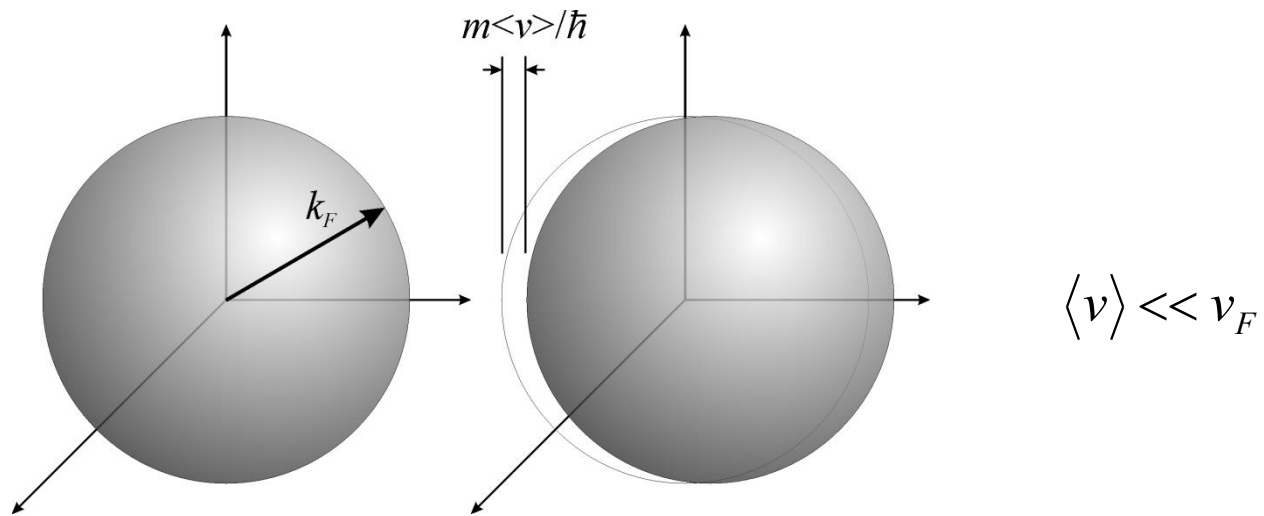
ELEMENT	FREE ELECTRON γ (in 10^{-4} cal-mole $^{-1}$ -K $^{-2}$)	MEASURED γ	RATIO ^a (m^*/m)
Li	1.8	4.2	2.3
Na	2.6	3.5	1.3
K	4.0	4.7	1.2
Rb	4.6	5.8	1.3
Cs	5.3	7.7	1.5
Cu	1.2	1.6	1.3
Ag	1.5	1.6	1.1
Au	1.5	1.6	1.1
Be	1.2	0.5	0.42
Mg	2.4	3.2	1.3
Ca	3.6	6.5	1.8
Sr	4.3	8.7	2.0
Ba	4.7	6.5	1.4
Nb	1.6	20	12
Fe	1.5	12	8.0
Mn	1.5	40	27
Zn	1.8	1.4	0.78
Cd	2.3	1.7	0.74
Hg	2.4	5.0	2.1
Al	2.2	3.0	1.4
Ga	2.4	1.5	0.62
In	2.9	4.3	1.5
Tl	3.1	3.5	1.1
Sn	3.3	4.4	1.3
Pb	3.6	7.0	1.9
Bi	4.3	0.2	0.047
Sb	3.9	1.5	0.38

Consequences to the transport properties:

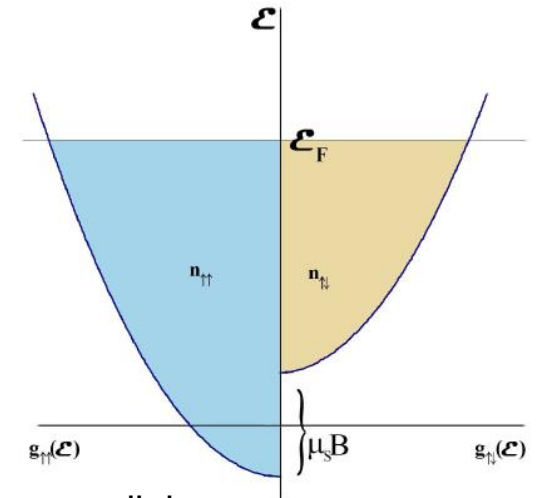
mean free path $l = v_F \tau \gg l^{\text{Drude}}$

the Wiedemann-Franz law: $\frac{\kappa}{\sigma T} = \frac{\pi^2}{3} \left(\frac{k_B}{e} \right)^2 \approx \left(\frac{\kappa}{\sigma T} \right)^{\text{Drude}} = \frac{3}{2} \left(\frac{k_B}{e} \right)^2$

Only the electrons at the Fermi surface do contribute to the electric or heat transport.



Pauli paramagnetism of free electrons



Spin magnetic moment of electron: $\mathbf{m}_S = -g_0 \mu_B \mathbf{S}$

In an external magnetic field \mathbf{B} the magnetic spin moments are either parallel or antiparallel to \mathbf{B} . The interaction energy with the magnetic field is

$$\mathcal{E} = -\mathbf{m}_S \cdot \mathbf{B} = \mp g_0 \mu_B \mathbf{S} \cdot \mathbf{B} \approx \mp 2 \mu_B \mathbf{S} \cdot \mathbf{B}$$

Resulting magnetization: $M_{\text{para}} = g_0 \mu_B S (n_{\uparrow} - n_{\downarrow}) \approx \mu_B (n_{\uparrow} - n_{\downarrow})$

Populations of spin-ups and spin-downs:

$$n_{\uparrow} - n_{\downarrow} = \frac{1}{2} \int_{\mathcal{E}_F - \mu_B B}^{\mathcal{E}_F + \mu_B B} d\mathcal{E} g(\mathcal{E}) \approx g(\mathcal{E}_F) \mu_B B$$

$$M_{\text{para}} = \mu_B^2 g(\mathcal{E}_F) B = \mu_0 \mu_B^2 g(\mathcal{E}_F) H$$

Pauli susceptibility

$$\chi = \mu_0 \mu_B^2 g(\mathcal{E}_F)$$

External magnetic field interacts also with the orbital magnetic moment of electron, leading to a diamagnetic contribution (Landau diamagnetism)

$$M_{\text{dia}} = -\frac{1}{3} M_{\text{para}}$$

so that the total susceptibility is

$$\chi = \frac{2}{3} \mu_0 \mu_B^2 g(\mathcal{E}_F) = \mu_0 \mu_B^2 \frac{n}{\mathcal{E}_F}$$

The susceptibility is independent of the temperature, paramagnetism of atoms is temperature dependent

Paramagnetic susceptibility [10 ⁻⁵]	
FeO	720
U	40
Pt	26
W	6.8
Cs	5.1
Al	2.2
Li	1.4
Mg	1.2
Na	0.72

V.2. Electrons in a periodic crystal field

Electron gas in a periodic crystal field – the electrons are independent but not free \Rightarrow the many-particle wave function is a direct product of one-particle wave functions

$$\Psi(\mathbf{r}_1, s_1, \dots, \mathbf{r}_N, s_N) = \prod_{j=1}^N \psi(\mathbf{r}_j) \chi(s_j)$$

We do not consider the spins, i.e. we solve the one-particle Schroedinger equation

$$-\frac{\hbar^2}{2m} \Delta \psi(\mathbf{r}) + U(\mathbf{r}) \psi(\mathbf{r}) = E \psi(\mathbf{r})$$

The potential energy is periodic, i.e.

$$U(\mathbf{r}) = U(\mathbf{r} + \mathbf{R}), \quad \mathbf{R} = n_1 \mathbf{a}_1 + n_2 \mathbf{a}_2 + n_3 \mathbf{a}_3$$

It can be expressed in the form of the Fourier series

$$U(\mathbf{r}) = \sum_{\mathbf{g}} U_{\mathbf{g}} e^{i\mathbf{g} \cdot \mathbf{r}}, \quad \mathbf{g} = g_1 \mathbf{b}_1 + g_2 \mathbf{b}_2 + g_3 \mathbf{b}_3$$

The solution of the Schroedinger equation is the Bloch wave

$$\psi_{nk}(\mathbf{r}) = e^{i\mathbf{k}\cdot\mathbf{r}} u_{nk}(\mathbf{r}), \quad u_{nk}(\mathbf{r}) = \sum_g u_{nkg} e^{i\mathbf{g}\cdot\mathbf{r}}, \quad \psi_{nk}(\mathbf{r} + \mathbf{R}) = e^{i\mathbf{k}\cdot\mathbf{R}} \psi_{nk}(\mathbf{r})$$

usually, $\mathbf{k} \in 1^{\text{st}}$ BZ, n is a positive integer (index of the energy band)

Proof of the Bloch theorem:

Let us define the translation operator $\hat{T}_R \psi(\mathbf{r}) = \psi(\mathbf{r} + \mathbf{R})$

Then $\hat{T}_R \hat{H} \psi = \hat{T}_R E \psi = E \hat{T}_R \psi,$

$$\hat{H} \hat{T}_R \psi = -\frac{\hbar^2}{2m} \Delta \psi(\mathbf{r} + \mathbf{R}) + U(\mathbf{r} + \mathbf{R}) \psi(\mathbf{r} + \mathbf{R}) = E \hat{T}_R \psi(\mathbf{r})$$

and therefore $\hat{T}_R \hat{T}_{R'} = \hat{T}_{R+R'}, \quad [\hat{T}_R, \hat{H}] = 0$

The Bloch waves are the eigenfunctions of \hat{T}_R and \hat{H} simultaneously

$$\hat{H} \psi = E \psi, \quad \hat{T}_R \psi = c(\mathbf{R}) \psi$$

Then $c(\mathbf{R} + \mathbf{R}') = c(\mathbf{R})c(\mathbf{R}')$ and we can always write $c(\mathbf{a}_j) = e^{2\pi i x_j}$ and

$$c(\mathbf{R}) = e^{i\mathbf{k}\cdot\mathbf{R}}, \quad \mathbf{k} = x_1 \mathbf{b}_1 + x_2 \mathbf{b}_2 + x_3 \mathbf{b}_3$$

and thus $\hat{T}_R \psi = c(\mathbf{R}) \psi = e^{i\mathbf{k}\cdot\mathbf{R}} \psi$ q.e.d.

Born-von Kármán boundary conditions

$$\psi(\mathbf{r}) = \psi(\mathbf{r} + N_1\mathbf{a}_1) = \psi(\mathbf{r} + N_2\mathbf{a}_2) = \psi(\mathbf{r} + N_3\mathbf{a}_3)$$

The Born-von Kármán region contains $N_1N_2N_3$ unit cells

Possible values of \mathbf{k} are
$$\mathbf{k} = \sum_{j=1}^3 \mathbf{b}_j \frac{m_j}{N_j}$$

Usually, we choose \mathbf{k} from the 1st BZ. If we choose \mathbf{k} from the 2nd BZ, for instance, then

$$\mathbf{k} = \mathbf{k}' + \mathbf{g}, \mathbf{k}' \in 1^{\text{st}} \text{ BZ}$$

and
$$\psi_{nk'}(\mathbf{r}) = e^{i\mathbf{g}\cdot\mathbf{r}} \psi_{nk}(\mathbf{r}) = e^{i\mathbf{k}\cdot\mathbf{r}} u_{nk}(\mathbf{r}) e^{i\mathbf{g}\cdot\mathbf{r}} = e^{i\mathbf{k}\cdot\mathbf{r}} u'_{nk}(\mathbf{r})$$

If we do not choose \mathbf{k} from the 1st BZ, then we do not need the band index n .

The number of one-electron states in the 1st BZ equals the number $N_1N_2N_3$ of the unit cells in the Born-von Kármán region

Putting the Bloch wave into the Schroedinger equation, we obtain

$$\hat{H}_k u_{nk}(\mathbf{r}) = \left[\frac{\hbar^2}{2m} (-i\nabla + \mathbf{k})^2 + U(\mathbf{r}) \right] u_{nk}(\mathbf{r}) = E_n(\mathbf{k}) u_{nk}(\mathbf{r})$$

The solutions of this equation are indexed by the band index n . ($\mathbf{k}\cdot\mathbf{p}$ method)

If we allow \mathbf{k} to range through all the \mathbf{k} -space, for given n ,

$$E_n(\mathbf{k} + \mathbf{g}) = E_n(\mathbf{k}), \psi_{n\mathbf{k}+\mathbf{g}}(\mathbf{r}) = \psi_{n\mathbf{k}}(\mathbf{r}) \quad (\text{repeated band scheme})$$

Comments:

1. $\hbar\mathbf{k}$ is the pseudo-momentum $\mathbf{v}_n(\mathbf{k}) = \frac{1}{\hbar} \nabla_{\mathbf{k}} E_n(\mathbf{k})$

2. the mean velocity of the electron in state $n\mathbf{k}$ is

This is a contradiction to the Drude model, in which the mean velocity is zero!!

Fermi surface

Insulators, intrinsic semiconductors: completely filled and completely empty bands at 0K

Metals: partially filled bands at 0K

Equation of the Fermi surface: $\mathcal{E}_n(\mathbf{k}) = \mathcal{E}_F$

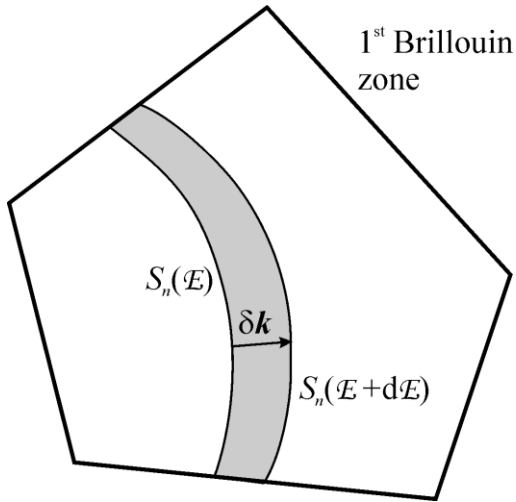
Density of states

Total energy of the electron gas

$$E = 2 \sum_n \sum_{\mathbf{k} \in 1BZ} f_{nk} \mathcal{E}_n(\mathbf{k}) \approx \frac{V}{4\pi^3} \sum_n \int_{1BZ} d^3\mathbf{k} f_{nk} \mathcal{E}_n(\mathbf{k}) = V \int_0^{\infty} d\mathcal{E} f(\mathcal{E}) g(\mathcal{E}) \mathcal{E}$$

The density of states $g(\mathcal{E}) = \sum_n g_n(\mathcal{E}) = \sum_n \frac{1}{4\pi^3} \int_{1BZ} d^3\mathbf{k} \delta^{(3)}(\mathcal{E} - \mathcal{E}_n(\mathbf{k}))$

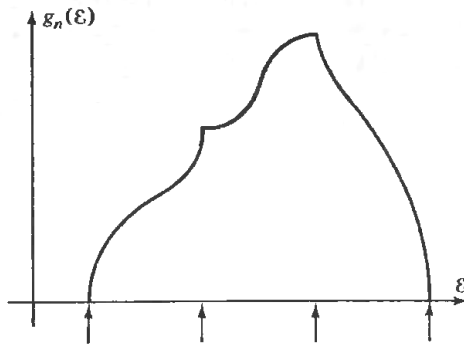
$$g_n(\mathcal{E}) = \frac{\text{number of states in band } n \text{ with the energies } \mathcal{E} \in \langle \mathcal{E}, \mathcal{E} + d\mathcal{E} \rangle}{V d\mathcal{E}}$$



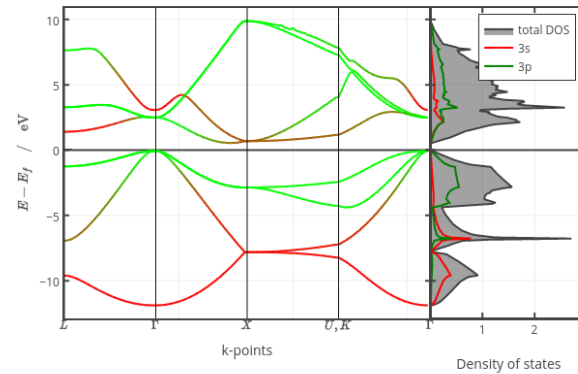
$$g_n(\mathcal{E})d\mathcal{E} = \frac{1}{4\pi^3} \int_{S_n(\mathcal{E})} d^2S |\delta \mathbf{k}|$$

$$g_n(\mathcal{E}) = \frac{1}{4\pi^3} \int_{S_n(\mathcal{E})} \frac{d^2S}{|\nabla_{\mathbf{k}} \mathcal{E}_n(\mathbf{k})|}$$

If $\nabla_{\mathbf{k}} \mathcal{E}_n(\mathbf{k}) = 0$, the slope $\frac{dg_n(\mathcal{E})}{d\mathcal{E}}$ diverges – van Hove singularity



Bands diagram and density of states of Silicon



How to solve the one-electron Schroedinger equation?

Several methods, we discuss

1. Nearly-free electron method
2. Tight-binding method

Nearly-free electron method

We look for the solution of the Schroedinger equation in the form of the Bloch wave

$$\psi(\mathbf{r}) = e^{i\mathbf{k}\cdot\mathbf{r}} u(\mathbf{r}) = \sum_{\mathbf{g}} u_{\mathbf{g}} e^{i(\mathbf{k}+\mathbf{g})\cdot\mathbf{r}}$$

We express the potential energy using the Fourier series

$$U(\mathbf{r}) = \sum_{\mathbf{g}} U_{\mathbf{g}} e^{i\mathbf{g}\cdot\mathbf{r}}$$

We obtain an infinite system of linear algebraic equations for the coefficients $u_{\mathbf{g}}$:

$$\left(\frac{\hbar^2}{2m} |\mathbf{k} + \mathbf{g}|^2 - E \right) u_{\mathbf{g}} + \sum_{\mathbf{g}'} U_{\mathbf{g}'} u_{\mathbf{g}-\mathbf{g}'} = 0$$

This system can be solved, if we limit the number of terms in the expression for $\psi(\mathbf{r})$

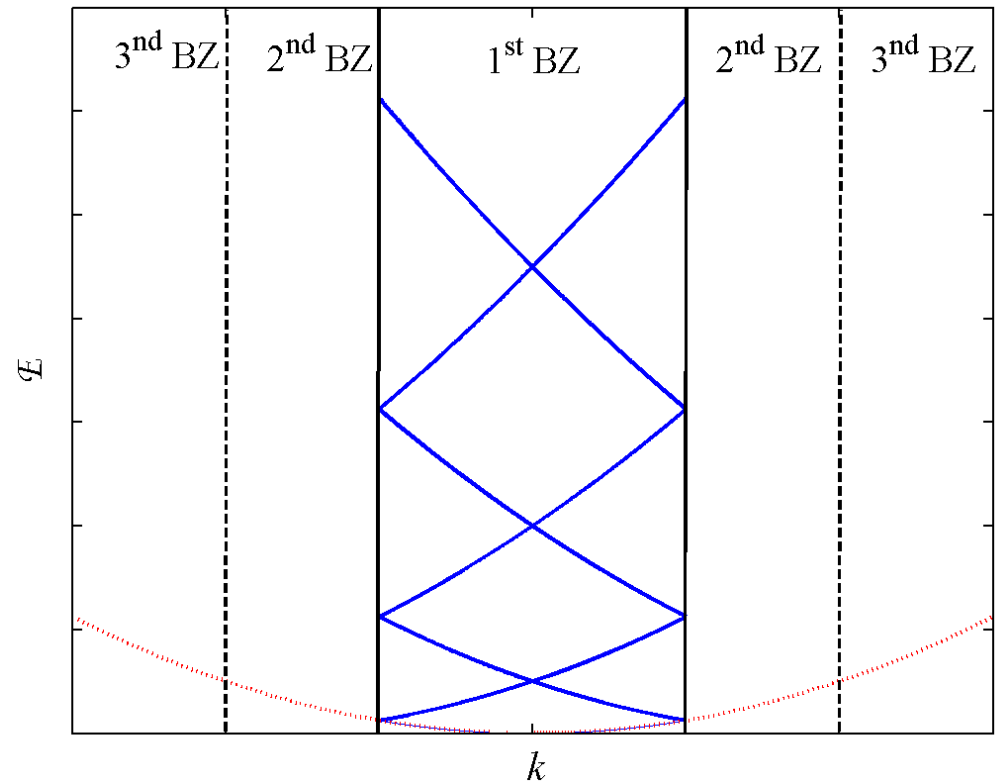
The simplest case – **empty lattice** $U_g = 0$

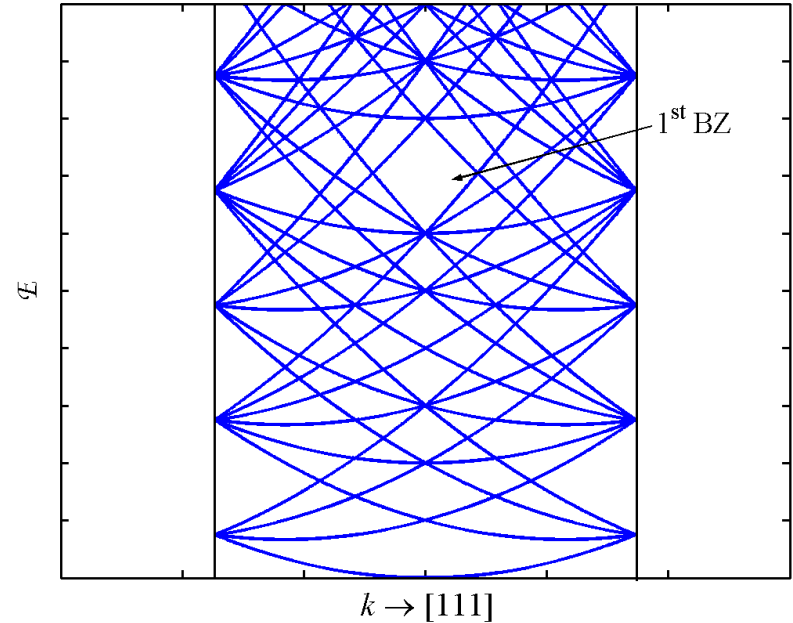
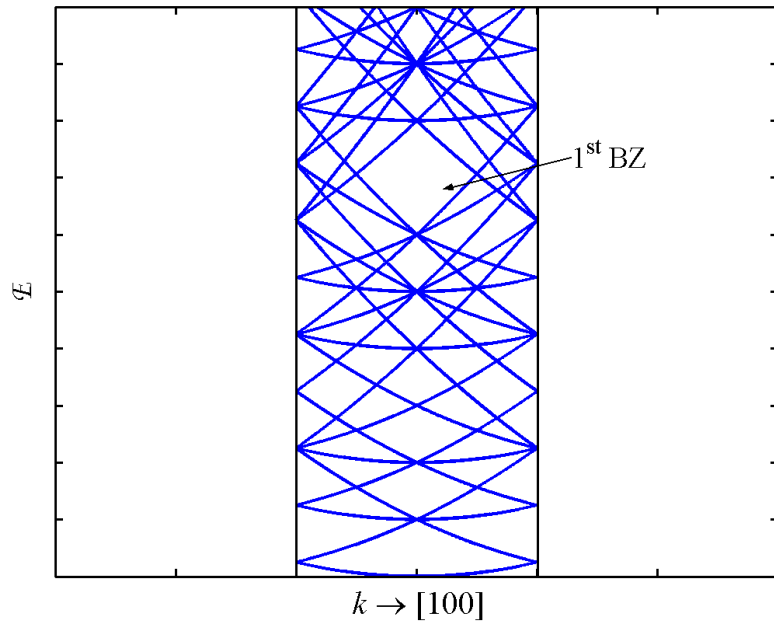
The condition for the existence of a non-trivial solution $u_g \neq 0$

$$E_g(\mathbf{k}) = \frac{\hbar^2}{2m} |\mathbf{k} + \mathbf{g}|^2, \mathbf{k} \in \text{1st BZ}$$

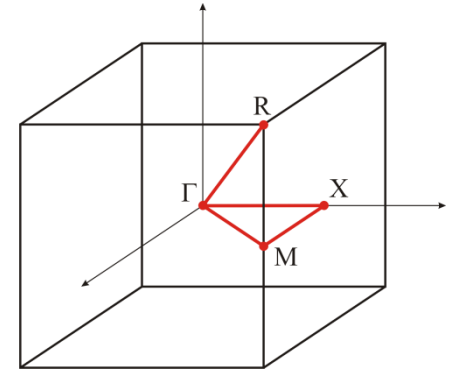
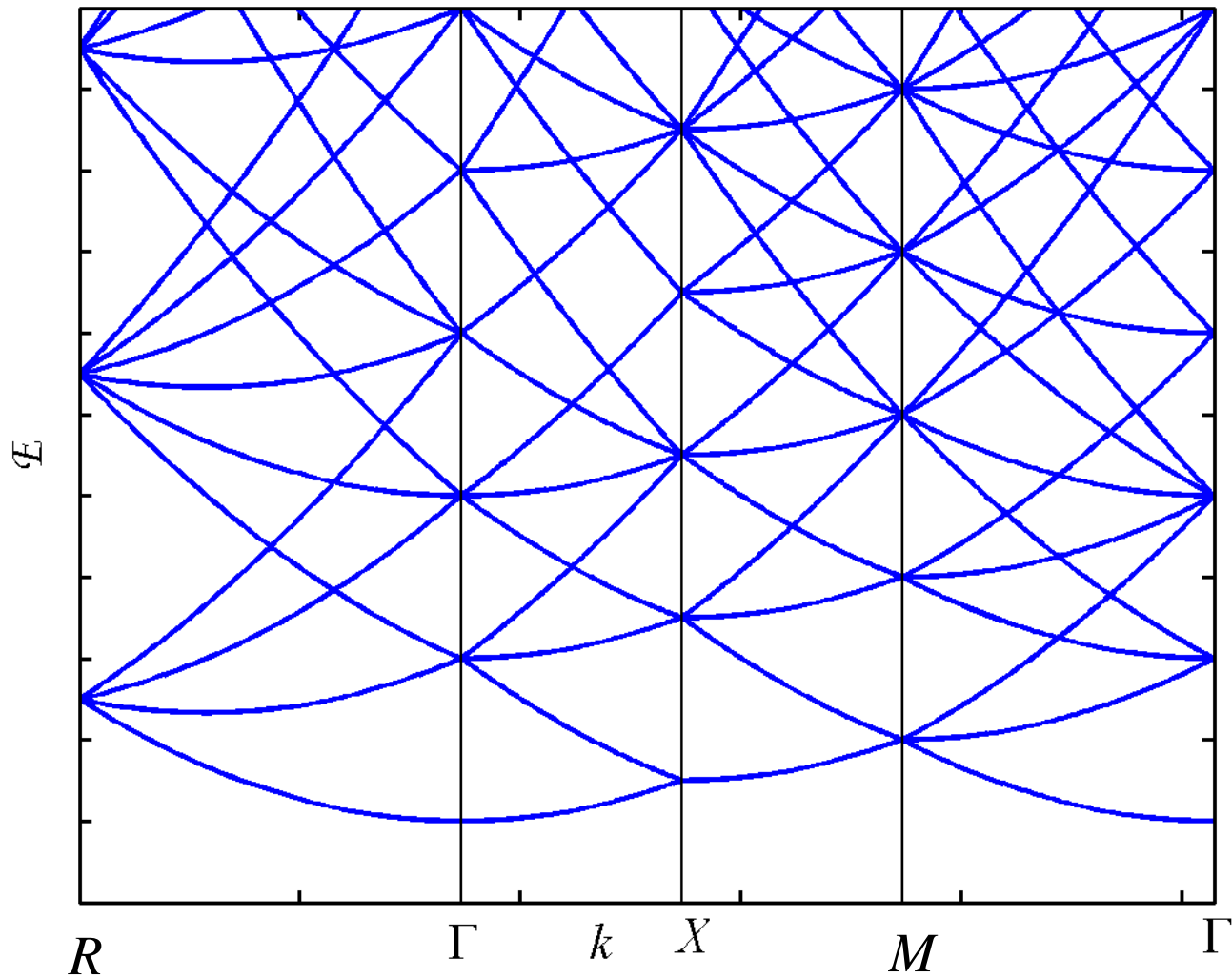
1D case – periodic chain of atoms:

all bands are non-degenerated

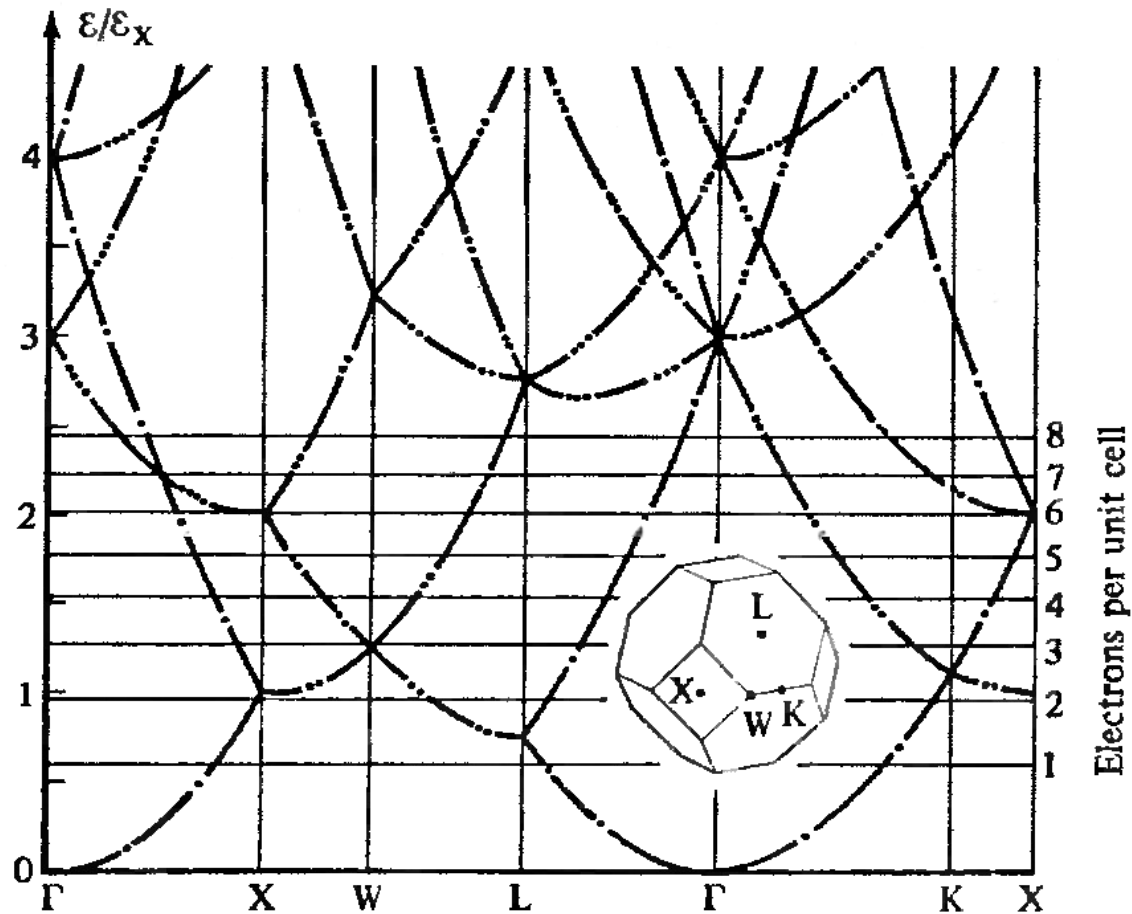




3D case – cubic lattice; some bands are degenerated



simple cubic empty lattice

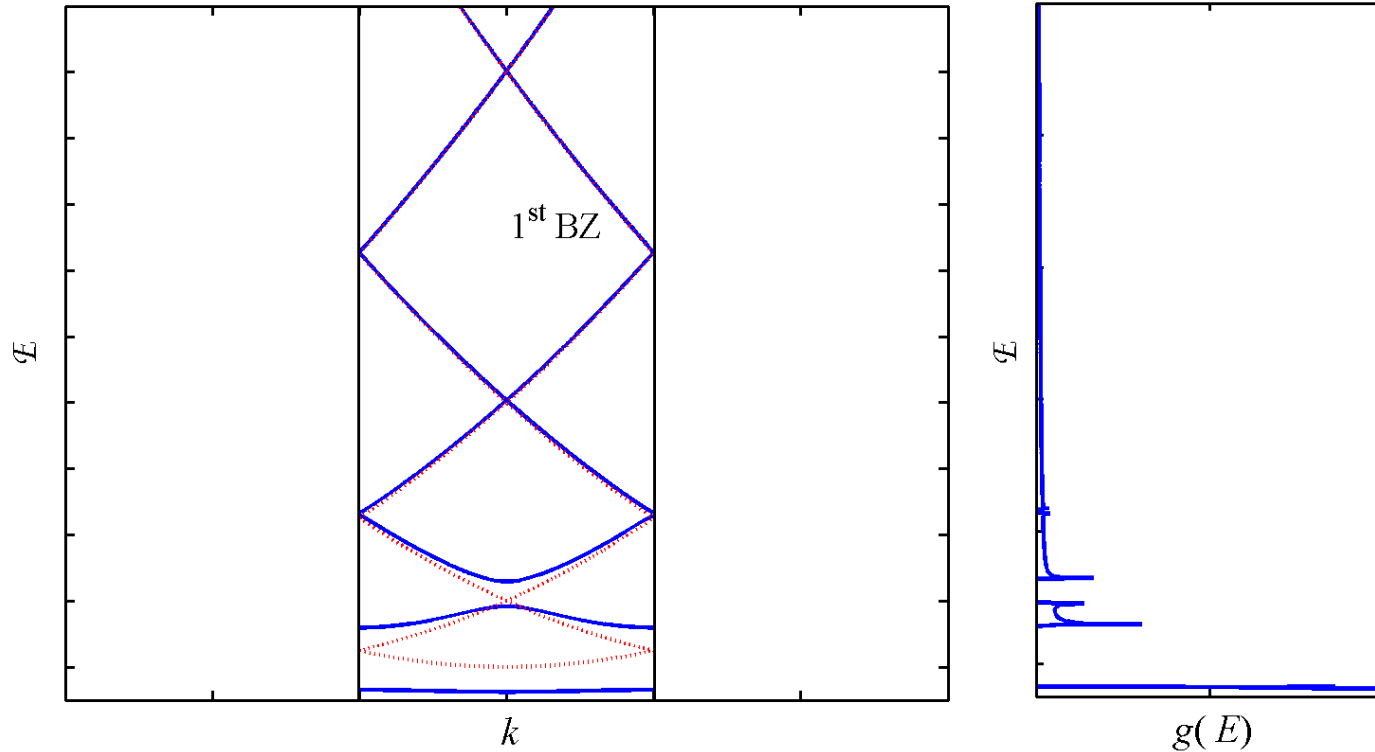


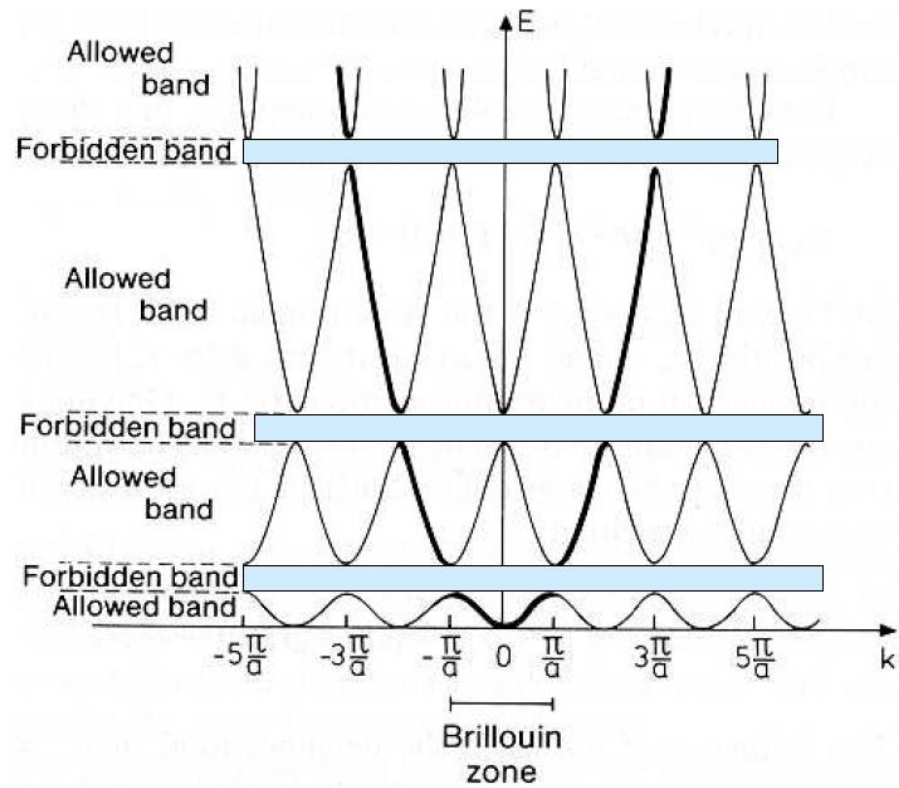
fcc empty lattice – the numbers of the dots in the lines denote the degeneracy

Another simple case: **cosine-like potential**

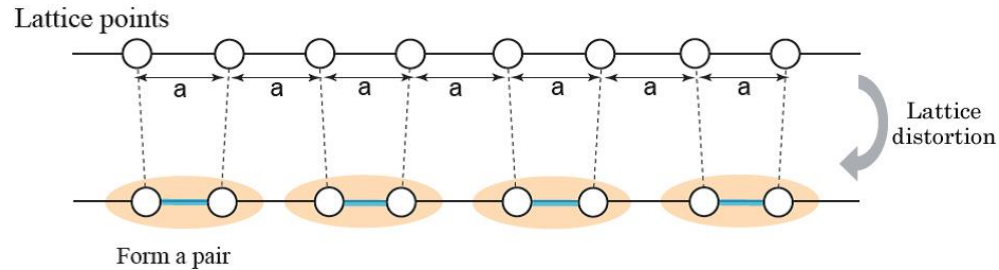
1D case: $U(x) = U_0 \cos(Gx) = \frac{U_0}{2} (e^{iGx} + e^{-iGx})$, $G = \frac{2\pi}{a}$

Seminar

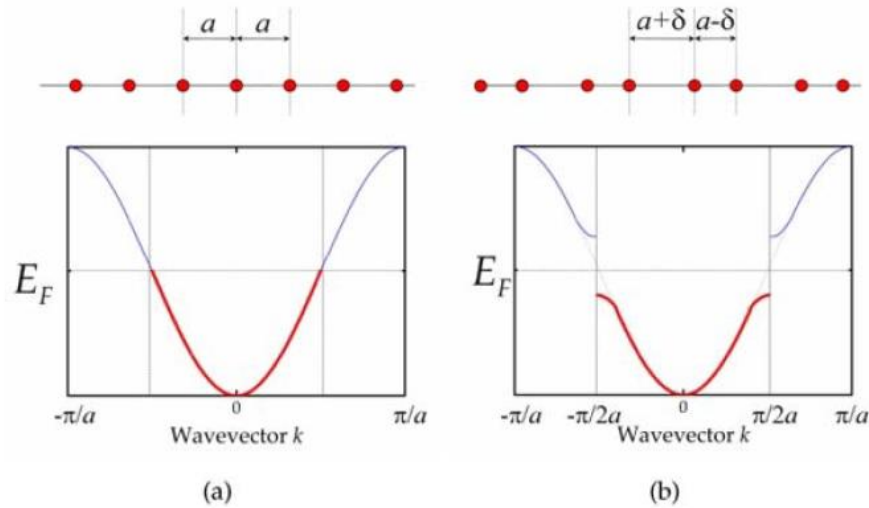




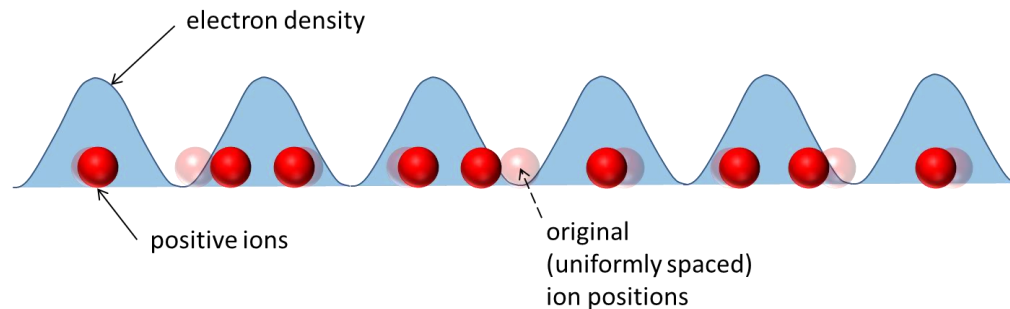
Peierls distortion \Rightarrow spontaneous metal to insulator transition (visible at low temperatures)

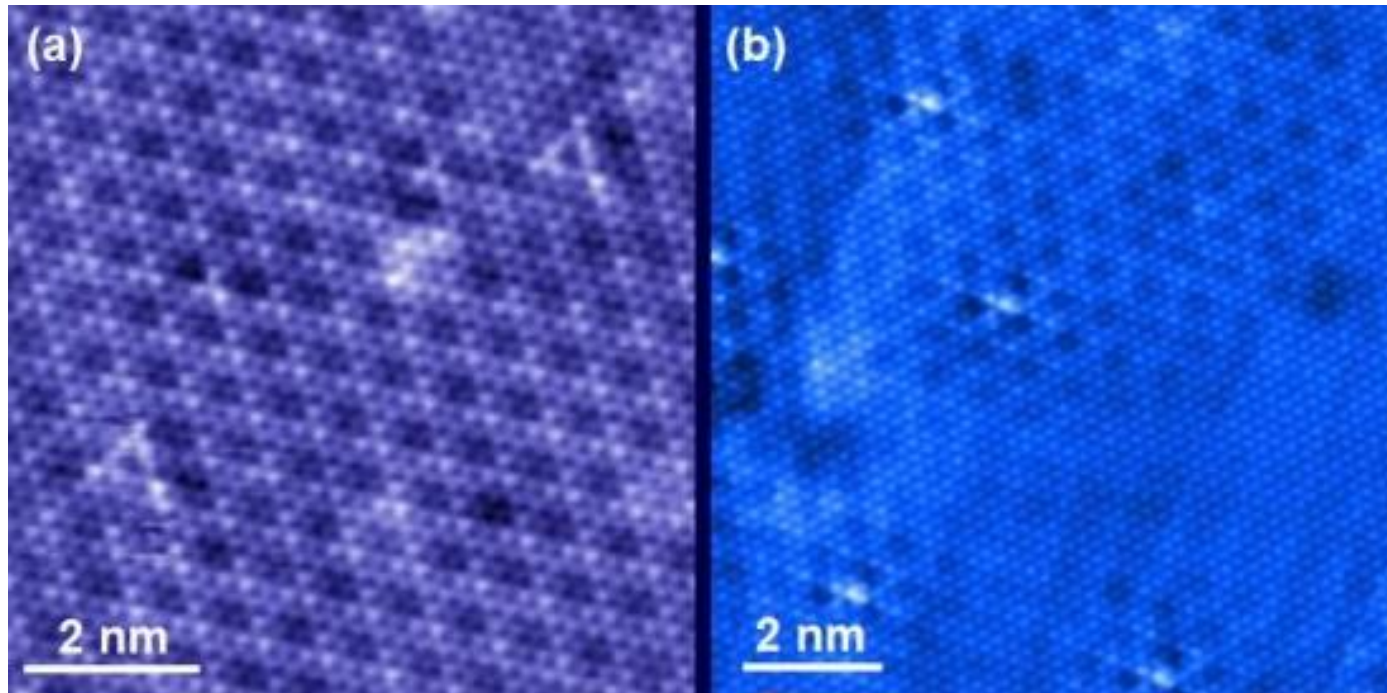


the total energy is reduced!!



Charge-density waves





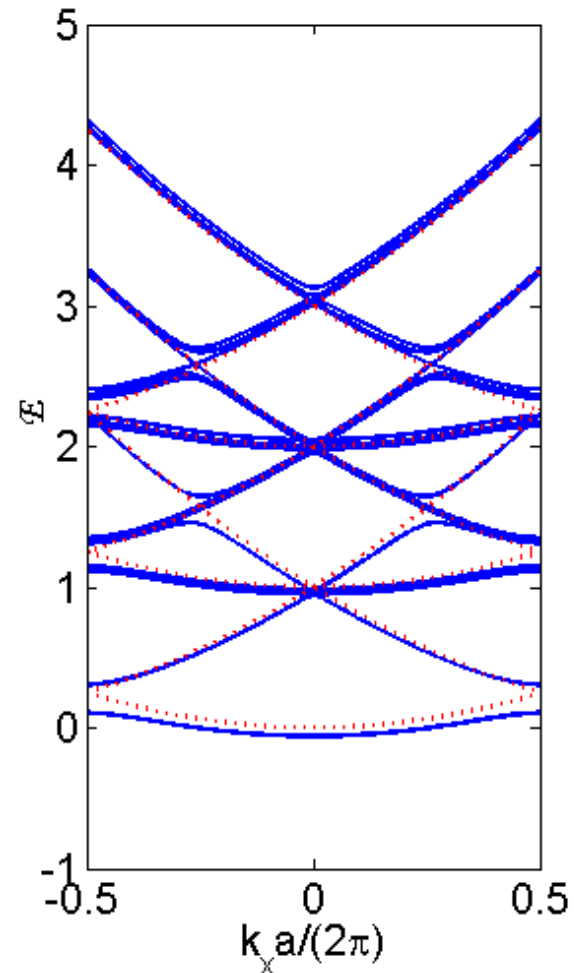
Atomically resolved STM topographies ($10 \text{ nm} \times 10 \text{ nm}$) of doped NbSe_2 , showing a hexagonal lattice and triangular impurities. **(a)** Topography taken at temperature below the CDW transition. The CDW is well defined and has a three-atom periodicity. **(b)** Topography taken at a temperature above the transition temperature. Above the transition the long-range phase coherence is broken and the CDW is pinned to impurities.

http://hoffman.physics.harvard.edu/research/STMresearch_replaced_2014_06_12.php
Anjan Soumyanarayanan et al., PNAS 110,1623-1627 (2013).

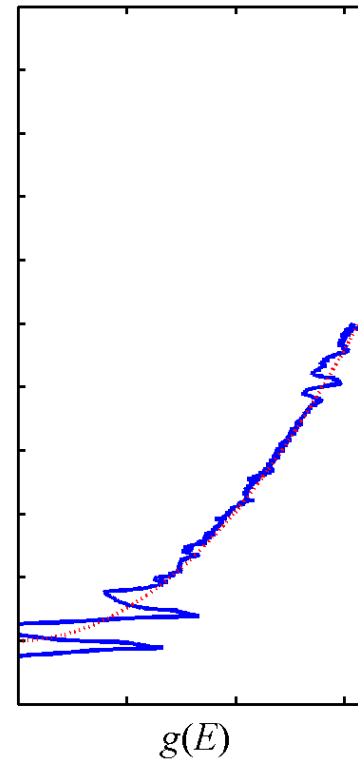
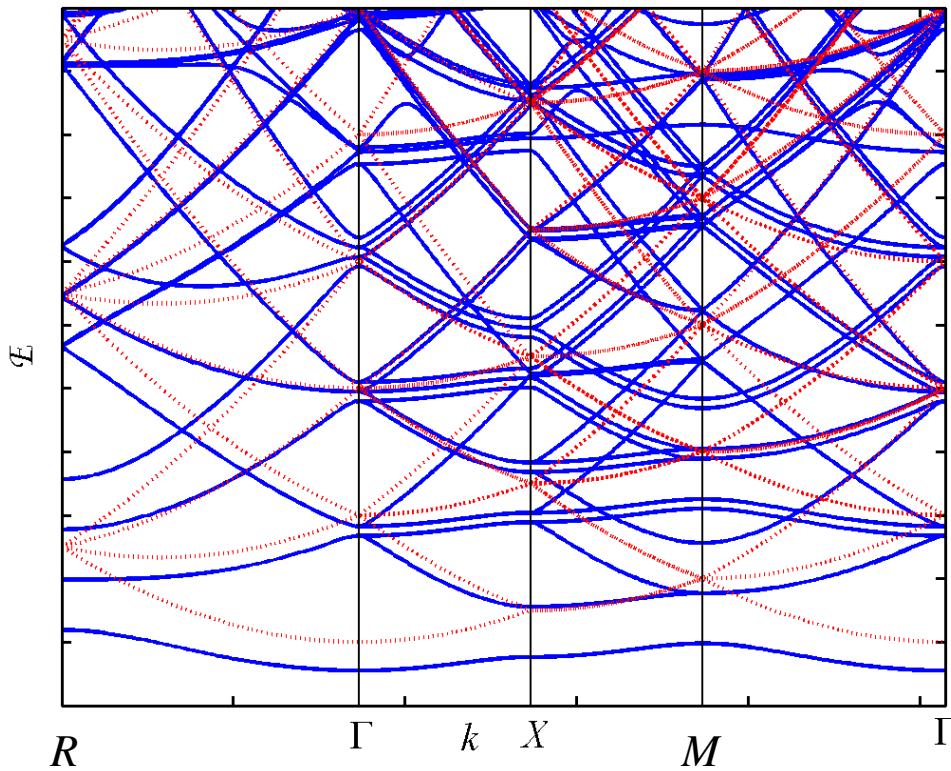
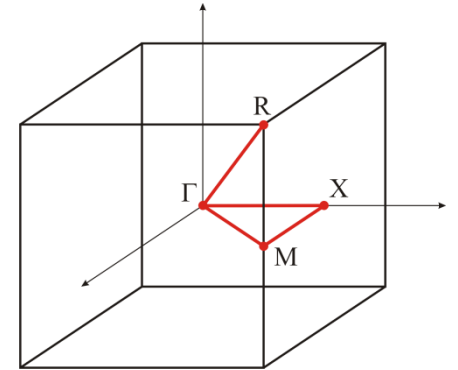
3D case – simple cubic lattice:

$$U(\mathbf{r}) = \frac{U_0}{3} [\cos(Gx) + \cos(Gy) + \cos(Gz)], \quad G = \frac{2\pi}{a}$$

The crystal field removes the degeneracy



Along the line in the 1st Brillouin zone:



Neighborhood of a boundary of the Brillouin zone

We consider only 2 terms in the series $\psi(\mathbf{r}) = e^{i\mathbf{k}\cdot\mathbf{r}} u(\mathbf{r}) = \sum_{\mathbf{g}} u_{\mathbf{g}} e^{i(\mathbf{k}+\mathbf{g})\cdot\mathbf{r}}$

We put $U_0 = 0$ and $U_{-\mathbf{g}} = U_{\mathbf{g}}^*$

Seminar

$$\left(\frac{\hbar^2}{2m} |\mathbf{k}|^2 - E \right) u_0 + U_{\mathbf{g}}^* u_{\mathbf{g}} = 0$$

$$\left(\frac{\hbar^2}{2m} |\mathbf{k} + \mathbf{g}|^2 - E \right) u_{\mathbf{g}} + U_{\mathbf{g}} u_0 = 0$$

We investigate the neighborhood of the boundary of the 1st BZ:

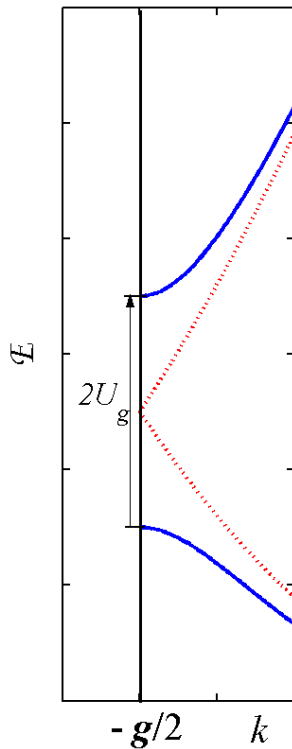
$$\mathbf{k} \approx -\mathbf{g} / 2$$

We obtain

$$\mathcal{E}(\mathbf{k}) = \frac{1}{2} [\mathcal{E}_0(\mathbf{k}) + \mathcal{E}_0(\mathbf{k} + \mathbf{g})] \pm \sqrt{\frac{1}{4} [\mathcal{E}_0(\mathbf{k}) - \mathcal{E}_0(\mathbf{k} + \mathbf{g})]^2 + |U_{\mathbf{g}}|^2}$$

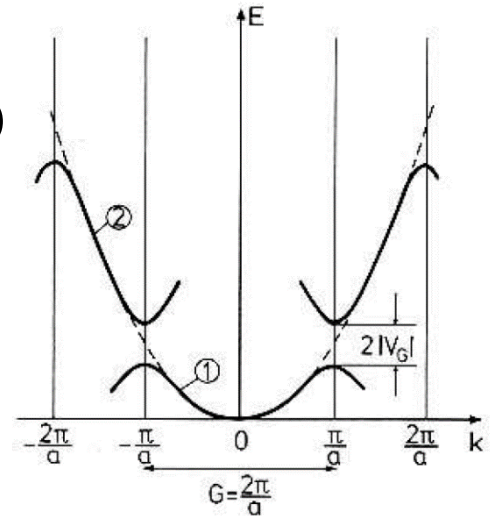
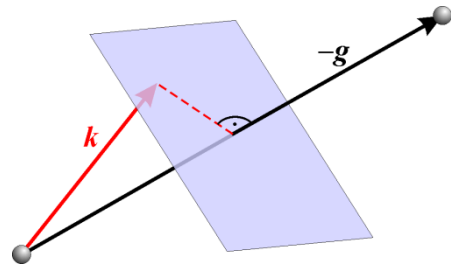
where

$$E_0(\mathbf{k}) = \frac{\hbar^2 k^2}{2m}$$



At the Brillouin zone boundary

$$\nabla_{\mathbf{k}} E(\mathbf{k}) \approx \frac{\hbar^2}{m} \left(\mathbf{k} + \frac{\mathbf{g}}{2} \right) \text{ if } E_0(\mathbf{k}) = E_0(\mathbf{k} + \mathbf{g})$$



At the Brillouin zone boundary, the gradient of the energy is parallel to the boundary
 \Rightarrow **the iso-energetic surfaces are perpendicular to the Brillouin zone boundaries**

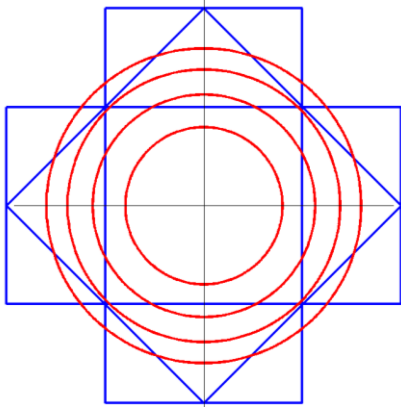
The eigenfunctions:

$$|\psi_{\mathbf{k}}(\mathbf{r})|^2 \propto |\cos(\mathbf{g} \cdot \mathbf{r} / 2)|^2 \text{ for } \mathcal{E} = \mathcal{E}_0(\mathbf{g}) + U_g$$

$$|\psi_{\mathbf{k}}(\mathbf{r})|^2 \propto |\sin(\mathbf{g} \cdot \mathbf{r} / 2)|^2 \text{ for } \mathcal{E} = \mathcal{E}_0(\mathbf{g}) - U_g$$

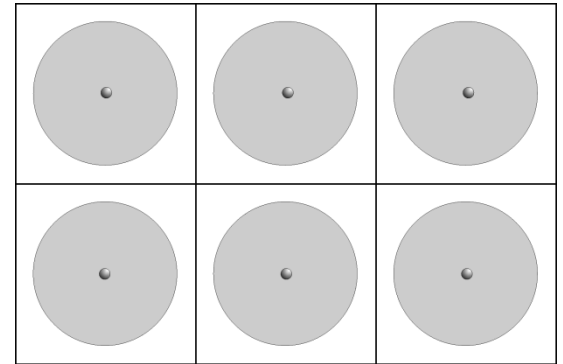
Qualitative construction of the Fermi surface – 2D quadratic lattice

Seminar

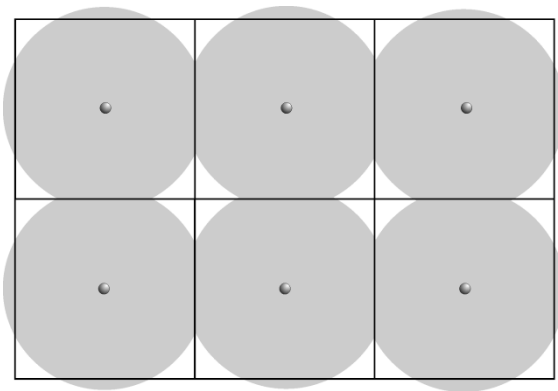


$$k_F = \frac{1}{a} \sqrt{2\pi Z}$$

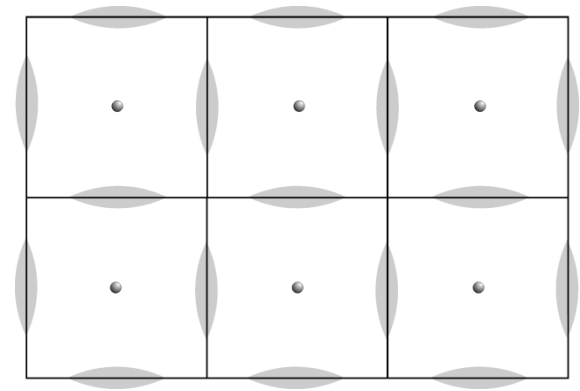
$$Z = 1, n = 1$$



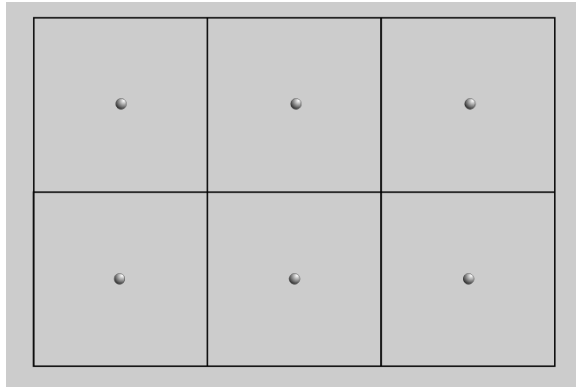
$$Z = 2, n = 1$$



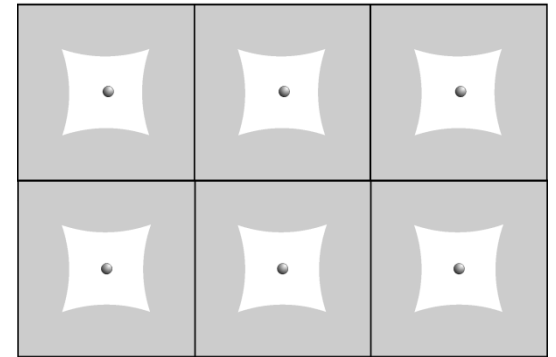
$$Z = 2, n = 2$$



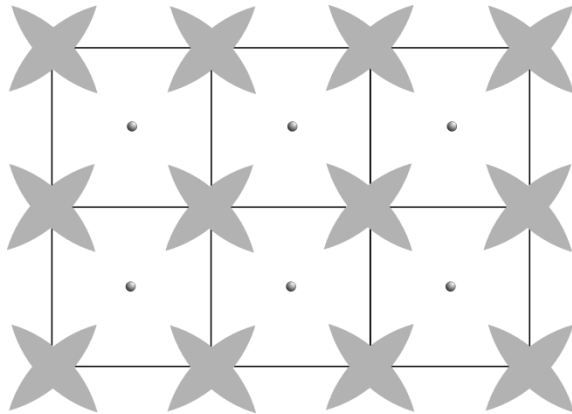
$Z = 4, n = 1$



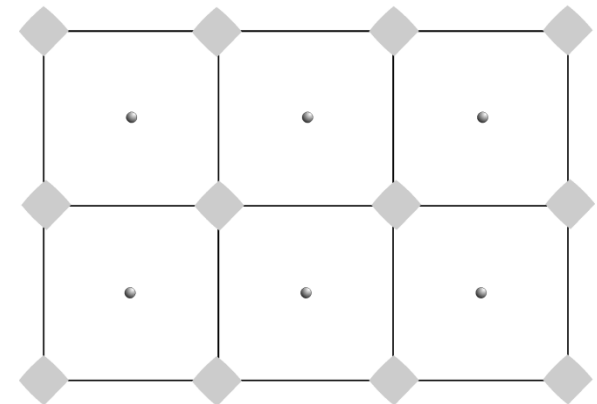
$Z = 4, n = 2$



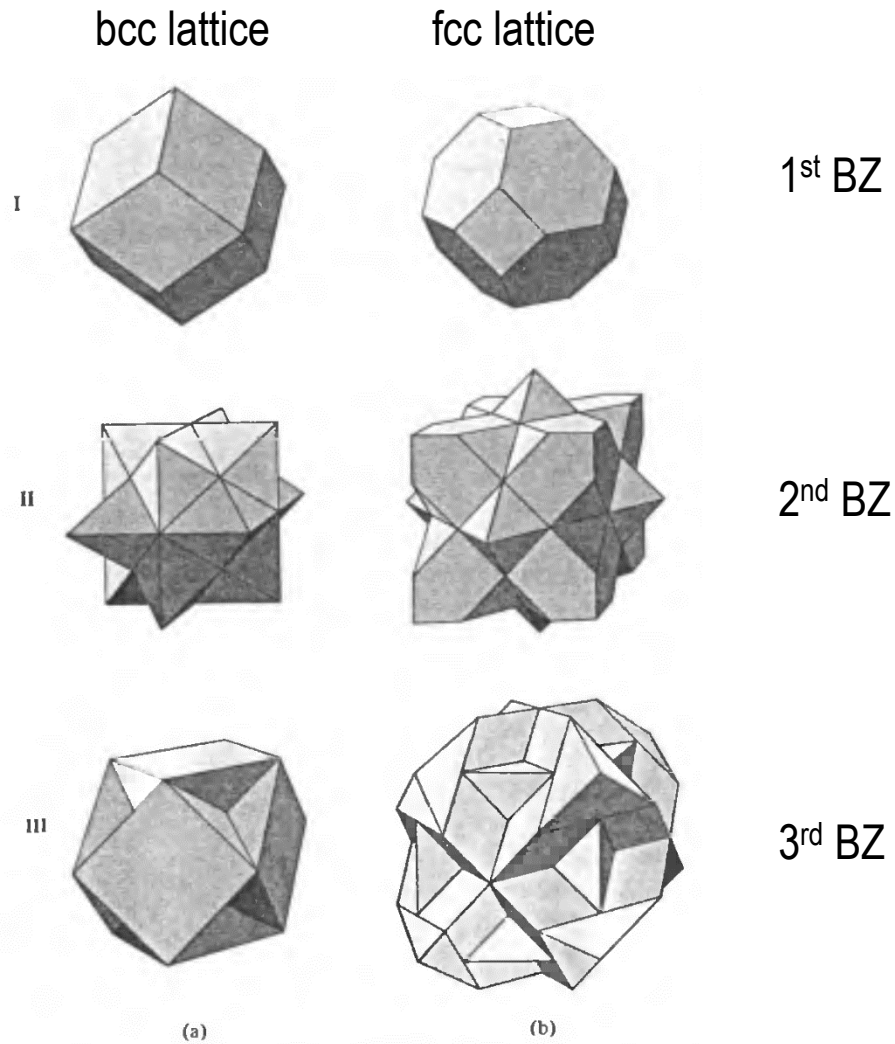
$Z = 4, n = 3$

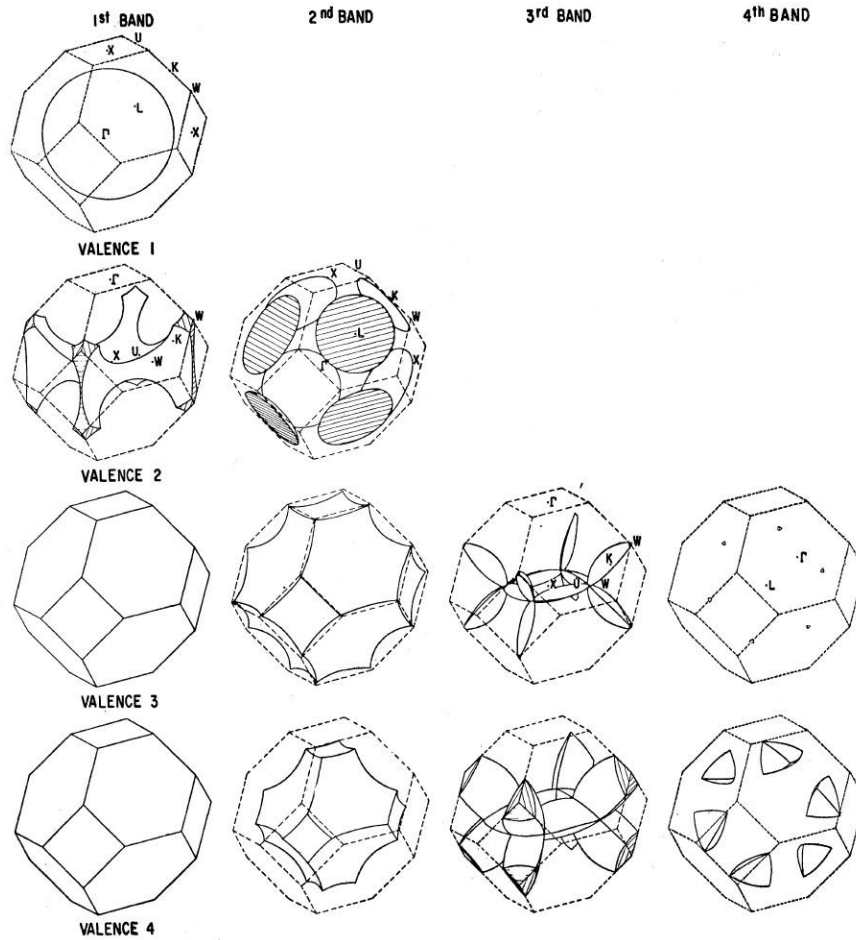


$Z = 4, n = 4$



Fermi surfaces, 3D lattices





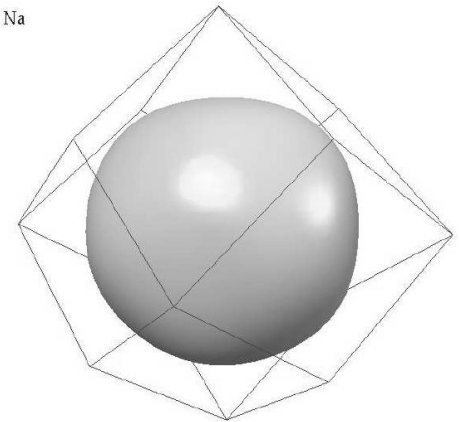
<http://lampx.tugraz.at/>

fcc lattice, the Fermi surfaces for $Z=1, \dots, 4$.

Examples of Fermi surfaces:

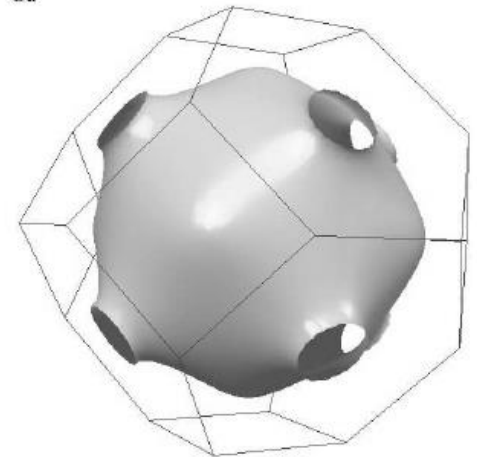
Alkali metals: The radius of the Fermi sphere in bcc alkali metals is less than the shortest distance from the center of the zone to a zone face and therefore the Fermi sphere lies entirely within the first Brillouin zone. The crystal potential does not distort much the free electron Fermi surface and it remains very similar to a sphere.

Na



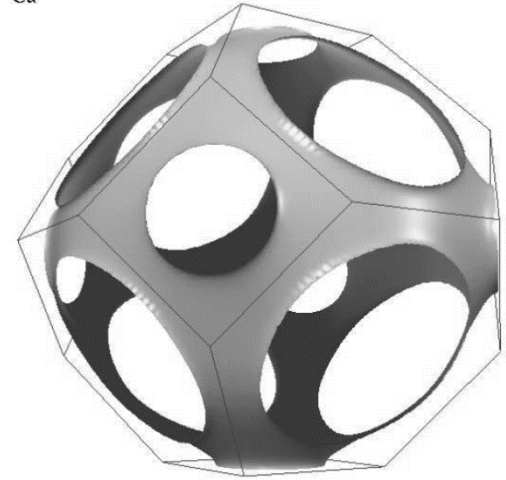
The noble metals: The Fermi surface for a single half-filled free electron band in an fcc Bravais lattice is a sphere entirely contained within the first Brillouin zone, approaching the surface of the zone most closely in the $[111]$ directions, where it reaches 0.903 of the distance from the origin to the center of the hexagonal face. For all three noble metals therefore their Fermi surfaces are closely related to the free electron sphere.

Cu



The cubic divalent metals: With two electrons per primitive cell, calcium, strontium, and barium could, in principle, be insulators. In the free electron model, the Fermi sphere has the same volume as the first zone and therefore intersects the zone faces. The free electron Fermi surface is thus a fairly complex structure in the first zone, and pockets of electrons in the second. The question is whether the effective lattice potential is strong enough to shrink the second-zone pockets down to zero volume, thereby filling up all the unoccupied levels in the first zone. Evidently this is not the case, since the group II elements are all metals. Calculations show that the first Brillouin zone is completely filled and a small number of electrons in the second zone determine the non-zero conductance.

Ca



Trivalent metals: The Fermi surface of aluminum is close to that of the free electron surface for fcc cubic monoatomic lattice with three conduction electrons per atom. The first Brillouin zone is filled and the Fermi surface of free electrons is entirely contained in the second, third and fourth Brillouin zones. When displayed in a reduced-zone scheme the second-zone surface is a closed structure containing unoccupied levels, while the third-zone surface is a complex structure of narrow tubes (see above). The amount of surface in the fourth zone is very small, enclosing tiny pockets of occupied levels. The effect of a weak periodic potential is to eliminate the fourth-zone pockets of electrons, and reduce the third-zone surface to a set of disconnected "rings" (above). Aluminum provides a striking illustration of the theory of Hall coefficients. The high-field Hall coefficient should be

$$R = -1/[e(n_e - n_h)],$$

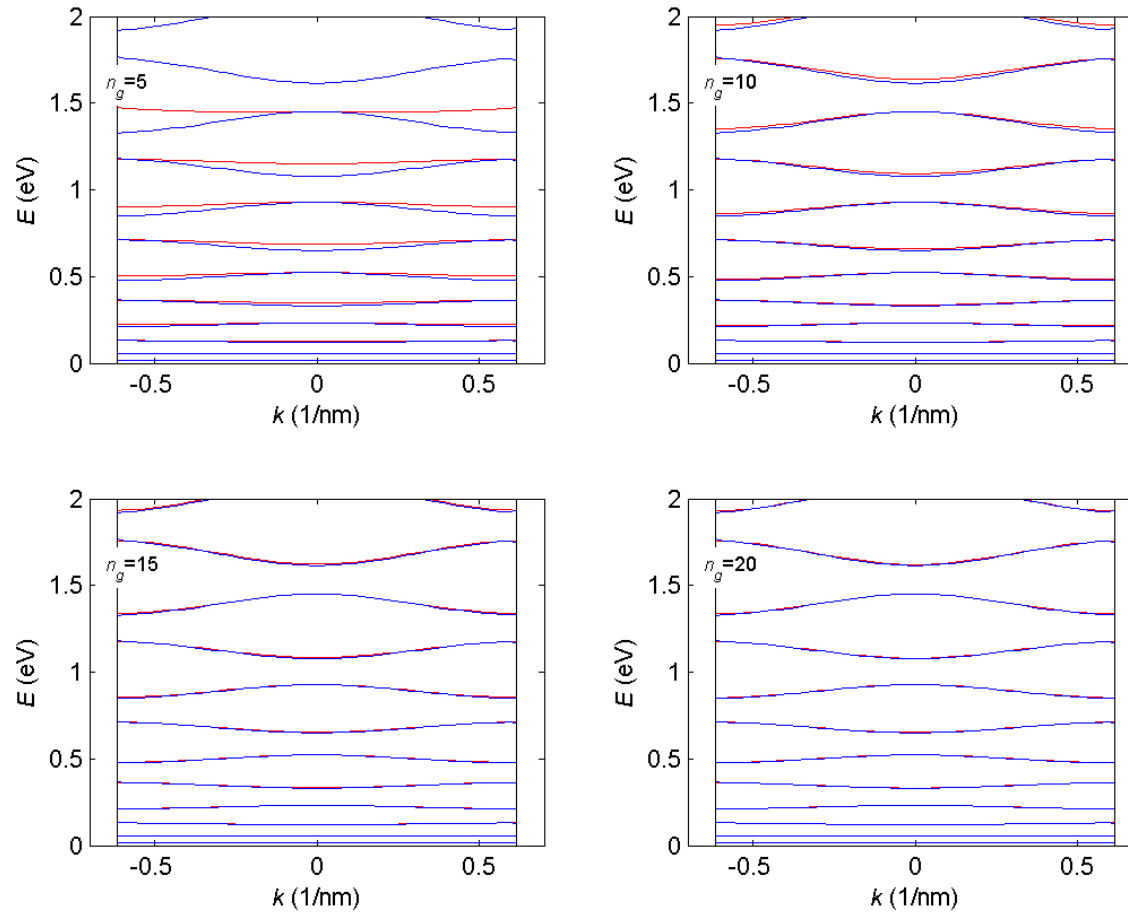
where n_e and n_h are the number of levels per unit volume enclosed by the particle-like and hole-like branches of the Fermi surface. Since the first zone of aluminum is completely filled and accommodates two electrons per atom, one of the three valence electrons per atom remains to occupy second- and third-zone levels. Thus $n_e^{(2)} + n_e^{(3)} = n/3$

On the other hand, since the total number of levels in any zone is enough to hold two electrons per atom, we also have $n_e^{(2)} + n_h^{(2)} = 2n/3 \Rightarrow n_e^{(3)} - n_h^{(2)} = -n/3$

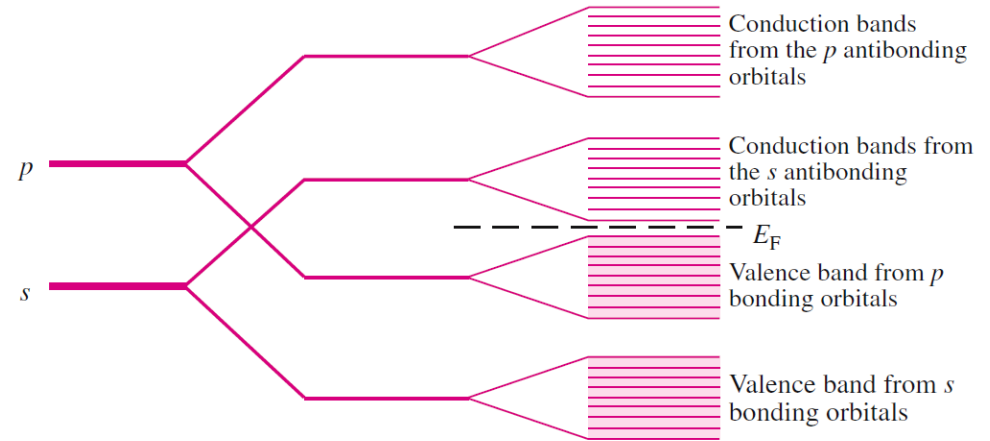
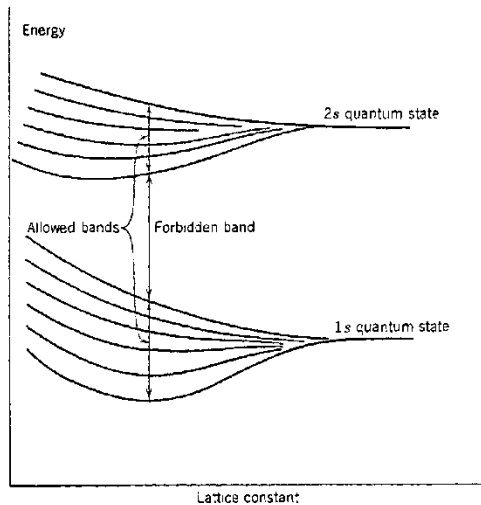
Thus the Hall coefficient should have a positive sign and yield an effective density of carriers a third of the free electron value

From <https://unlcms.unl.edu/cas/physics/tsymbal/teaching/SSP-927/index.shtml>

Comparison of the results of the Kronig-Penney model (blue) with the nearly-free electron method (red) with various numbers of the plane-wave components; $U_0 = 5\text{eV}$, $a = 5\text{nm}$, $b = 0.1\text{nm}$, only the lowest bands are shown



Tight-binding method



Evolution of the atomic s and p orbitals into valence and conduction bands in a semiconductor with tetragonal bonds (after Yu & Cardona)

The eigenstates of an isolated atom lying in origin:

$$\hat{\mathbf{H}}_{at}\varphi_n(\mathbf{r}) = E_n\varphi_n(\mathbf{r})$$

If the crystal hamiltonian \mathbf{H} differs from \mathbf{H}_{at} at distances, where $\varphi_n(\mathbf{r}) \approx 0$, then a superposition of functions φ_n centered around different atoms is a good approximation of a full solution. In order to keep the translation symmetry (the Bloch wave!!) we perhaps could choose

$$\psi_{nk}(\mathbf{r}) = \sum_{\mathbf{R}} e^{i\mathbf{k}\cdot\mathbf{R}} \varphi_n(\mathbf{r} - \mathbf{R})$$

A better choice that accounts also for degenerated atomic levels, is

$$\psi_{\mathbf{k}}(\mathbf{r}) = \sum_{\mathbf{R}} e^{i\mathbf{k}\cdot\mathbf{R}} \sum_n b_n \phi_n(\mathbf{r} - \mathbf{R}) \equiv |\mathbf{k}\rangle = \sum_{\mathbf{R}} e^{i\mathbf{k}\cdot\mathbf{R}} \sum_n b_n |\mathbf{R}n\rangle$$

where b_n are unknown constants. This function obeys the Bloch theorem.

We also denote $\hat{H} = \hat{H}_{at} + \Delta U(\mathbf{r})$ and $\hat{\mathbf{H}}|\mathbf{k}\rangle = \mathcal{E}(\mathbf{k})|\mathbf{k}\rangle$

The Ritz variation method: we minimize the functional

$$\mathcal{E}(\mathbf{k}) = \frac{\langle \mathbf{k} | \hat{\mathbf{H}} | \mathbf{k} \rangle}{\langle \mathbf{k} | \mathbf{k} \rangle} \equiv \frac{\sum_{n,m} b_n b_m^* H_{nm}}{\sum_{n,m} b_n b_m^* S_{nm}}$$

The condition for the minimum is $\frac{\partial \mathcal{E}}{\partial b_m^*} = 0$

From which we get $\sum_n b_n [H_{nm} - \mathcal{E}(\mathbf{k})S_{nm}] \equiv \sum_n b_n A_{nm}(\mathbf{k}) = 0$ for each m (free index)

We have denoted

$$A_{nm}(\mathbf{k}) = \sum_{\mathbf{R}} \sum_{\mathbf{R}'} e^{i\mathbf{k}\cdot(\mathbf{R}-\mathbf{R}')} [\langle \mathbf{R}'m | \hat{\mathbf{H}} | \mathbf{R}n \rangle - \mathcal{E}(\mathbf{k})\langle \mathbf{R}'m | \mathbf{R}n \rangle] = N \sum_{\mathbf{R}} e^{i\mathbf{k}\cdot\mathbf{R}} [\langle \mathbf{R}m | \hat{\mathbf{H}} | \mathbf{0}n \rangle - \mathcal{E}(\mathbf{k})\langle \mathbf{R}m | \mathbf{0}n \rangle]$$

$$A_{nm}(\mathbf{k}) = N\{[\mathcal{E}_{at} - \mathcal{E}(\mathbf{k})][\delta_{nm} + \alpha_{nm}(\mathbf{k})] - \beta_{nm} - \gamma_{nm}(\mathbf{k})\}$$

where

$$\hat{\mathbf{H}}_{at}|\mathbf{R}n\rangle = \mathcal{E}_{at}|\mathbf{R}n\rangle \quad \alpha_{nm}(\mathbf{k}) = \sum_{\mathbf{R} \neq \mathbf{0}} e^{i\mathbf{k} \cdot \mathbf{R}} \langle \mathbf{R}m | \mathbf{0}n \rangle$$

$$\beta_{nm} = -\langle \mathbf{0}m | \Delta U | \mathbf{0}n \rangle \quad \gamma_{nm}(\mathbf{k}) = -\sum_{\mathbf{R} \neq \mathbf{0}} e^{i\mathbf{k} \cdot \mathbf{R}} \langle \mathbf{R}m | \Delta U | \mathbf{0}n \rangle$$

Special case: a s-band

only one term in the sum $\sum_n b_n$

Then

$$\begin{aligned} \mathcal{E}(\mathbf{k}) &= \mathcal{E}_{at} - \frac{\beta + \gamma(\mathbf{k})}{1 + \alpha(\mathbf{k})} \approx \mathcal{E}_{at} - \beta - \gamma(\mathbf{k}) = \text{const} + \sum_{\mathbf{R} \neq \mathbf{0}} e^{i\mathbf{k} \cdot \mathbf{R}} \langle \mathbf{R} | \Delta U | \mathbf{0} \rangle = \\ &= \text{const} - \sum_{\mathbf{R} \neq \mathbf{0}} e^{i\mathbf{k} \cdot \mathbf{R}} \gamma(\mathbf{R}) \end{aligned}$$

Simplification: we include only the nearest neighbors in the sum $\sum_{R \neq 0}$

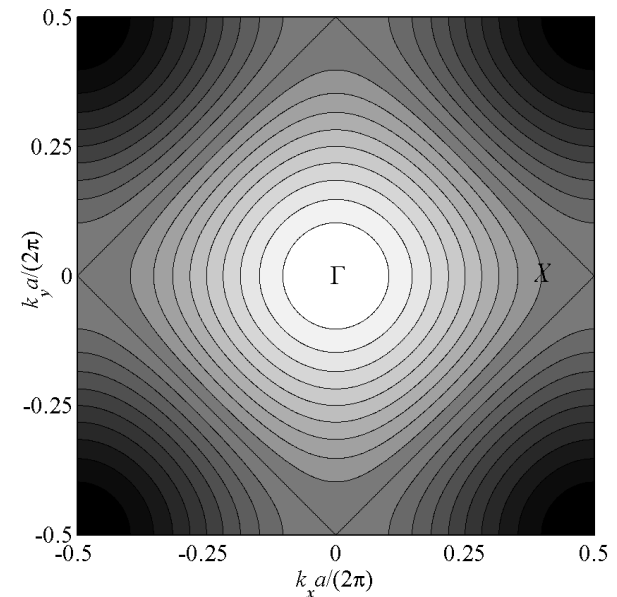
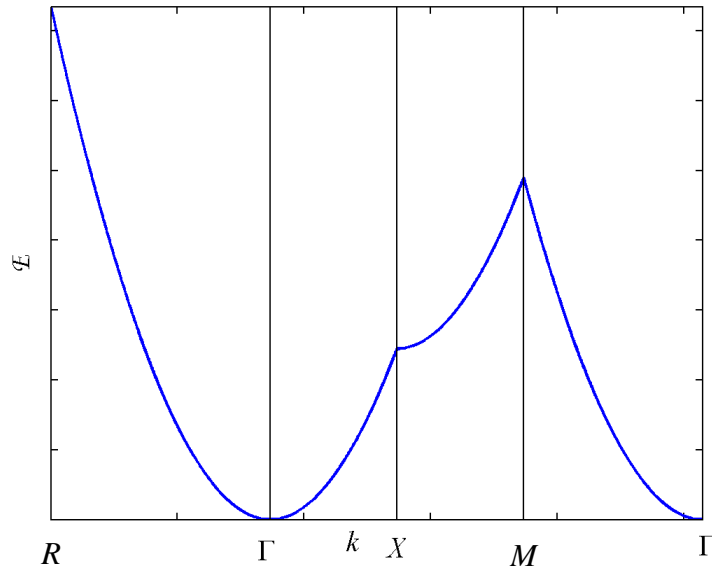
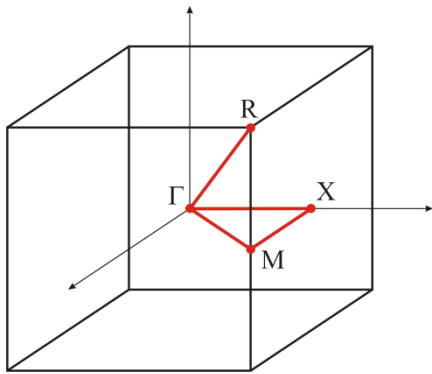
Since the nearest neighbors are crystallographically equivalent,

$$\mathcal{E}(\mathbf{k}) \approx \text{const} - \gamma \sum_{R \in (\text{n.n.})} e^{i\mathbf{k} \cdot \mathbf{R}}$$

effective mass in point Γ :

$$m^* = \frac{\hbar^2}{2\gamma a^2}$$

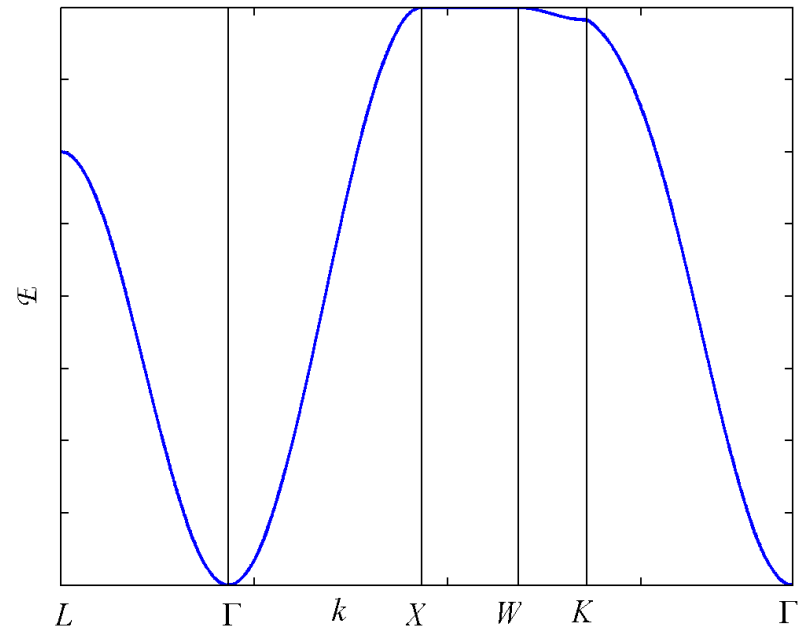
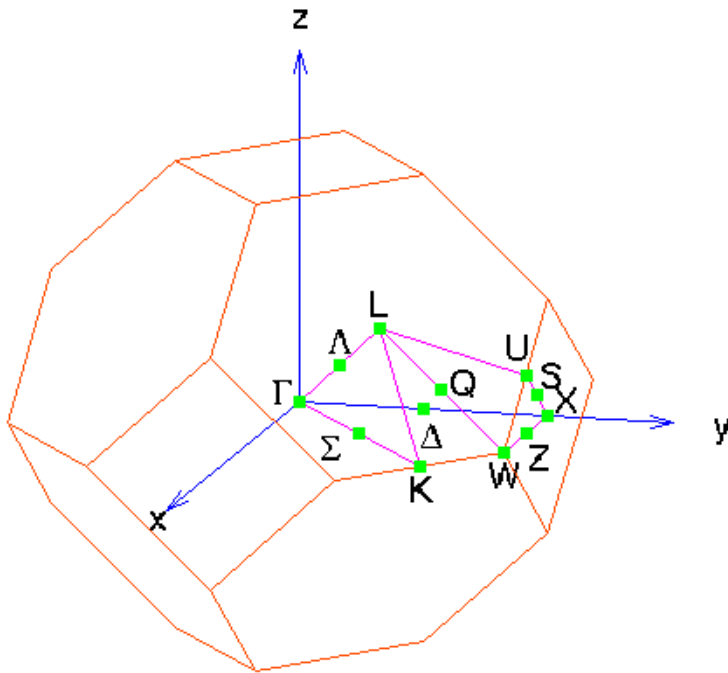
Simple cubic lattice: $\mathcal{E}(\mathbf{k}) = E_s - \beta - 2\gamma[\cos(k_x a) + \cos(k_y a) + \cos(k_z a)]$



fcc lattice:
$$E(\mathbf{k}) = E_s - \beta - 4\gamma[\cos(k_x a / 2) \cos(k_y a / 2) + \cos(k_y a / 2) \cos(k_z a / 2) + \cos(k_z a / 2) \cos(k_x a / 2)]$$

effective mass in point Γ :

$$m^* = \frac{\hbar^2}{2\gamma a^2}$$

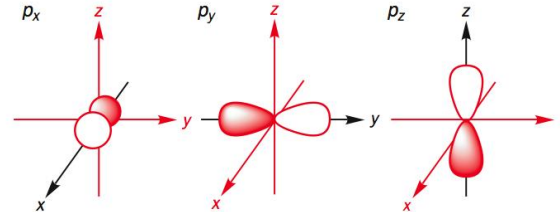


a p-band: three terms in the sum $\sum_n b_n$

The dispersion relation:

$$\det[A_{nm}(\mathbf{k})] = \det\{[\mathcal{E}_{at} - \mathcal{E}(\mathbf{k})][\delta_{nm} + \alpha_{nm}(\mathbf{k})] - \beta_{nm} - \gamma_{nm}(\mathbf{k})\} = 0$$

we choose $|\mathbf{0}n\rangle = x_n f(r), x_n = x, y, z$



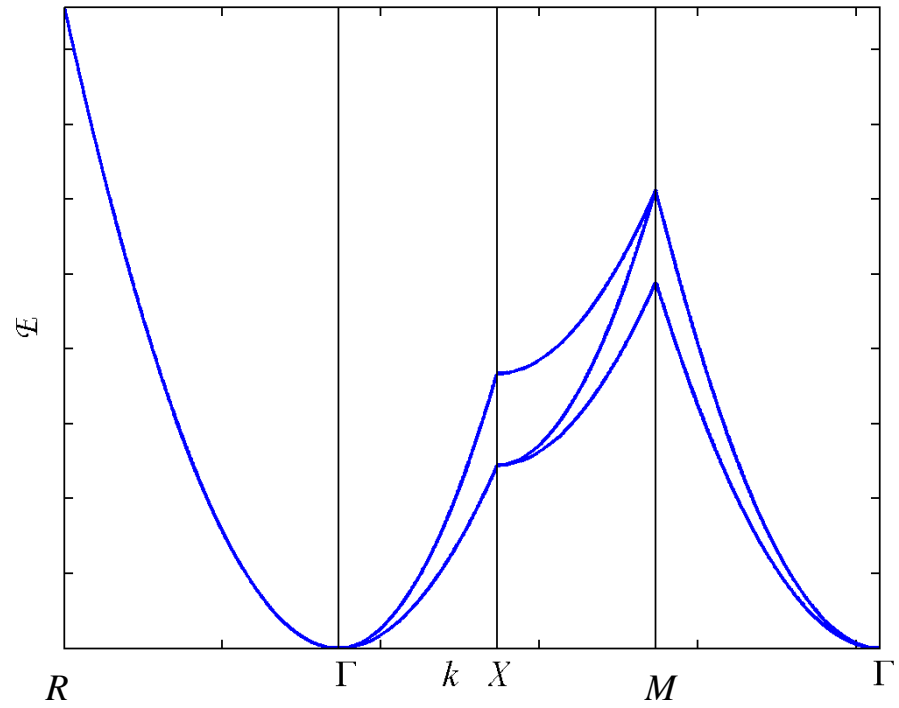
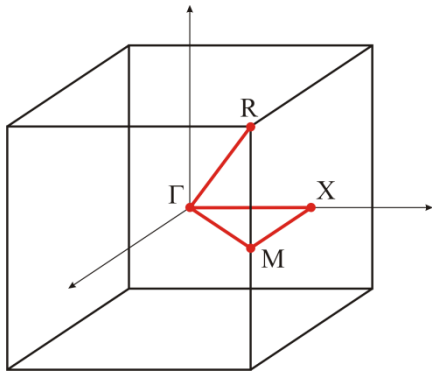
simple cubic lattice, nearest neighbors only:

$$\langle (0,0,0)p_x | \Delta U | (a,0,0)p_x \rangle = \gamma_1, \langle (0,0,0)p_{y,z} | \Delta U | (a,0,0)p_{y,z} \rangle = \gamma_2$$

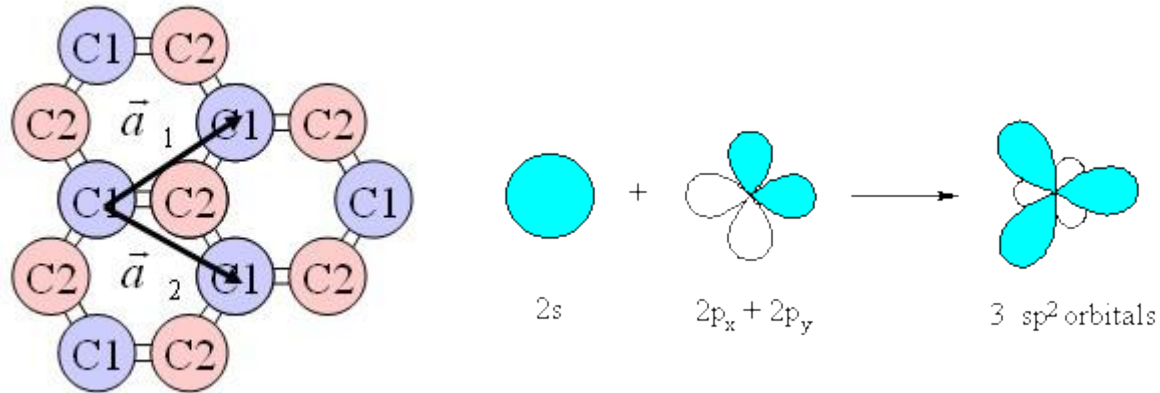
Then from symmetry it follows:

$$\beta_{ij} = \beta \delta_{ij}, \gamma_{ij} = \begin{pmatrix} \gamma_x & 0 & 0 \\ 0 & \gamma_y & 0 \\ 0 & 0 & \gamma_z \end{pmatrix} \quad \begin{aligned} \gamma_x &= 2[\gamma_1 \cos(k_x a) + \gamma_2 \cos(k_y a) + \gamma_2 \cos(k_z a)], \\ \gamma_y &= 2[\gamma_2 \cos(k_x a) + \gamma_1 \cos(k_y a) + \gamma_2 \cos(k_z a)], \\ \gamma_z &= 2[\gamma_2 \cos(k_x a) + \gamma_2 \cos(k_y a) + \gamma_1 \cos(k_z a)] \end{aligned}$$

The 3-fold degeneracy is removed: $E_{x,y,z}(\mathbf{k}) = E_p - \beta - \gamma_{x,y,z}$



Graphene:



Each C atom has a free p_z orbital $|\mathbf{R}\rangle$, the orbitals p_x and p_y are used in the sp^2 hybridized bonds

The LCAO test function can be written in the form

$$|\mathbf{k}\rangle = \sum_{\mathbf{R}} e^{i\mathbf{k}\cdot\mathbf{R}} [c_1|\mathbf{R}\rangle + c_2|\mathbf{R} + \mathbf{d}\rangle]$$

where $\mathbf{d} = (\mathbf{a}_1 + \mathbf{a}_2)/3$ is the position of the 2nd atom in the cell

For the unknown coefficients $c_{1,2}$ we obtain the equations

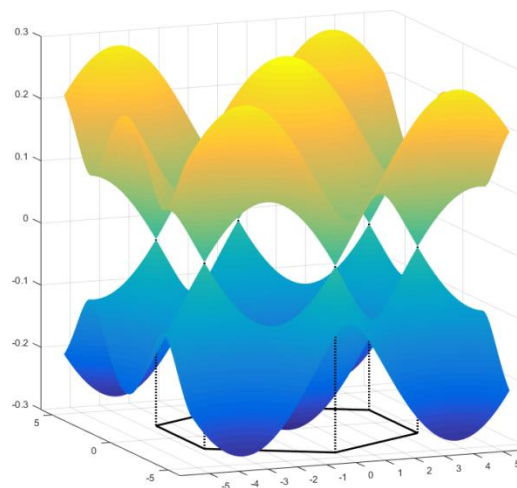
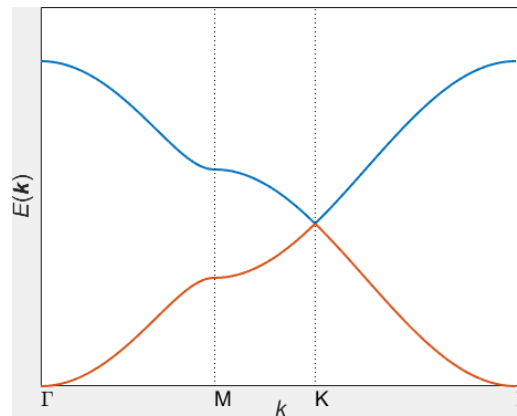
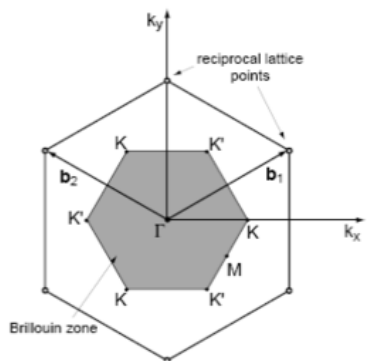
$$\begin{pmatrix} \varepsilon - E(\mathbf{k}) & -t [1 + \exp(-i\mathbf{k}\cdot\mathbf{a}_1) + \exp(-i\mathbf{k}\cdot\mathbf{a}_2)] \\ -t [1 + \exp(i\mathbf{k}\cdot\mathbf{a}_1) + \exp(i\mathbf{k}\cdot\mathbf{a}_2)] & \varepsilon - E(\mathbf{k}) \end{pmatrix} \begin{pmatrix} c_1 \\ c_2 \end{pmatrix} = 0$$

where $\varepsilon = \langle 0|\Delta U|0\rangle$, $t = -\langle 0|\Delta U|\mathbf{d}\rangle$

therefore

$$E(\mathbf{k}) = \varepsilon \pm t \sqrt{1 + 4 \cos\left(\frac{\sqrt{3}}{2} k_x a\right) \cos\left(\frac{1}{2} k_y a\right) + 4 \left[\cos\left(\frac{1}{2} k_y a\right)\right]^2}$$

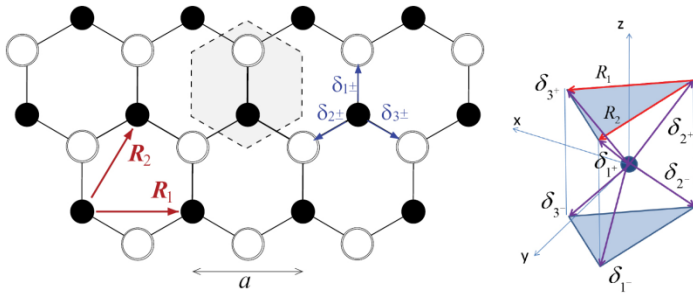
1st Brillouin zone



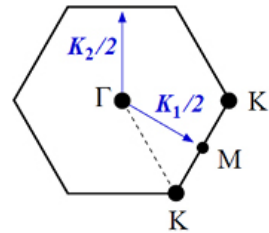
Another example - MoS₂:

MoS₂: direct bandgap, large mobilities, spin-valley correlations due to LS coupling

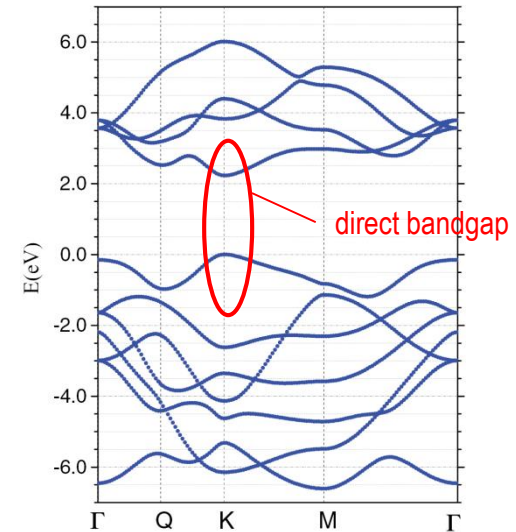
Lattice:



1BZ:



DFT calculation:



Let \mathbf{r}_i denote the Mo atom location in the i th unit cell. Following Cappelluti and collaborators [27, 28], we consider a tight-binding model with five d orbitals in the Mo atom, namely,

$$|\mathbf{r}_i; d_0\rangle = |d_{3z^2-r^2}\rangle, \quad |\mathbf{r}_i; d_1\rangle = |d_{x^2-y^2}\rangle,$$

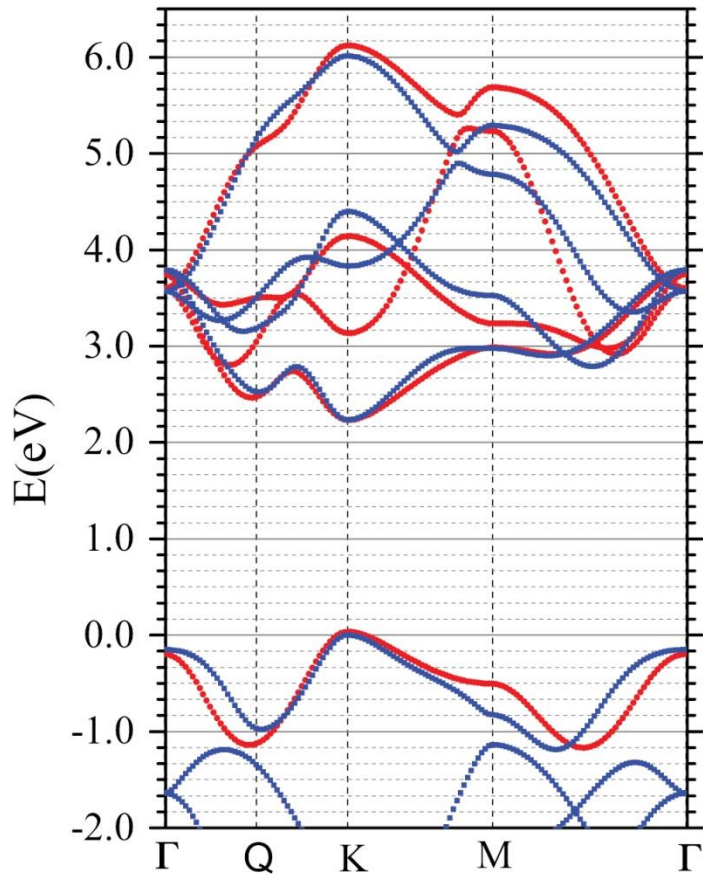
$$|\mathbf{r}_i; d_2\rangle = |d_{xy}\rangle, \quad |\mathbf{r}_i; d_3\rangle = |d_{xz}\rangle, \quad |\mathbf{r}_i; d_4\rangle = |d_{yz}\rangle,$$

and six p orbitals for the S atoms, three for the top t (+) and three for the bottom b (-) layers,

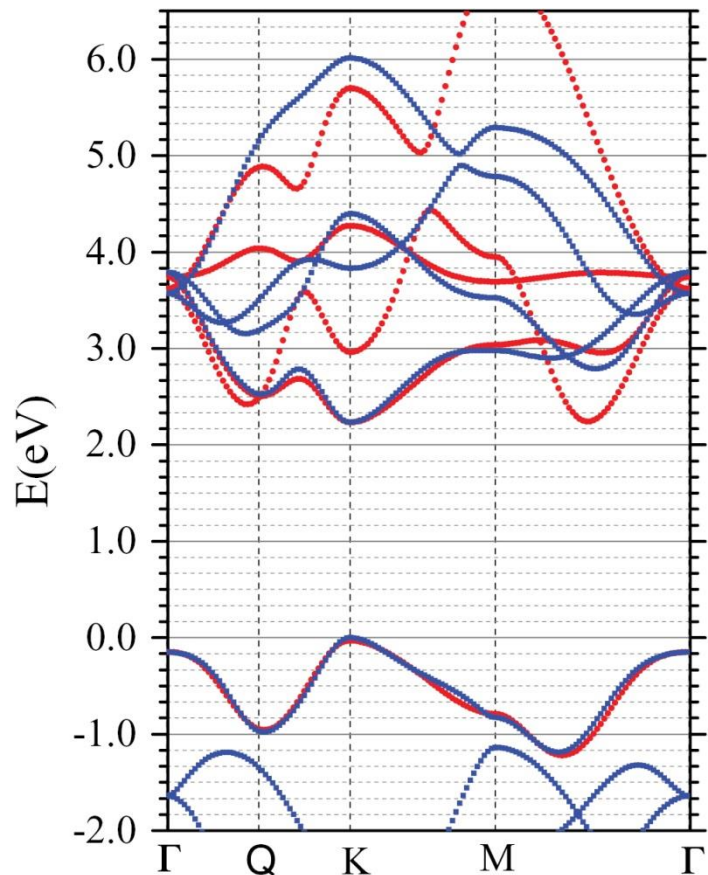
$$|\mathbf{r}_i + \boldsymbol{\delta}_{1\pm}; p_1\rangle = |p_x^{t,b}\rangle, \quad |\mathbf{r}_i + \boldsymbol{\delta}_{1\pm}; p_2\rangle = |p_y^{t,b}\rangle,$$

$$|\mathbf{r}_i + \boldsymbol{\delta}_{1\pm}; p_3\rangle = |p_z^{t,b}\rangle.$$

E Ridolfi et al., J. Phys. Cond. Mat. **27**,365501 (2015).



Comparison between the band structures obtained with the DFT-HSE06 (blue squares) and with the optimized tight-binding model using the parameters from the CB-VB optimization (red circles) near the gap region.



Comparison between the band structures obtained with the DFT-HSE06 (blue squares) and with the optimized tight-binding model using the parameters from the VB optimization (red circles) near the gap region.

Group IV semiconductors: from the Cardona textbook:

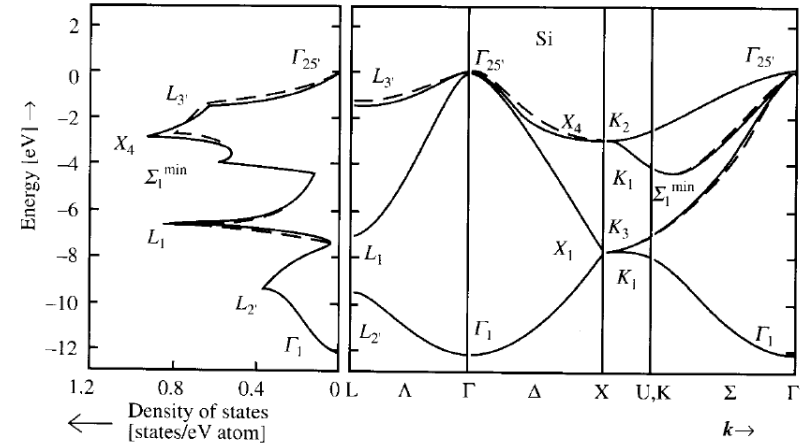


Fig. 2.24. The valence band structure and density of states (see Sect. 4.3.1 for definition) of Si calculated by the tight-binding method (*broken curves*) and by the empirical pseudopotential method (*solid lines*) [2.19]

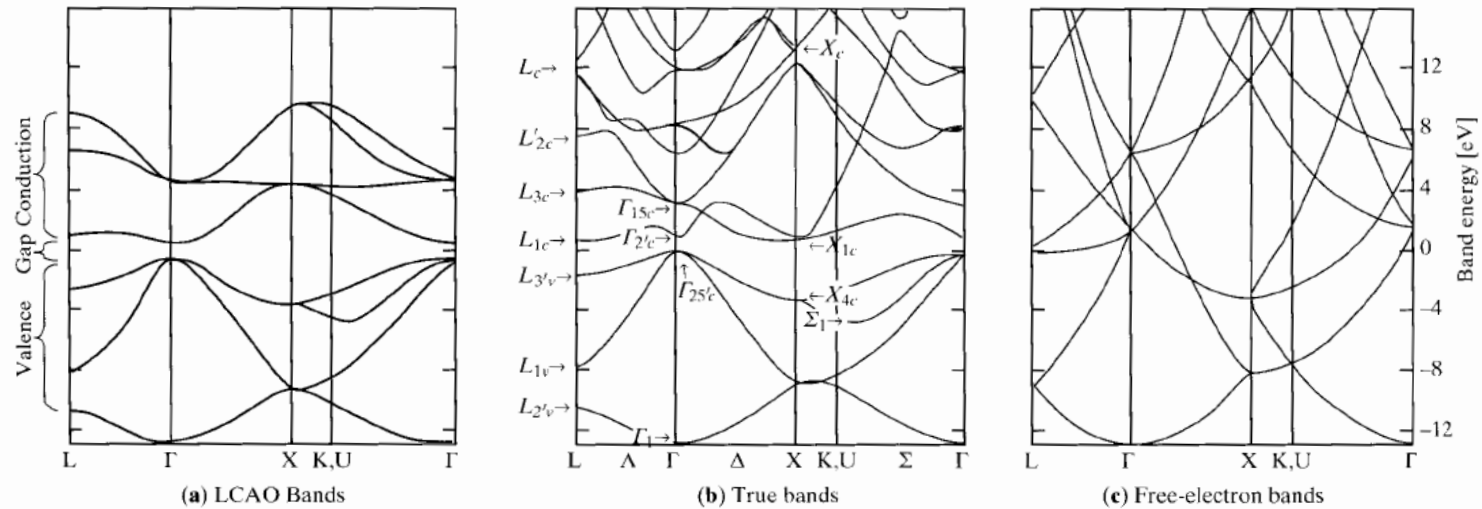
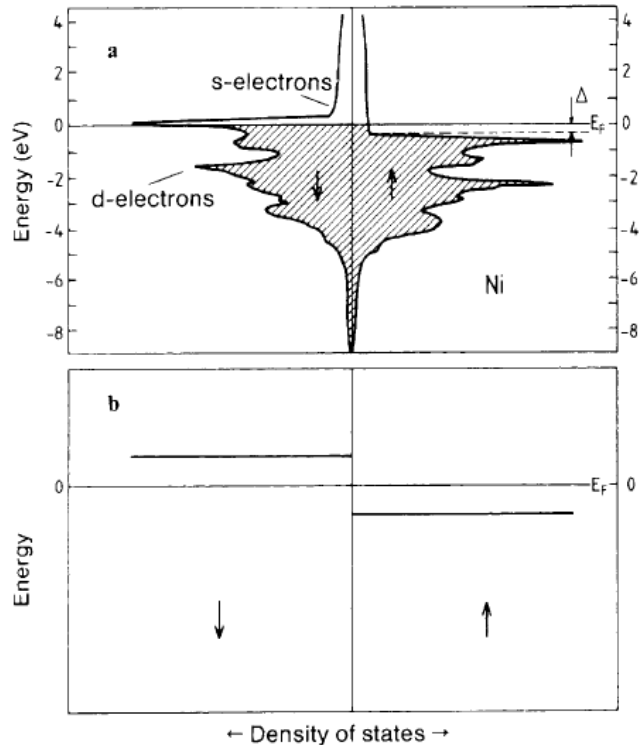


Fig. 2.25. A comparison between the band structure of Ge calculated by (a) the tight-binding method, (b) the empirical pseudopotential method, and (c) the nearly free electron model [Ref. 2.18, p. 79]

Stoner model for band ferromagnetism



Spin-dependent electron energies

$$E_{\uparrow}(k) = E(k) - \frac{1}{2} \frac{(n_{\downarrow} - n_{\uparrow})}{n} I = E(k) - \Delta$$

$$E_{\downarrow}(k) = E(k) + \frac{1}{2} \frac{(n_{\downarrow} - n_{\uparrow})}{n} I = E(k) + \Delta$$

I ...Stoner parameter describing the electrostatic repulsion of the electrons with opposite spins in the same state (the Hubbard model)

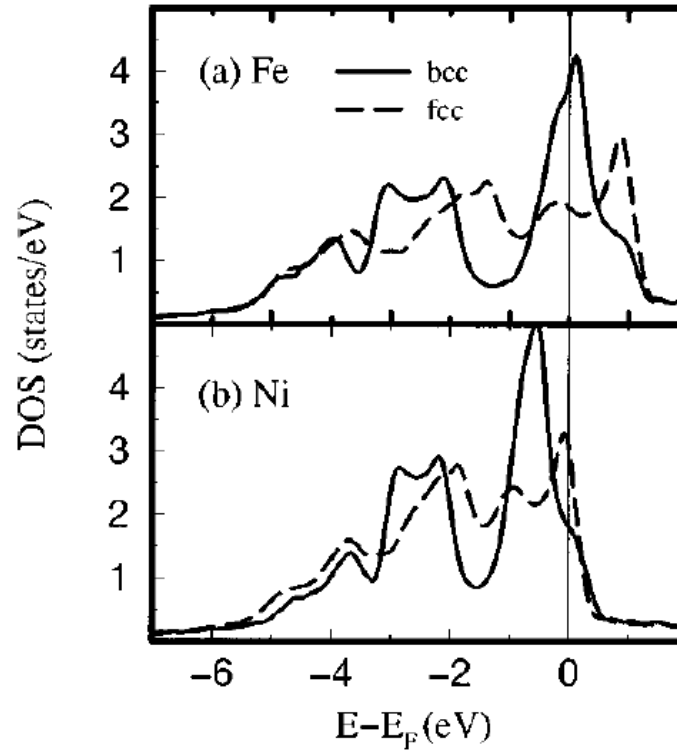
Difference in electron populations

$$n_{\downarrow} - n_{\uparrow} = \frac{3}{4} \frac{n}{E_F} \Delta = \frac{1}{2} g(E_F) \Delta$$

At $T=0K$, the criterion for ferromagnetic ordering is $I \cdot g(E_F) > 1$

Where $g(E_F)$ is the density of states normalized per one electron

bcc Fe is ferromagnetic,
fcc Ni is ferromagnetic



Calculated magnetic properties of binary alloys between Fe, Co, Ni, and Cu

P. James

Condensed Matter Theory Group, Physics Department, Uppsala University, S-75121 Uppsala, Sweden

O. Eriksson

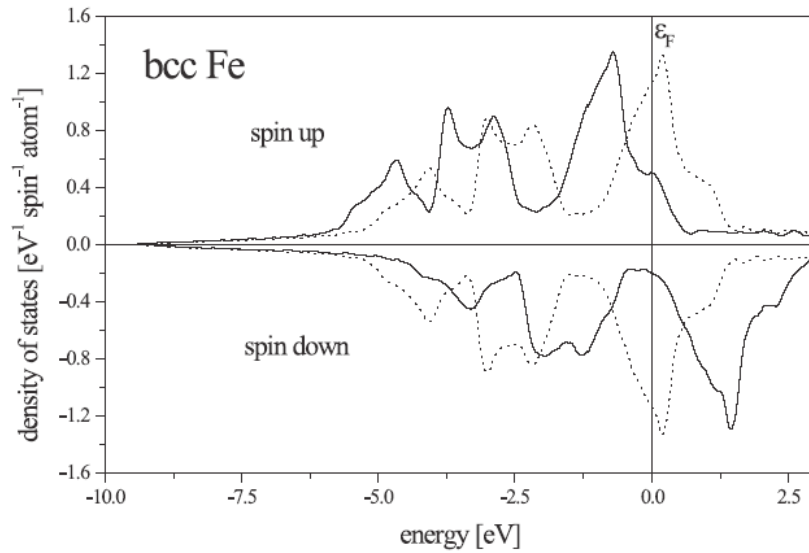
*Condensed Matter Theory Group, Physics Department, Uppsala University, S-75121 Uppsala, Sweden
and Theoretical Division and Center for Materials Science, Los Alamos National Laboratory, Los Alamos, New Mexico 87545*

B. Johansson and I. A. Abrikosov

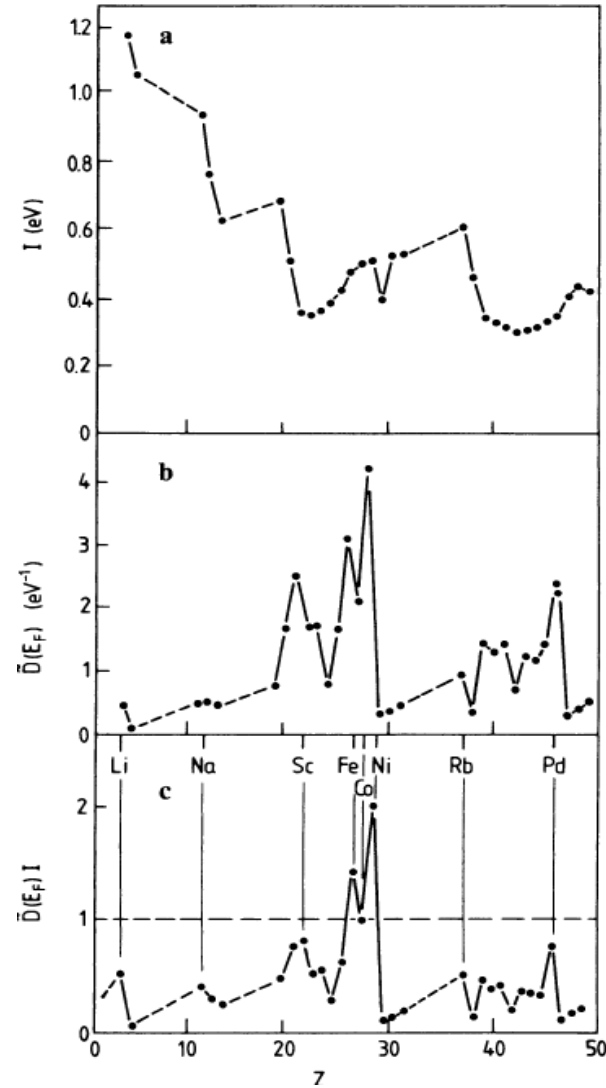
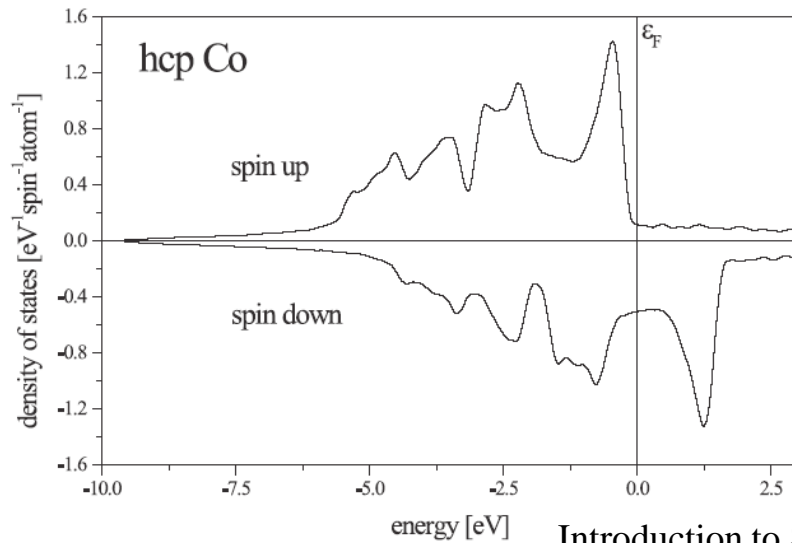
Condensed Matter Theory Group, Physics Department, Uppsala University, S-75121 Uppsala, Sweden

(Received 11 May 1998)

Fe: weak ferromagnet



Co: strong ferromagnet



Comment on electron-electron interactions

Many-particle wave function $\Psi(\mathbf{r}_1, s_1, \dots, \mathbf{r}_N, s_N)$ is a solution of the many-particle Schroedinger equation

$$\hat{\mathbf{H}}\Psi = \sum_{j=1}^N \left[-\frac{\hbar^2}{2m} \Delta_j \Psi - Ze^2 \sum_{\mathbf{R}} \frac{1}{|\mathbf{R} - \mathbf{r}_j|} \Psi \right] + \frac{1}{2} \sum_{j \neq k=1}^N \frac{e^2}{|\mathbf{r}_j - \mathbf{r}_k|} \Psi = \mathcal{E}\Psi$$

It is impossible to solve this equation and one has to find suitable approximation(s). One possible approximation is to replace the electron-electron interaction term by an effective potential:

$$U(\mathbf{r}) = U_{ion}(\mathbf{r}) + U_{el}(\mathbf{r}) = -Ze^2 \sum_{\mathbf{R}} \frac{1}{|\mathbf{R} - \mathbf{r}|} - e \int d^3\mathbf{r}' \frac{\rho(\mathbf{r}')}{|\mathbf{r} - \mathbf{r}'|}$$

where $\rho(\mathbf{r}) = -e \sum_{j=1}^N |\psi_j(\mathbf{r})|^2$ is the charge density calculated from the one-electron wave functions. From this we obtain the one-electron Schroedinger equation (the Hartree equation):

$$-\frac{\hbar^2}{2m} \Delta_j \psi_j(\mathbf{r}) + U_{ion}(\mathbf{r}) \psi_j(\mathbf{r}) + \left[e^2 \int d^3\mathbf{r}' \sum_{k=1}^N \frac{|\psi_k(\mathbf{r}')|^2}{|\mathbf{r} - \mathbf{r}'|^2} \right] \psi_j(\mathbf{r}) = \mathcal{E}_j \psi_j(\mathbf{r})$$

This equation is nonlinear and can be solved by iterations. The equation contains a non-physical term $j = k$.

In the Hartree equation, the many-electron wave function is replaced by a product of one-electron wave functions

$$\Psi(\mathbf{r}_1, s_1, \dots, \mathbf{r}_N, s_N) = \prod_{j=1}^N \psi_j(\mathbf{r}_j, s_j)$$

However, this function does not obey the Pauli principle. The simplest generalization of the Hartree approach is the Slater determinant obeying the Pauli principle

1st electron in position (\mathbf{r}_2, s_2)

$$\Psi(\mathbf{r}_1, s_1, \dots, \mathbf{r}_N, s_N) = \begin{vmatrix} \psi_1(\mathbf{r}_1, s_1) & \psi_1(\mathbf{r}_2, s_2) & \psi_1(\mathbf{r}_{N-1}, s_{N-1}) & \psi_1(\mathbf{r}_N, s_N) \\ \psi_2(\mathbf{r}_1, s_1) & \psi_2(\mathbf{r}_2, s_2) & \dots & \psi_2(\mathbf{r}_N, s_N) \\ \dots & \dots & \dots & \dots \\ \psi_N(\mathbf{r}_1, s_1) & \psi_N(\mathbf{r}_2, s_2) & \dots & \psi_N(\mathbf{r}_N, s_N) \end{vmatrix}$$

The Slater determinant is used for the calculation of mean energy:

$$\langle \mathcal{E} \rangle = \frac{\langle \Psi | \hat{\mathbf{H}} | \Psi \rangle}{\langle \Psi | \Psi \rangle}$$

From the condition of minimum mean energy the Hartree-Fock (HF) equation follows:

Electron-electron Coulomb repulsion

$$-\frac{\hbar^2}{2m} \Delta_j \psi_j(\mathbf{r}) + U_{ion}(\mathbf{r}) \psi_j(\mathbf{r}) + \left[e^2 \int d^3 \mathbf{r}' \sum_{k=1}^N \frac{|\psi_k(\mathbf{r}')|^2}{|\mathbf{r} - \mathbf{r}'|^2} \right] \psi_j(\mathbf{r})$$

$$- e^2 \sum_{k=1}^N \delta_{s_j s_k} \int d^3 \mathbf{r}' \frac{\psi_k^*(\mathbf{r}') \psi_k(\mathbf{r}) \psi_j(\mathbf{r}')}{|\mathbf{r} - \mathbf{r}'|} = \varepsilon_j \psi_j(\mathbf{r})$$

Electron-electron exchange interaction

The nonphysical terms $j = k$ cancel mutually. Relatively simple solution of the HF equation exists only for free electron gas, see specialized lectures on many-particle theory.

V. 3. Electrons in external fields – quasiclassical approximation

Bloch electrons in an external field – how to describe their motion?

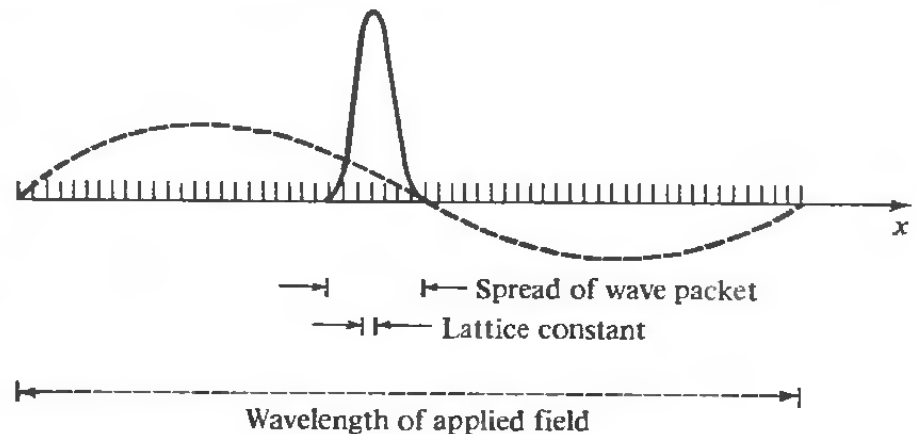
The Bloch electrons are described by a stationary solution of the Schrodinger equation, their velocity is

$$v_n(\mathbf{k}) = \frac{1}{\hbar} \nabla_{\mathbf{k}} E_n(\mathbf{k})$$

The interaction with the crystal field does not lead to an energy dissipation.

In the following we do not consider the collisions (i.e. $\tau \rightarrow \infty$)

In the quasiclassical approximation, the external field is described **classically**. This is possible, if the wave packet describing a Bloch electron is much smaller than a characteristic size of the external field (wavelength). On the other hand, the wave packet is much broader than the crystal unit cell (thus, the crystal field is described using a quantum approach).



Basic assumptions of the quasiclassical approach:

1. The band index n is constant (inter-band transitions are not considered)
2. Equations of motion:

$$\dot{\mathbf{r}} = \mathbf{v}_n(\mathbf{k}) = \frac{1}{\hbar} \nabla_{\mathbf{k}} E_n(\mathbf{k})$$

$$\hbar \dot{\mathbf{k}} = -e[\mathbf{E}(\mathbf{r}, t) + \mathbf{v}_n(\mathbf{k}) \times \mathbf{B}(\mathbf{r}, t)]$$

3. The wave vector \mathbf{k} is defined within an additive reciprocal lattice vector \mathbf{g}

Consequence for the transport properties: A filled band remain filled during the motion

The electric current density:

$$\mathbf{j}_n = -e \int_{\text{filled}} d^3 \mathbf{k} \frac{1}{4\pi^3} \frac{1}{\hbar} \nabla_{\mathbf{k}} E_n(\mathbf{k})$$

The contribution of a fully filled band $\mathbf{j}_n = 0$

The contribution of a partially filled band:

$$\mathbf{j}_n = -e \int_{\text{filled}} d^3\mathbf{k} \frac{1}{4\pi^3} \frac{1}{\hbar} \nabla_{\mathbf{k}} E_n(\mathbf{k}) = \underbrace{-e \int_{\text{BZ}} d^3\mathbf{k} \frac{1}{4\pi^3} \frac{1}{\hbar} \nabla_{\mathbf{k}} E_n(\mathbf{k})}_{=0} + e \underbrace{\int_{\text{empty}} d^3\mathbf{k} \frac{1}{4\pi^3} \frac{1}{\hbar} \nabla_{\mathbf{k}} E_n(\mathbf{k})}_{\text{Holes}}$$

Equation of the hole motion:

$$\hbar \dot{\mathbf{k}} = -e[\mathbf{E}(\mathbf{r}, t) + \mathbf{v}_n(\mathbf{k}) \times \mathbf{B}(\mathbf{r}, t)] \quad (\text{the same as for an electron})$$

Close to an extremal value of $E_n(\mathbf{k})$

$$E_n(\mathbf{k}) \approx E_n(\mathbf{k}_0) + A |\mathbf{k} - \mathbf{k}_0|^2 \quad \text{we denote } \frac{\hbar^2}{2m^*} = A$$

m^* is the effective mass

$$\text{Then } \mathbf{v}_n(\mathbf{k}) \approx \frac{\hbar(\mathbf{k} - \mathbf{k}_0)}{m^*}$$

Local minimum in $\mathbf{k}_0 \Rightarrow$ positive effective mass – electron

Local maximum in $\mathbf{k}_0 \Rightarrow$ negative effective mass - hole

We can also define a positive hole effective mass, then the hole charge is positive

In a general case – effective mass tensor

$$[\hat{m}^{-1}]_{jk} = \pm \frac{1}{\hbar^2} \frac{\partial^2 E_n(\mathbf{k})}{\partial k_j \partial k_k} \Big|_{\mathbf{k}=\mathbf{k}_0}$$

and the equation of motion is

$$m(\mathbf{k}) \frac{d\mathbf{v}}{dt} = \pm e [\mathbf{E} + \mathbf{v}_n(\mathbf{k}) \times \mathbf{B}]$$

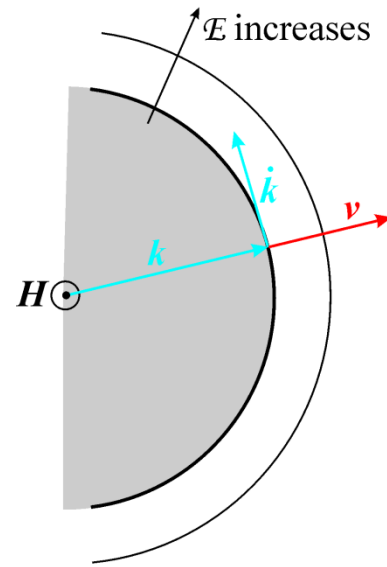
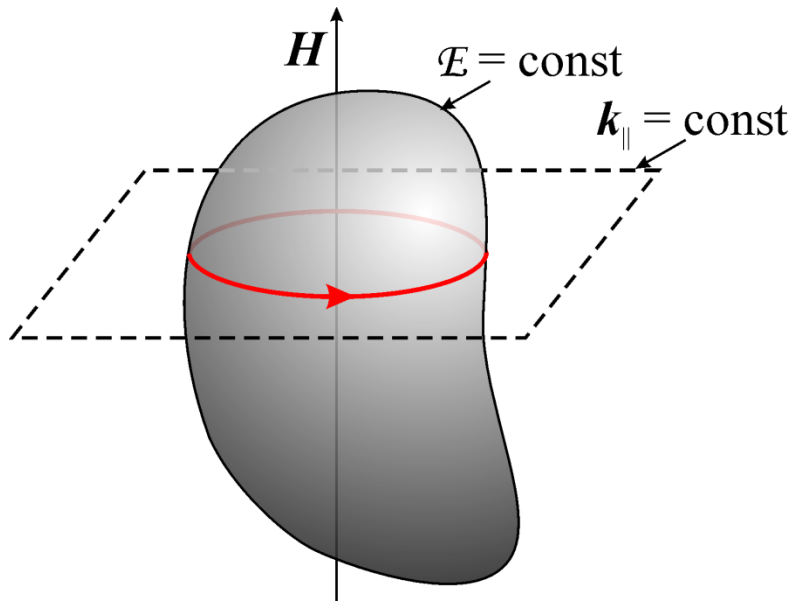
Electron in an external magnetic field

Equations of movement:

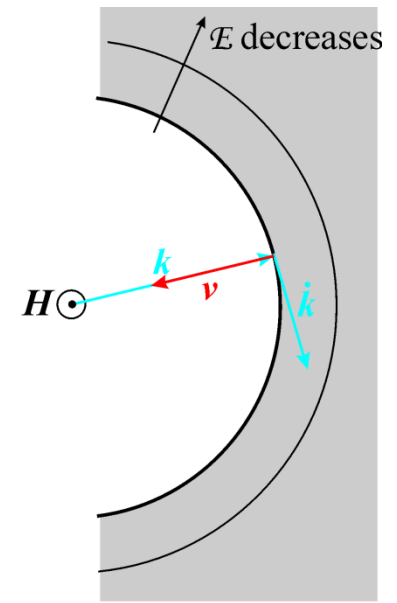
$$\dot{\mathbf{r}} = \mathbf{v}_n(\mathbf{k}) = \frac{1}{\hbar} \nabla_{\mathbf{k}} E_n(\mathbf{k})$$

$$\hbar \dot{\mathbf{k}} = -e \mathbf{v}_n(\mathbf{k}) \times \mathbf{B}(\mathbf{r}, t)$$

The energy and the component of \mathbf{k} along \mathbf{H} are constant during the motion

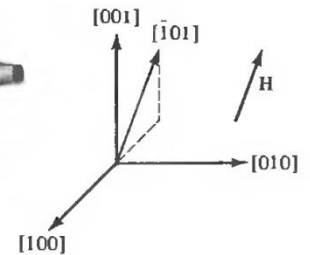
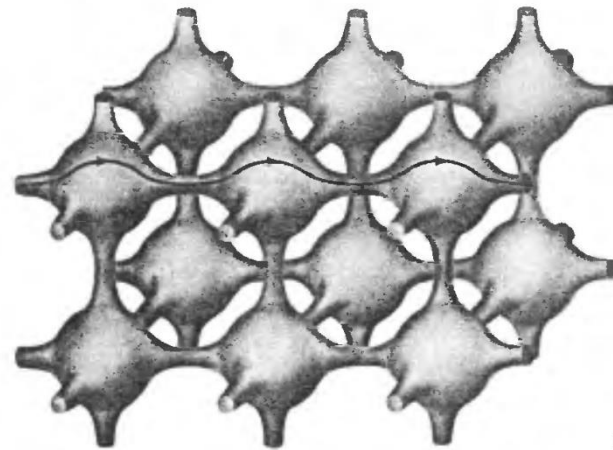


electron orbit



hole orbit

open orbit in a repeated zone scheme:



Quasiclassical electron trajectory in direct space:

the component of the position vector perpendicular to \mathbf{B} :

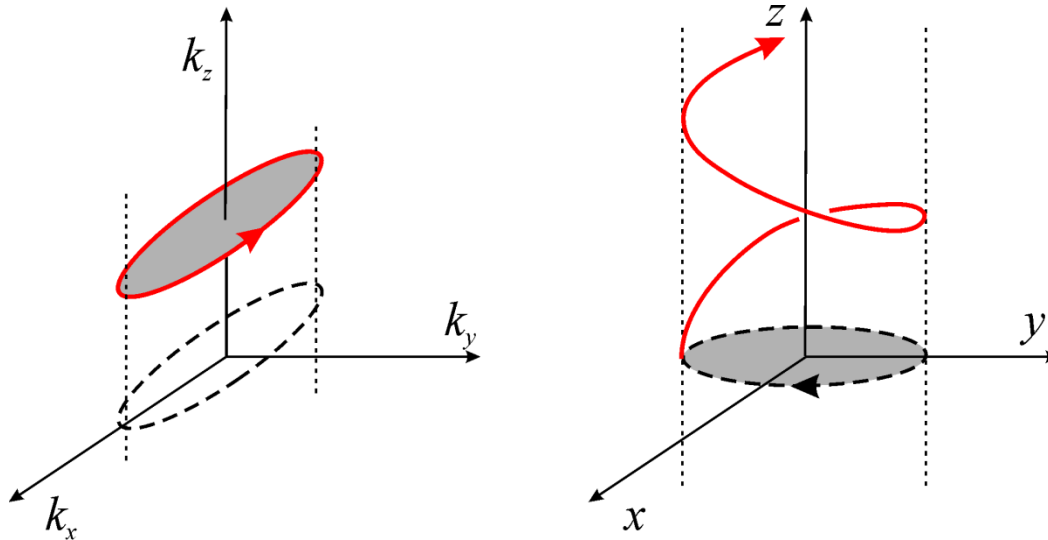
$$\mathbf{r}_\perp = \mathbf{r} - \mathbf{B}^0(\mathbf{B}^0 \cdot \mathbf{r}), \dot{\mathbf{r}}_\perp = \dot{\mathbf{r}} - \mathbf{B}^0(\mathbf{B}^0 \cdot \dot{\mathbf{r}}) = \mathbf{B}^0 \times (\dot{\mathbf{r}} \times \mathbf{B}^0)$$

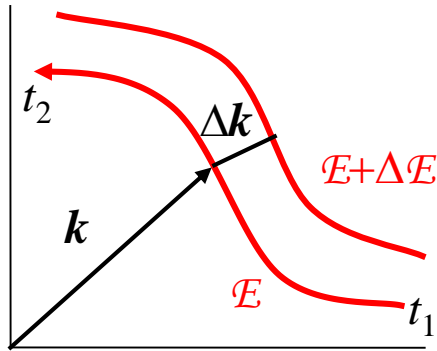
The equation of motion:

$$\mathbf{B}^0 \times (\hbar \dot{\mathbf{k}}) = -e\mathbf{B}^0 \times (\dot{\mathbf{r}} \times \mathbf{B}) = -eB\dot{\mathbf{r}}_\perp$$

After integration:

$$\mathbf{r}(t) - \mathbf{r}(0) = -\frac{\hbar}{eB} \mathbf{B}^0 \times (\mathbf{k}(t) - \mathbf{k}(0))$$





$$\begin{aligned}
 t_2 - t_1 &= \int_1^2 dt = \int_1^2 dk \left| \frac{dt}{dk} \right| = \frac{\hbar^2}{e} \int_1^2 \frac{dk}{|\nabla_{\mathbf{k}} E(\mathbf{k}) \times \mathbf{B}|} \\
 &= \frac{\hbar^2}{eB} \int_1^2 dk \frac{\Delta k}{\Delta E} = \frac{\hbar^2}{eB} \frac{\partial A_{12}}{\partial E}
 \end{aligned}$$

Period of the movement around a closed orbit:

$$T = \frac{\hbar^2}{eB} \frac{\partial A}{\partial E}$$

For a free electron:

$$A = \pi k_{\perp}^2 = \pi \left(\frac{2m}{\hbar^2} E - k_z^2 \right) \Rightarrow T = \frac{2\pi m}{eB}$$

cyclotron frequency: $\omega_c = \frac{eB}{m}$

cyclotron frequency of the Bloch electrons: $\omega_c = \frac{eB}{m_c^*}$

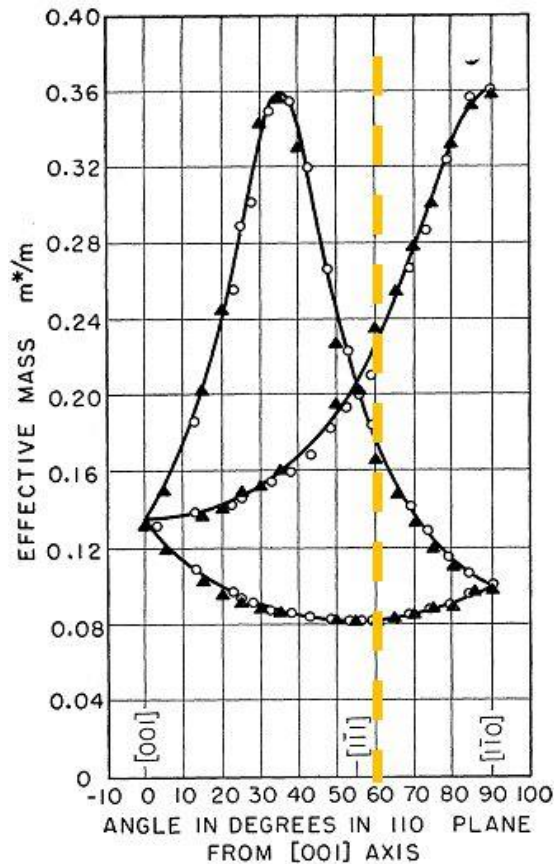
the cyclotron effective mass depends on the effective mass tensor m^* and on the direction of \mathbf{H}

Cyclotron Resonance (CR) in Ge

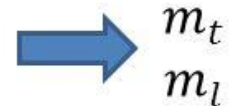
In general, effective mass are anisotropic,

For Ge, constant energy surfaces near band edge are spheroidal

$$E(\mathbf{k}) = \hbar^2 \left(\frac{k_x^2 + k_y^2}{2m_t} + \frac{k_z^2}{2m_l} \right)$$

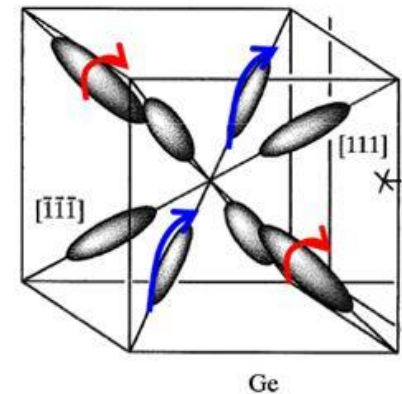
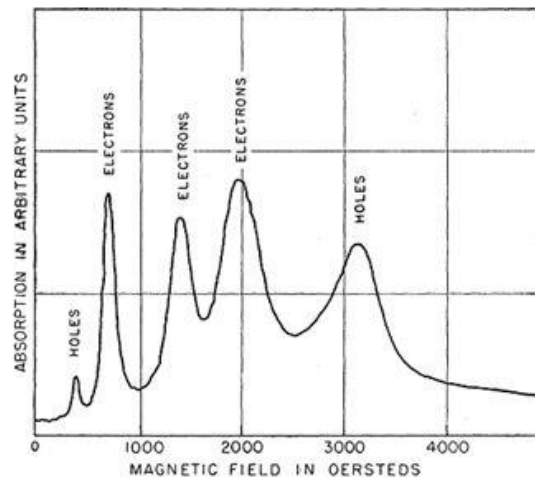


$$\left(\frac{1}{m^*} \right)^2 = \frac{\cos^2\theta}{m_t^2} + \frac{\sin^2\theta}{m_t m_l}$$



1. Measuring CR at different field angles θ

2. Extract cyclotron mass by $\omega_c = \frac{eB}{m_c}$



G. Dresselhaus et al., Phys. Rev. **98**, 368 (1955)

<https://slideplayer.com/slide/5261837/>

Quantization of the cyclotron orbits

Beyond the quasiclassical approximation!!

Free electrons in a homogeneous magnetic field:

$$\frac{1}{2m} (\hat{\mathbf{p}} - e\mathbf{A})^2 \psi(\mathbf{r}) = E\psi(\mathbf{r})$$

The electron spin is not considered.

The magnetic field: $\mathbf{B} = (0, 0, B) \Rightarrow \mathbf{A} = (-yB, 0, 0)$

We assume the wavefunction in the form

$$\psi(x, y, z) = e^{i(k_x x + k_z z)} \varphi(y)$$

Then

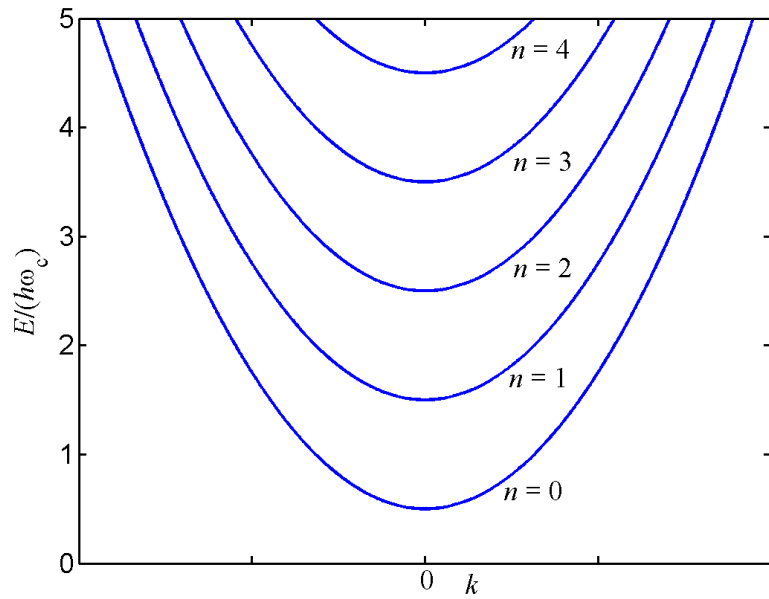
$$-\frac{\hbar^2}{2m} \frac{d^2 \varphi}{dy'^2} + \frac{1}{2} m \omega_c^2 y'^2 \varphi = E' \varphi, \quad y' = y + \frac{\hbar k_x}{eB}, \quad E' = E - \frac{\hbar^2 k_z^2}{2m}$$

Harmonic oscillator equation. The eigenenergies are

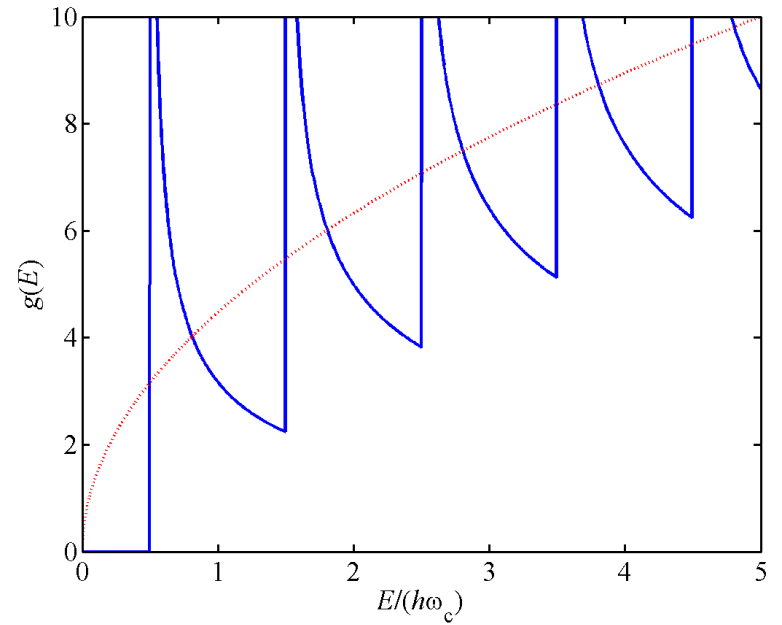
$$E_n(\mathbf{k}) = \frac{\hbar^2 k^2}{2m} + \hbar \omega_c \left(n + \frac{1}{2} \right)$$

There are about 10^4 levels up to E_F (for the magnetic field of about 1 T).

energy bands



density of states



de Haas-van Alphen effect: the inverse susceptibility oscillates in magnetic field as the field intensity is increased. The period of the oscillation is

$$\Delta(1/\chi) = 2\pi e / (\hbar S)$$

where S is the area of the Fermi surface normal to the direction of \mathbf{B}

A detailed de Haas–van Alphen effect study of the overdoped cuprate $\text{Ti}_2\text{Ba}_2\text{CuO}_{6+\delta}$

P M C Rourke¹, A F Bangura¹, T M Benseman², M Matusiak²,
J R Cooper², A Carrington¹ and N E Hussey^{1,3}

New Journal of Physics **12** (2010) 105009 (29pp)

Received 23 July 2010

Published 29 October 2010

Online at <http://www.njp.org/>

doi:10.1088/1367-2630/12/10/105009

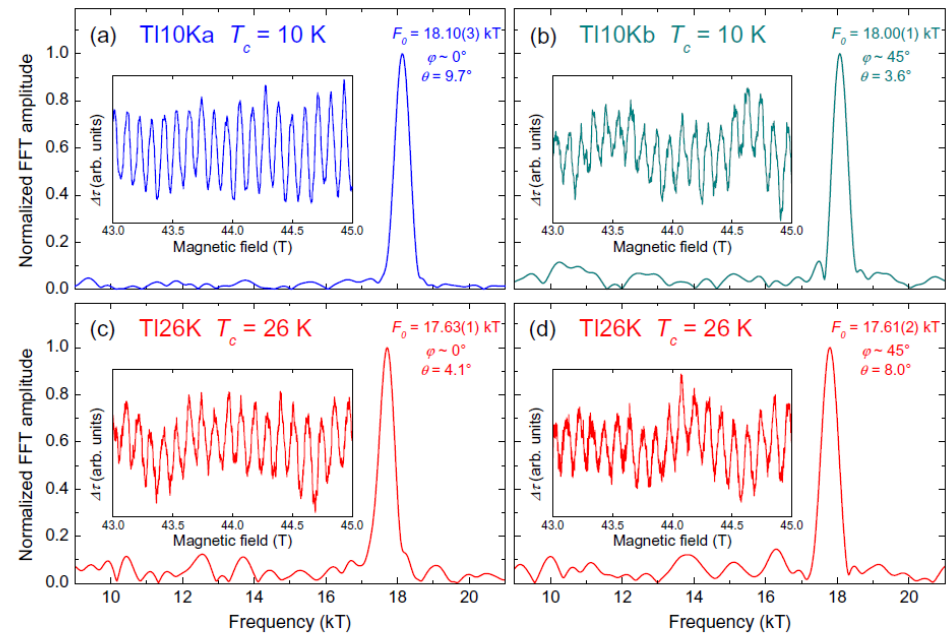
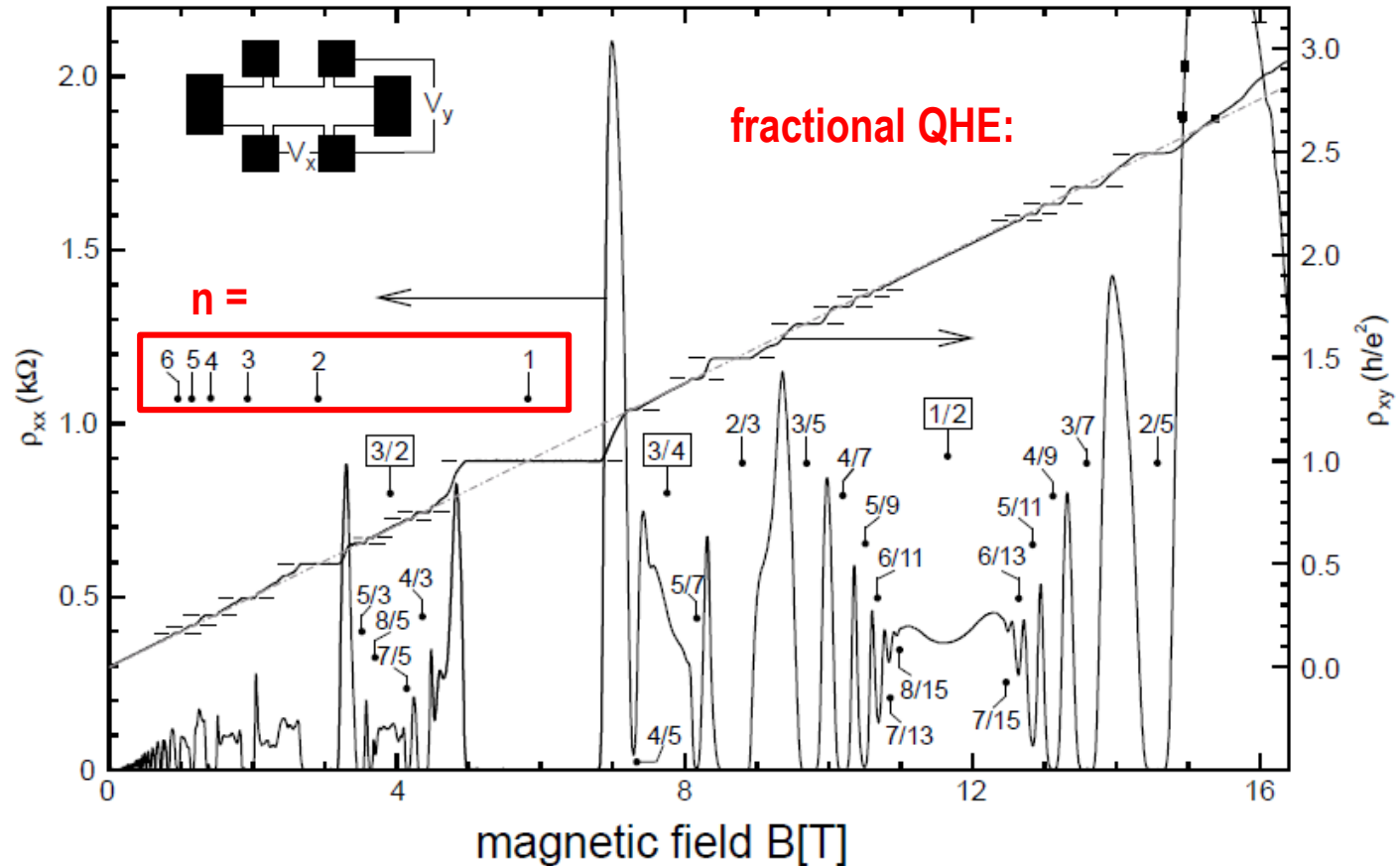
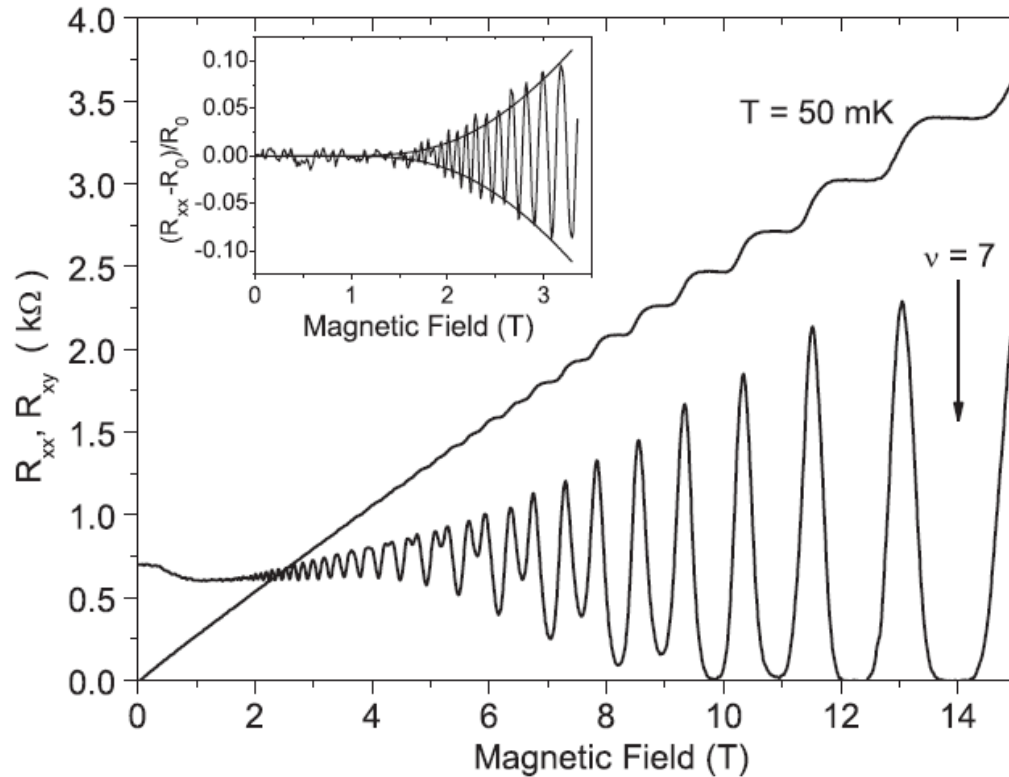


Figure 3. FFTs of torque data between 38 and 45 T (38.5 and 45 T for (d)) at $T = 0.4$ K for (a) TI10Ka, (b) TI10Kb, (c) TI26K ($\varphi \sim 0^\circ$ configuration) and (d) TI26K ($\varphi \sim 45^\circ$ configuration). High-field portions of the corresponding background-subtracted raw data for each sample are shown in the insets.

This is similar to Shubnikov-de Haas effect (oscillation of σ_{xx} in 2D systems in magnetic field) and to the quantum Hall effect:

$$\rho_{xy} = \frac{1}{n} \frac{h}{e^2}, n \text{ is integer}$$





Longitudinal R_{xx} and transverse R_{xy} magnetoresistance versus magnetic field at 50mK, AlGaIn/GaN heterostructure. The inset shows the low field part of the SdHO after normalization by the low field resistance value, R_0 , and the fit of the SdHO amplitude. The arrow marks the magnetic field corresponding to $\nu = 7$. W Knap *et al* 2004 *J. Phys.: Condens. Matter* **16** 3421

The difference of the neighboring levels

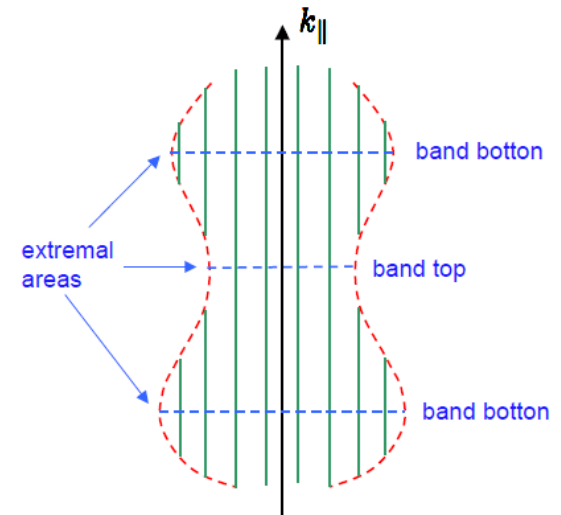
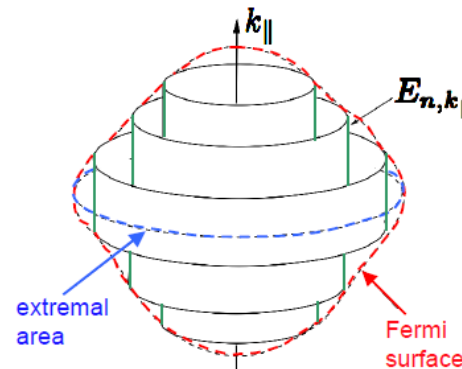
$$E_{n+1}(k_z) - E_n(k_z) = \frac{e\hbar B}{m} = \frac{h}{T}$$

The period is given by

$$T = \frac{\hbar^2}{eB} \frac{\partial A}{\partial E} \approx \frac{\hbar^2}{eB} \frac{A_{n+1} - A_n}{E_{n+1} - E_n}$$

The Lifshitz-Onsager quantization rule:

$$A(E_n(k_z), k_z) = (n + \lambda) \frac{2\pi eB}{\hbar}$$



Anomalous Hall effect

The anomalous Hall effect AHE occurs in solids with broken time-reversal symmetry, typically in a ferromagnetic phase, as a consequence of spin-orbit coupling. Sometimes it could be much larger than the normal Hall effect.

See Nagaosa N. et al., Rev. Mod. Phys **82**, 1539 (2010).

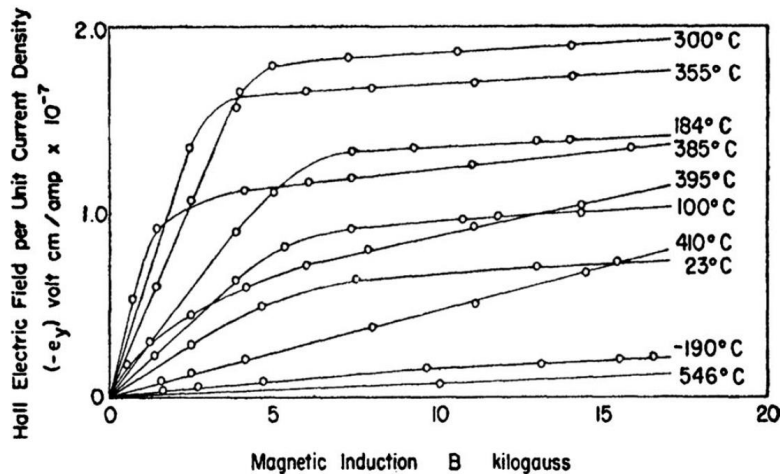


FIG. 1. The Hall effect in Ni (data from Smith, 1910). From Pugh and Rostoker, 1953.

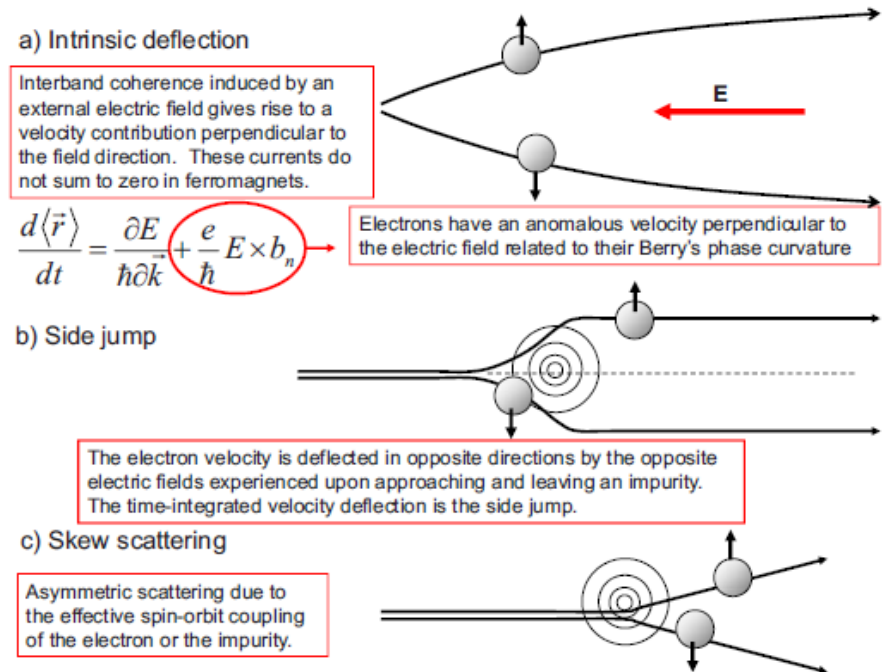


FIG. 3. (Color online) Illustration of the three main mechanisms that can give rise to an AHE. In any real material all of these mechanisms act to influence electron motion.

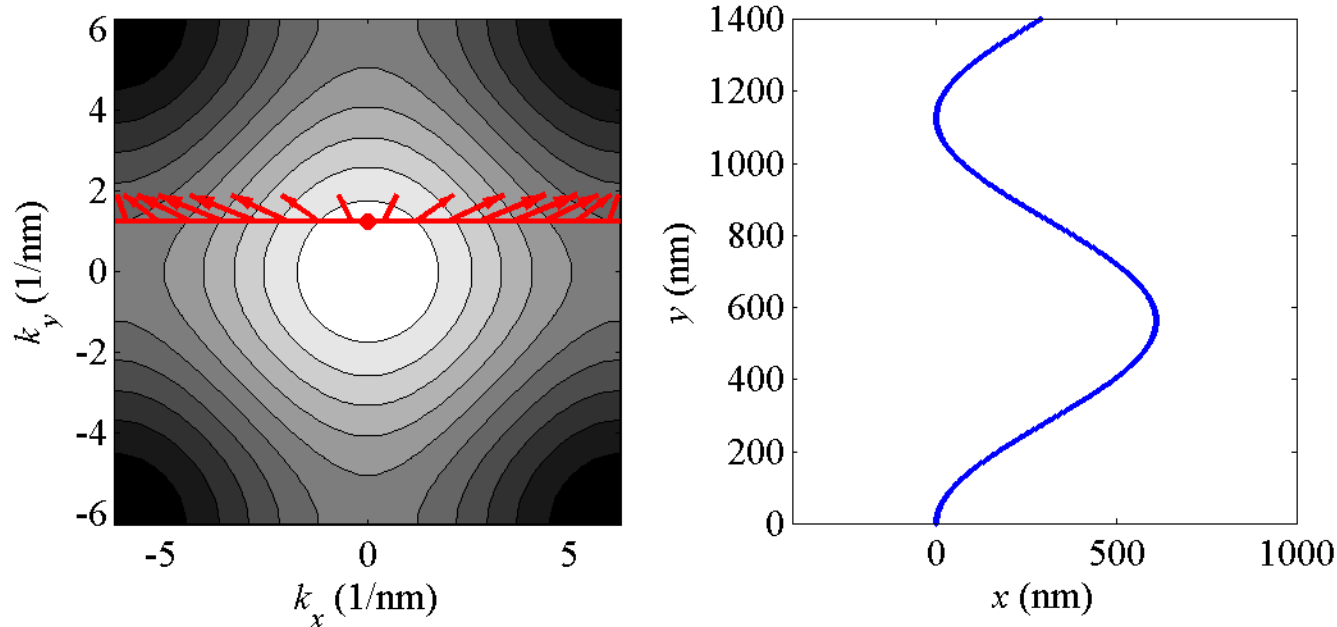
Electron in an external electric field

Equations of movement: $\mathbf{v} = \dot{\mathbf{r}} = \frac{1}{\hbar} \nabla_{\mathbf{k}} \mathcal{E}(\mathbf{k}), \hbar \dot{\mathbf{k}} = -e\mathbf{E}$

We consider a 2D square lattice. The tight-binding band structure is

$$\mathcal{E}(\mathbf{k}) = \mathcal{E}_0 - \beta - 2\gamma[\cos(k_x a) + \cos(k_y a)]$$

Therefore $\mathbf{v}(t) = \frac{2a\gamma}{\hbar} [\sin(k_x(t)a), \sin(k_y(t)a)]; \mathbf{k}(t) = \mathbf{k}(0) - e\mathbf{E}t/\hbar$



The Bloch oscillations, it generates THz electromagnetic waves

Bloch oscillations at room temperature

T. Dekorsy, R. Ott, and H. Kurz

Institut für Halbleitertechnik, Rheinisch-Westfälische Technische Hochschule Aachen, D-52056 Aachen, Germany

K. Köhler

Fraunhofer-Institut für Angewandte Festkörperphysik, D-79108 Freiburg, Germany

(Received 10 March 1995)

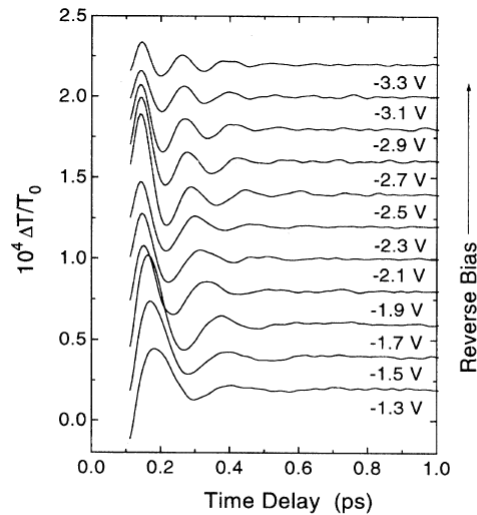


FIG. 2. Extracted oscillatory contributions from TEOS data at different reverse bias voltages applied.

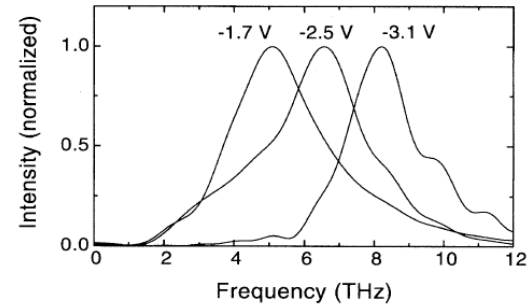


FIG. 3. Fourier transform of the time-domain data at -1.7 V, -2.5 V, and -3.1 V reverse bias.

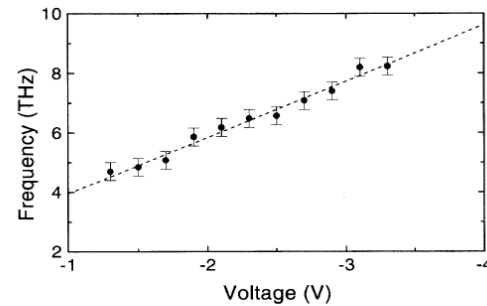


FIG. 4. Frequency of Bloch oscillations versus voltage applied to the superlattice. The straight line is a linear fit to the data with a slope of 2.1 ± 0.3 THz/V.

Quasiclassical description of the scattering of electrons

Sources of scattering:

- scattering from impurities and structure defects
- scattering from thermal vibrations
- electron-electron scattering (less important)

Simple description of the scattering (as used in the Drude and Sommerfeld models) using the relaxation time is not correct. Let us make it better now.

The same assumptions as in the semikinematical approach: the band index n is constant, the electron spin is preserved during the scattering process, and the collisions are localized both in direct (\mathbf{r}) and reciprocal (\mathbf{k}) spaces.

We denote $W_{kk'} \frac{dt d^3\mathbf{k}'}{8\pi^3}$ the probability of scattering of an electron with the wave vector \mathbf{k} into $d^3\mathbf{k}'$ in dt

We define the non-equilibrium distribution function $g_n(\mathbf{r}, \mathbf{k}, t)$ so that $g_n(\mathbf{r}, \mathbf{k}, t) d^3\mathbf{r} d^3\mathbf{k} / (4\pi^3)$ equals the number of electrons in time t and in element $d^3\mathbf{r} d^3\mathbf{k}$

In equilibrium $g_n^0(\mathbf{r}, \mathbf{k}, t) = f(\mathcal{E}_n(\mathbf{k}))$ (f is the Fermi-Dirac distribution function)

Total probability per unit time of scattering of an electron with the wave vector \mathbf{k} is (we omit the variables \mathbf{r} and t)

$$\frac{1}{\tau(\mathbf{k})} = \int \frac{d^3\mathbf{k}'}{8\pi^3} W_{\mathbf{k}\mathbf{k}'} [1 - g(\mathbf{k}')]]$$

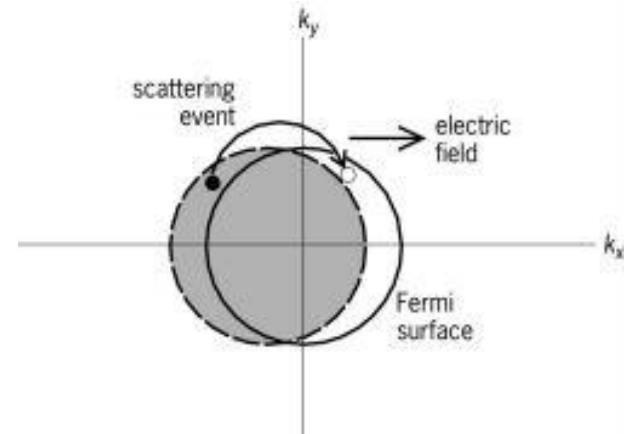
Let us calculate the changes of the non-equilibrium distribution functions due to collisions

Due to the scattering from the state \mathbf{k}

$$\left(\frac{dg(\mathbf{k})}{dt} \right)_{\text{out}} = -\frac{g(\mathbf{k})}{\tau(\mathbf{k})} = -g(\mathbf{k}) \int \frac{d^3\mathbf{k}'}{8\pi^3} W_{\mathbf{k}\mathbf{k}'} [1 - g(\mathbf{k}')]]$$

Due to the scattering into the state \mathbf{k}

$$\left(\frac{dg(\mathbf{k})}{dt} \right)_{\text{in}} = \frac{g^0(\mathbf{k})}{\tau(\mathbf{k})} = [1 - g(\mathbf{k})] \int \frac{d^3\mathbf{k}'}{8\pi^3} W_{\mathbf{k}\mathbf{k}'} g(\mathbf{k}')$$



Total change of the distribution function

$$\left(\frac{dg(\mathbf{k})}{dt} \right)_{\text{tot}} = \frac{g^0(\mathbf{k}) - g(\mathbf{k})}{\tau(\mathbf{k})} = \int \frac{d^3\mathbf{k}'}{8\pi^3} \{ W_{\mathbf{k}\mathbf{k}'} g(\mathbf{k}') [1 - g(\mathbf{k})] - W_{\mathbf{k}\mathbf{k}'} g(\mathbf{k}) [1 - g(\mathbf{k}')]] \}$$

If the relaxation time approximation is not fulfilled, the time development of the non-equilibrium distribution function cannot be reconstructed. Instead, we can calculate the distribution function in time $t+dt$ from its value in time t .

In the quasiclassical approximation, the electron in point $(\mathbf{r}, \mathbf{k}, t)$ was also in point

$$\left(\mathbf{r} - \mathbf{v}(\mathbf{k})dt, \mathbf{k} - \frac{\mathbf{F}(\mathbf{r}, t)dt}{\hbar}, t - dt \right)$$

if no collisions occurred in this time interval. Therefore, without collisions

$$g(\mathbf{r}, \mathbf{k}, t) = g\left(\mathbf{r} - \mathbf{v}(\mathbf{k})dt, \mathbf{k} - \frac{\mathbf{F}(\mathbf{r}, t)dt}{\hbar}, t - dt\right)$$

With collisions

$$g(\mathbf{r}, \mathbf{k}, t) = g\left(\mathbf{r} - \mathbf{v}(\mathbf{k})dt, \mathbf{k} - \frac{\mathbf{F}(\mathbf{r}, t)dt}{\hbar}, t - dt\right) + \left(\frac{dg(\mathbf{r}, \mathbf{k}, t)}{dt}\right)_{\text{out}} dt + \left(\frac{dg(\mathbf{r}, \mathbf{k}, t)}{dt}\right)_{\text{in}} dt$$

Expanding the distribution function, we get the Boltzmann transport equation

$$\frac{\partial g}{\partial t} + \mathbf{v} \cdot \nabla_{\mathbf{r}} g + \frac{1}{\hbar} \mathbf{F} \cdot \nabla_{\mathbf{k}} g = \left(\frac{dg}{dt}\right)_{\text{tot}} = -\frac{g(\mathbf{k}) - g^0(\mathbf{k})}{\tau(\mathbf{k})}$$

Scattering from impurities:

$$W_{\mathbf{k}\mathbf{k}'} = \frac{2\pi}{\hbar} |V_{\mathbf{k}\mathbf{k}'}|^2 \delta(E(\mathbf{k}) - E(\mathbf{k}'))$$

Where

$$V_{\mathbf{k}\mathbf{k}'} = \langle \mathbf{k} | V | \mathbf{k}' \rangle = \frac{1}{V} \sum_n e^{i(\mathbf{k}-\mathbf{k}') \cdot \mathbf{R}_n} v_{\mathbf{k}\mathbf{k}'} = \frac{1}{V} \sum_n e^{i(\mathbf{k}-\mathbf{k}') \cdot \mathbf{R}_n} \langle u_{\mathbf{k}} | v(\mathbf{r}) | u_{\mathbf{k}'} \rangle$$

is the matrix element of the perturbation potential due to the impurity atoms, the sum runs over the impurity atoms, $u_{\mathbf{k}}(\mathbf{r})$ is the periodic part of the Bloch wave.

Finally, we obtain the collision integral in the form

$$\left(\frac{dg(\mathbf{k})}{dt} \right)_{\text{tot}} \propto \frac{2\pi}{\hbar} n_i \int dS_E |v_{\mathbf{k}\mathbf{k}'}|^2 (g(\mathbf{k}') - g(\mathbf{k}))$$

i.e., it is proportional to the density n_i of the impurities

Matthiessen rule

Two independent sources of scattering (impurities and thermal vibrations):

$$W = W^{(1)} + W^{(2)}$$

In the relaxation-time approximation

$$\frac{1}{\tau} = \frac{1}{\tau^{(1)}} + \frac{1}{\tau^{(2)}} \Rightarrow \rho = \rho^{(1)} + \rho^{(2)}$$

If the relaxation time depends on k , this formula is not valid, even in the relaxation-time approximation

Beyond this approximation

$$\rho \geq \rho^{(1)} + \rho^{(2)}$$

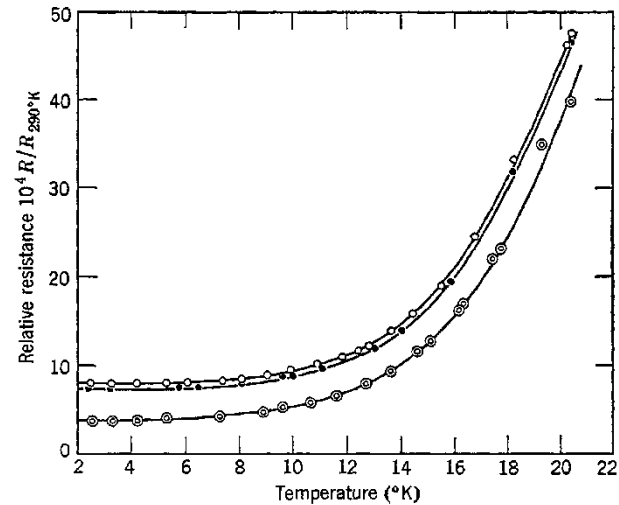


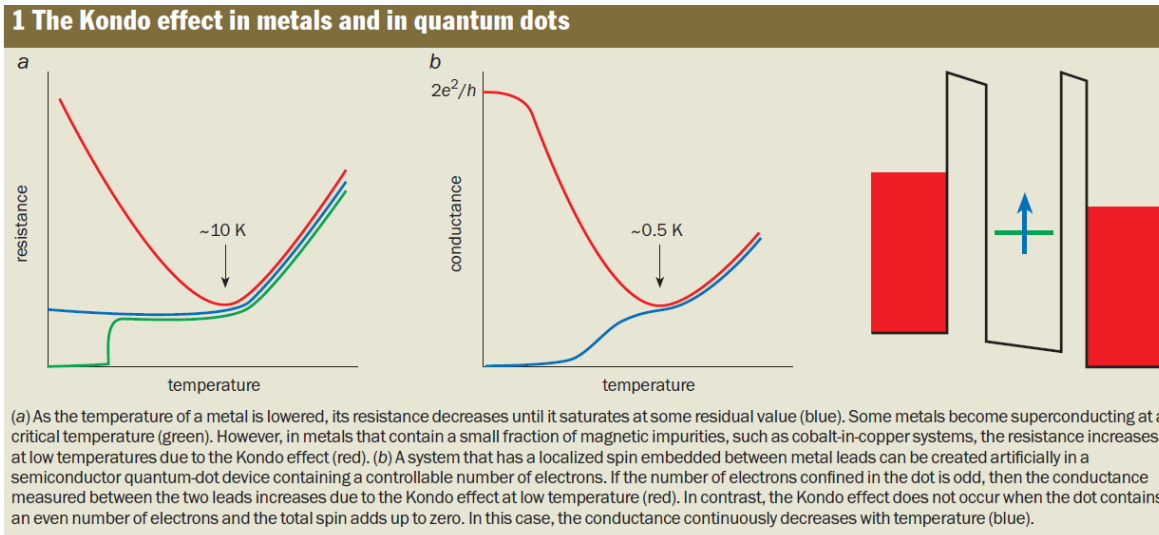
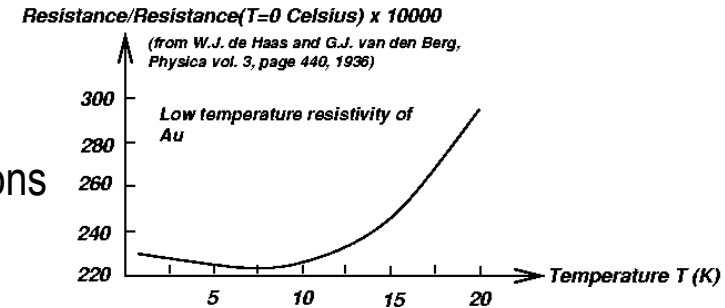
Fig. 13.10. Resistance of sodium below $20^{\circ}K$, as measured on three specimens by MacDonald and Mendlessohn [Proc. Roy. Soc. (London) **A202**, 103 (1950)].

Kondo effect – scattering of conduction electrons from magnetic impurities due to a strong coupling of the itinerant electron spins with the spins of fixed impurity atoms.

From the theory it follows the following temperature dependence of the specific resistivity:

$$\rho(T) = \rho_0 + aT^2 + c \ln \frac{\mu}{T} + bT^5$$

from Fermi liquid properties
Kondo term
from phonons



From L. Kouwenhoven and L. Glazman, *Physics World* 33 (2001)

Kondo, Jun (1964). "Resistance Minimum in Dilute Magnetic Alloys". *Progress of Theoretical Physics*. **32**: 37

V. 4. Semiconductors

The width of the energy gap smaller than approx. 3 eV.

The density of the electrons in the conduction band is proportional to $\exp[-E_g / (2k_B T)]$

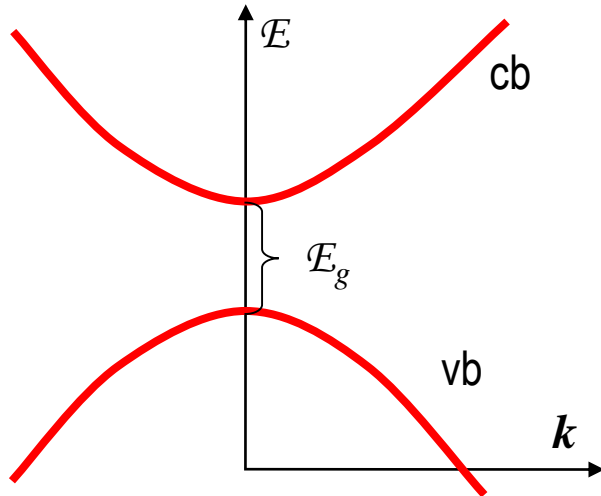
For $E_g = 4$ eV and room temperature we obtain $\exp[-E_g / (2k_B T)] \approx 10^{-35}$

For $E_g = 0.25$ eV it is $\exp[-E_g / (2k_B T)] \approx 10^{-2}$

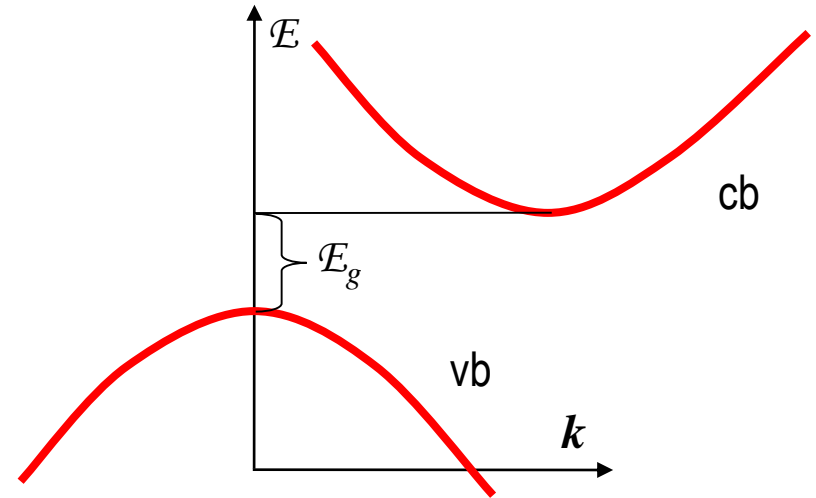
ENERGY GAPS OF SELECTED SEMICONDUCTORS

MATERIAL	E_g ($T = 300$ K)	E_g ($T = 0$ K)	E_0 (LINEAR EXTRAPOLATION TO $T = 0$)	LINEAR DOWN TO
Si	1.12 eV	1.17	1.2	200 K
Ge	0.67	0.75	0.78	150
PbS	0.37	0.29	0.25	
PbSe	0.26	0.17	0.14	20
PbTe	0.29	0.19	0.17	
InSb	0.16	0.23	0.25	100
GaSb	0.69	0.79	0.80	75
AlSb	1.5	1.6	1.7	80
InAs	0.35	0.43	0.44	80
InP	1.3		1.4	80
GaAs	1.4		1.5	
GaP	2.2		2.4	
Grey Sn	0.1			
Grey Se	1.8			
Te	0.35			
B	1.5			
C (diamond)	5.5			

Direct gap:



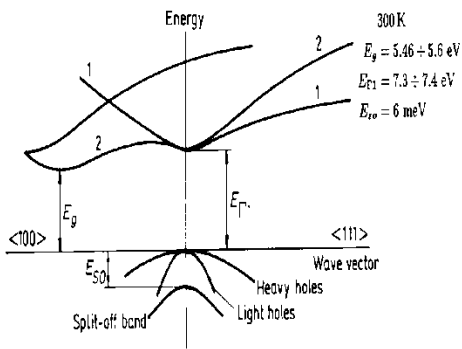
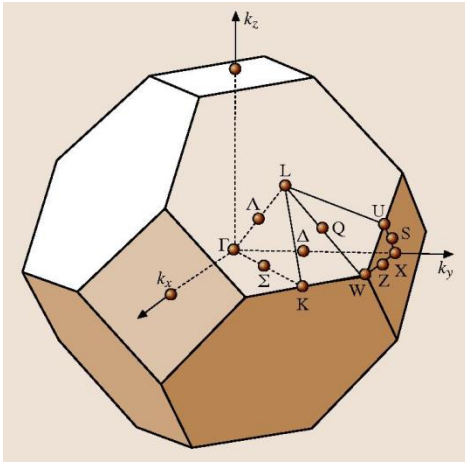
Indirect gap:



Close to the extrema of the bands, the energy can be approximated by

$$E(\mathbf{k}) = E_c + \frac{\hbar^2}{2} \sum_{jl} (k_j - k_{0j})(\hat{m})_{jl}^{-1} (k_l - k_{0l}) \quad \text{electrons}$$

$$E(\mathbf{k}) = E_v - \frac{\hbar^2}{2} \sum_{jl} k_j (\hat{m})_{jl}^{-1} k_l \quad \text{holes}$$



$a=3.567\text{\AA}$, $E_g=5.46\text{eV}$
 $m_L=1.40m$, $m_T=0.36m$
 $m_{LH}=0.70m$, $m_{HH}=2.12m$
 $m_{SO}=1.06m$

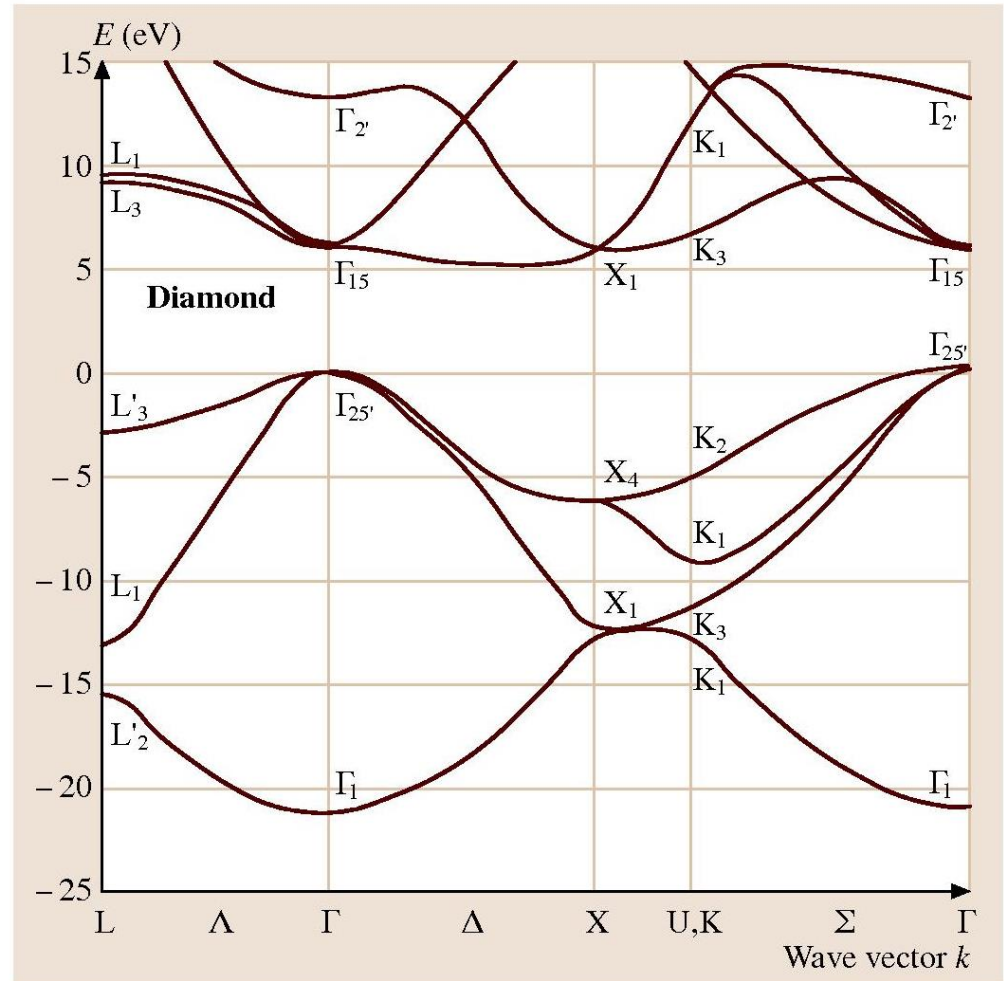
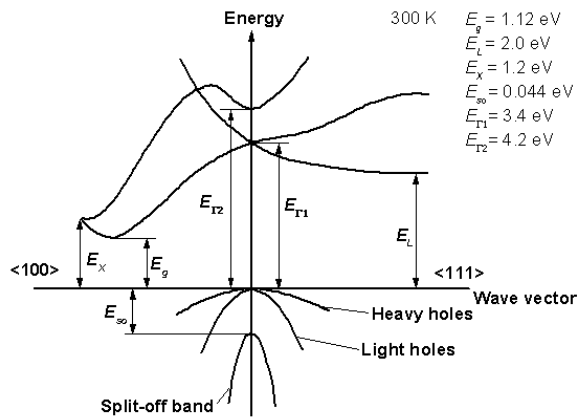
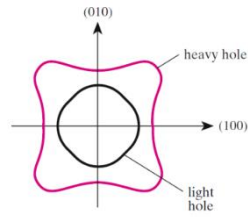
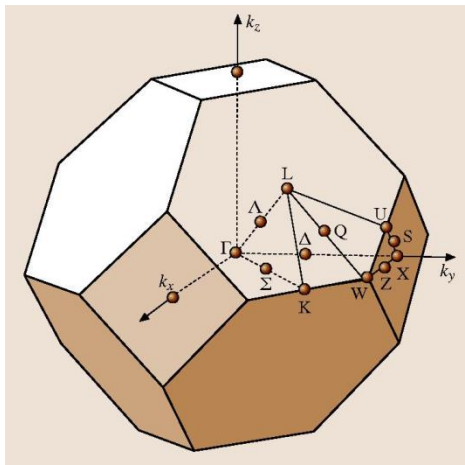


Fig. 4.1-25 Band structure of diamond



$a = 5.431 \text{ \AA}$, $E_g = 1.12 \text{ eV}$
 $m_L = 0.98m$, $m_T = 0.19m$
 $m_{LH} = 0.16m$, $m_{HH} = 0.49m$
 $m_{SO} = 0.24m$

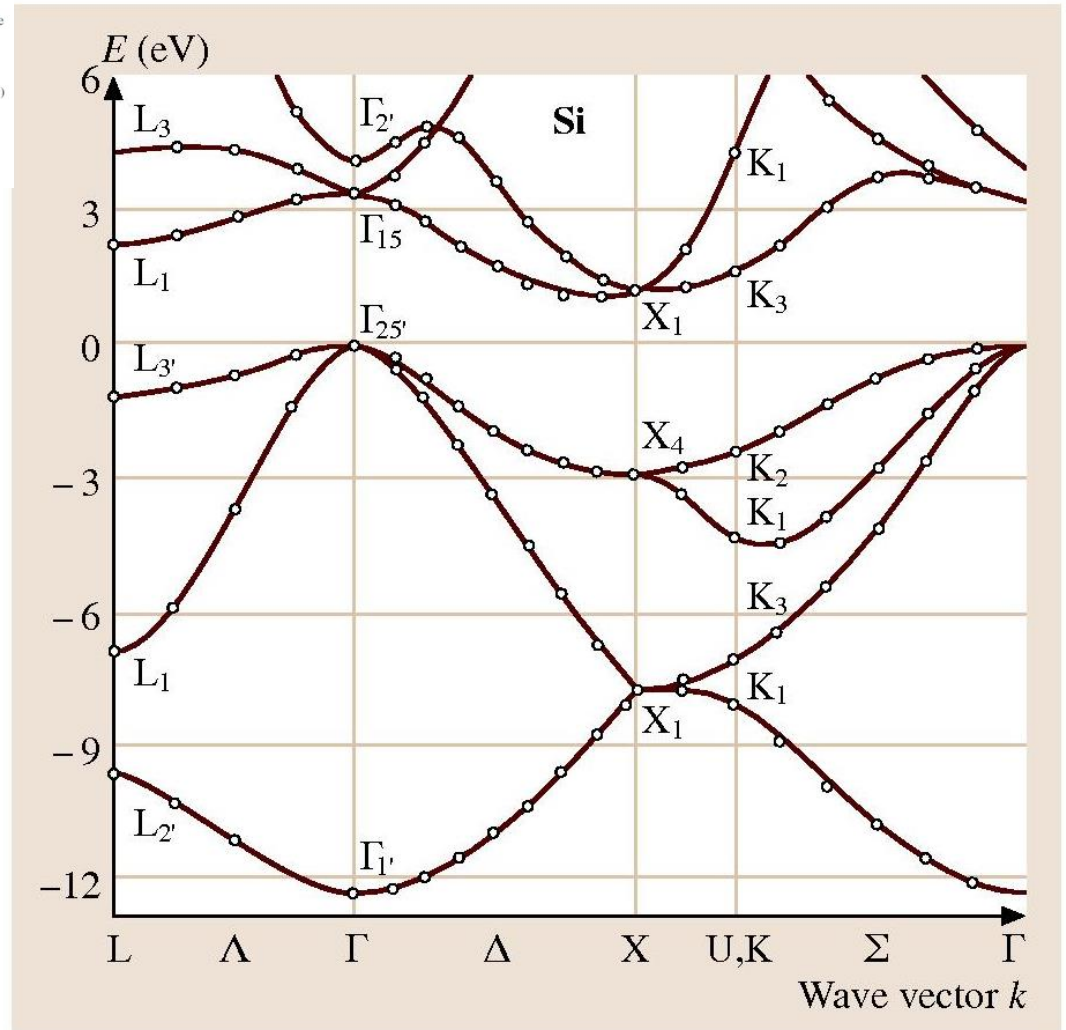


Fig. 4.1-26 Band structure of silicon

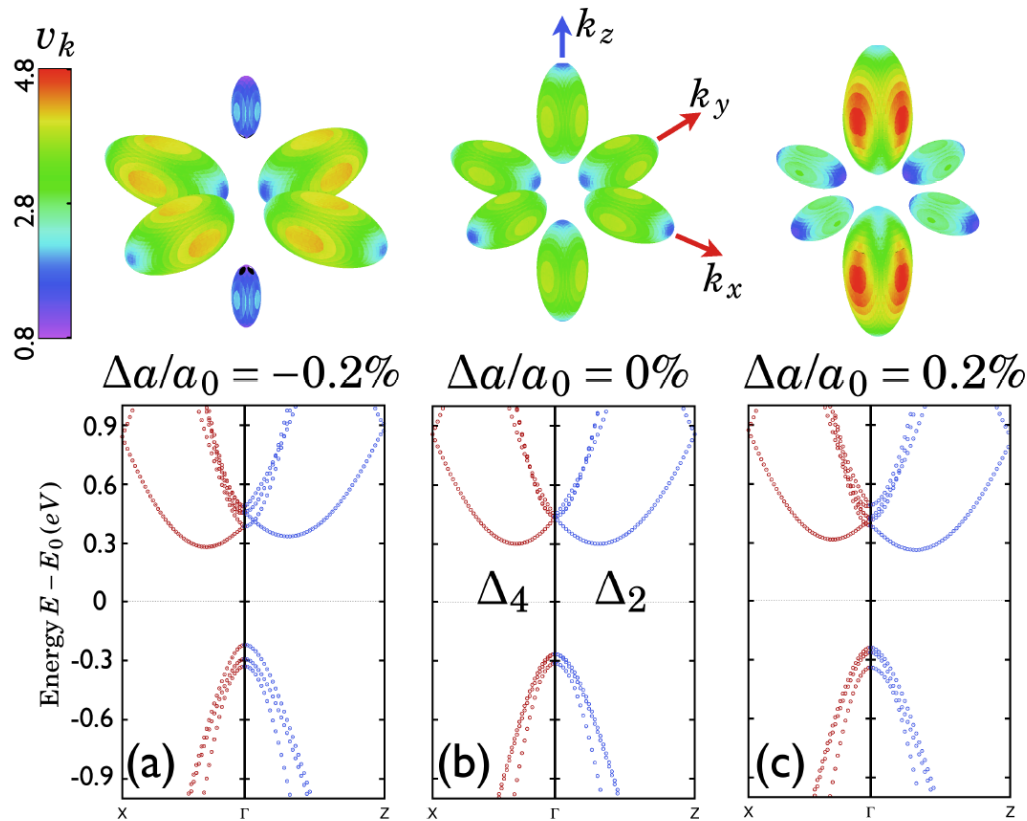
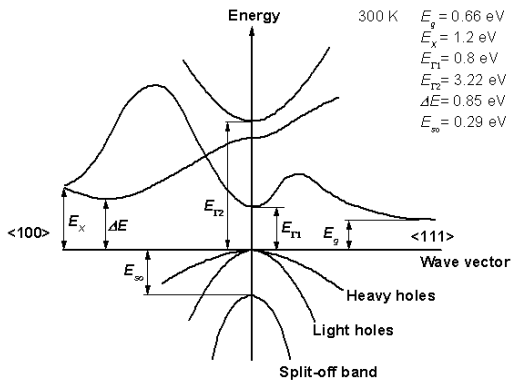
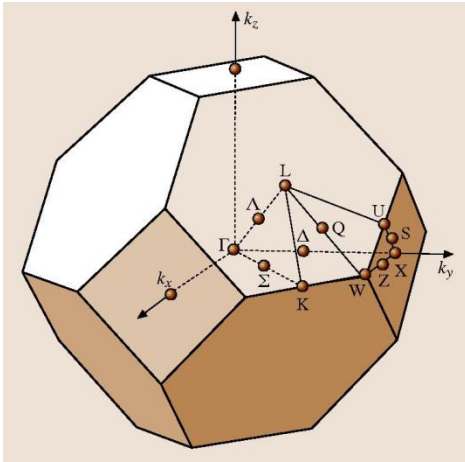


Figure 3. (color online) Fermi surfaces of electron doped silicon under compressive strain (left), no strain (middle) and tensile strain (right). On the Fermi surfaces the absolute value of the group velocities are plotted in units of $0.08 \cdot 10^6$ m/s. As reference the band structure on two high symmetry lines is given below. The doping corresponds to additionally 0.01 electrons per unit cell which causes carrier densities of $6.25 \cdot 10^{19} \text{ cm}^{-3}$.

N. F. Hinsche et al. J. Phys.: Condens. Matter **23** (2011) 295502



$a = 5.657 \text{ \AA}$, $E_g = 0.67 \text{ eV}$
 $m_L = 1.6m$, $m_T = 0.08m$
 $m_{LH} = 0.043m$, $m_{HH} = 0.33m$
 $m_{SO} = 0.084m$

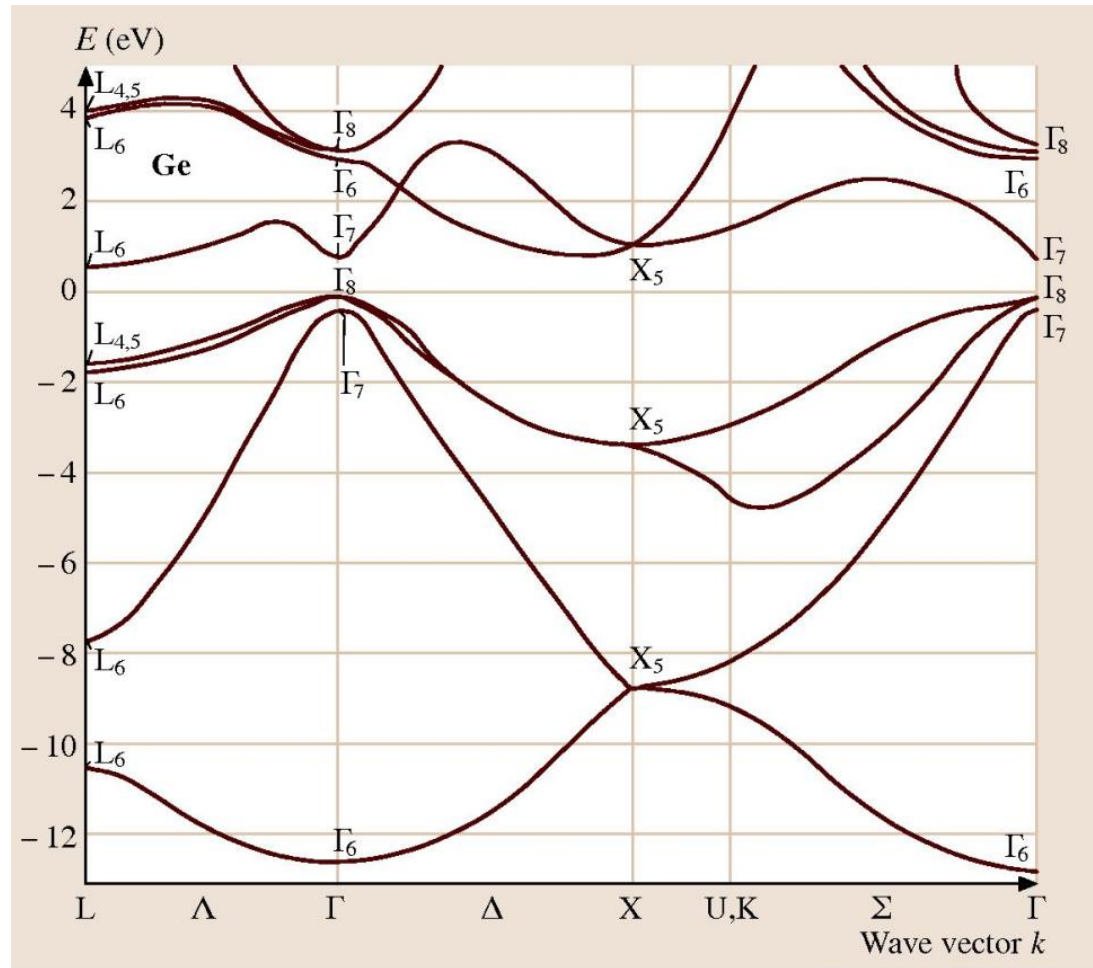
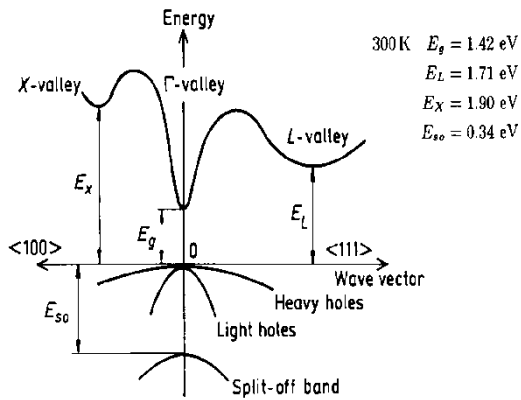
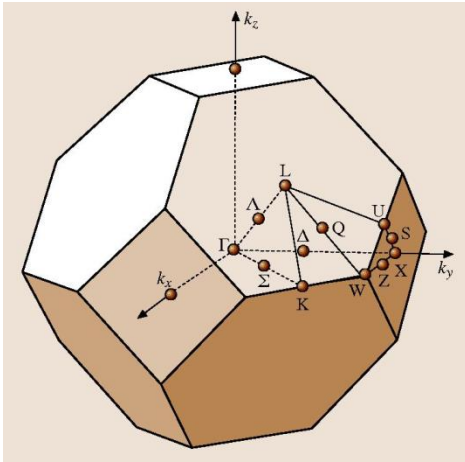


Fig. 4.1-27 Band structure of germanium



$a = 5.632 \text{ \AA}$, $E_g = 1.42 \text{ eV}$
 $m_e = 0.063 m$,
 $m_{LH} = 0.082 m$, $m_{HH} = 0.51 m$
 $m_{SO} = 0.015 m$

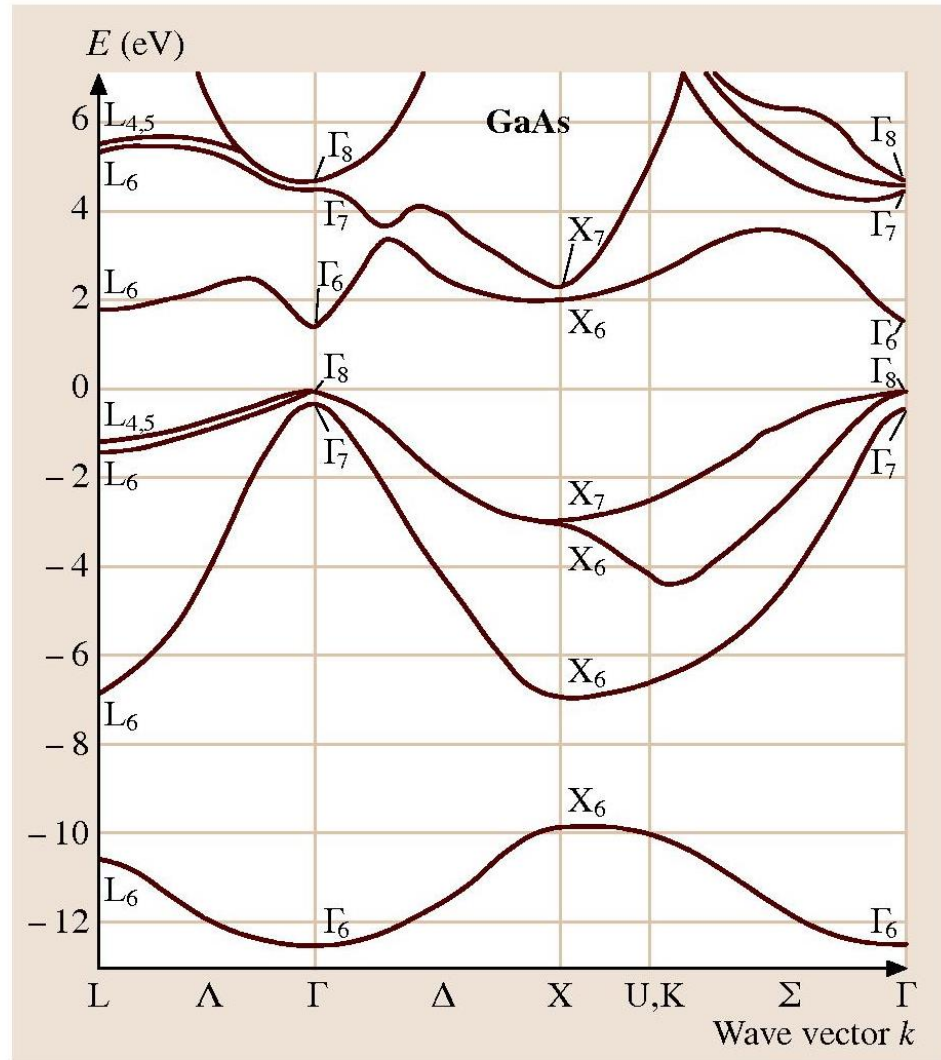
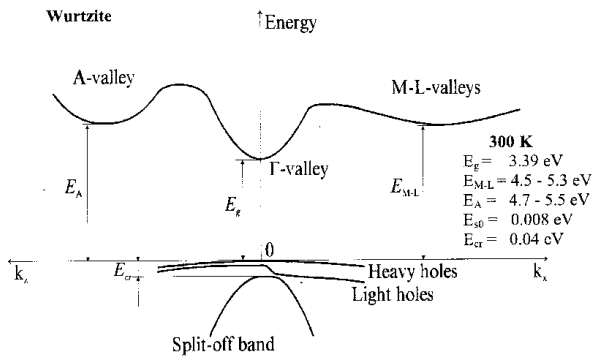
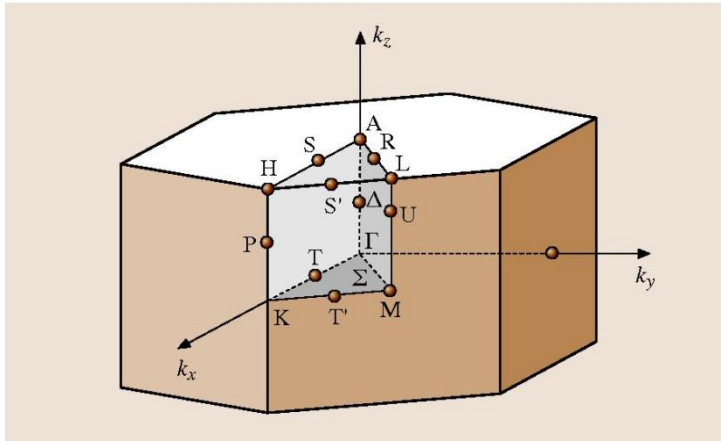


Fig. 4.1-88 Band structure of gallium arsenide



$a=3.189\text{\AA}$, $c=5.186\text{\AA}$, $E_g=3.39\text{eV}$
 $m_e=0.2m$,
 $m_{LH}=0.3m$, $m_{HH}=1.4m$
 $m_{SO}=0.6m$

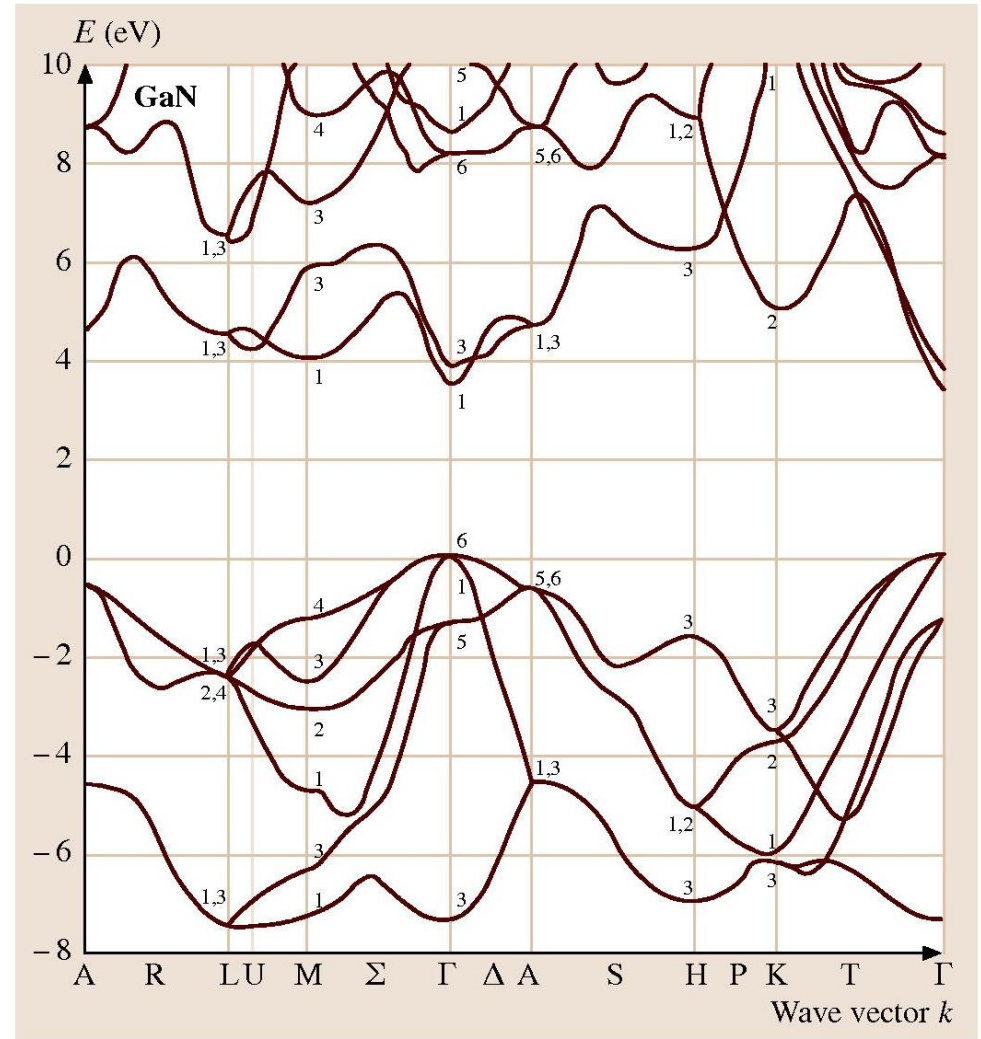
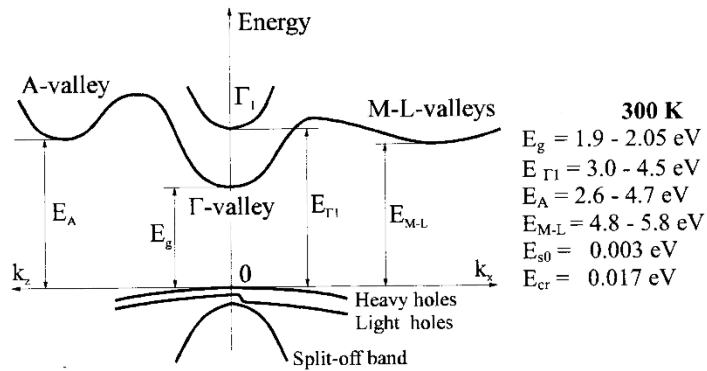
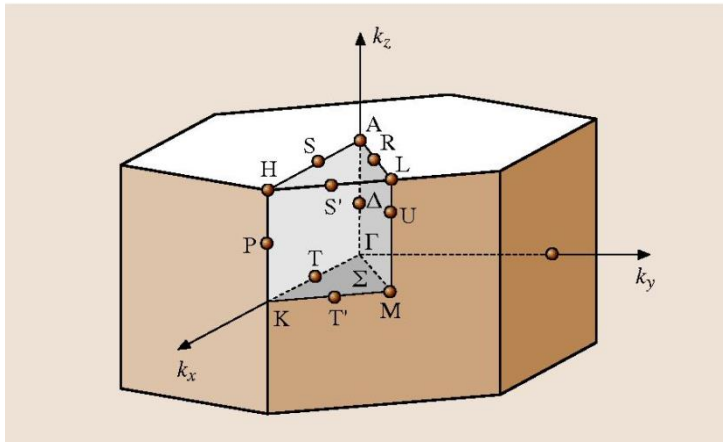


Fig. 4.1-87 Band structure of gallium nitride



$a=3.533A$, $c=5.693A$, $E_g=1.9\text{eV}$
 $m_e=0.11m$,
 $m_{LH}=0.27m$, $m_{HH}=1.63m$
 $m_{SO}=0.65m$

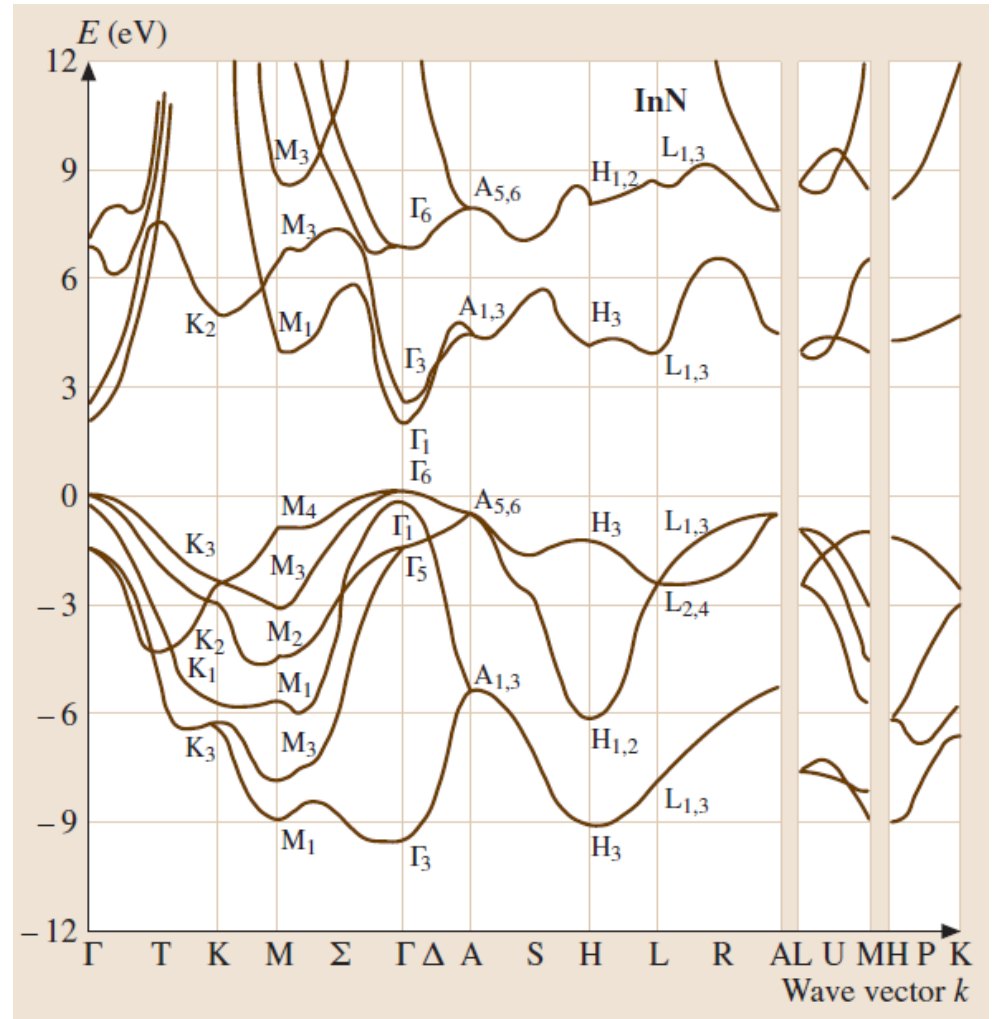
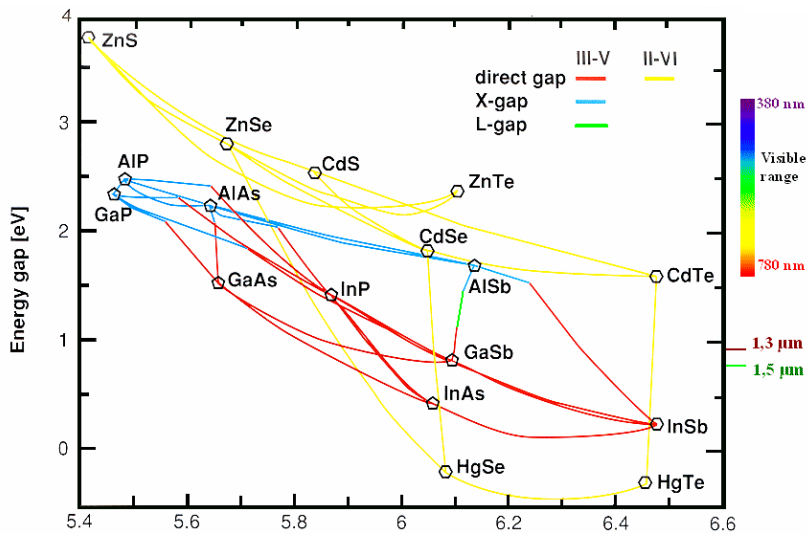
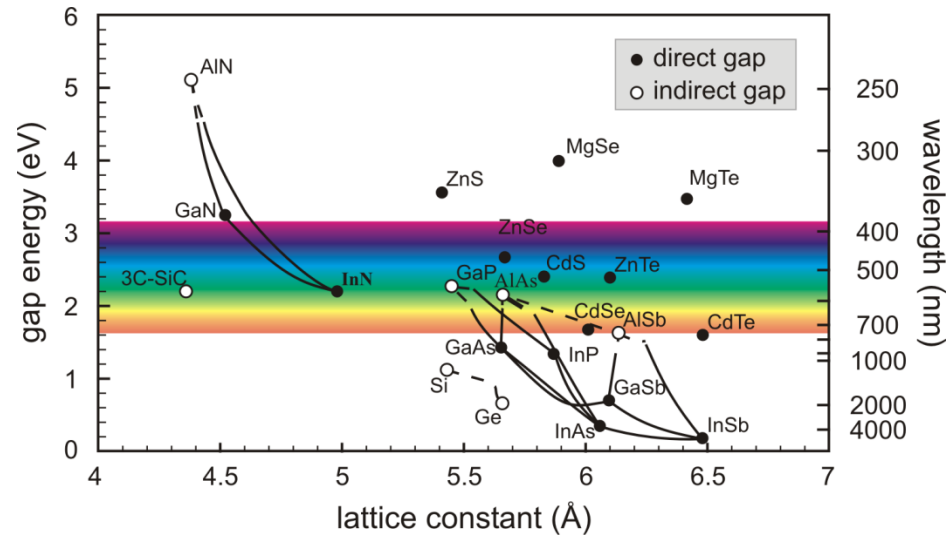


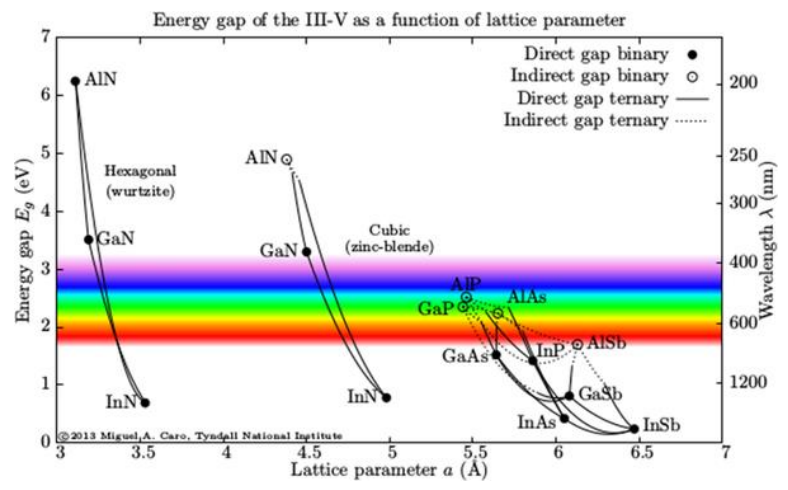
Fig. 4.1-114 Band structure of indium nitride



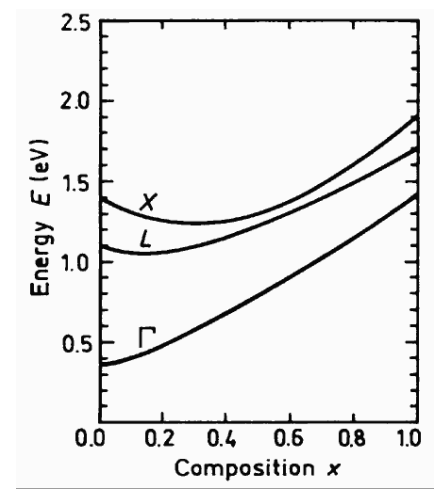
<http://www.tf.uni-kiel.de>



<http://web.tiscali.it>



<https://www.quora.com/>



Direct bandgap of $\text{Ga}_x\text{In}_{1-x}\text{As}$
 W. Porod, D.K. Ferry, Phys. Rev., B27, 2587 (1983).

Density of carriers in a homogeneous semiconductor

we denote: n_c, p_v the densities of electrons in cb and of holes in vb, respectively, $g_c(\mathcal{E}), g_v(\mathcal{E})$ are the densities of states, $f(\mathcal{E})$ is the FD distribution function. Then

$$n_c(T) = \int_{E_c}^{\infty} d\mathcal{E} g_c(\mathcal{E}) f(\mathcal{E}),$$

$$p_v(T) = \int_{-\infty}^{E_v} d\mathcal{E} g_v(\mathcal{E}) [1 - f(\mathcal{E})] = \int_{-\infty}^{E_v} d\mathcal{E} g_v(\mathcal{E}) \frac{1}{e^{(\mu - \mathcal{E})/(k_B T)} + 1}$$

Numerically complicated – we do not know $\mu(T)$. Simplification: **non-degenerated semiconductor:**

$$E_c - \mu \gg k_B T \text{ and } \mu - E_v \gg k_B T$$

Then

$$\frac{1}{\exp\left(\frac{E - \mu}{k_B T}\right) + 1} \approx \exp\left(-\frac{E - \mu}{k_B T}\right) \text{ if } E > E_c$$

$$\frac{1}{\exp\left(\frac{\mu - E}{k_B T}\right) + 1} \approx \exp\left(-\frac{\mu - E}{k_B T}\right) \text{ if } E < E_v$$

and

$$n_c(T) = N_c(T) e^{-\frac{E_c - \mu}{k_B T}}, N_c(T) = \int_{E_c}^{\infty} dE g_c(E) e^{-(E - E_c)/(k_B T)} = \frac{1}{4} \left(\frac{2m_c k_B T}{\pi \hbar^2} \right)^{3/2}$$

$$p_v(T) = P_v(T) e^{+\frac{E_v - \mu}{k_B T}}, P_v(T) = \int_{-\infty}^{E_v} dE g_v(E) e^{+(E - E_v)/(k_B T)} = \frac{1}{4} \left(\frac{2m_v k_B T}{\pi \hbar^2} \right)^{3/2}$$

“conservation law” $n_c p_v = N_c P_v e^{-E_g/(k_B T)}$

a special case: **intrinsic semiconductor**

$$n_c = p_v \equiv n_i = \sqrt{N_c P_v} e^{-E_g/(2k_B T)}$$

the chemical potential:

$$\mu_i = E_v + \frac{1}{2} E_g + \frac{1}{2} k_B T \ln \left(\frac{P_v}{N_c} \right)$$

Semiconductor with impurities (extrinsic semiconductor)

LEVELS OF GROUP V (DONORS) AND GROUP III (ACCEPTORS) IMPURITIES IN SILICON AND GERMANIUM

GROUP III ACCEPTORS (TABLE ENTRY IS $\epsilon_a - \epsilon_v$)

	B	Al	Ga	In	Tl
Si	0.046 eV	0.057	0.065	0.16	0.26
Ge	0.0104	0.0102	0.0108	0.0112	0.01

GROUP V DONORS (TABLE ENTRY IS $\epsilon_c - \epsilon_d$)

	P	As	Sb	Bi
Si	0.044 eV	0.049	0.039	0.069
Ge	0.0120	0.0127	0.0096	—

ROOM TEMPERATURE ENERGY GAPS ($E_g = \epsilon_c - \epsilon_v$)

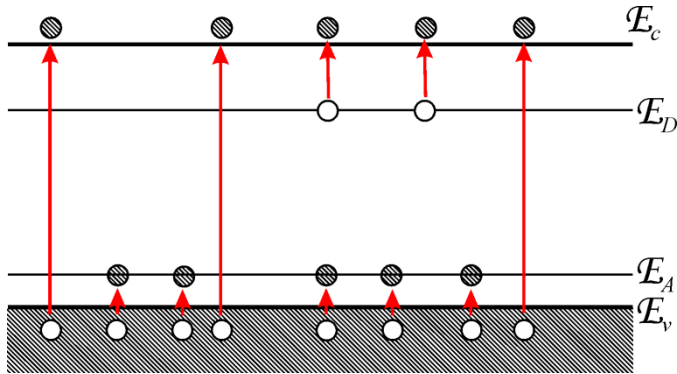
Si	1.12 eV
Ge	0.67 eV

The impurity levels are affected by:

1. screening of the electric field of the impurity ion
2. small effective mass of the free carriers

The binding energy of an electron to the impurity ion $E = \mathcal{R} \frac{1}{\epsilon^2} \frac{m^*}{m}$, $\mathcal{R} = 13.6 \text{ eV}$

We denote N_A, N_D the concentrations of the donor and acceptor impurities
 n_D, p_A are the densities of electrons on the donor level and holes on the acceptor level, respectively



Electric neutrality:

$$p_v + N_D^+ = n_c + N_A^-$$

mean densities of the electrons and holes on the impurity levels:

The donor level:

The level population:

N_j	\mathcal{E}_j
0	0
1 \uparrow	\mathcal{E}_D
1 \downarrow	\mathcal{E}_D
2	$2\mathcal{E}_D$

$$n_D = N_D \frac{\sum_j N_j e^{-(\mathcal{E}_j - \mu N_j)/(k_B T)}}{\sum_j e^{-(\mathcal{E}_j - \mu N_j)/(k_B T)}} \approx \frac{N_D}{\frac{1}{2} e^{(\mathcal{E}_D - \mu)/(k_B T)} + 1}$$

The acceptor level:

The level population:

N_j	\mathcal{E}_j
0	$2\mathcal{E}_A$
1 \uparrow	\mathcal{E}_A
1 \downarrow	\mathcal{E}_A
2	0

$$p_A = N_A \frac{\sum_j N_j e^{-(\mathcal{E}_j - \mu N_j)/(k_B T)}}{\sum_j e^{-(\mathcal{E}_j - \mu N_j)/(k_B T)}} \approx \frac{N_A}{\frac{1}{2} e^{(\mu - \mathcal{E}_A)/(k_B T)} + 1}$$

For simplicity, we consider a semiconductor with a single donor level only – the n-type

The conservation law $n_c p_v = N_c P_v e^{-\mathcal{E}_g/(k_B T)}$ is still valid

Electric neutrality: $n_c = p_v + N_D^+ \quad N_D^+ \equiv p_D = \frac{N_D}{2e^{(\mu - \mathcal{E}_D)/(k_B T)} + 1}$

Special case: low temperatures: $p_v \ll N_D^+ \Rightarrow n_c \approx p_D$

$$N_c e^{-(\mathcal{E}_c - \mu)/(k_B T)} = \frac{N_D}{2e^{(\mu - \mathcal{E}_D)/(k_B T)} + 1} \Rightarrow \text{equation for } \mu$$

Solution:

$$\mu = k_B T \ln \left[\frac{1}{4} e^{\mathcal{E}_D / (k_B T)} \left(\sqrt{1 + 8 \frac{N_D}{N_c} e^{(\mathcal{E}_c - \mathcal{E}_D) / (k_B T)}} - 1 \right) \right]$$

if, in addition $8 \frac{N_D}{N_c} e^{(\mathcal{E}_c - \mathcal{E}_D) / (k_B T)} \gg 1$ then

$$\mu = \frac{1}{2} (\mathcal{E}_c + \mathcal{E}_D) + \frac{1}{2} k_B T \ln \frac{N_D}{2N_c} \quad \text{and} \quad n_c = \sqrt{\frac{1}{2} N_c N_D} e^{-(\mathcal{E}_c - \mathcal{E}_D) / (2k_B T)}$$

if, in addition $8 \frac{N_D}{N_c} e^{(\mathcal{E}_c - \mathcal{E}_D) / (k_B T)} \ll 1$ then

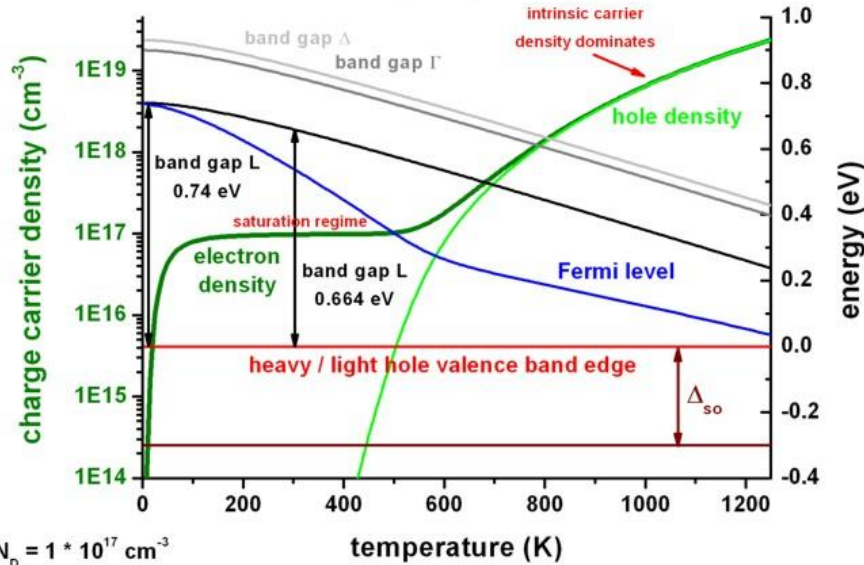
$$\mu = \mathcal{E}_c + k_B T \ln \frac{N_D}{N_c} \quad \text{and} \quad n_c = N_D$$

Special case: high temperatures $n_c = p_v + N_D$

$$\text{then} \quad n_c = \frac{n_i^2}{n_c} + N_D \Rightarrow n_c = \frac{1}{2} N_D \left(1 + \sqrt{1 + 4 \frac{n_i^2}{N_D^2}} \right)$$

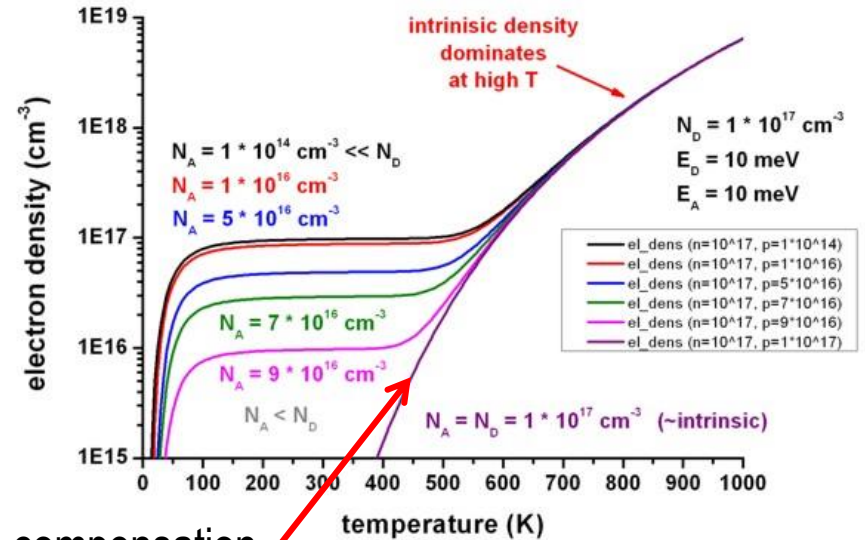
$$\mu = \mathcal{E}_c + k_B T \ln \left[\frac{N_D}{2N_c} \left(1 + \sqrt{1 + 4 \frac{N_c p_v}{N_D^2} e^{-\mathcal{E}_g / (k_B T)}} \right) \right]$$

Charge carrier density and Fermi level vs. temperature for n-type doped Ge



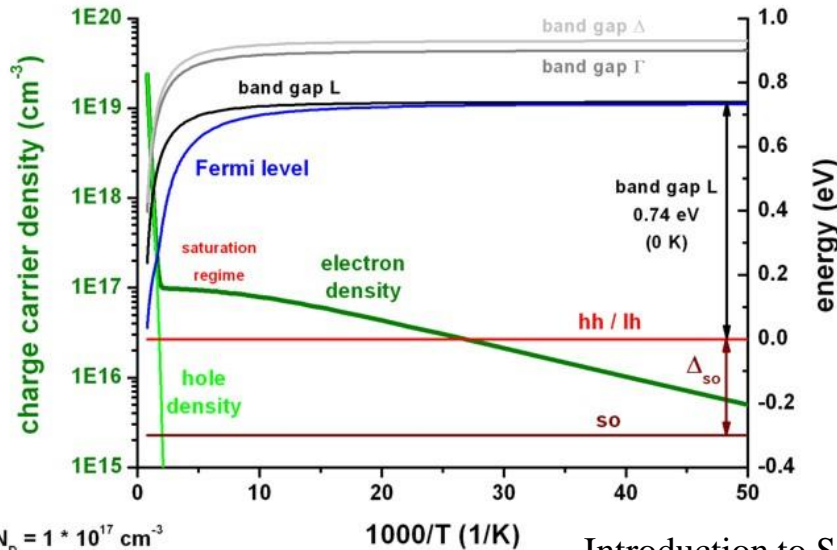
$N_D = 1 \cdot 10^{17} \text{ cm}^{-3}$
 $E_D = 10 \text{ meV}$

Electron density in Ge vs. temperature for different acceptor densities N_A



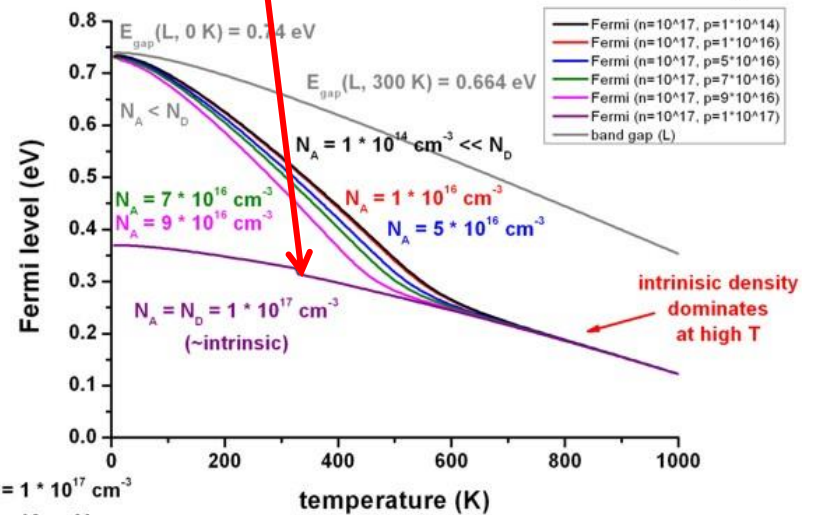
compensation

Charge carrier density and Fermi level vs. inverse temperature for n-type doped Ge



$N_D = 1 \cdot 10^{17} \text{ cm}^{-3}$
 $E_D = 10 \text{ meV}$

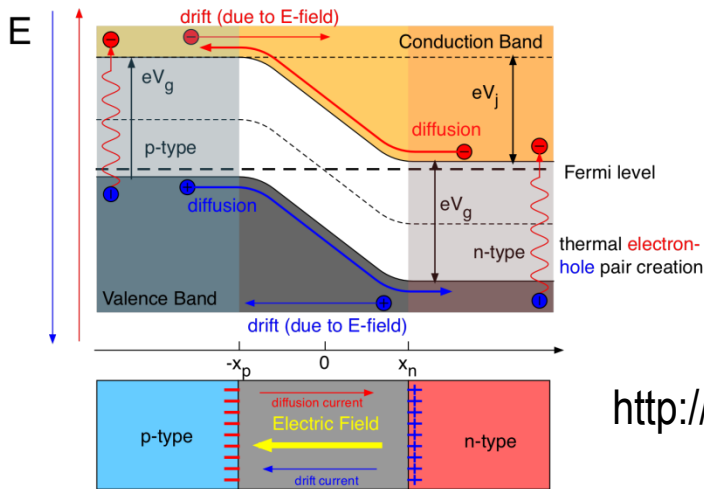
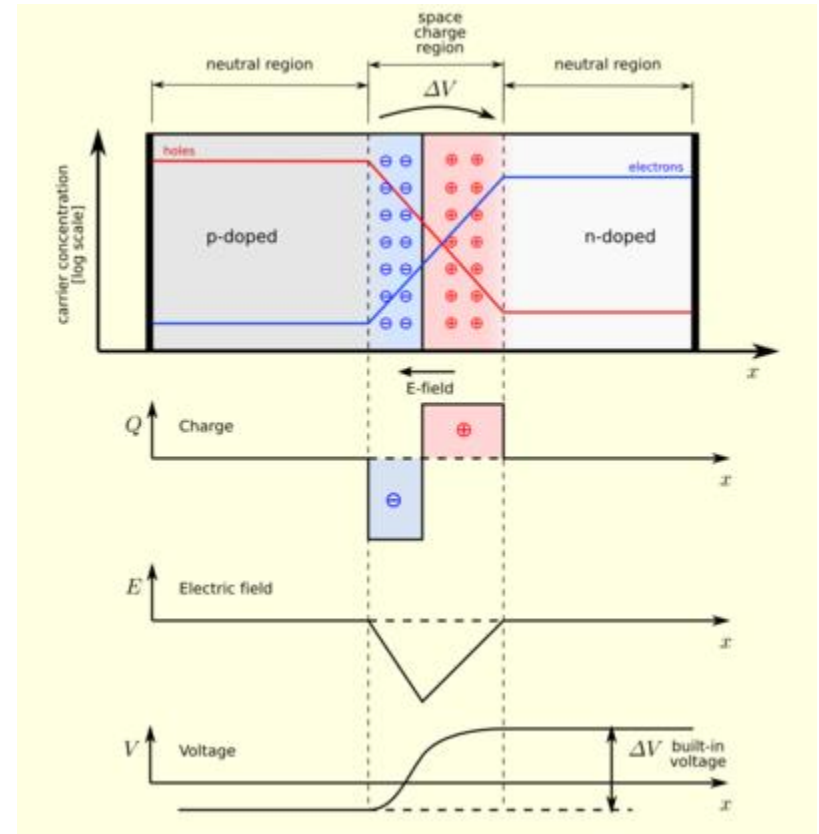
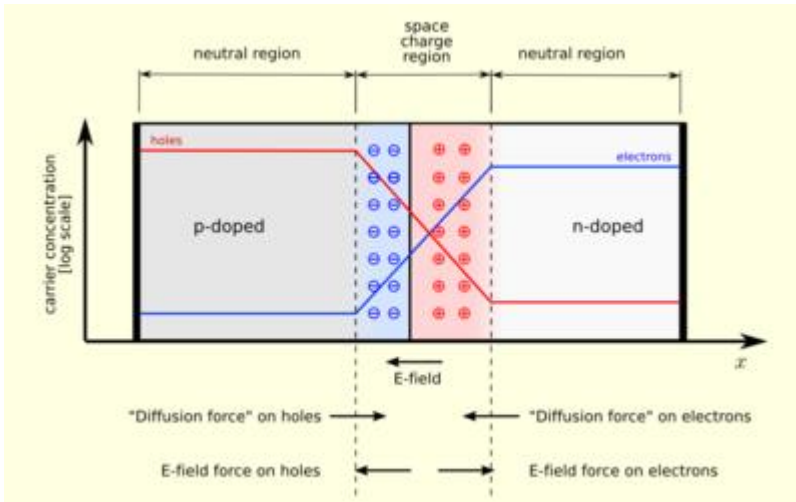
Fermi level in Ge vs. temperature for different acceptor densities N_A



$N_D = 1 \cdot 10^{17} \text{ cm}^{-3}$
 $E_D = 10 \text{ meV}$

p-n junction

en.wikipedia.org



Schematic of pn-junction



<http://wanda.fiu.edu>

a n-type and a p-type semiconductors are in contact in a thermodynamic equilibrium $\Rightarrow \mu$ is constant thorough the sample

Quasiclassical approximation: for a given energy band, the hamiltonian is

$$\hat{H}_n = E_n \left(\frac{\mathbf{p}}{\hbar} \right) - e\varphi(x)$$

The electrostatic potential must be a slowly varying function

$$e[\varphi(x + a) - \varphi(x)] \ll E_g$$

We restrict us to the equilibrium case, then

$$n_c(x) = N_c(T) \exp \left[-\frac{E_c - e\varphi(x) - \mu}{k_B T} \right] \quad p_v(x) = P_v(T) \exp \left[-\frac{\mu - E_v + e\varphi(x)}{k_B T} \right]$$

The potential is determined self-consistently using the Poisson equation

$$-\nabla^2 \phi = \frac{1}{\varepsilon} \rho(x)$$

$$\rho(x) = e[N_D^+(x) - N_A^-(x) - n_c(x) + p_v(x)], \quad N_D^+(x) \approx N_D, \quad N_A^-(x) \approx N_A$$

The potential difference $\Delta\phi = \phi(\infty) - \phi(-\infty)$ can be estimated as follows

Far from the junction at the n-side, the density of the free electrons approx. equals the density of the donor atoms (we assume all donor atoms are ionized):

$$n_c(\infty) \approx N_D = N_c \exp\left[-\frac{E_c - e\phi(\infty) - \mu}{k_B T}\right]$$

and similarly

$$p_v(-\infty) \approx N_A = P_v \exp\left[-\frac{\mu - E_v + e\phi(-\infty)}{k_B T}\right]$$

thus

$$e\Delta\phi = E_g + k_B T \ln\left(\frac{N_D N_A}{N_c P_v}\right)$$

depleted zones of thicknesses d_n, d_p :

$$d_{n,p} = \sqrt{\frac{(N_A / N_D)^{\pm 1} 2\epsilon\epsilon_0 \Delta\phi}{N_A + N_D} \frac{1}{e}}$$

numerically $\sim 10^2 \div 10^4 \text{ \AA}$.

The field strength in the depleted region is roughly

$$\frac{\Delta\phi}{d_n + d_p} \sim 10^5 \div 10^7 \text{ V/m} \quad \text{for } E_g = 0.1 \text{ eV}$$

Rectification effect of a p-n junction

the depletion layer has much smaller carrier density \Rightarrow much smaller electric conductivity

If we apply an external voltage V , the potential difference across the depletion layer is

$$\Delta\phi(V) = \Delta\phi(0) - V$$

and the width of the depletion layer is

$$d_{n,p}(V) = d_{n,p}(0) \sqrt{1 - \frac{\Delta\phi(V)}{\Delta\phi(0)}}$$

The carrier currents across the junction:

1. the generation current of the minority carriers – independent of V
2. the recombination current of the majority carriers – depends on V

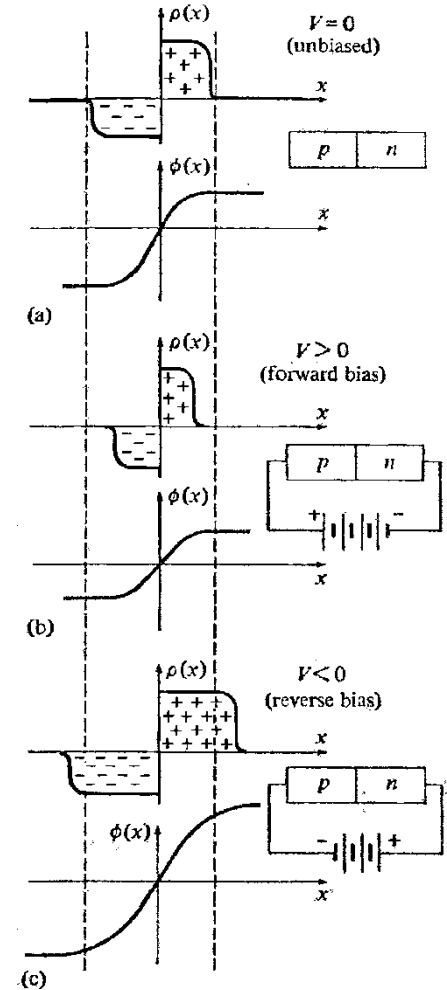
$$j_{\text{rec}}(V) \propto e^{-e[\Delta\phi(0)-V]/(k_B T)}$$

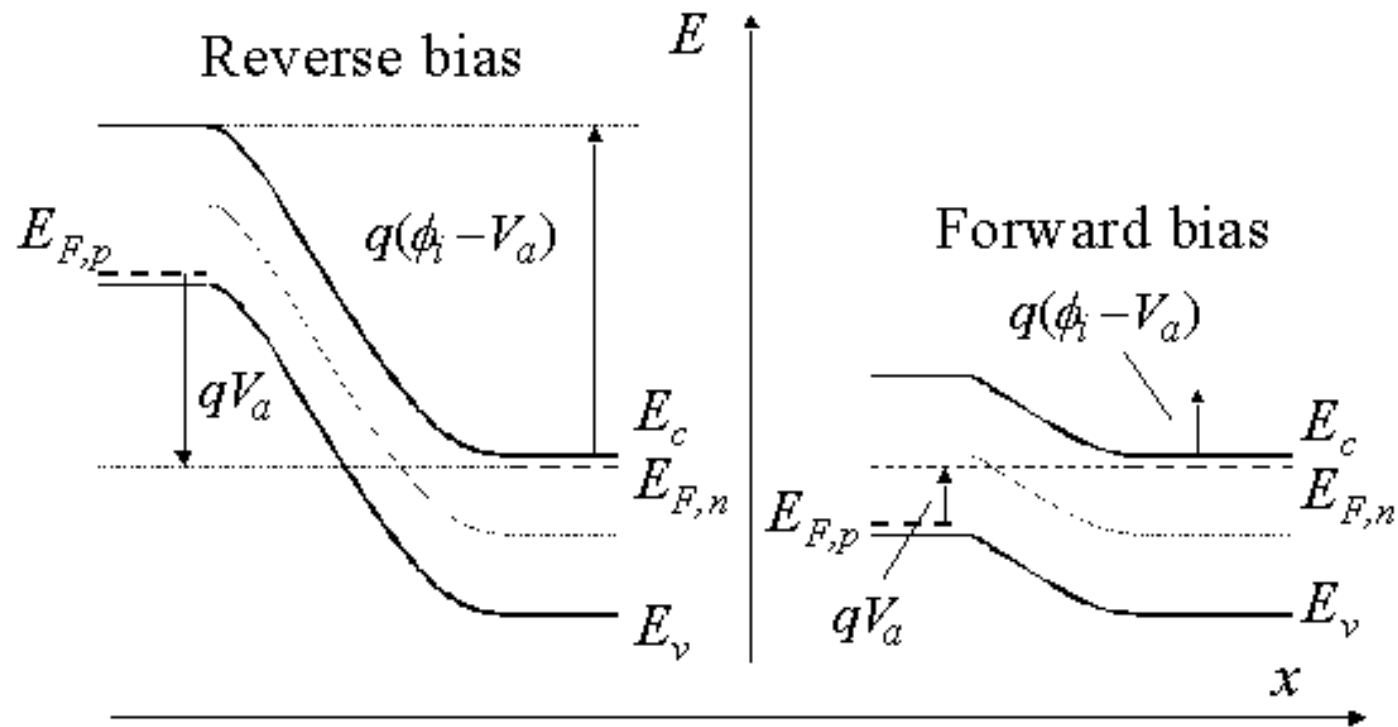
Equilibrium for $V = 0$:

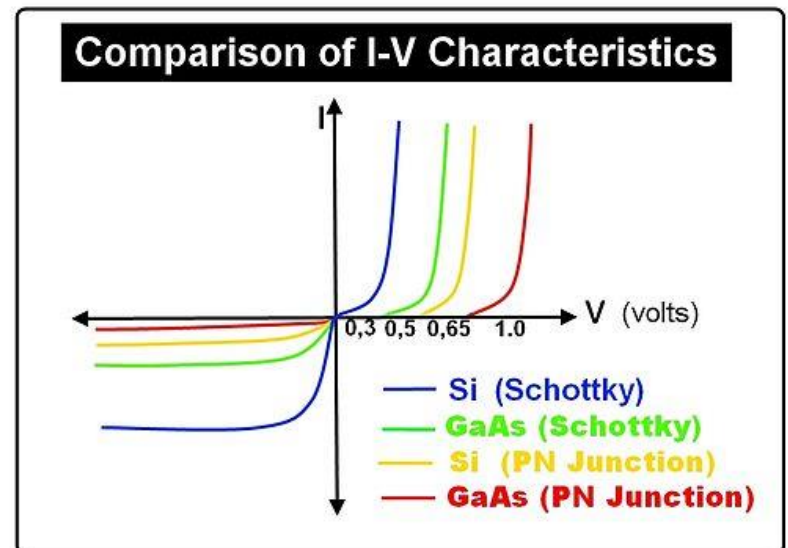
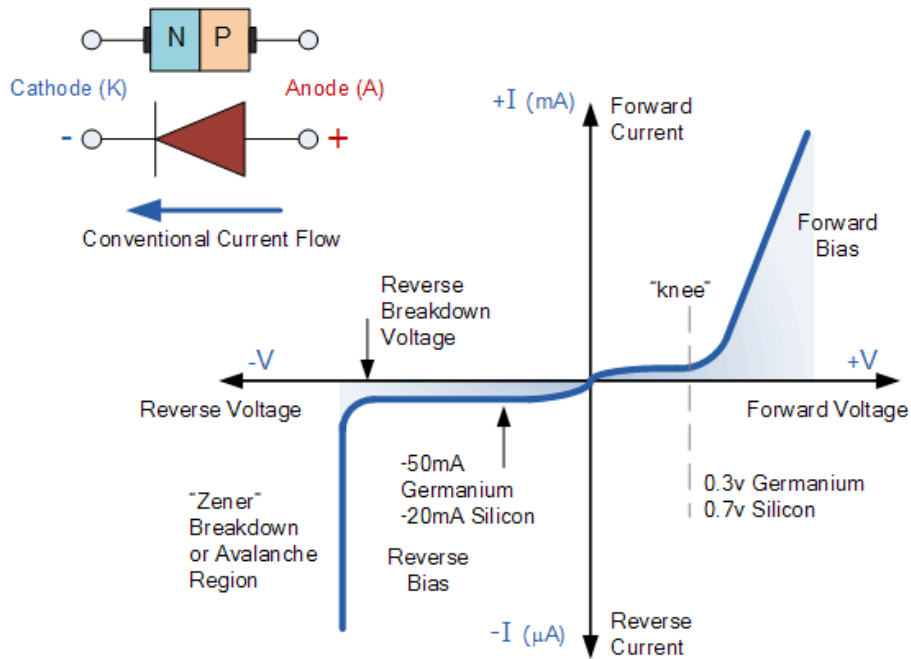
$$j_{\text{rec}}^h(0) = j_{\text{gen}}^h, j_{\text{rec}}^e(0) = j_{\text{gen}}^e$$

therefore

$$j(V) = (j_{\text{gen}}^e + j_{\text{gen}}^h) (e^{eV/(k_B T)} - 1)$$



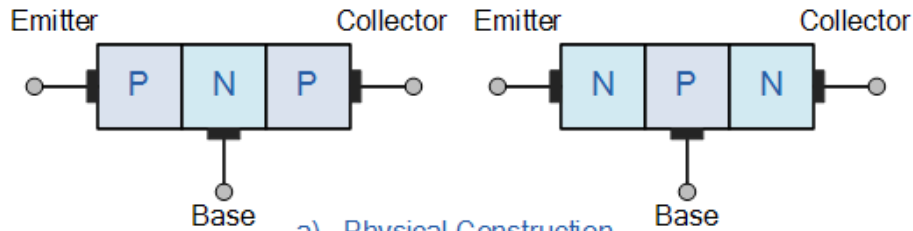




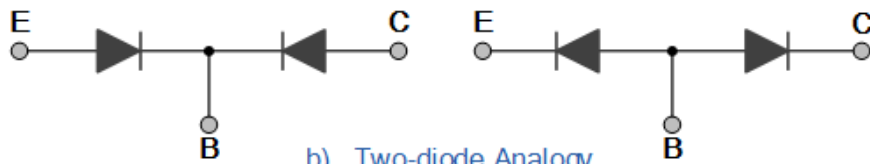
Bipolar junction transistor

PNP Transistor

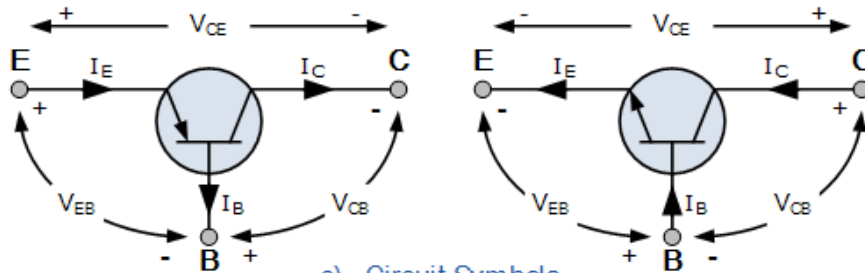
NPN Transistor



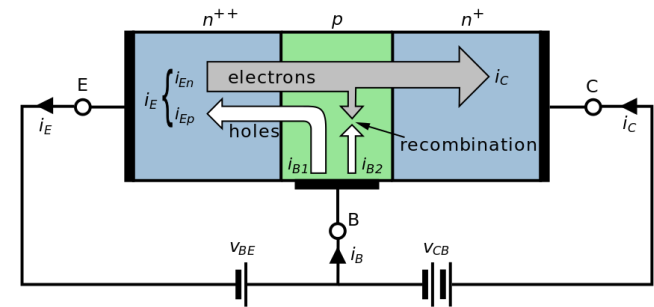
a). [Physical Construction](#)



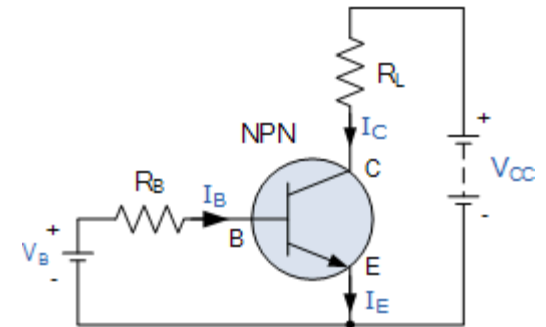
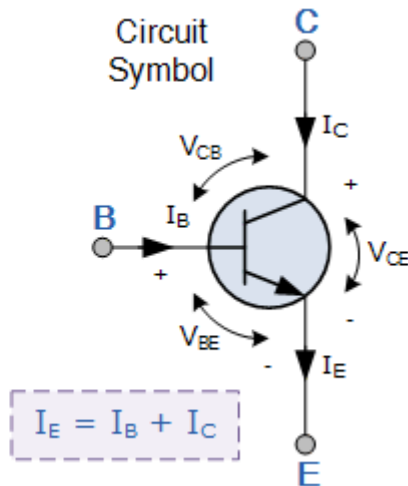
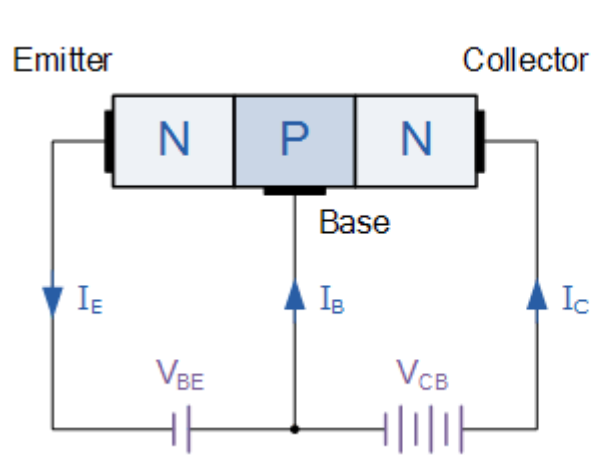
b). [Two-diode Analogy](#)



c). [Circuit Symbols](#)



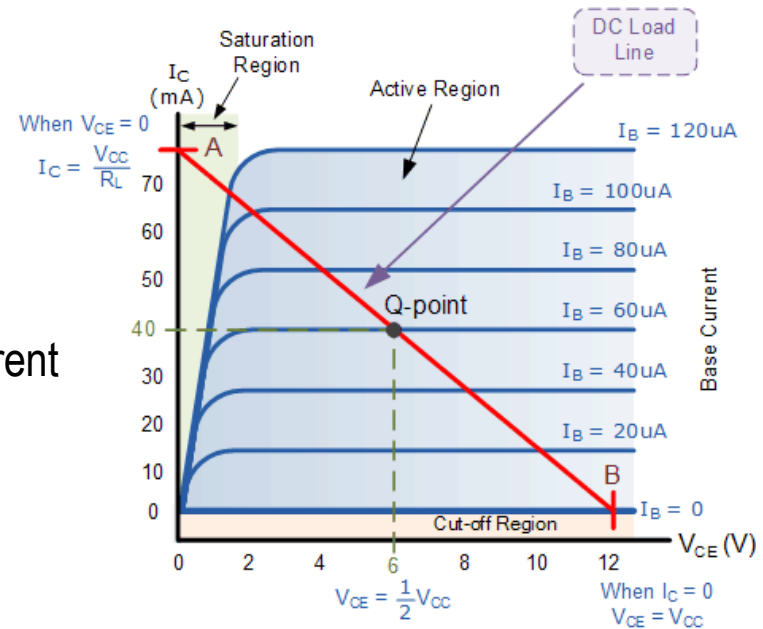
npn bipolar junction transistor



We define $\beta = \frac{I_C}{I_B}$, $\alpha = \frac{I_C}{I_E}$

then $\beta = \frac{\alpha}{1 - \alpha}$

Usually, $\alpha \rightarrow 1$ so that β is large \Rightarrow amplification of the current



VI. ELEMENTARY EXCITATIONS IN SOLIDS – PHONONS, MAGNONS

VI.1. Classical theory of a harmonic crystal

Basic assumptions:

1. The mean positions of the atoms corresponds to the Bravais lattice sites (\Rightarrow no diffusion assumed)
2. The amplitude of the atomic oscillations is much smaller than the inter-atomic distance (\Rightarrow harmonic approximation is applicable)

We denote $\mathbf{u}(\mathbf{R}, t)$ the displacement of the atom in the site \mathbf{R} . The potential energy of the crystal is

$$U = \frac{1}{2} \sum_{\mathbf{R} \neq \mathbf{R}'} \varphi(\mathbf{R} + \mathbf{u}(\mathbf{R}, t) - \mathbf{R}' - \mathbf{u}(\mathbf{R}', t))$$

Due to the assumptions:

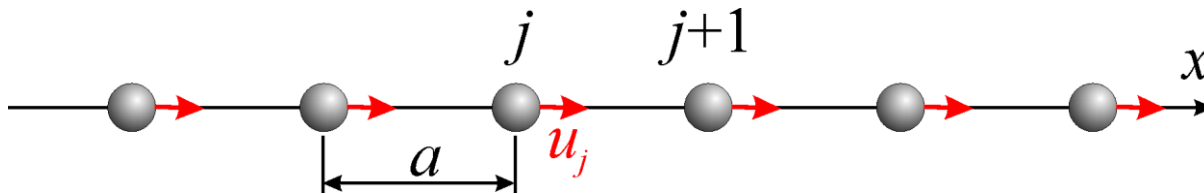
$$U \approx \frac{N}{2} \sum_{\mathbf{R} \neq 0} \varphi(\mathbf{R}) + \frac{1}{2} \sum_{\mathbf{R} \neq \mathbf{R}'} [\mathbf{u}(\mathbf{R}) - \mathbf{u}(\mathbf{R}')].\nabla \varphi(\mathbf{R} - \mathbf{R}') + \frac{1}{4} \sum_{\mathbf{R} \neq \mathbf{R}'} [(\mathbf{u}(\mathbf{R}) - \mathbf{u}(\mathbf{R}')).\nabla]^2 \varphi(\mathbf{R} - \mathbf{R}') = U_{\text{eq}} + U_{\text{harm}}$$

The harmonic part of the potential energy is

$$U_{\text{harm}} = \frac{1}{4} \sum_{\mathbf{R} \neq \mathbf{R}'} (u_j(\mathbf{R}) - u_j(\mathbf{R}')) \varphi_{jk}(\mathbf{R} - \mathbf{R}') (u_k(\mathbf{R}) - u_k(\mathbf{R}')), \quad \varphi_{jk}(\mathbf{r}) = \frac{\partial^2 \varphi(\mathbf{r})}{\partial x_j \partial x_k}$$

The components of the matrix φ can be calculated ab-initio by a exact quantum-mechanical approach or using empirical potentials. In these calculations, the adiabatic approximation is used (i.e., the role of the electrons is neglected).

Normal modes of an one-dimensional monoatomic lattice



Assumption: harmonic interaction of nearest neighbors:

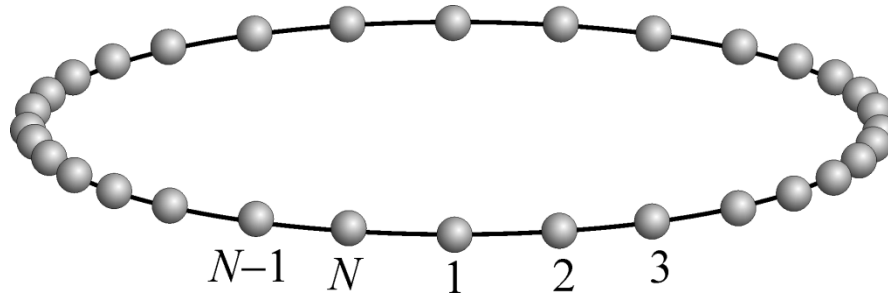
$$U_{\text{harm}} = \frac{1}{2} K \sum_j (u_{j+1} - u_j)^2, \quad K = \left. \frac{\partial^2 \varphi}{\partial x^2} \right|_{x=a}$$

Equation of movement: $M\ddot{u}_j = -\frac{\partial U_{\text{harm}}}{\partial u_j} = K(u_{j+1} + u_{j-1} - 2u_j), j = 1, \dots, N$

Periodic Born-von Kármán boundary conditions:

$$u_{N+1}(t) = u_1(t)$$

i.e., the nearest neighbors of atom N are the atoms N-1 and 1



We seek the solution of the equations of movement in the form

$$u_j(t) \propto e^{-i(\omega t - kja)}$$

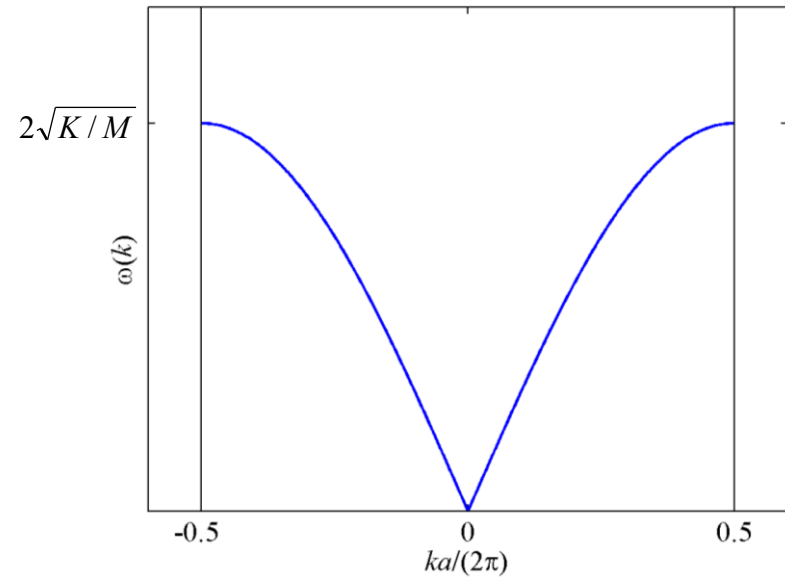
Possible values of k : $e^{ikNa} = 1 \Rightarrow k_m = m \frac{2\pi}{Na}$

We choose N values of k from the 1st Brillouin zone: $m \in \{-N/2, -N/2+1, \dots, N/2-1\}$

We obtain the dispersion relation

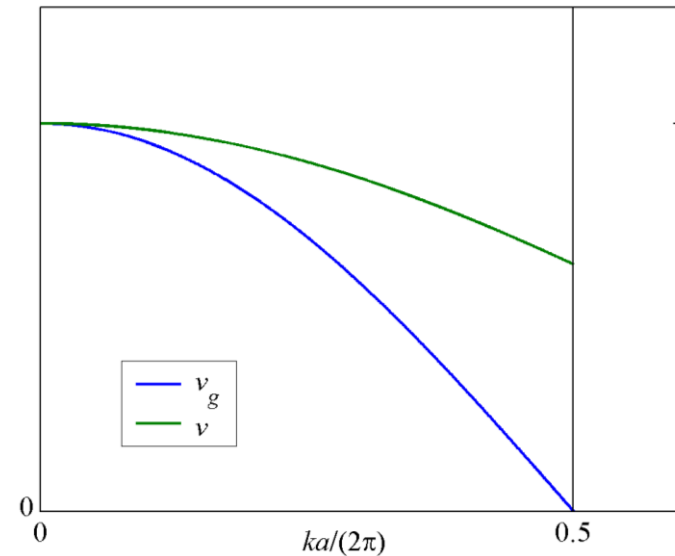
$$\omega(k) = 2\sqrt{\frac{K}{M}} \left| \sin\left(\frac{1}{2}ka\right) \right|$$

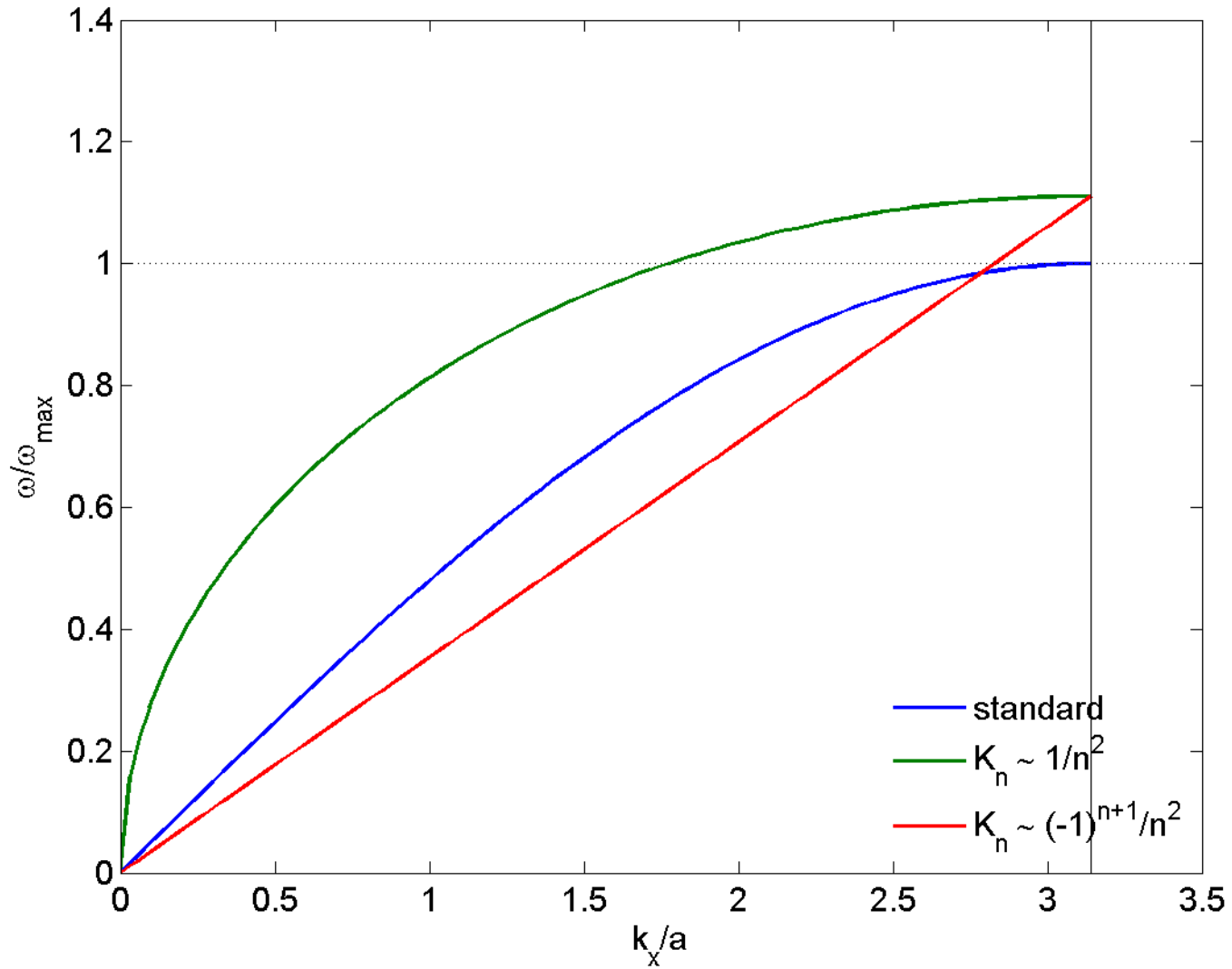
N/2 possible frequencies and N normal modes



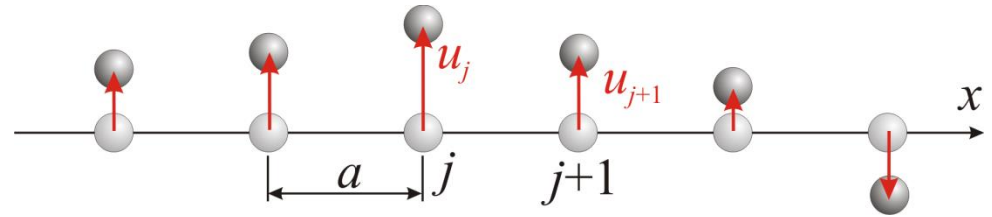
the group velocity $v_g = a\sqrt{\frac{K}{M}} \cos\left(\frac{1}{2}ka\right)$

the phase velocity $v = a\sqrt{\frac{K}{M}} \frac{\sin\left(\frac{1}{2}ka\right)}{\frac{1}{2}ka}$





Comment on transversal oscillations



Harmonic part of the potential energy (l is the length of free spring):

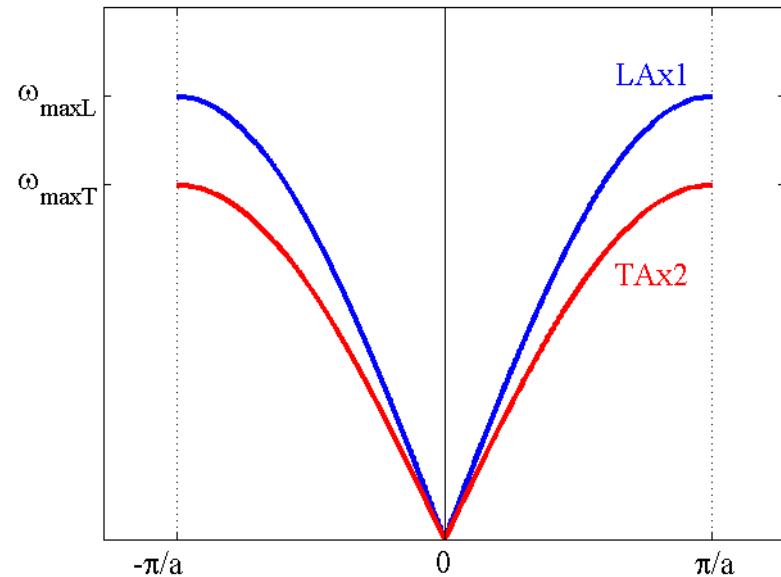
$$U_{\text{harm}} = \frac{1}{2} K \sum_j \left(\sqrt{(u_{j+1} - u_j)^2 + a^2} - l \right)^2$$

Equation of movement (approximation of small displacements):

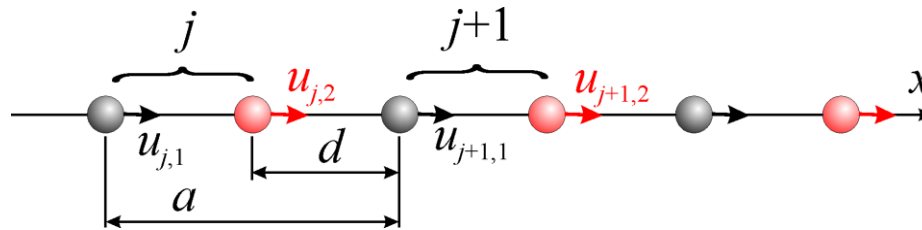
$$M \ddot{u}_j = - \frac{\partial U_{\text{harm}}}{\partial u_j} = K \frac{a-l}{a} (u_{j+1} + u_{j-1} - 2u_j), j = 1, \dots, N$$

Effective stiffness constant

$$K_T = K \frac{a-l}{a} < K$$



Normal modes of an one-dimensional diatomic lattice



The harmonic part of the potential energy:

$$U_{\text{harm}} = \frac{1}{2} K \sum_j (u_{j,1} - u_{j,2})^2 + \frac{1}{2} G \sum_j (u_{j,2} - u_{j+1,1})^2$$

The equations of movement (we assume the same masses of the atoms but different force constants):

$$\begin{aligned} M_1 \ddot{u}_{j,1} &= -K(u_{j,1} - u_{j,2}) - G(u_{j,1} - u_{j-1,2}) \\ M_2 \ddot{u}_{j,2} &= -K(u_{j,2} - u_{j,1}) - G(u_{j,2} - u_{j+1,1}), j = 1, \dots, N \end{aligned}$$

We seek the solution of the equations of movement in the form

$$u_{j1}(t) = u_1 e^{-i(\omega t - kja)}, \quad u_{j2}(t) = u_2 e^{-i(\omega t - kja)}$$

Then we obtain

$$\begin{aligned} (M_1\omega^2 - K - G)u_1 + (K + Ge^{-ika})u_2 &= 0 \\ (K + Ge^{ika})u_1 + (M_2\omega^2 - K - G)u_2 &= 0 \end{aligned}$$

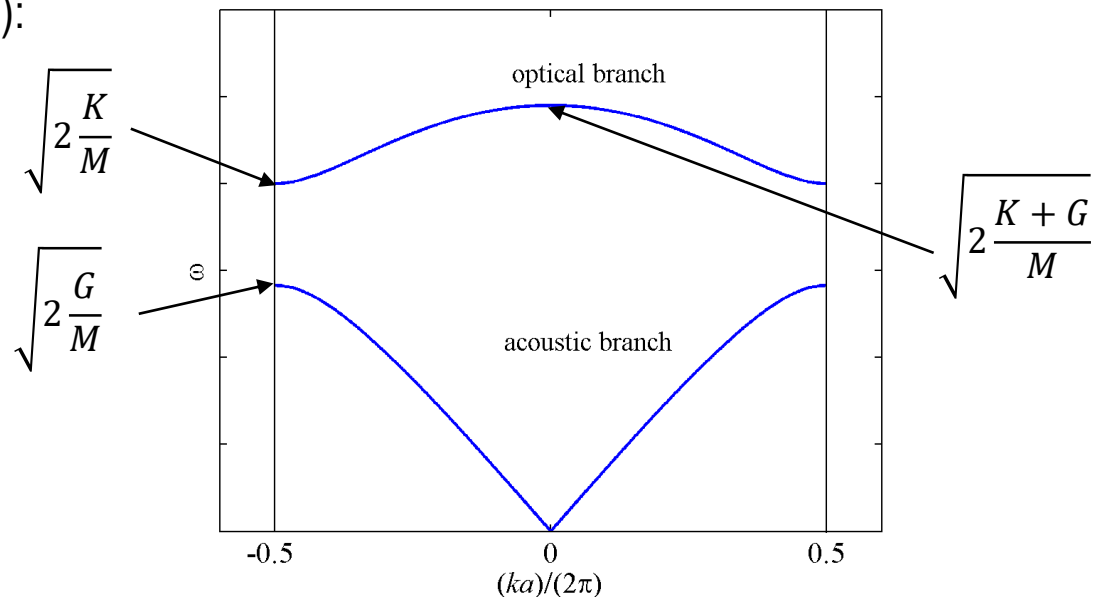
and the dispersion relation is

$$\omega^2 = \frac{M_1 + M_2}{2M_1M_2} \left[K + G \pm \sqrt{(K + G)^2 - 8 \frac{M_1M_2}{(M_1 + M_2)^2} KG(1 - \cos(ka))} \right]$$

two frequencies for a given $k \Rightarrow$ two frequency branches

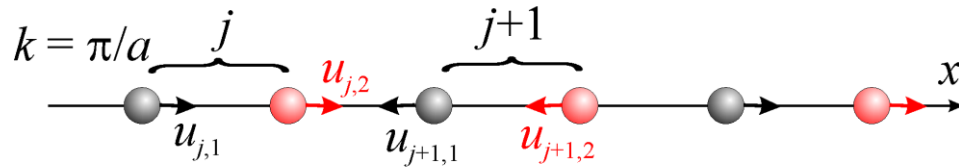
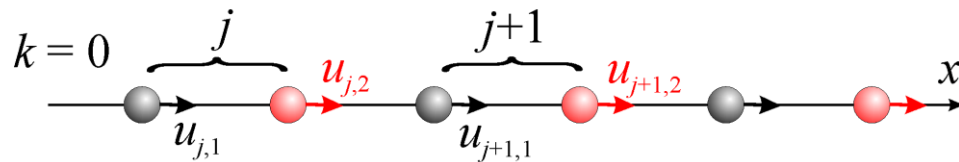
Ratio of the amplitudes (for $M_1 = M_2$):

$$\frac{u_2}{u_1} = \mp \frac{K + Ge^{ika}}{|K + Ge^{ika}|}$$

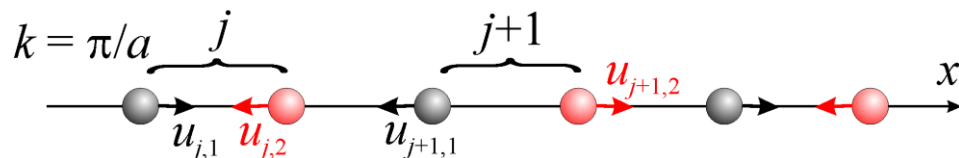
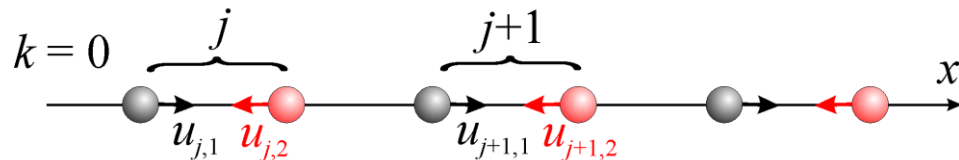


The lower (acoustic) branch: around $k = 0$: $u_1 \approx u_2, u_{j,1} \approx u_{j+1,1}$
 around $k = \pi/a$: $u_1 \approx u_2, u_{j,1} \approx -u_{j+1,1}$ (if $K > G$)

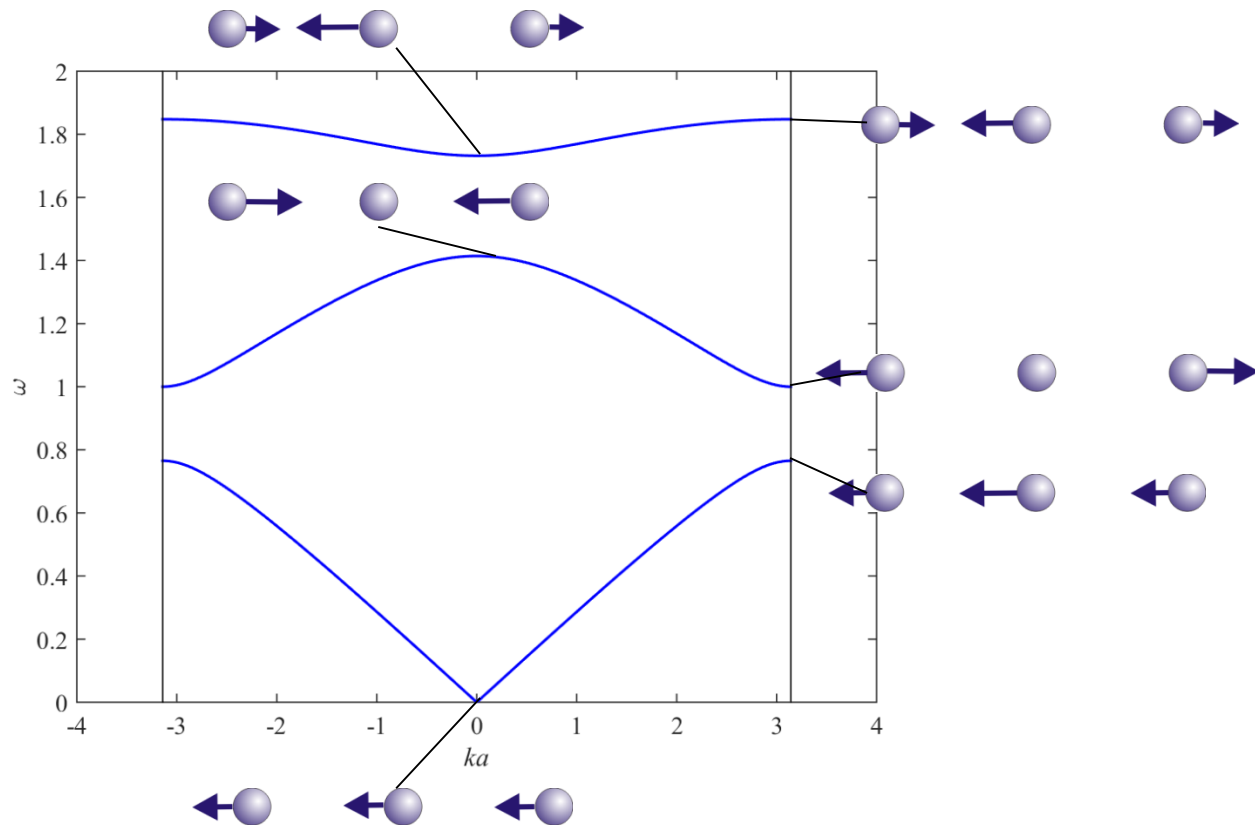
The upper (optical) branch: around $k = 0$: $u_1 \approx -u_2, u_{j,1} \approx u_{j+1,1}$
 around $k = \pi/a$: $u_1 \approx -u_2, u_{j,1} \approx -u_{j+1,1}$ (if $K > G$)
 acoustic:



optical:



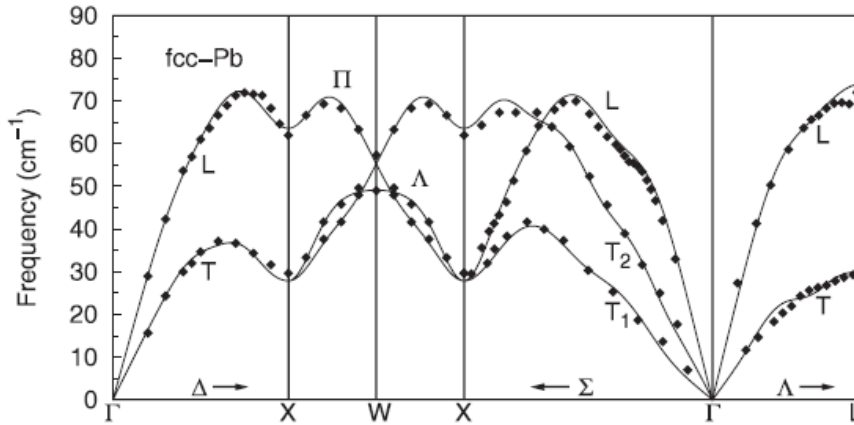
Three atoms in a molecule, 1D chain, longitudinal polarization



one acoustic branch, two optical branches

3D-case

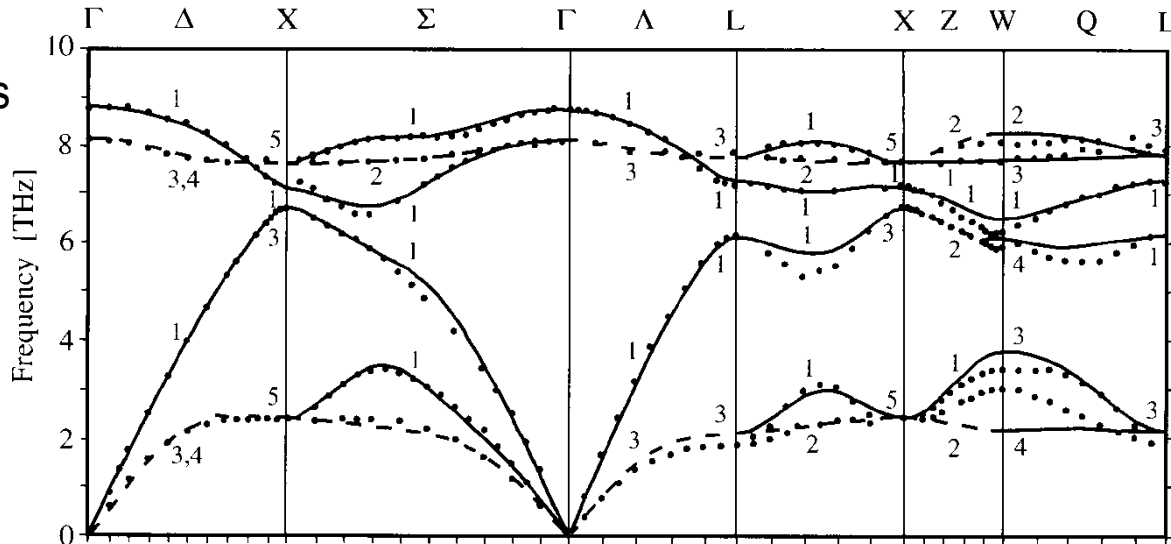
Pb

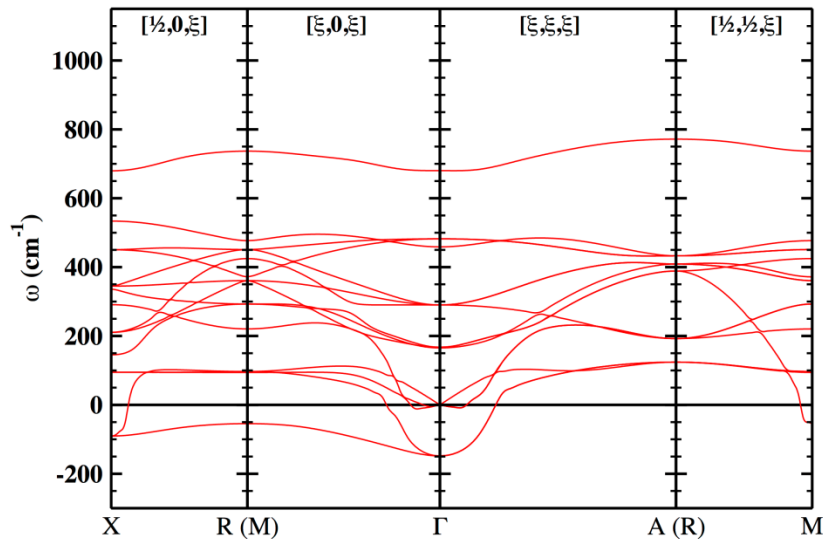
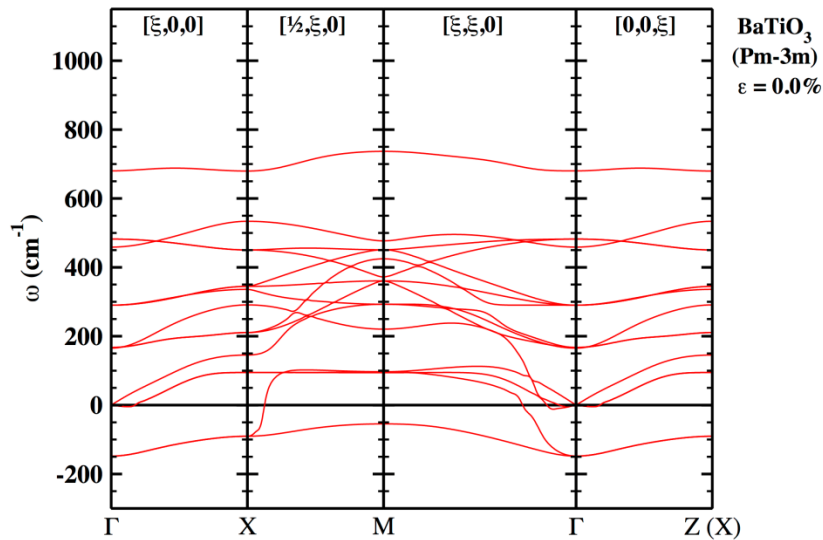


3 acoustic branches, $3(p-1)$ optical branches, p is the number of atoms in the **primitive** unit cell

Figure 1. LDA phonon dispersions (solid lines) for fcc-Pb calculated at the theoretical lattice constant compared to inelastic neutron scattering data (solid diamonds) at $T = 100$ K [1]. A FR-PP with 5d, 6s and 6p valence electrons and an $8 \times 8 \times 8$ Fourier interpolation grid have been used.

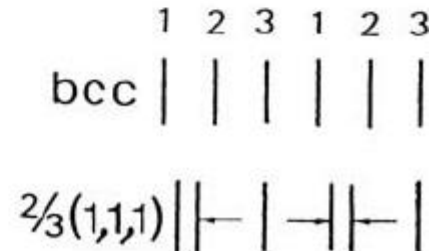
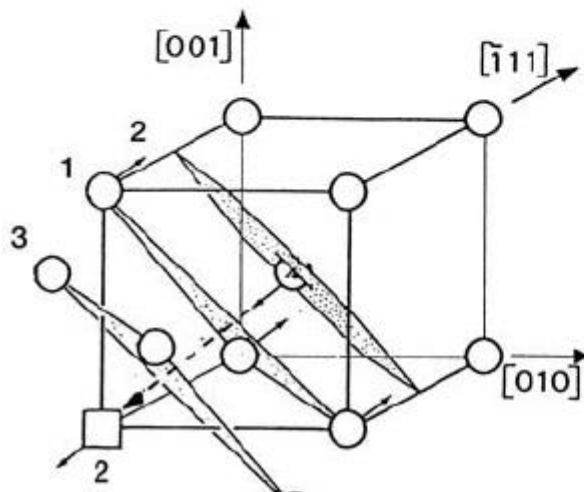
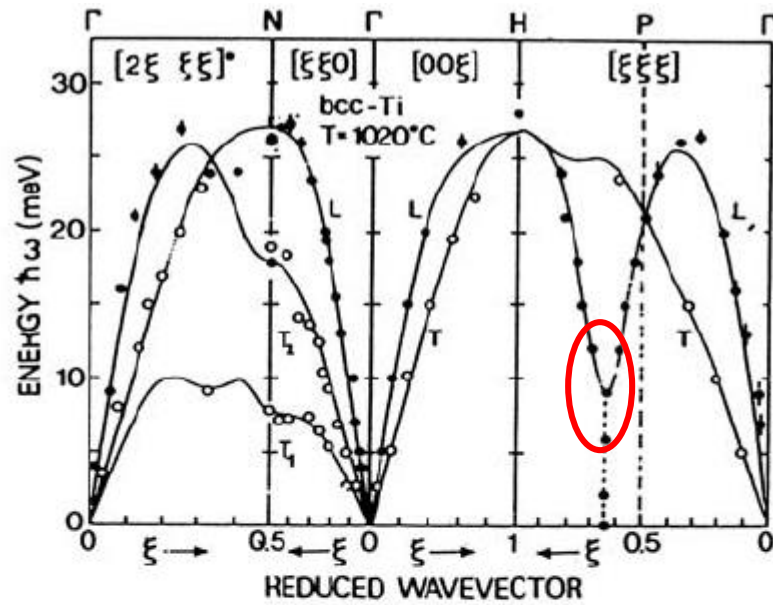
GaAs





- BaTiO₃ in cubic symmetry has several instabilities:
1. FerroElectric (FE) instability at Γ (0,0,0) reciprocal point
 2. AntiFerroElectric (AFE) instability at X (0.5,0,0)
 3. AntiFerroDistortive (AFD) instabilities at M (0.5,0.5,0) and R (0.5,0.5,0.5)
 4. Freezing in the eigenvector at Γ (0,0,0), reduces the symmetry to Tetragonal ($P4mm$)

Weak phonons in β -Ti



VI.2. Heat capacity of a crystal lattice

The classical approach:

The energy density of a lattice

$$u = \frac{1}{V} \frac{\int d\Gamma \mathcal{E} e^{-\mathcal{E}/k_B T}}{\int d\Gamma e^{-\mathcal{E}/k_B T}}, \quad d\Gamma = d^3 \mathbf{u}_1 d^3 \mathbf{u}_2 \dots d^3 \mathbf{u}_N d^3 \mathbf{p}_1 d^3 \mathbf{p}_2 \dots d^3 \mathbf{p}_N$$

$$u = -\frac{1}{V} \frac{\partial}{\partial \beta} \ln \int d\Gamma e^{-\beta \mathcal{E}}, \quad \beta = 1/(k_B T)$$

The total energy of the lattice is

$$\begin{aligned} \mathcal{E} &= \sum_{\mathbf{R}} \frac{p(\mathbf{R})^2}{2M} + U_{\text{eq}} + U_{\text{harm}} = \sum_{\mathbf{R}} \frac{p(\mathbf{R})^2}{2M} + U_{\text{eq}} + \\ &+ \frac{1}{4} \sum_{\mathbf{R} \neq \mathbf{R}'} [u_j(\mathbf{R}) - u_j(\mathbf{R}')] \varphi_{jk}(\mathbf{R} - \mathbf{R}') [u_k(\mathbf{R}) - u_k(\mathbf{R}')] \end{aligned}$$

Let us make the substitution $\mathbf{u}(\mathbf{R}) = \beta^{-1/2} \tilde{\mathbf{u}}(\mathbf{R})$, $\mathbf{p}(\mathbf{R}) = \beta^{-1/2} \tilde{\mathbf{p}}(\mathbf{R})$

Then

$$\int d\Gamma e^{-\beta\mathcal{E}} = e^{-\beta U_{\text{eq}}} \beta^{-3N} \int \prod_{\mathbf{R}} d^3\mathbf{u}(\mathbf{R}) d^3\mathbf{p}(\mathbf{R}) \exp \left[- \sum_{\mathbf{R}} \frac{\tilde{p}^2(\mathbf{R})}{2M} - \frac{1}{2} \sum_{\mathbf{R} \neq \mathbf{R}'} \tilde{u}_j(\mathbf{R}) \varphi_{jk}(\mathbf{R} - \mathbf{R}') \tilde{u}_k(\mathbf{R}') \right]$$

and the entire integral is independent of temperature.

Therefore

$$u = -\frac{1}{V} \frac{\partial}{\partial \beta} (-\beta U_{\text{eq}} - 3N \ln \beta + \text{const}) = \frac{U_{\text{eq}}}{V} + 3nk_B T$$

and

$$c_V = \left(\frac{\partial u}{\partial T} \right)_V = 3nk_B \quad \text{the rule Dulong-Petit}$$

The quantum-mechanical approach:

$$u = -\frac{1}{V} \frac{\partial}{\partial \beta} \ln \left(\sum_i \exp \left(-\beta \sum_{ks} \left(n_{ks}^{(i)} + \frac{1}{2} \right) \hbar \omega_s(\mathbf{k}) \right) \right)$$

where $n_{ks}^{(i)}$ is the quantum number of a harmonic oscillator in the state $|\mathbf{k}s\rangle$

the sum \sum_i is calculated over all possible values of the quantum numbers $n_{ks}^{(i)}$

$$\begin{aligned} \sum_i \exp \left(-\beta \sum_{ks} \left(n_{ks}^{(i)} + \frac{1}{2} \right) \hbar \omega_s(\mathbf{k}) \right) &= \sum_i \prod_{ks} \exp \left(-\beta \sum_{ks} \left(n_{ks}^{(i)} + \frac{1}{2} \right) \hbar \omega_s(\mathbf{k}) \right) = \\ &= \prod_{ks} \left[\sum_{n=0}^{\infty} \exp \left(-\beta \sum_{ks} \left(n_{ks}^{(i)} + \frac{1}{2} \right) \hbar \omega_s(\mathbf{k}) \right) \right] = \prod_{ks} \frac{e^{-\beta \hbar \omega_s(\mathbf{k})/2}}{1 - e^{-\beta \hbar \omega_s(\mathbf{k})}} \end{aligned}$$

We obtain

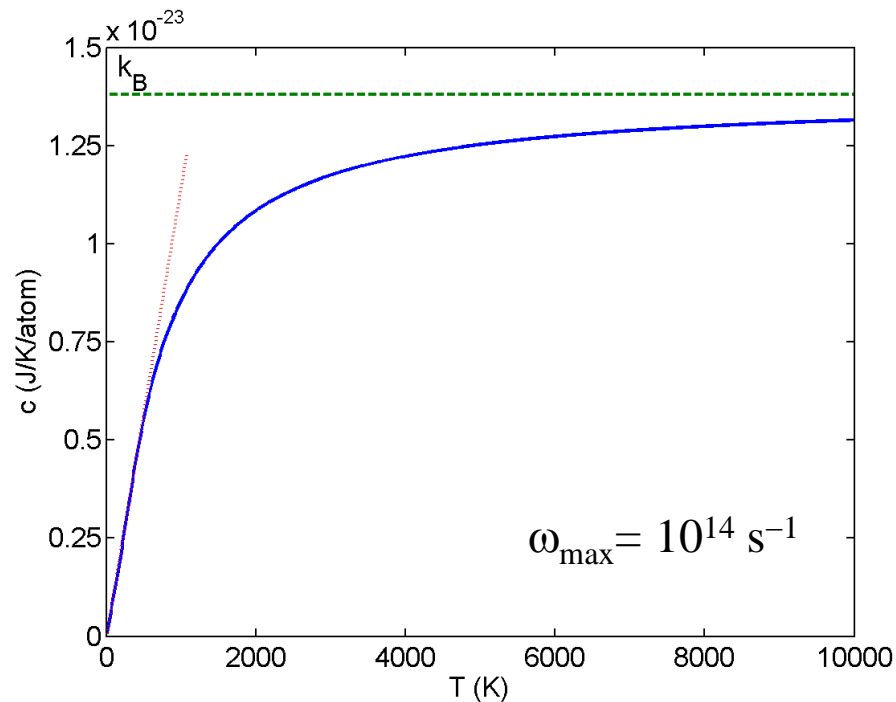
$$u = \frac{1}{V} \sum_{ks} \hbar \omega_s(\mathbf{k}) \left[n_s(\mathbf{k}) + \frac{1}{2} \right], \quad n_s(\mathbf{k}) = \frac{1}{e^{\beta \hbar \omega_s(\mathbf{k})} - 1}$$

The Bose-Einstein statistics

Exact calculation of c_V : 1D monoatomic chain

Specific heat capacity per one atom:

$$c = \frac{1}{N} \frac{\hbar^2}{k_B T^2} \sum_{n=-N/2}^{\frac{N}{2}-1} \left[\frac{\omega_n}{\exp\left(\frac{\hbar\omega_n}{k_B T}\right) - 1} \right]^2$$

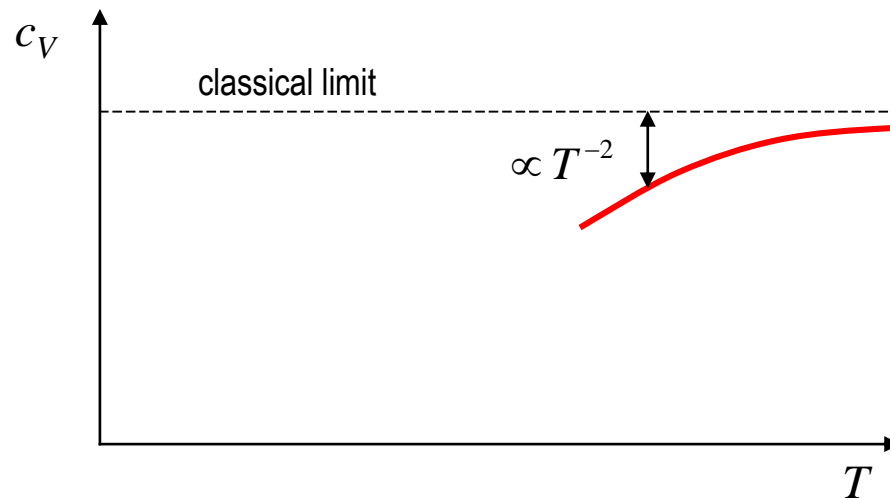


Calculation of c_V in 3D case:
$$u = \frac{1}{V} \sum_{ks} \hbar \omega_s(\mathbf{k}) \left[n_s(\mathbf{k}) + \frac{1}{2} \right], n_s(\mathbf{k}) = \frac{1}{e^{\beta \hbar \omega_s(\mathbf{k})} - 1}$$

1. High temperatures: $\beta \hbar \omega_s(\mathbf{k}) \ll 1$

and
$$\frac{1}{\exp(x) - 1} \approx \frac{1}{x} \left(1 - \frac{x}{2} + \frac{x^2}{12} + O(x^3) \right)$$

Finally we obtain
$$c_V \approx 3nk_B \left[1 - \frac{\hbar^2}{12(k_B T)^2} \frac{1}{3N} \sum_{ks} (\omega_s(\mathbf{k}))^2 \right]$$



2. low temperatures: $\beta \hbar \omega_s(\mathbf{k}) \gg 1$

Then only the lowest-frequency modes contribute to the specific heat (long-wave acoustic phonons)

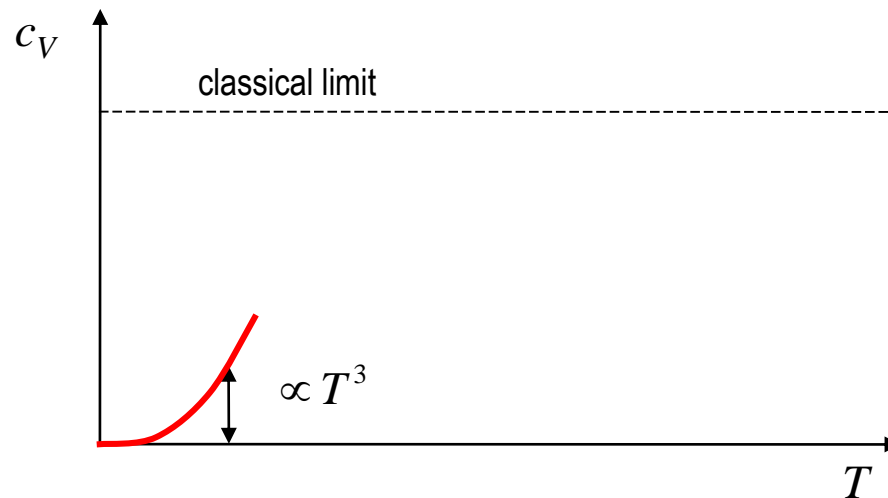
$$c_V \approx \frac{\partial}{\partial T} \sum_s \int \frac{d^3 \mathbf{k}}{8\pi^3} \frac{\hbar k c_s(\mathbf{k}^0)}{\exp\left(\frac{\hbar k c_s(\mathbf{k}^0)}{k_B T}\right) - 1}$$

because $\omega_s(\mathbf{k}) = k c_s(\mathbf{k}^0)$

for long-wave acoustic phonons

Then $c_V \approx \frac{2\pi^2}{5} k_B \left(\frac{k_B T}{\hbar c}\right)^3 \propto T^3$ where

$$\frac{1}{c^3} = \frac{1}{3} \sum_s \int \frac{d^2 \mathbf{k}^0}{4\pi} \frac{1}{[c_s(\mathbf{k}^0)]^3}$$



3. Whole temperature range, the Einstein model:

assumption – all phonons have the same frequency ω

$$c_V^E = nk_B \left(\frac{\hbar\omega}{k_B T} \right)^2 \frac{\exp\left(\frac{\hbar\omega}{k_B T}\right)}{\left[\exp\left(\frac{\hbar\omega}{k_B T}\right) - 1 \right]^2}$$

4. Whole temperature range, the Debye model:

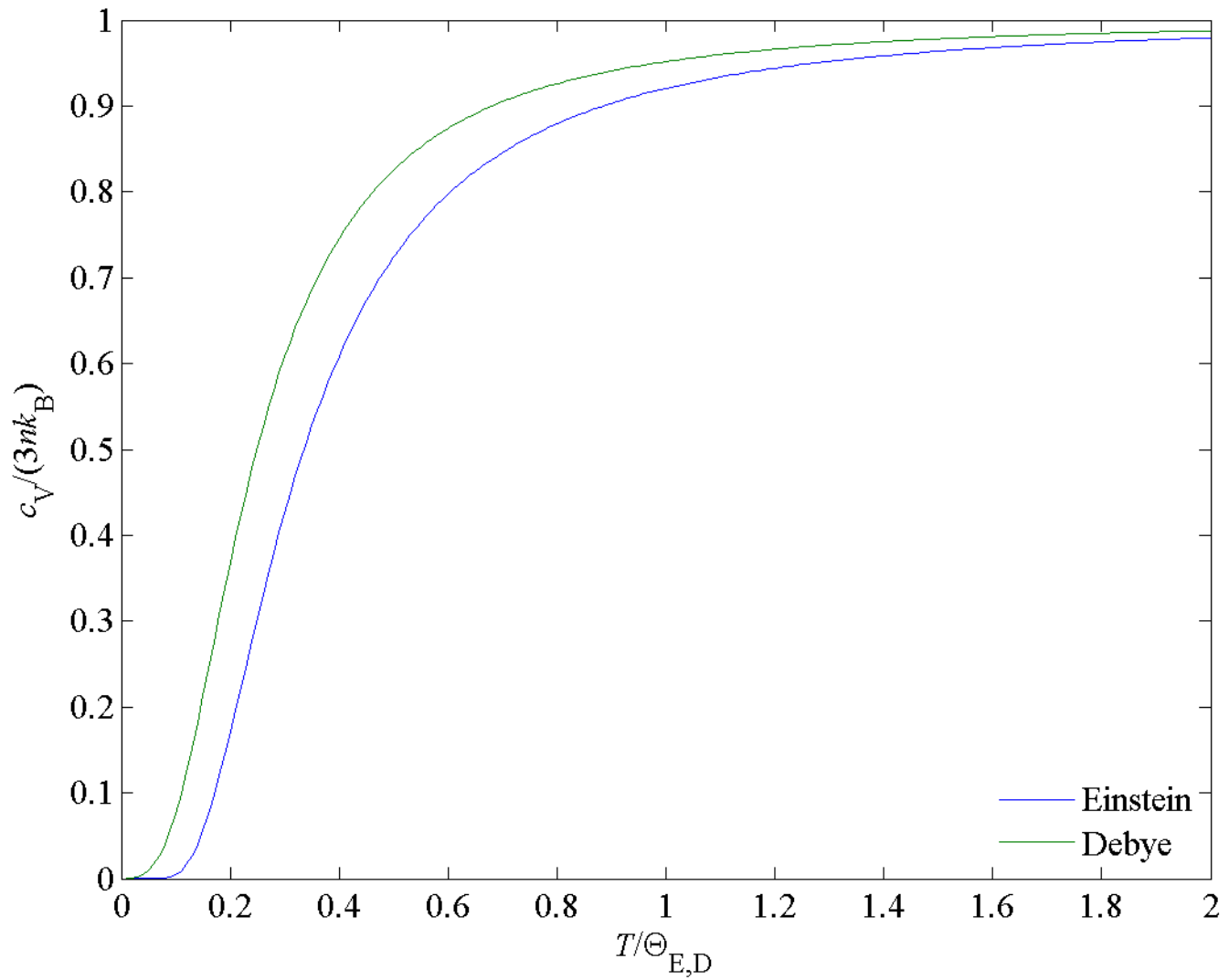
assumptions – all phonons have the same phase velocity $\omega = c|\mathbf{k}|$

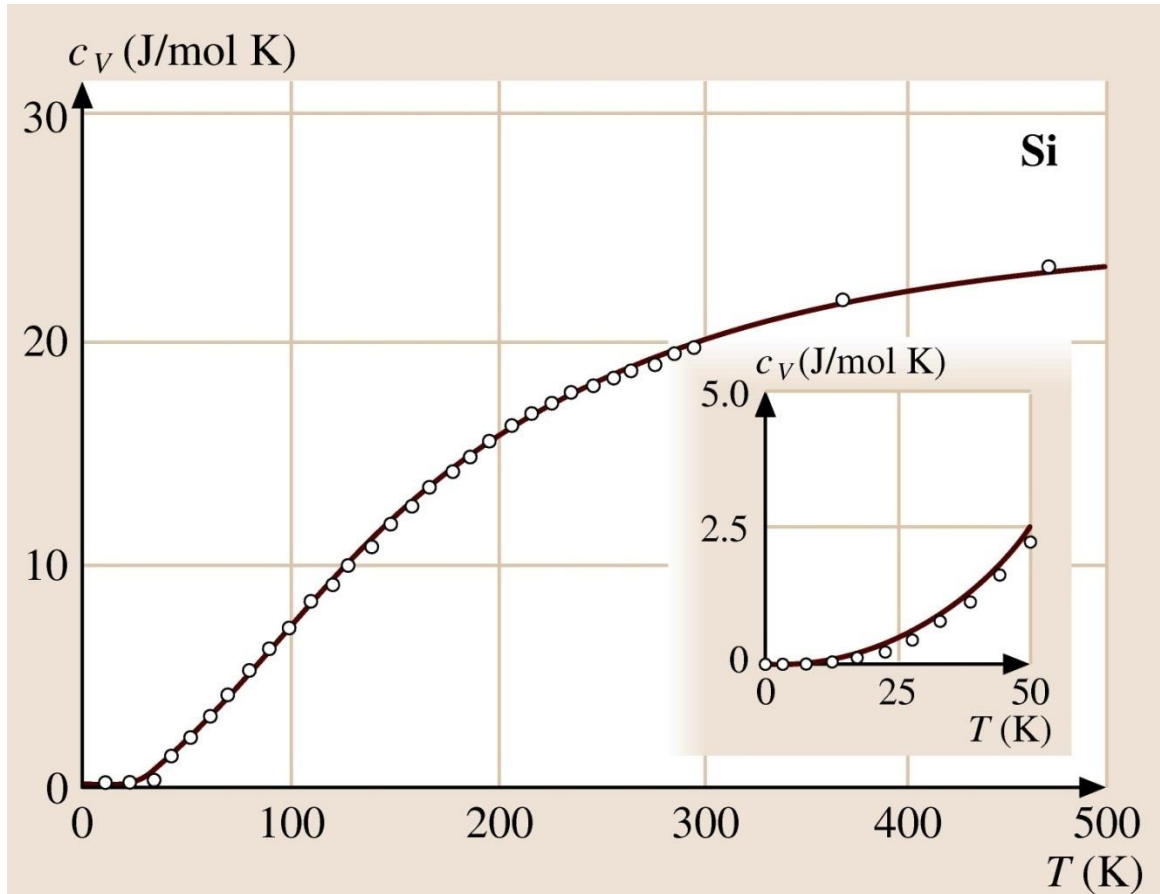
– the 1BZ is replaced by a sphere of radius k_D

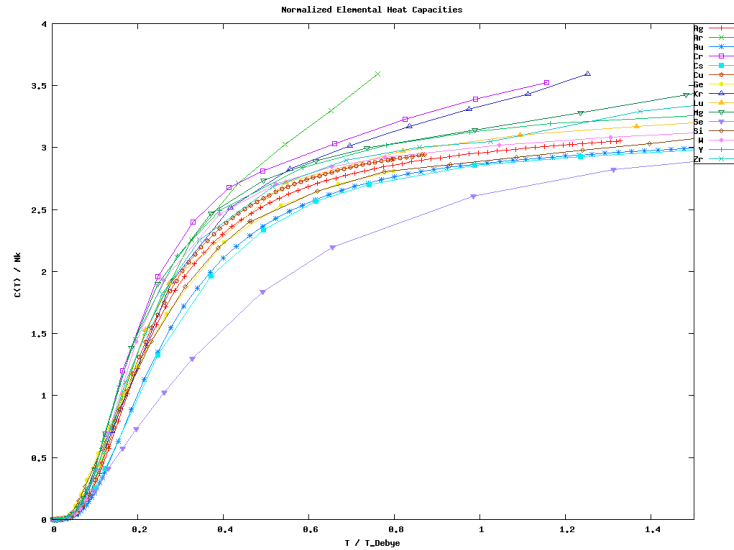
$$c_V^D = 9nk_B \left(\frac{T}{\Theta_D} \right)^3 \int_0^{\Theta_D/T} dx \frac{x^4 e^x}{(e^x - 1)^2}$$

Θ_D is the Debye temperature

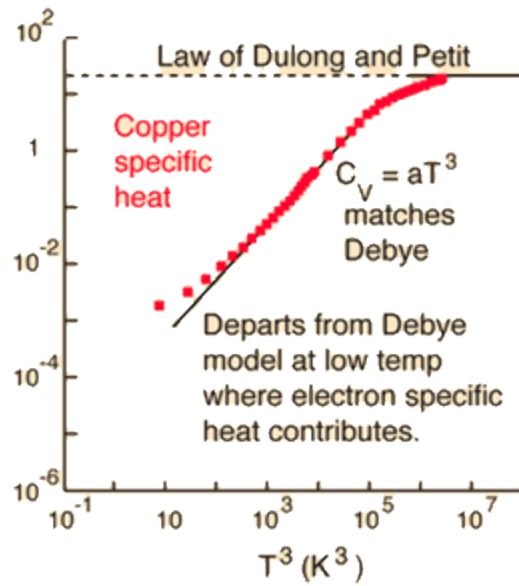
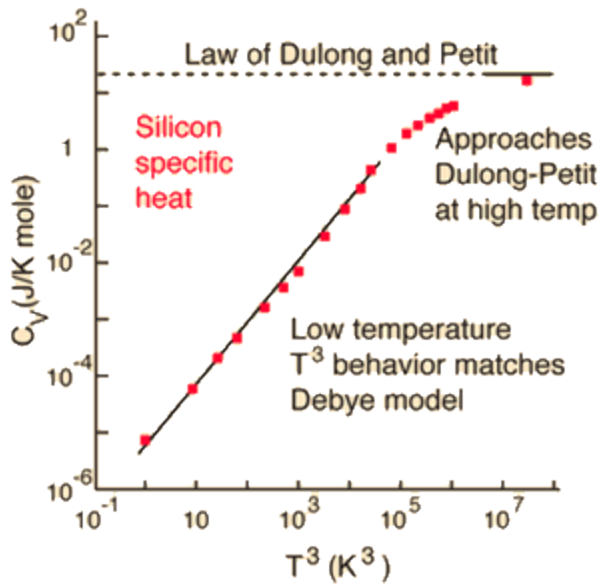
$$k_B \Theta_D = \hbar c k_D = \hbar \omega_D$$







chemwiki.ucdavis.edu



people.virginia.edu

Magnetic transitions influence the heat capacity:

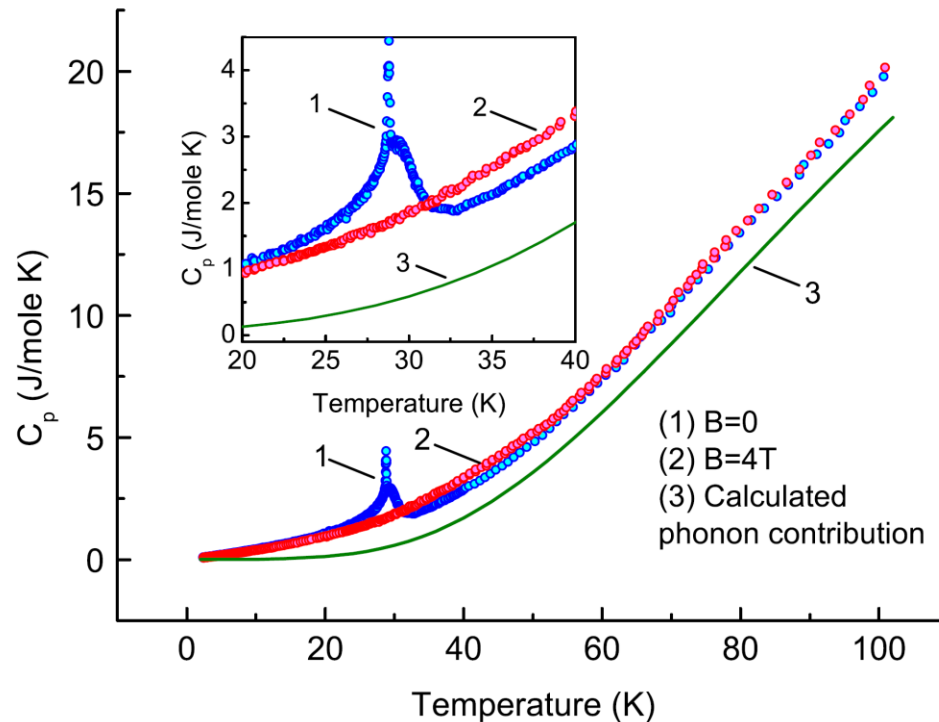


FIG. 2 (color online). The experimental heat capacity of MnSi at $B = 0$ (1) and $B = 4$ T (2) and the calculated phonon contribution (3).

Lost Heat Capacity and Entropy in the Helical Magnet MnSi

Sergei M. Stishov,^{1,*} Alla E. Petrova,¹ Anatoly A. Shikov,² Thomas A. Lograsso,³ Eyvaz I. Isaev,⁴
Börje Johansson,⁵ and Luke L. Daemen⁶

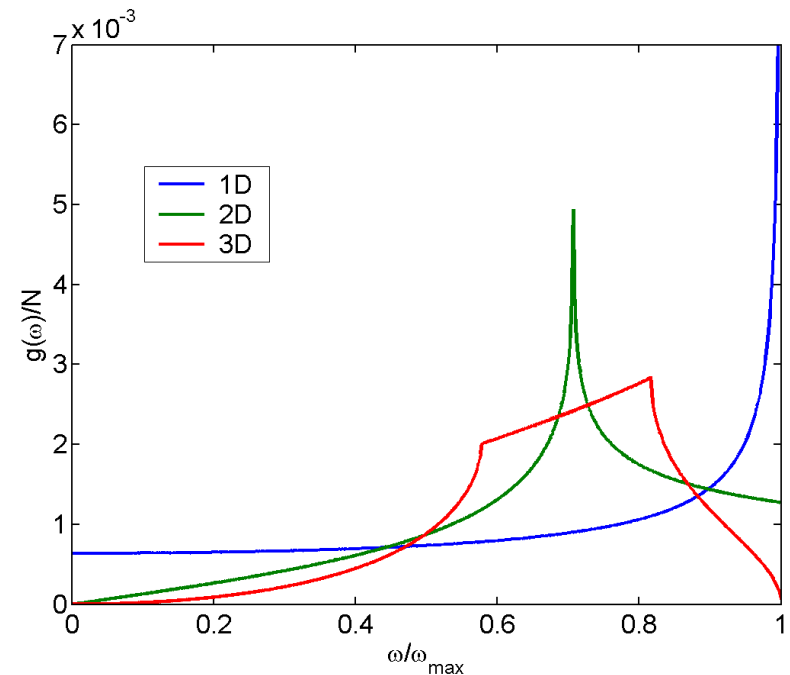
Density of phonon states:

calculation of the mean value of quantity Q depending on frequency:

$$q = \frac{1}{V} \sum_{ks} Q(\omega_s(\mathbf{k})) \approx \frac{1}{8\pi^3} \sum_s \int_{1BZ} d^3\mathbf{k} Q(\omega_s(\mathbf{k})) = \int_0^\infty d\omega g(\omega) Q(\omega) \Rightarrow$$

$$\Rightarrow g(\omega) = \frac{1}{8\pi^3} \sum_s \int_{1BZ} d^3\mathbf{k} \delta(\omega - \omega_s(\mathbf{k}))$$

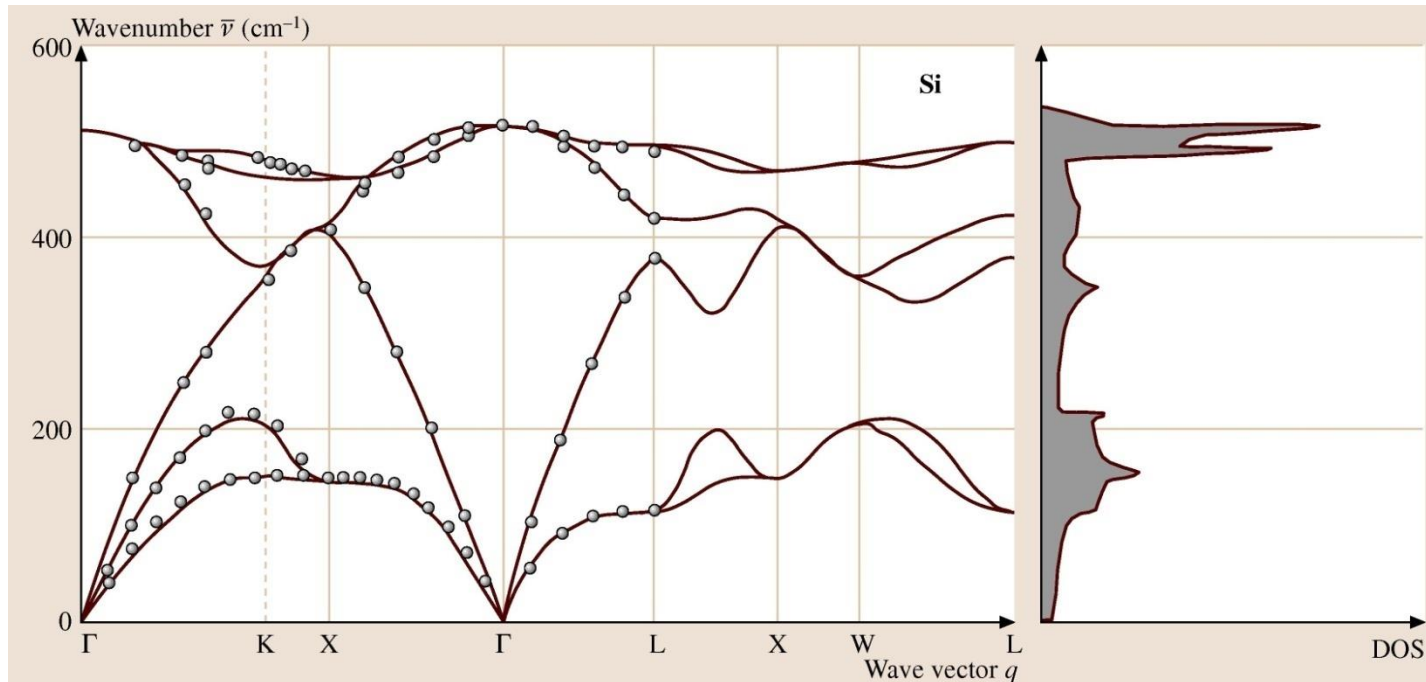
monoatomic 1D, 2D or 3D cubic lattices,
a direct calculation:



The Debye model, density of phonon states:

$$g_D(\omega) = \begin{cases} 3\omega^2 / (2\pi^2 c^3) & \text{for } \omega < \omega_D \\ 0 & \text{for } \omega \geq \omega_D \end{cases}$$

phonon dispersion relation and density of states in Si



IV. 6. Interaction of a ionic crystal with light - polaritons

Polarizability of an ionic lattice – relative displacement of cations with respect to anions in an external electric field. Equations of movement of the positive and negative sublattices

$$\begin{aligned} M_+ \ddot{\mathbf{u}}_+ &= -K(\mathbf{u}_+ - \mathbf{u}_-) + e\mathbf{E}_{Loc} && \text{long-range electrostatic interaction} \\ M_- \ddot{\mathbf{u}}_- &= -K(\mathbf{u}_- - \mathbf{u}_+) - e\mathbf{E}_{Loc} && \text{between the ions is included in } \mathbf{E}_{loc} \end{aligned}$$

long-wave phonons are assumed ($k \ll 1\text{BZ}$) \Rightarrow all the ions of the same kind have the same displacements

Equation for the relative displacement

$$\ddot{\mathbf{w}} = \ddot{\mathbf{u}}_+ - \ddot{\mathbf{u}}_- = \frac{e}{M} \mathbf{E}_{Loc} - \frac{K}{M} \mathbf{w}, \quad M = \frac{M_+ M_-}{M_+ + M_-}$$

Amplitude of the stationary solution

$$\mathbf{w}_0 = \frac{e\mathbf{E}_0}{M(\bar{\omega}^2 - \omega^2)}, \quad \bar{\omega}^2 = \frac{K}{M} \quad \mathbf{E}_0 \text{ is the amplitude of } \mathbf{E}_{loc}$$

The amplitude of the dipole moment of one molecule is $\mathbf{p}_0 = e\mathbf{w}_0$ and the polarizability is

$$\alpha = \frac{p_0}{E_0} = \frac{e^2}{M(\bar{\omega}^2 - \omega^2)}$$

How to include the polarizability of the ions (electron polarizability)?

The resonant frequency of the electrons is roughly

$$\hbar\omega_0 \propto 100 \div 1000 \text{ eV}$$

while $\hbar\bar{\omega} \approx \hbar\omega_D \propto 10 \div 100 \text{ meV}$

Since $M \approx 10^4 m_e$, both polarizabilities are comparable at frequencies close to $\bar{\omega}$

Intuitively:

$$\alpha = \alpha_+ + \alpha_- + \frac{e^2}{M(\bar{\omega}^2 - \omega^2)}$$

“Static” case $\omega \ll \bar{\omega} \ll \omega_0$

$$\frac{\varepsilon(0) - 1}{\varepsilon(0) + 2} = \frac{1}{3\varepsilon_0 V_c} \left(\alpha_+ + \alpha_- + \frac{e^2}{M\bar{\omega}^2} \right) \quad \text{See the Clausius-Mossotti equation}$$

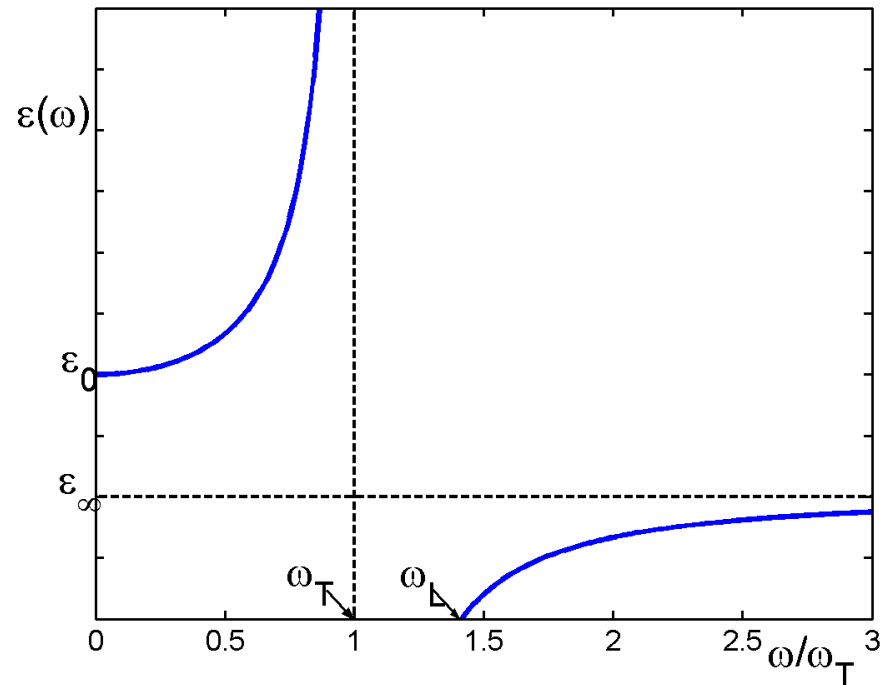
High-frequency case $\bar{\omega} \ll \omega \ll \omega_0$

$$\frac{\varepsilon(\infty) - 1}{\varepsilon(\infty) + 2} = \frac{1}{3\varepsilon_0 V_c} (\alpha_+ + \alpha_-)$$

Since
$$\frac{\epsilon(\omega) - 1}{\epsilon(\omega) + 2} = \frac{1}{3\epsilon_0 V_c} \left(\alpha_+ + \alpha_- + \frac{e^2}{M(\bar{\omega}^2 - \omega^2)} \right)$$

we obtain

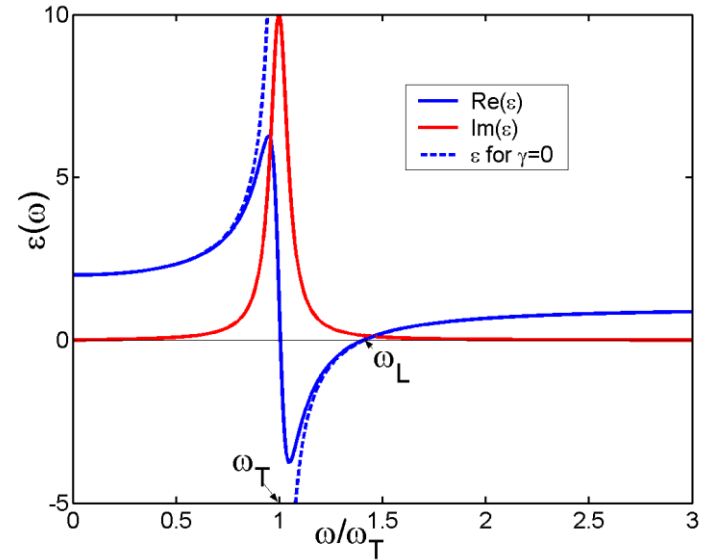
$$\epsilon(\omega) = \epsilon(\infty) + \frac{\epsilon(\infty) - \epsilon(0)}{\frac{\omega^2}{\omega_T^2} - 1}, \quad \omega_T^2 = \bar{\omega}^2 \frac{\epsilon(\infty) + 2}{\epsilon(0) + 2}$$



Frequency gap for $\omega_T < \omega < \omega_L \Rightarrow$ total reflection of light

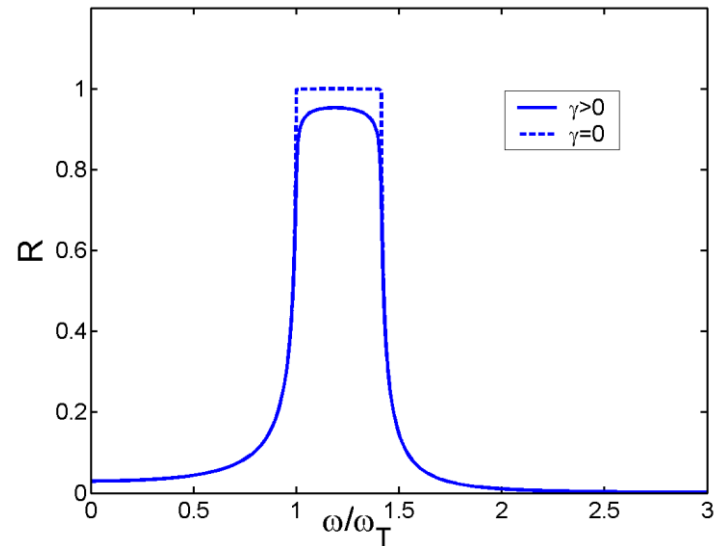
With absorption

$$\epsilon(\omega) = \epsilon(\infty) + \frac{\epsilon(\infty) - \epsilon(0)}{\frac{\omega^2}{\omega_T^2} - 1 + i\gamma \frac{\omega}{\omega_T}}$$



Reflectivity of light at normal incidence

$$R = \left| \frac{1 - \sqrt{\epsilon}}{1 + \sqrt{\epsilon}} \right|^2$$



Ab initio calculations of indium arsenide in the wurtzite phase: structural, electronic and optical properties

Luis C O Dacal¹ and A Cantarero²

¹Instituto de Estudos Avançados, IEAv-CTA, PO Box 6044, 12228-970, São José dos Campos-SP, Brazil

²Materials Science Institute, University of Valencia, PO Box 22085, E46071 Valencia, Spain
E-mail: lcodacal@gmail.com and cantarero@uv.es

Received 3 December 2013, revised 24 January 2014

Accepted for publication 29 January 2014

Published 25 February 2014

Materials Research Express 1 (2014) 015702

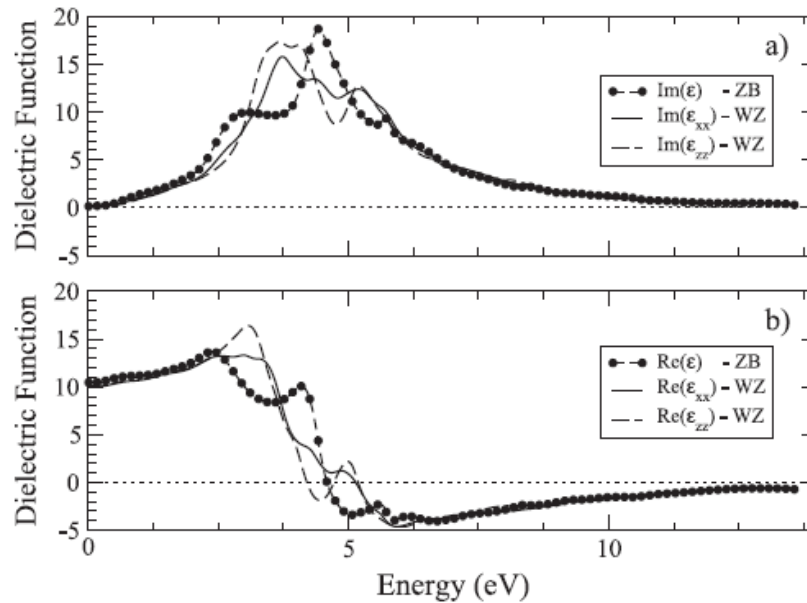
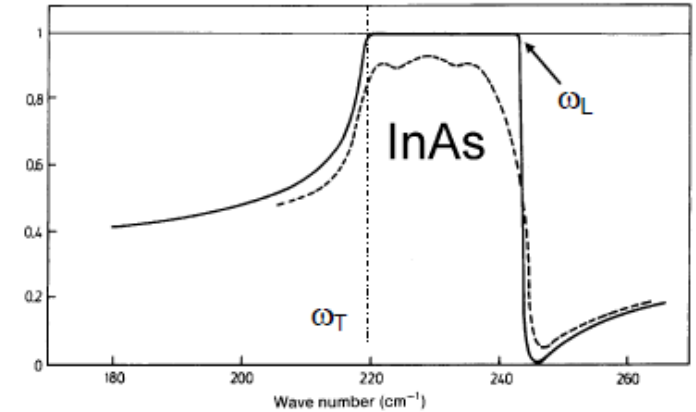


Figure 4. Imaginary (a) and real (b) parts of the complex dielectric function of WZ InAs as a function of incident photon energy for polarizations in the xy plane and along the z -axis. The results for ZB InAs are included for comparison.

Long-wave optical phonons

we assume that all equivalent ions have the same displacements.

The Maxwell equations

$$\mathbf{D} = \varepsilon_0 \mathbf{E} + \mathbf{P}, \quad \text{div} \mathbf{D} = 0,$$

$$\text{rot} \mathbf{E} = -\frac{\partial \mathbf{B}}{\partial t} \approx 0 \quad (\text{electrostatic approximation})$$

we restrict ourselves to cubic crystals, where ε is a scalar $\Rightarrow \mathbf{D} \parallel \mathbf{E} \parallel \mathbf{P}$; we assume plane monochromatic waves.

$$\begin{Bmatrix} \mathbf{D} \\ \mathbf{E} \\ \mathbf{P} \end{Bmatrix} = \begin{Bmatrix} \mathbf{D}_0 \\ \mathbf{E}_0 \\ \mathbf{P}_0 \end{Bmatrix} e^{i\mathbf{k} \cdot \mathbf{r}}$$

Then

$$\text{div} \mathbf{D} = 0 \Rightarrow \mathbf{k} \cdot \mathbf{D}_0 = 0 \Rightarrow \mathbf{D}_0 = 0 \text{ or } \mathbf{D}, \mathbf{E}, \mathbf{P} \perp \mathbf{k}$$

$$\text{rot} \mathbf{E} = 0 \Rightarrow \mathbf{k} \times \mathbf{E}_0 = 0 \Rightarrow \mathbf{E}_0 = 0 \text{ or } \mathbf{D}, \mathbf{E}, \mathbf{P} \parallel \mathbf{k}$$

Longitudinal optical phonon:

$$\mathbf{P} \parallel \mathbf{k} \Rightarrow \mathbf{D} = 0 \Rightarrow \varepsilon = 0 \quad \text{frequency } \omega_L$$

Transversal optical phonon:

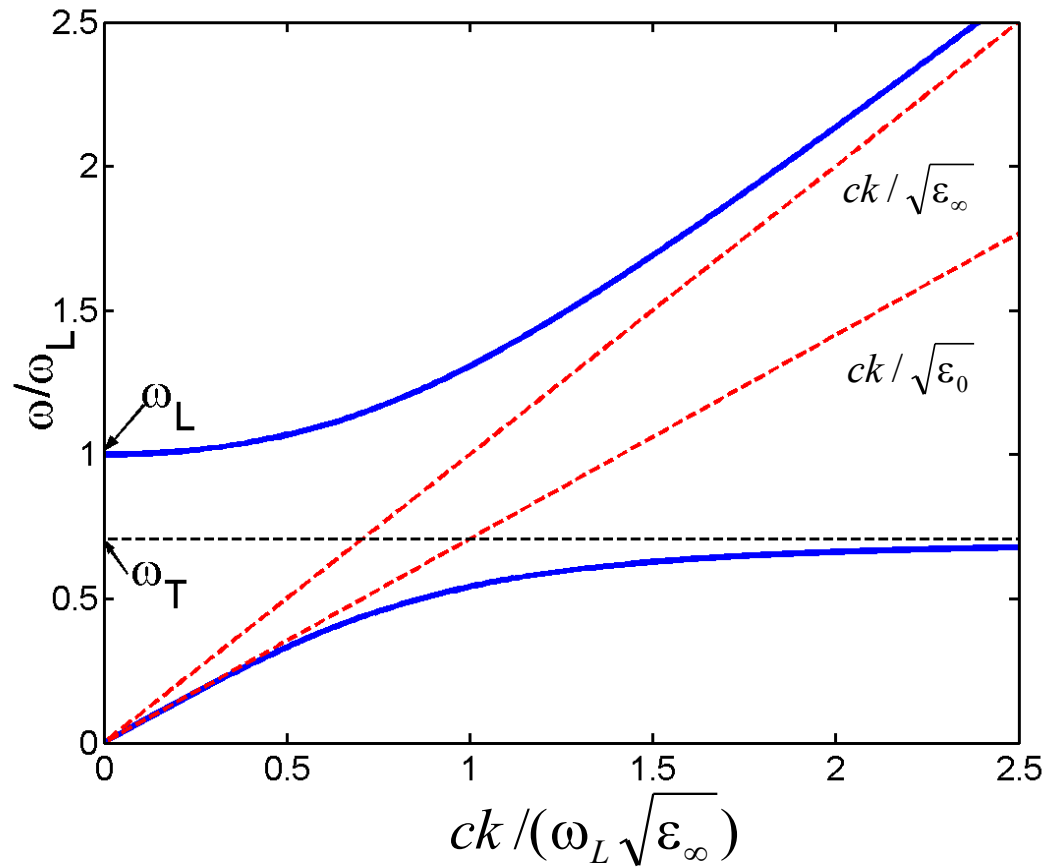
$$\mathbf{P} \perp \mathbf{k} \Rightarrow \mathbf{E} = 0 \Rightarrow \varepsilon = \infty \quad \text{frequency } \omega_T$$

Lyddane-Sachs-Teller formula (LST):

$$\frac{\omega_L^2}{\omega_T^2} = \frac{\varepsilon(0)}{\varepsilon(\infty)}$$

Dispersion relation for phonons/photons for small k

$$\omega = \frac{ck}{\sqrt{\varepsilon(\omega)}} \Rightarrow \omega^2 = \frac{1}{2} \left[\omega_L^2 + \frac{(kc)^2}{\varepsilon(\infty)} \pm \sqrt{\left(\omega_L^2 + \frac{(kc)^2}{\varepsilon(\infty)} \right)^2 - 4\omega_L^2 \frac{(kc)^2}{\varepsilon(0)}} \right]$$



collective excitation - **polariton**

IV. 7. Magnons

The Heisenberg hamiltonian $\hat{H}_S = - \sum_{i \neq j} J_{ij} \hat{\mathbf{S}}_i \cdot \hat{\mathbf{S}}_j - g\mu_B B \sum_j \hat{S}_{zj}$

The ground state of the Heisenberg hamiltonian is $|0\rangle = \prod_R |S\rangle_R$, in which all spins are parallel to the external field

What is the first excited state? Let us consider the state, in which in a given position \mathbf{R} the value of S_z is $S-1$ (instead of S)

$$|\mathbf{R}\rangle = \frac{1}{\sqrt{2S}} \hat{S}_-(\mathbf{R})|0\rangle$$

We have denoted $\hat{S}_\pm = \hat{S}_x(\mathbf{R}) \pm i\hat{S}_y(\mathbf{R})$ the creation and annihilation operators

$$\hat{S}_\pm(\mathbf{R})|S_z\rangle_{\mathbf{R}} = \sqrt{(S \mp S_z)(S + 1 \pm S_z)}|S_z \pm 1\rangle_{\mathbf{R}}$$

$|\mathbf{R}\rangle$ is NOT an eigenvector of the Heisenberg hamiltonian.

Let us express an eigenvector of the Heisenberg hamiltonian as a linear combination of the states $|\mathbf{R}\rangle$

If the exchange integrals depend only on the distance $\mathbf{R} - \mathbf{R}'$, an eigenstate of the Heisenberg hamiltonian can be expressed as a linear combination

$$|\mathbf{k}\rangle = \frac{1}{\sqrt{N}} \sum_{\mathbf{R}} e^{i\mathbf{k}\cdot\mathbf{R}} |\mathbf{R}\rangle, \mathbf{k} \in 1BZ \quad \text{spin wave – magnon}$$

Let us calculate the corresponding eigenvalue of energy

$$\hat{H}_S |\mathbf{k}\rangle = E(\mathbf{k}) |\mathbf{k}\rangle$$

We obtain

$$E(\mathbf{k}) = E_0 + g\mu_B B + S \sum_{\mathbf{R}} J(\mathbf{R}) (1 - e^{i\mathbf{k}\cdot\mathbf{R}})$$

Since $J(\mathbf{R}) = J(-\mathbf{R})$ we obtain for zero field

$$E(\mathbf{k}) - E_0 = 2S \sum_{\mathbf{R}} J(\mathbf{R}) \sin^2(\mathbf{k}\cdot\mathbf{R} / 2)$$

For small \mathbf{k} , $E(\mathbf{k}) - E_0 \propto k^2$

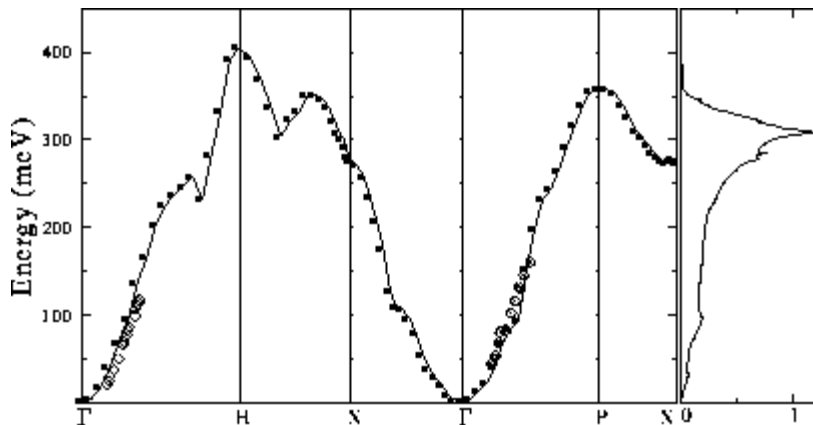
For an antiferromagnet $E(\mathbf{k}) \propto k$

The total spin of the state $|\mathbf{k}\rangle$ is $NS - 1$. The probability of finding a reduced spin value in point \mathbf{R}

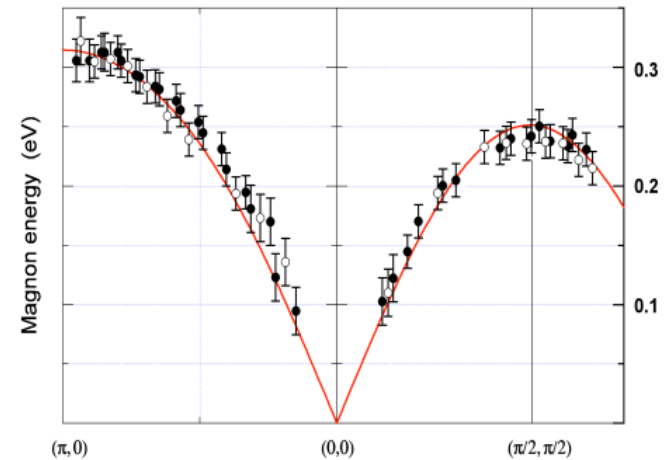
$$|\langle \mathbf{k} | \mathbf{R} \rangle|^2 = \frac{1}{N} \left| \sum_{\mathbf{R}'} e^{-i\mathbf{k} \cdot \mathbf{R}'} \langle \mathbf{R}' | \mathbf{R} \rangle \right|^2 = \frac{1}{N} = \text{const.}$$

S. V. Halilov et al. Europhys. Lett. **39**, 91 (1997).

M. Guarise et al. Phys. Rev. Lett. **105**, 157006 (2010)



ferromagnetic α -Fe

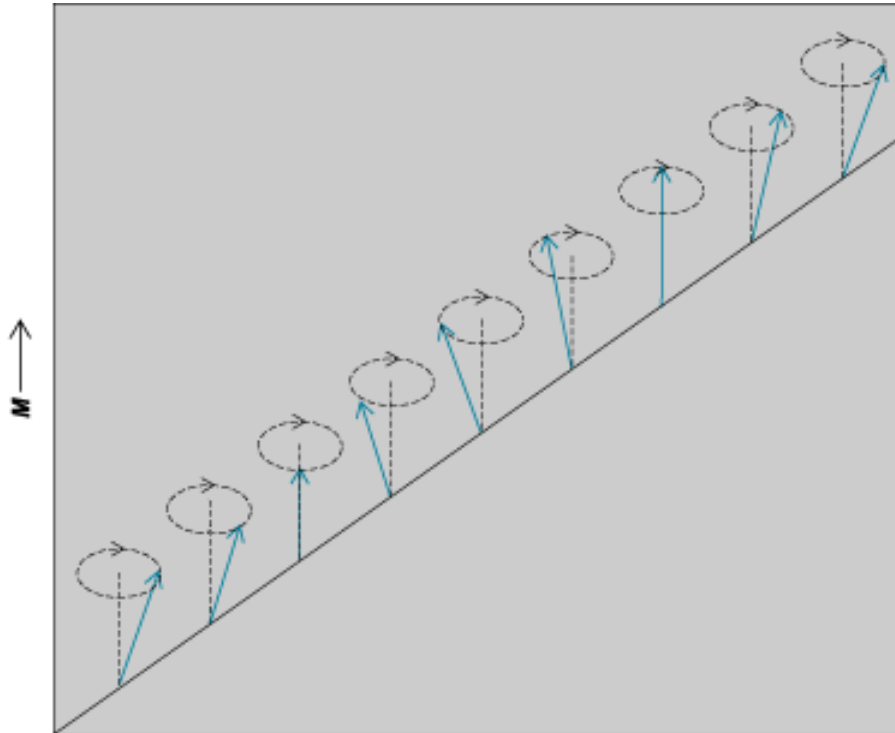


Magnon dispersion in antiferromagnetic $\text{Sr}_2\text{CuO}_2\text{Cl}_2$

Let us calculate the mean value of the correlation of the transversal components of the spins

$$\langle \mathbf{k} | \widehat{\mathbf{S}}_{\perp}(\mathbf{R}) \widehat{\mathbf{S}}_{\perp}(\mathbf{R}') | \mathbf{k} \rangle \quad \text{where} \quad \widehat{\mathbf{S}}_{\perp}(\mathbf{R}) \widehat{\mathbf{S}}_{\perp}(\mathbf{R}') = \widehat{S}_x(\mathbf{R}) \widehat{S}_x(\mathbf{R}') + \widehat{S}_y(\mathbf{R}) \widehat{S}_y(\mathbf{R}')$$

We obtain $\langle \mathbf{k} | \widehat{\mathbf{S}}_{\perp}(\mathbf{R}) \widehat{\mathbf{S}}_{\perp}(\mathbf{R}') | \mathbf{k} \rangle = \frac{2S}{N} \cos[\mathbf{k} \cdot (\mathbf{R} - \mathbf{R}')]]$



Magnon statistics:

The mean number of magnons with the wave vector \mathbf{k} in the unit volume of sample

$$n(\mathbf{k}) = \frac{1}{\exp\left(\frac{E(\mathbf{k})}{k_B T}\right) - 1}$$

The mean value of magnetization $M(T) = M(0) \left[1 - \frac{1}{NS} \sum_{\mathbf{k} \in 1BZ} n(\mathbf{k}) \right]$

for small T only the lowest magnon states are occupied, therefore

$$\begin{aligned} \sum_{\mathbf{k} \in 1BZ} n(\mathbf{k}) &\approx \frac{V}{(2\pi)^3} \int_{E_3^*} d^3\mathbf{k} \left[\exp\left(2S \sum_{\mathbf{R}} J(\mathbf{R}) \sin^2(\mathbf{k} \cdot \mathbf{R} / 2) / (k_B T)\right) - 1 \right]^{-1} \approx \\ &\approx \frac{V}{(2\pi)^3} \int_{E_3^*} d^3\mathbf{k} \left[\exp\left(S \sum_{\mathbf{R}} J(\mathbf{R}) (\mathbf{k} \cdot \mathbf{R})^2 / (2k_B T)\right) - 1 \right]^{-1} \end{aligned}$$

Using the substitution $\mathbf{k} = \mathbf{q} \sqrt{k_B T}$ we find

$$M(T) \approx M(0) \left\{ 1 - \frac{V}{NS} (k_B T)^{3/2} \int_{E_3^*} d^3\mathbf{q} \left[\exp\left(\frac{S}{2} \sum_{\mathbf{R}} J(\mathbf{R}) (\mathbf{q} \cdot \mathbf{R})^2\right) - 1 \right]^{-1} \right\} = M(0) (1 - \text{const.} T^{3/2})$$

The Bloch T^{3/2}-law

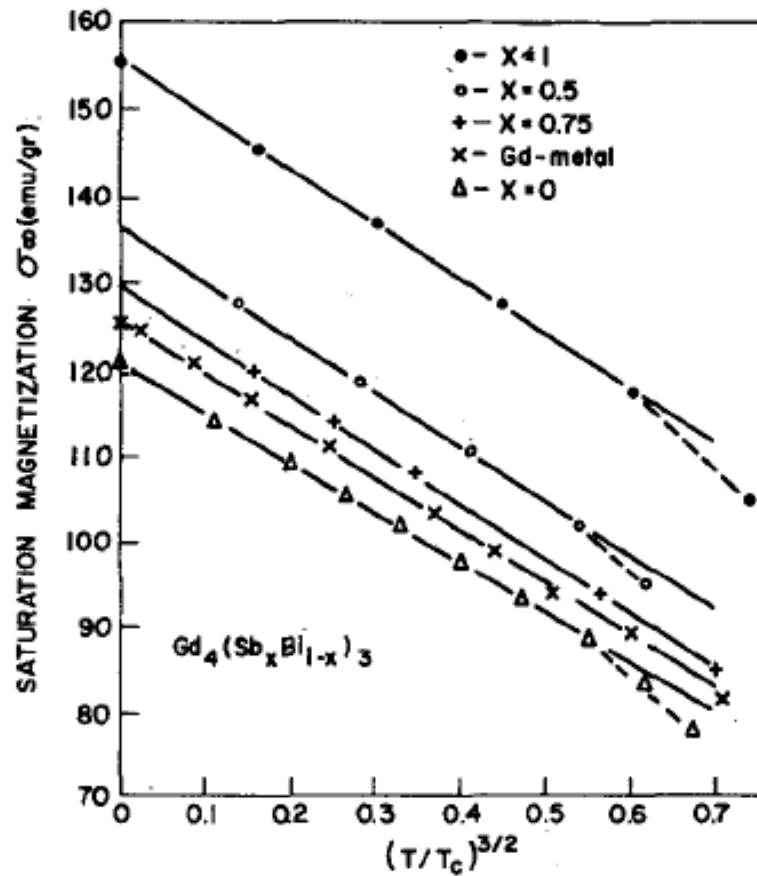


FIG. 4. Saturation magnetization of Gd metal and $Gd_4(Sb_xBi_{1-x})_3$ compounds compared with the T^3 law (solid lines). For Gd metal $\sigma_{\infty}/2$ has been plotted.

Even for nanoparticles

Bloch's law for epitaxial ultrathin dot arrays with uniaxial magnetic anisotropy

W. Kipferl,^{a)} M. Dumm, P. Kotissek, F. Steinbauer, and G. Bayreuther
Institut für Experimentelle und Angewandte Physik, Universität Regensburg, 93040 Regensburg, Germany

